U.S. DEPARTMENT OF ENERGY

OCRWM

YUCCA MOUNTAIN

YUCCA MOUNTAIN PROJECT

CONTROLLED COPY NO. 32 THIS IS A RED STAMP

Document No. YMP/CC-0003
Revision 0
CI No. CI.400000
Date 4/11/89
WBS No. 1.2.6
QA Level I

PROJECT CCB CONTROLLED DOCUMENT

EXPLORATORY SHAFT FACILITY (ESF)

SUBSYSTEM DESIGN REQUIREMENTS DOCUMENT (SDRD)

Received w/Ltr Dated 4/7/89

FOR TITLE II

VOLUME 2A

CHANGES TO THIS DOCUMENT REQUIRE PREPARATION AND APPROVAL OF A CHANGE REQUEST IN ACCORDANCE WITH PROJECT AP-3.3Q

DEPARTMENT OF ENERGY · UNITED STATES OF AMERICA

UNITED STATES DEPARTMENT OF ENERGY
NEVADA OPERATIONS OFFICE/YUCCA MOUNTAIN PROJECT OFFICE

WD 431-93-001

89\$523\$283 - Part 2

Box 28

SDRD APPENDIX A.1

ESF - REPOSITORY INTERFACE DRAWINGS

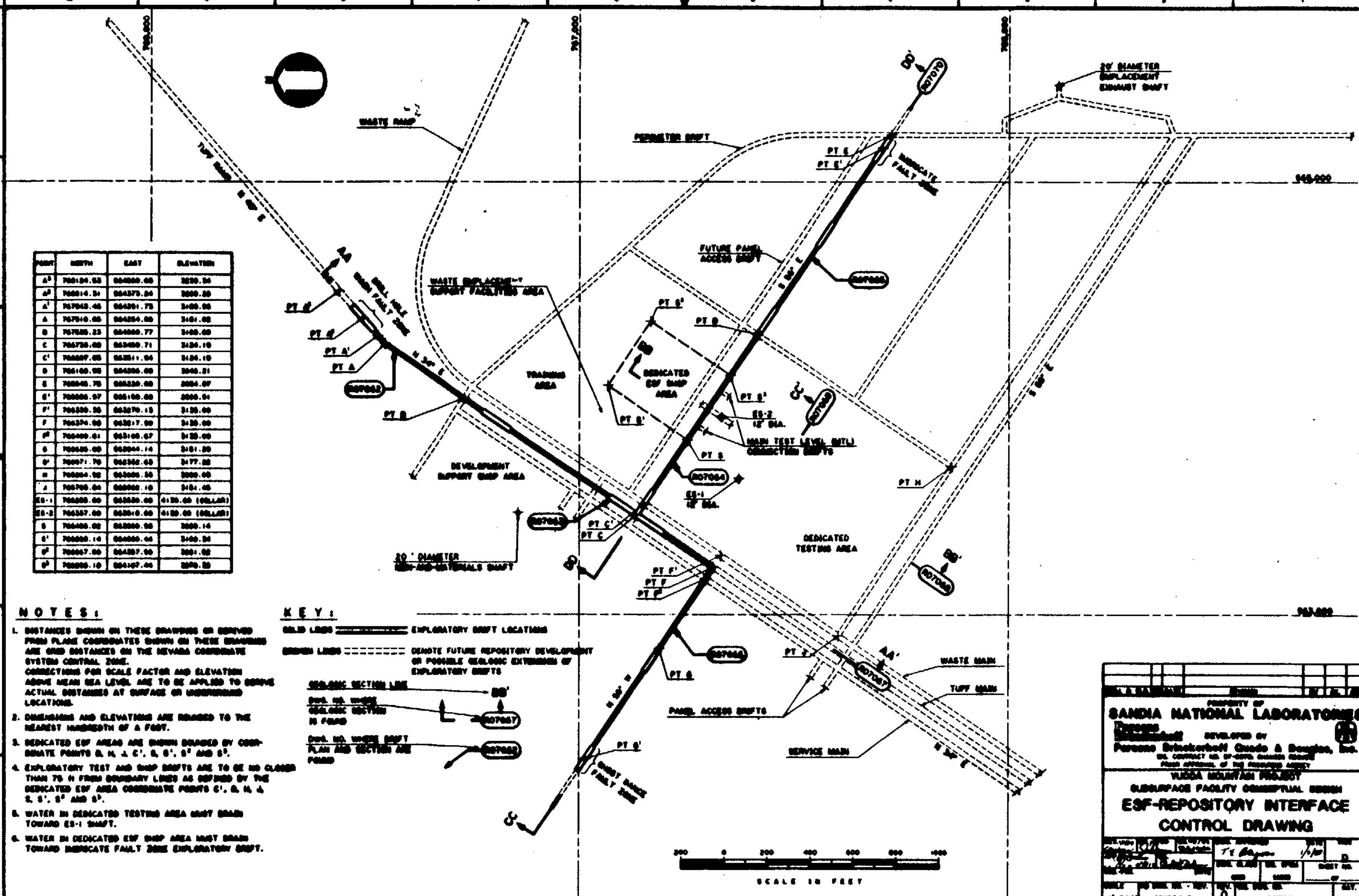

POINT	NORTH	EAST	ELEVATION
A³	[illegible]	[illegible]	[illegible]
A²	[illegible]	[illegible]	[illegible]
A'	[illegible]	[illegible]	[illegible]
A	[illegible]	[illegible]	[illegible]
B	[illegible]	[illegible]	[illegible]
C	[illegible]	[illegible]	[illegible]
C'	[illegible]	[illegible]	[illegible]
D	[illegible]	[illegible]	[illegible]
E	[illegible]	[illegible]	[illegible]
E'	[illegible]	[illegible]	[illegible]
F'	[illegible]	[illegible]	[illegible]
F	[illegible]	[illegible]	[illegible]
F²	[illegible]	[illegible]	[illegible]
G	[illegible]	[illegible]	[illegible]
G'	[illegible]	[illegible]	[illegible]
H	[illegible]	[illegible]	[illegible]
J	[illegible]	[illegible]	[illegible]
ES-1	[illegible]	[illegible]	[illegible] (COLLAR)
ES-2	[illegible]	[illegible]	[illegible] (COLLAR)
G	[illegible]	[illegible]	[illegible]
G'	[illegible]	[illegible]	[illegible]
G²	[illegible]	[illegible]	[illegible]
G³	[illegible]	[illegible]	[illegible]

NOTES:

1. DISTANCES SHOWN ON THESE DRAWINGS OR DERIVED FROM PLANE COORDINATES SHOWN ON THESE DRAWINGS ARE GRID DISTANCES ON THE NEVADA COORDINATE SYSTEM CENTRAL ZONE. CORRECTIONS FOR SCALE FACTOR AND ELEVATION ABOVE MEAN SEA LEVEL ARE TO BE APPLIED TO DERIVE ACTUAL DISTANCES AT SURFACE OR UNDERGROUND LOCATIONS.
2. DIMENSIONS AND ELEVATIONS ARE ROUNDED TO THE NEAREST HUNDREDTH OF A FOOT.
3. DEDICATED ESF AREAS ARE SHOWN BOUNDED BY COORDINATE POINTS D, H, J, C', G, G', G² AND G³.
4. EXPLORATORY TEST AND SHOP DRIFTS ARE TO BE NO CLOSER THAN 75 ft FROM BOUNDARY LINES AS DEFINED BY THE DEDICATED ESF AREA COORDINATE POINTS C', D, H, J, G, G', G² AND G³.
5. WATER IN DEDICATED TESTING AREA MUST DRAIN TOWARD ES-1 SHAFT.
6. WATER IN DEDICATED ESF SHOP AREA MUST DRAIN TOWARD IMBRICATE FAULT ZONE EXPLORATORY DRIFT.

KEY:

SOLID LINES — EXPLORATORY DRIFT LOCATIONS

BROKEN LINES — DENOTE FUTURE REPOSITORY DEVELOPMENT OR POSSIBLE GEOLOGIC EXTENSIONS OF EXPLORATORY DRIFTS

GEOLOGIC SECTION LINE

DWG. NO. WHERE GEOLOGIC SECTION IS FOUND

DWG. NO. WHERE DRIFT PLAN AND SECTION ARE FOUND

PROPERTY OF
SANDIA NATIONAL LABORATORIES

DEVELOPED BY
Parsons Brinckerhoff Quade & Douglas, Inc.

YUCCA MOUNTAIN PROJECT
SUBSURFACE FACILITY CONCEPTUAL DESIGN

ESF-REPOSITORY INTERFACE CONTROL DRAWING

SCALE 1"=200'

R07061

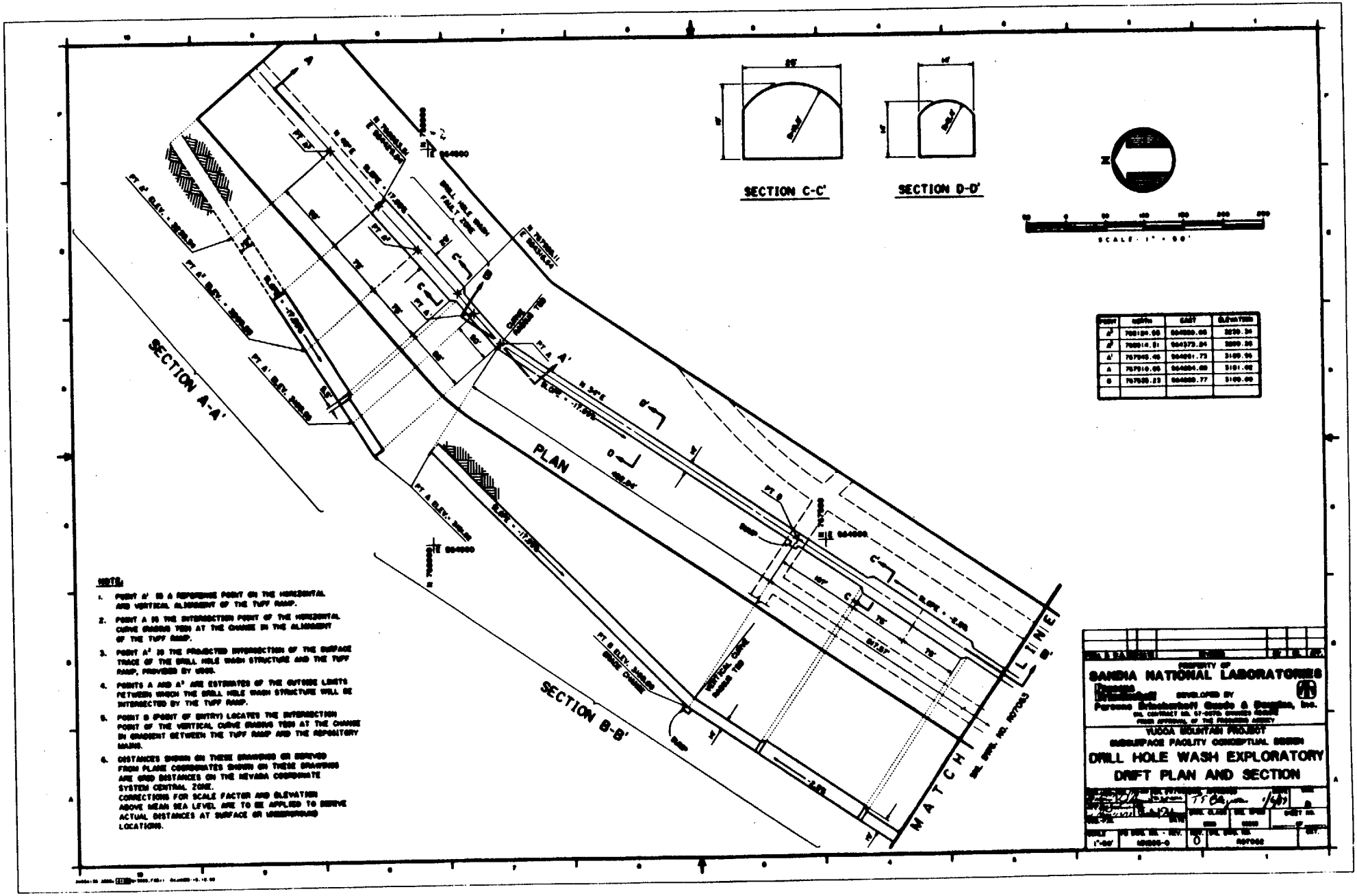
SECTION C-C'
SECTION D-D'
SCALE: 1" = 50'
SECTION A-A'
PLAN
SECTION B-B'
MATCH LINE
NOTES:
1. POINT A' IS A REFERENCE POINT ON THE HORIZONTAL AND VERTICAL ALIGNMENT OF THE TUFF RAMP.
2. POINT A IS THE INTERSECTION POINT OF THE HORIZONTAL CURVE ENDING TEN AT THE CHANGE IN THE ALIGNMENT OF THE TUFF RAMP.
3. POINT A² IS THE PROJECTED INTERSECTION OF THE SURFACE TRACE OF THE DRILL HOLE WASH STRUCTURE AND THE TUFF RAMP, PROVIDED BY USGS.
4. POINTS A AND A² ARE ESTIMATES OF THE OUTSIDE LIMITS BETWEEN WHICH THE DRILL HOLE WASH STRUCTURE WILL BE INTERSECTED BY THE TUFF RAMP.
5. POINT B (POINT OF ENTRY) LOCATES THE INTERSECTION POINT OF THE VERTICAL CURVE ENDING TEN AT THE CHANGE IN GRADIENT BETWEEN THE TUFF RAMP AND THE REPOSITORY MAINS.
6. DISTANCES SHOWN ON THESE DRAWINGS OR DERIVED FROM PLANE COORDINATES SHOWN ON THESE DRAWINGS ARE GRID DISTANCES ON THE NEVADA COORDINATE SYSTEM CENTRAL ZONE.
CORRECTIONS FOR SCALE FACTOR AND ELEVATION ABOVE MEAN SEA LEVEL ARE TO BE APPLIED TO DERIVE ACTUAL DISTANCES AT SURFACE OR UNDERGROUND LOCATIONS.
PROPERTY OF
SANDIA NATIONAL LABORATORIES
DEVELOPED BY
Parsons Brinckerhoff Quade & Douglas, Inc.
YUCCA MOUNTAIN PROJECT
SUBSURFACE FACILITY CONCEPTUAL DESIGN
DRILL HOLE WASH EXPLORATORY DRIFT PLAN AND SECTION

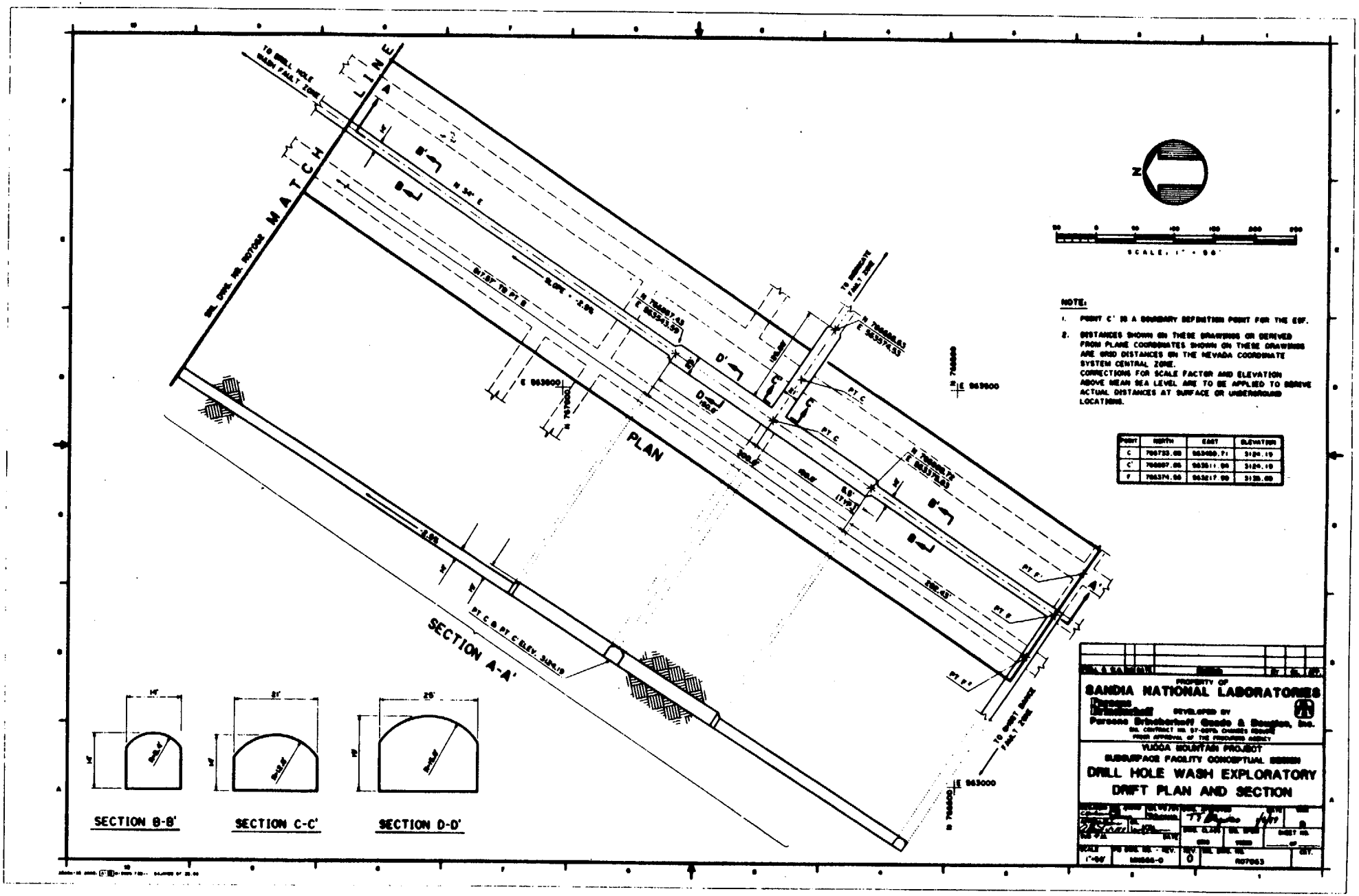
MATCH LINE
PLAN
SECTION A-A'
SECTION B-B'
SECTION C-C'
SECTION D-D'
NOTE:
1. POINT C' IS A BOUNDARY DEFINITION POINT FOR THE EXF.
2. DISTANCES SHOWN ON THESE DRAWINGS OR DERIVED FROM PLANE COORDINATES SHOWN ON THESE DRAWINGS ARE GRID DISTANCES ON THE NEVADA COORDINATE SYSTEM CENTRAL ZONE. CORRECTIONS FOR SCALE FACTOR AND ELEVATION ABOVE MEAN SEA LEVEL ARE TO BE APPLIED TO DERIVE ACTUAL DISTANCES AT SURFACE OR UNDERGROUND LOCATIONS.
PROPERTY OF
SANDIA NATIONAL LABORATORIES
YUCCA MOUNTAIN PROJECT
SUBSURFACE FACILITY CONCEPTUAL DESIGN
DRILL HOLE WASH EXPLORATORY
DRIFT PLAN AND SECTION

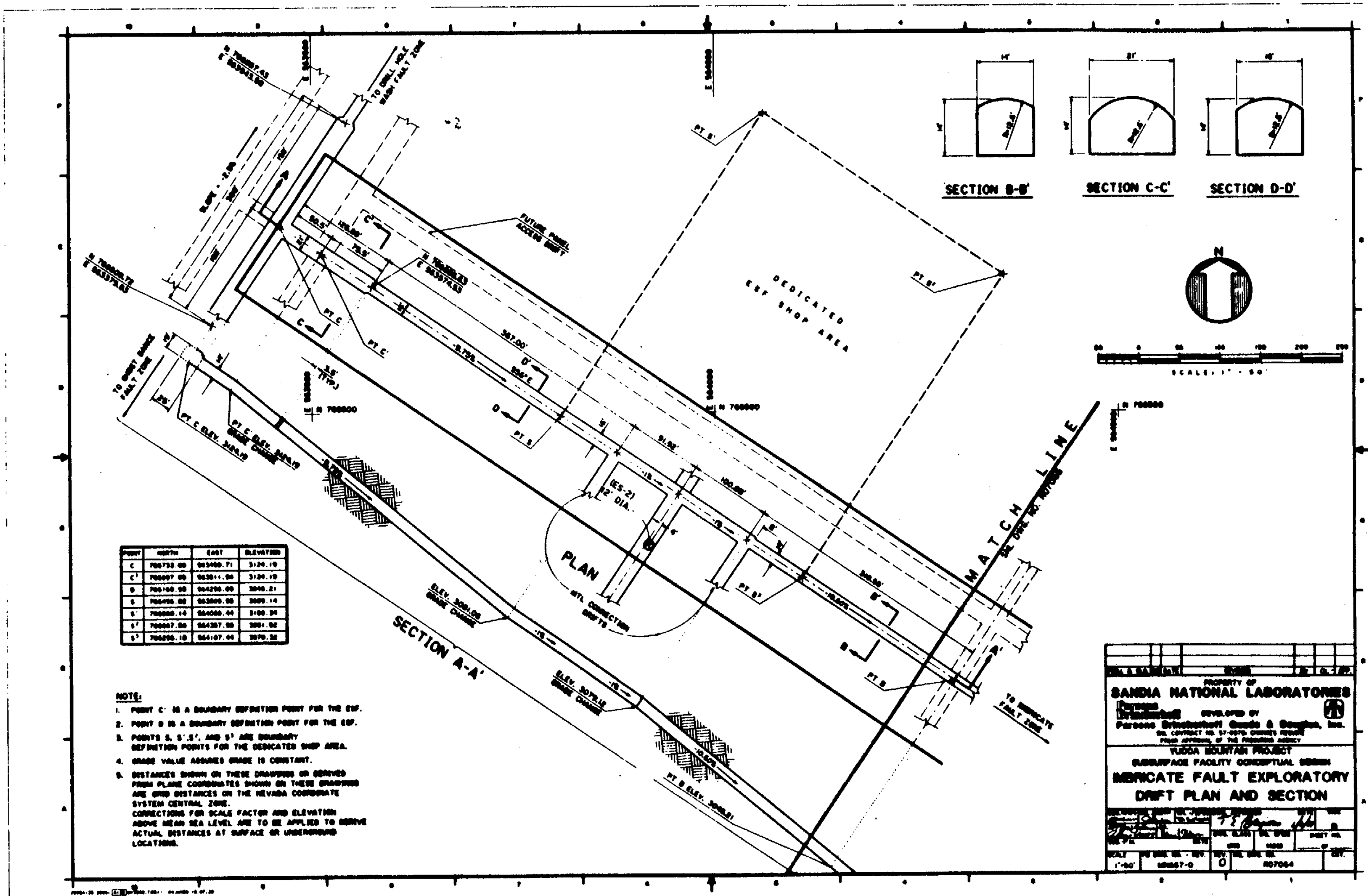
SECTION B-B'
SECTION C-C'
SECTION D-D'
N
SCALE: 1" = 50'
DEDICATED ESF SHOP AREA
FUTURE PANEL ACCESS DRIFT
TO DRILL HOLE WASH FAULT ZONE
TO GHOST DANCE FAULT ZONE
TO IMBRICATE FAULT ZONE
MATCH LINE
PT C
PT C'
PT B
PT S
PT S'
387.00'
100.00'
91.92'
ES-2 12' DIA.
PLAN
ALT. CONNECTING DRIFTS
SECTION A-A'
ELEV. 3081.06 GRADE CHANGE
ELEV. 3079.12 GRADE CHANGE
PT C' ELEV. 3124.19 GRADE CHANGE
PT C ELEV. 3124.19
PT B ELEV. 3048.21
N 765000
N 766000
POINT | NORTH | EAST | ELEVATION
C | 766733.00 | 963400.71 | 3124.19
C' | | | 3124.19
B | | | 3048.21
S | | | 3089.14
S' | | | 3100.34
S² | | | 3081.02
S³ | | | 3070.32
NOTE:
1. POINT C' IS A BOUNDARY DEFINITION POINT FOR THE ESF.
2. POINT B IS A BOUNDARY DEFINITION POINT FOR THE ESF.
3. POINTS S, S', S², AND S³ ARE BOUNDARY DEFINITION POINTS FOR THE DEDICATED SHOP AREA.
4. GRADE VALUE ASSUMES GRADE IS CONSTANT.
5. DISTANCES SHOWN ON THESE DRAWINGS OR DERIVED FROM PLANE COORDINATES SHOWN ON THESE DRAWINGS ARE GRID DISTANCES ON THE NEVADA COORDINATE SYSTEM CENTRAL ZONE.
CORRECTIONS FOR SCALE FACTOR AND ELEVATION ABOVE MEAN SEA LEVEL ARE TO BE APPLIED TO DERIVE ACTUAL DISTANCES AT SURFACE OR UNDERGROUND LOCATIONS.
PROPERTY OF
SANDIA NATIONAL LABORATORIES
DEVELOPED BY
Parsons Brinckerhoff Quade & Douglas, Inc.
YUCCA MOUNTAIN PROJECT
SUBSURFACE FACILITY CONCEPTUAL DESIGN
IMBRICATE FAULT EXPLORATORY DRIFT PLAN AND SECTION
SCALE 1"=50'
REV. 0
R07064

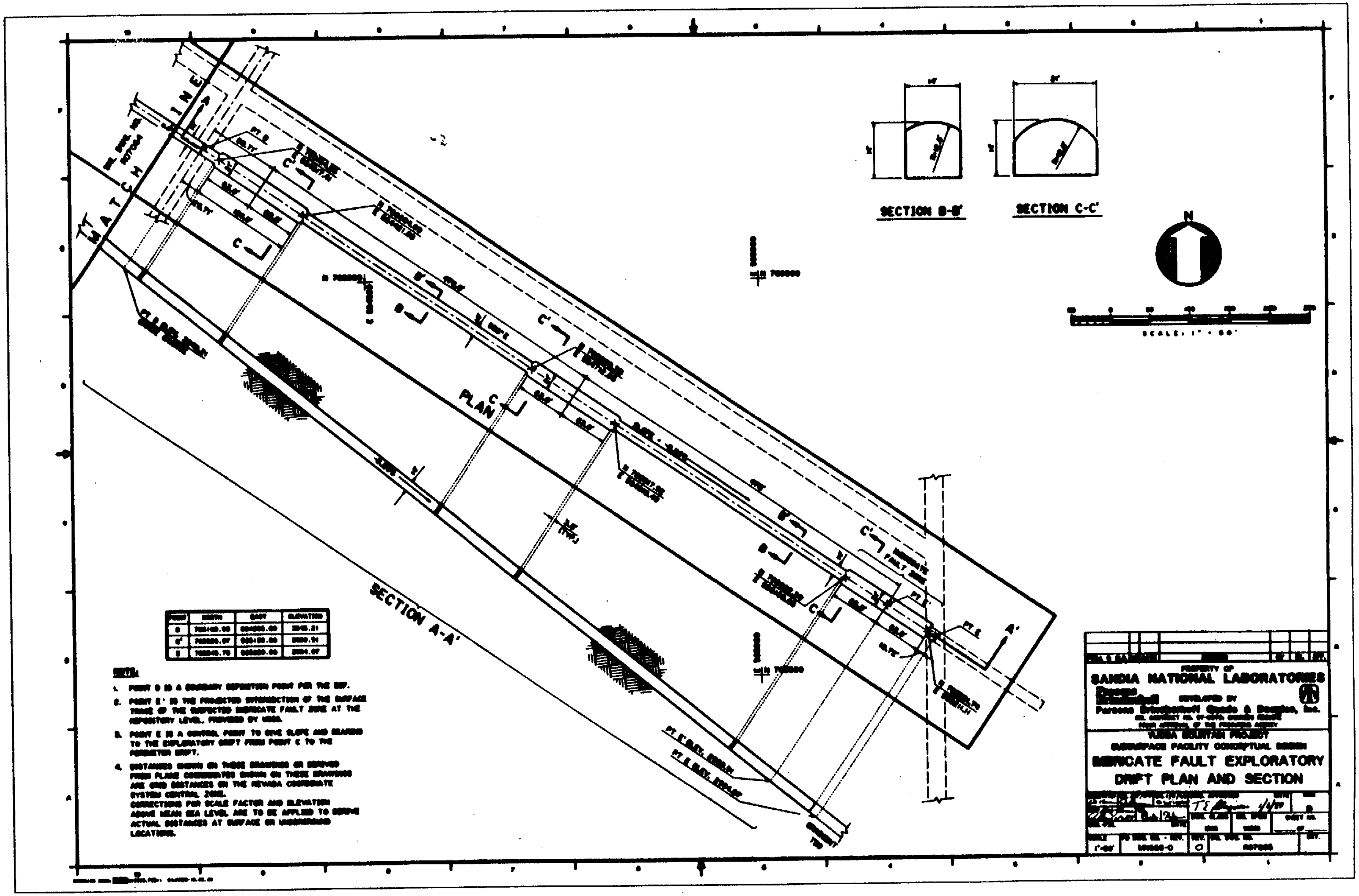

MATCH LINE
PLAN
SECTION A-A'
SECTION B-B'
SECTION C-C'
N
SANDIA NATIONAL LABORATORIES
FAULT EXPLORATORY
DRIFT PLAN AND SECTION

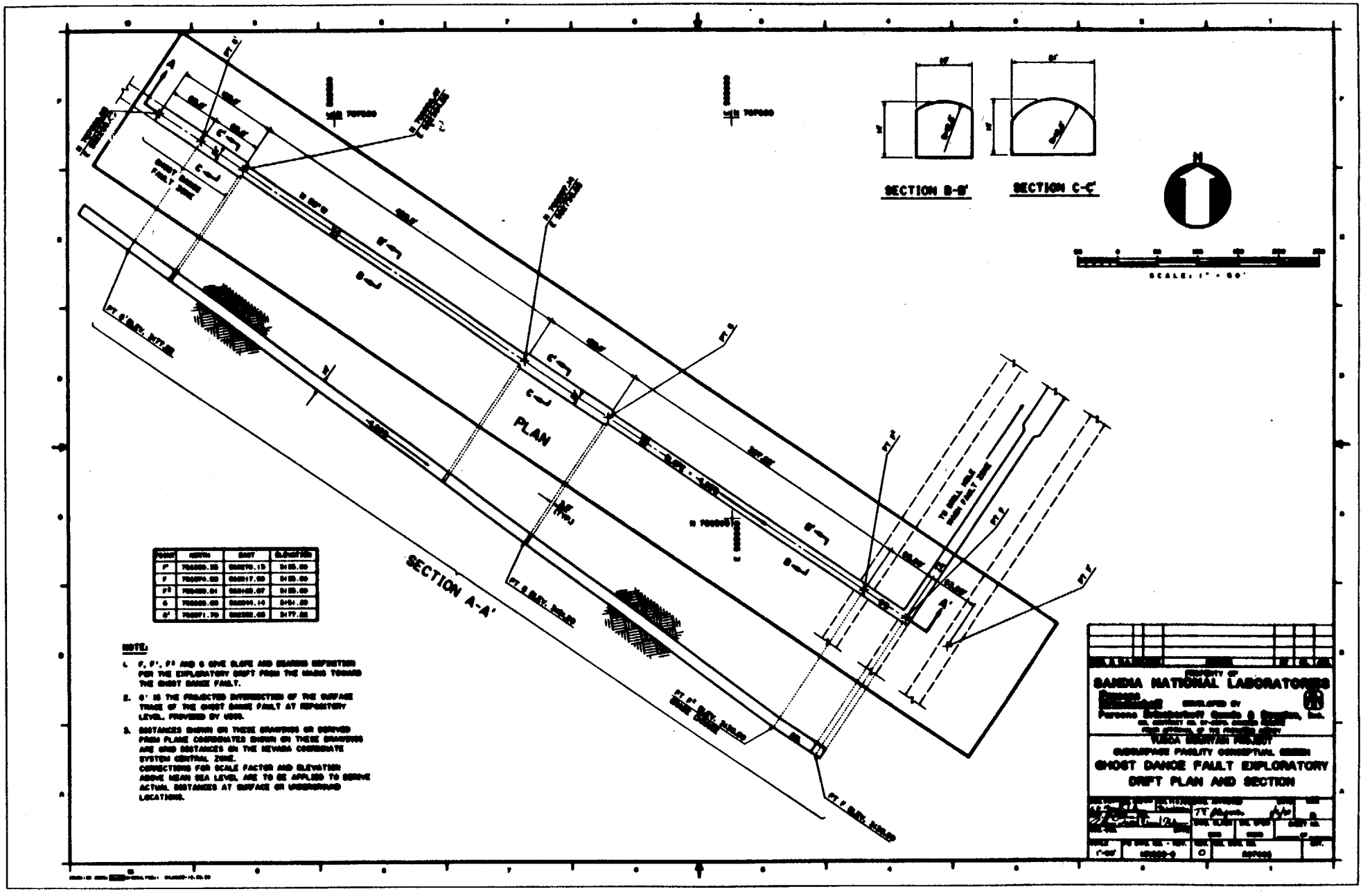
SECTION B-B'
SECTION C-C'
PLAN
SECTION A-A'
SANDIA NATIONAL LABORATORIES
GHOST DANCE FAULT EXPLORATORY
DRIFT PLAN AND SECTION

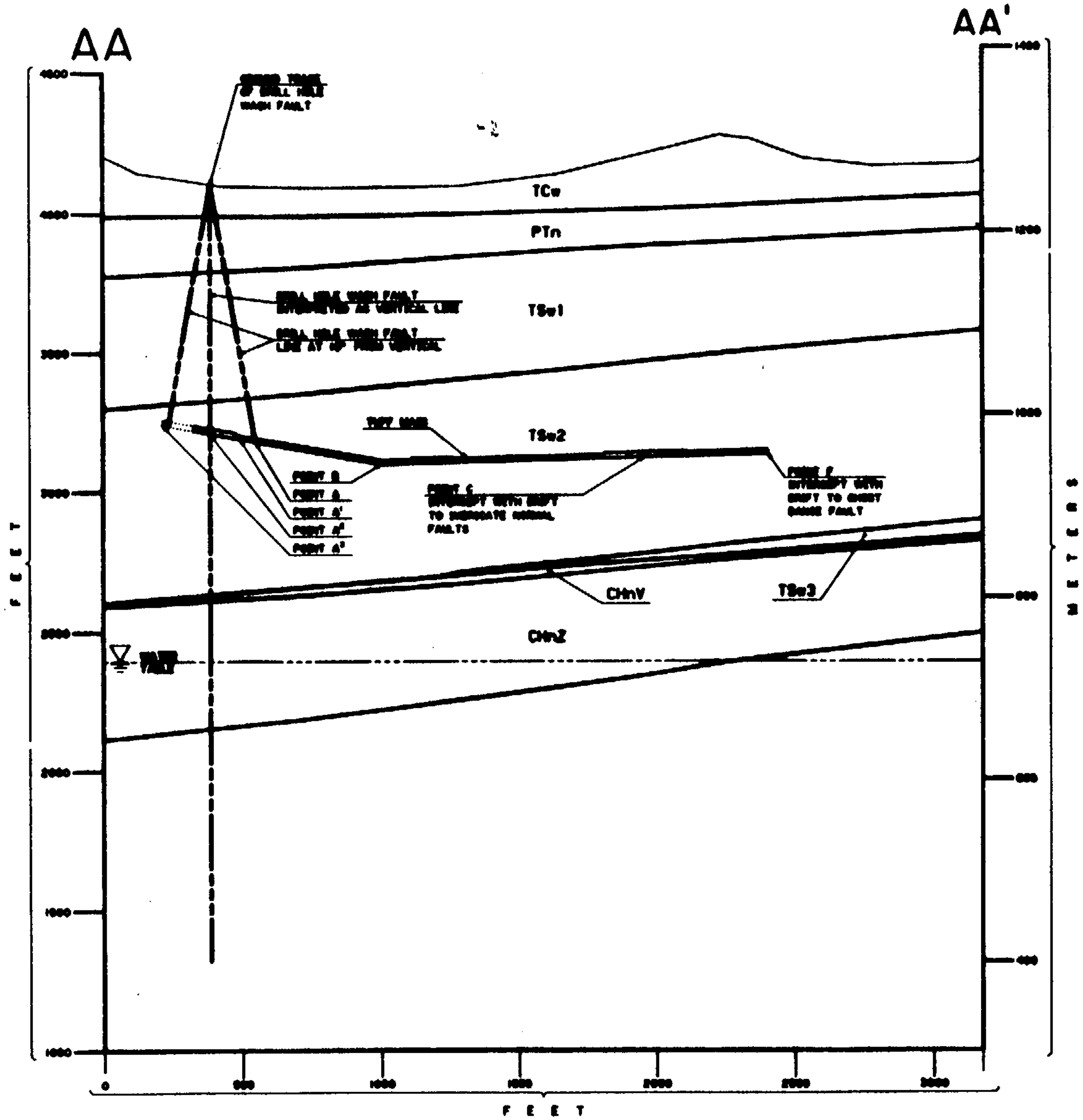

POINT	NORTH	EAST	ELEVATION
[illegible]	[illegible]	[illegible]	[illegible]
[illegible]	[illegible]	[illegible]	[illegible]
A'	[illegible]	[illegible]	[illegible]
A	[illegible]	[illegible]	[illegible]
B	[illegible]	[illegible]	[illegible]
C	[illegible]	[illegible]	[illegible]
F	[illegible]	[illegible]	[illegible]

NOTES:

1. DISTANCES SHOWN ON THESE DRAWINGS OR DERIVED FROM PLANE COORDINATES SHOWN ON THESE DRAWINGS ARE GRID DISTANCES ON THE NEVADA COORDINATE SYSTEM CENTRAL ZONE. CORRECTIONS FOR SCALE FACTOR AND ELEVATION ABOVE MEAN SEA LEVEL ARE TO BE APPLIED TO DERIVE ACTUAL DISTANCES AT SURFACE OR UNDERGROUND LOCATIONS.
2. PLAN POSITIONS OF ESF SHAFTS AND REPOSITORY MAINS ARE SHOWN ON DRAWING [illegible].
3. DRILL HOLE WASH EXPLORATORY DRIFT PLAN IS SHOWN ON DRAWINGS [illegible] AND [illegible].
4. GROUND TRACE OF DRILL HOLE WASH FAULT AND PROJECTED INTERCEPTS WITH EXPLORATORY DRIFTS AS PER LOCATIONS BY [illegible] FARMER, USGS 7/30/87.

SCALE: 1" = 200'

PROPERTY OF
SANDIA NATIONAL LABORATORIES
DEVELOPED BY
Parsons Brinckerhoff Quade & Douglas, Inc.
YUCCA MOUNTAIN PROJECT
SUBSURFACE FACILITY CONCEPTUAL DESIGN
GEOLOGIC SECTION
ON LINE AA-AA'

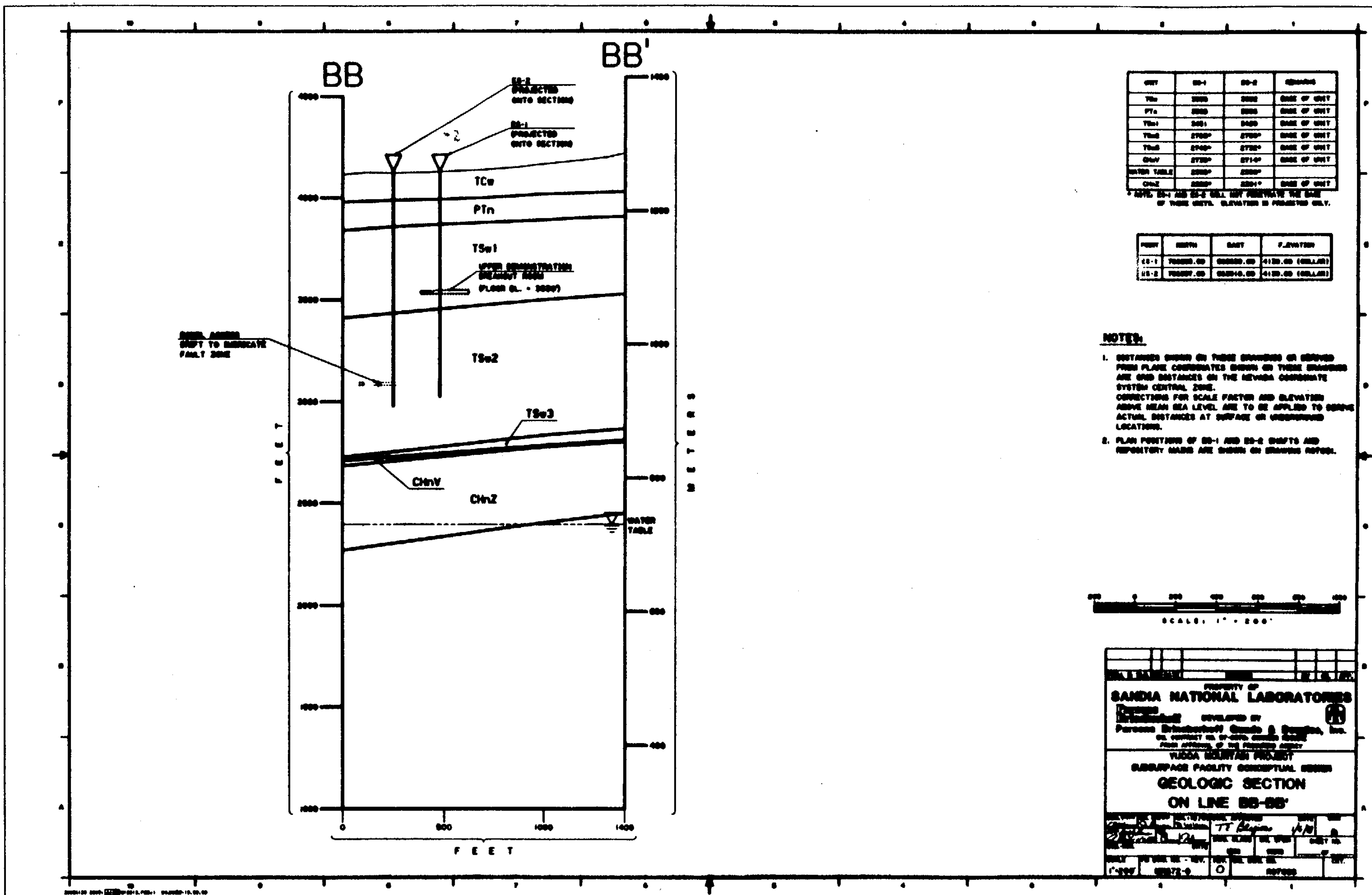

BB
BB'
ES-2 PROJECTED ONTO SECTION
ES-1 PROJECTED ONTO SECTION
TCw
PTn
TSw1
UPPER DEMONSTRATION BREAKOUT ROOM
TSw2
TSw3
CHnV
CHnZ
WATER TABLE
FEET
METERS
UNIT
ES-1
ES-2
BASE OF UNIT
WATER TABLE
EAST
ELEVATION
NOTES:
SYSTEM CENTRAL ZONE.
LOCATIONS.
SCALE: 1" = 200'
PROPERTY OF
SANDIA NATIONAL LABORATORIES
DEVELOPED BY
YUCCA MOUNTAIN PROJECT
SUBSURFACE FACILITY CONCEPTUAL DESIGN
GEOLOGIC SECTION
ON LINE BB-BB'

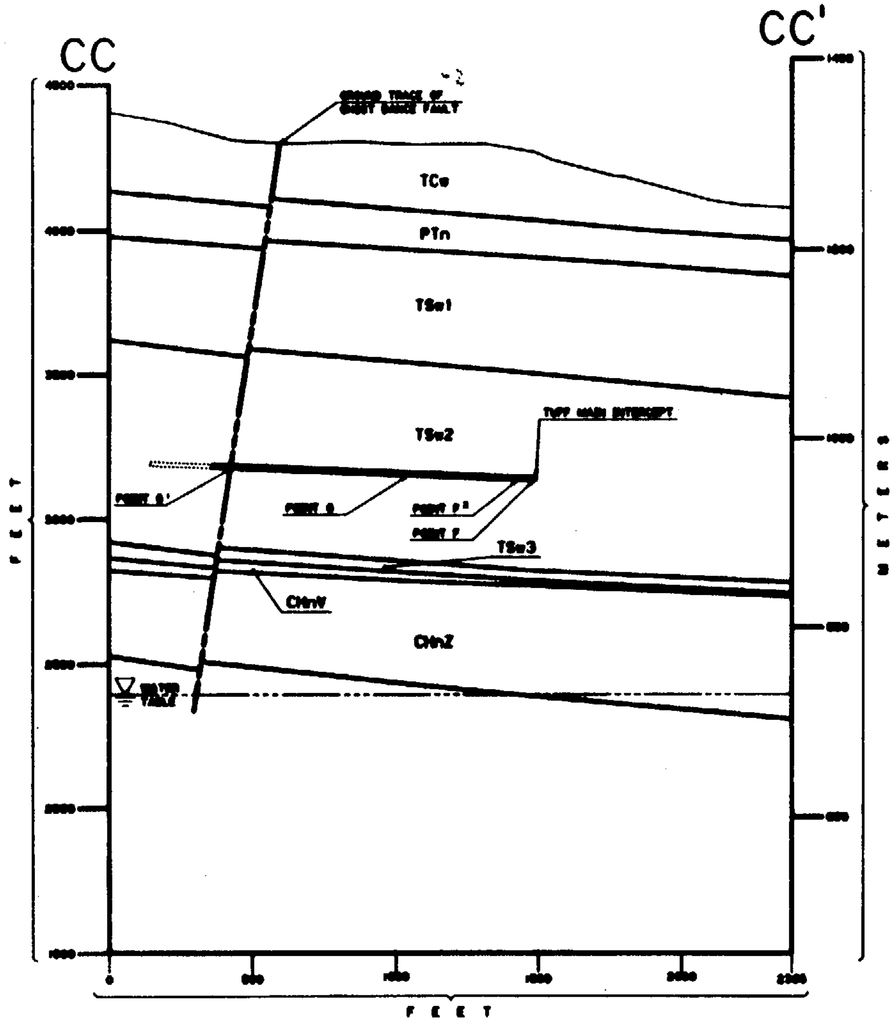

POINT	NORTH	EAST	ELEVATION
F	[illegible]	[illegible]	[illegible]
F²	[illegible]	[illegible]	[illegible]
G	[illegible]	[illegible]	[illegible]
G'	[illegible]	[illegible]	[illegible]

NOTES:

1. DISTANCES SHOWN ON THESE DRAWINGS OR DERIVED FROM PLANE COORDINATES SHOWN ON THESE DRAWINGS ARE GRID DISTANCES ON THE NEVADA COORDINATE SYSTEM CENTRAL ZONE.
   CORRECTIONS FOR SCALE FACTOR AND ELEVATION ABOVE MEAN SEA LEVEL ARE TO BE APPLIED TO DERIVE ACTUAL DISTANCES AT SURFACE OR UNDERGROUND LOCATIONS.
2. PLAN POSITIONS OF ESF SHAFTS AND REPOSITORY MAINS ARE SHOWN ON DRAWING [illegible].
3. GHOST DANCE FAULT EXPLORATORY DRIFT PLAN IS SHOWN ON DRAWING [illegible].
4. GROUND TRACE OF GHOST DANCE FAULT AND PROJECTED INTERCEPT WITH EXPLORATORY DRIFT AS PER LOCATIONS PROVIDED BY [illegible], USGS 7/30/87.

SCALE: 1" = 200'

PROPERTY OF
SANDIA NATIONAL LABORATORIES
DEVELOPED BY
Parsons Brinckerhoff Quade & Douglas, Inc.
YUCCA MOUNTAIN PROJECT
SUBSURFACE FACILITY CONCEPTUAL DESIGN
GEOLOGIC SECTION ON LINE CC-CC'

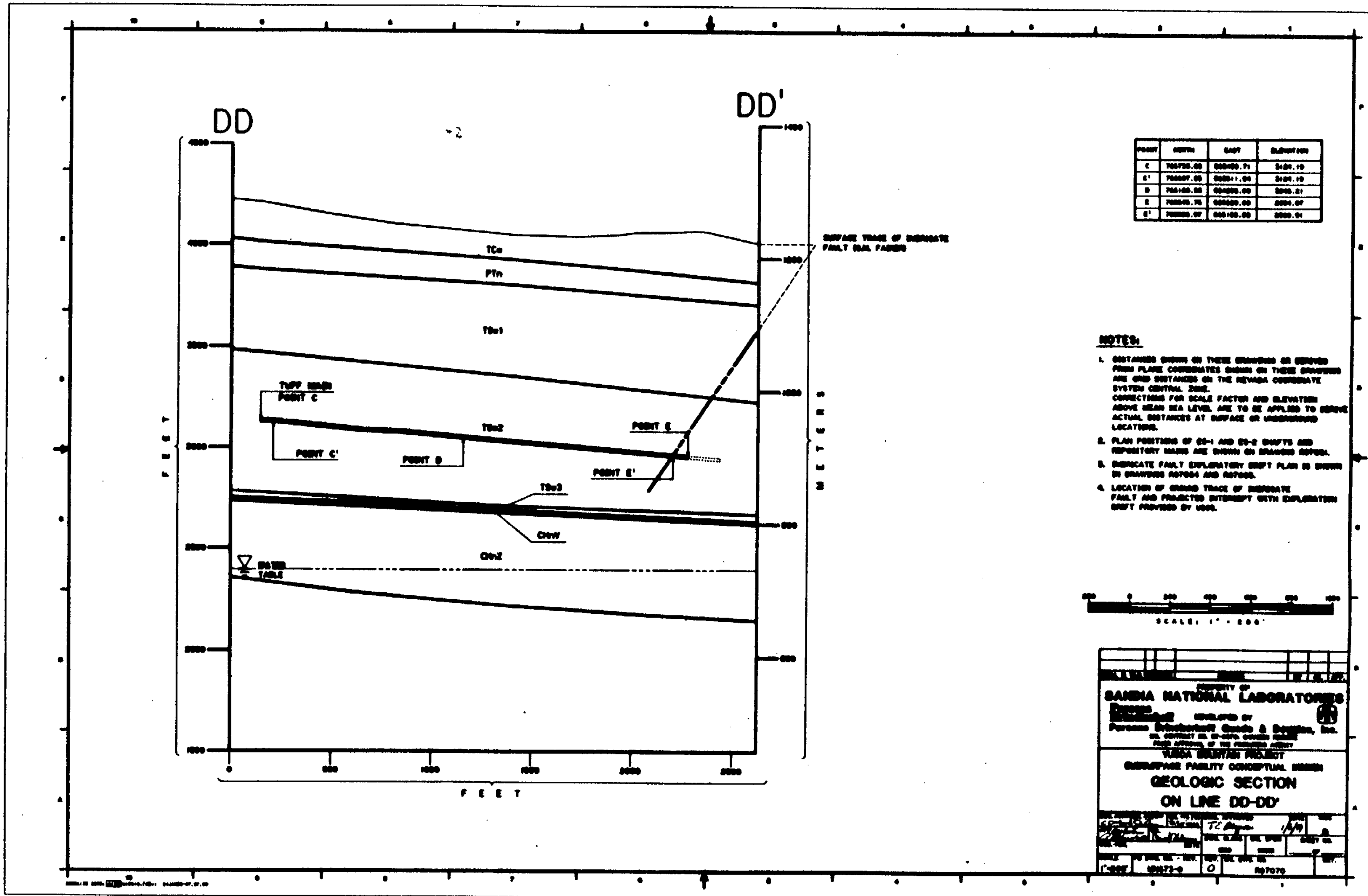
DD
DD'
TCc
PTn
TSw1
TSw2
TSw3
CHnV
CHn2
POINT C
POINT C'
POINT D
POINT E
POINT E'
WATER TABLE
FEET
METERS
NOTES:
SANDIA NATIONAL LABORATORIES
GEOLOGIC SECTION
ON LINE DD-DD'

SDRD APPENDIX A.2

ESF SEALING REQUIREMENTS IMPOSED BY REPOSITORY SEALING PLAN

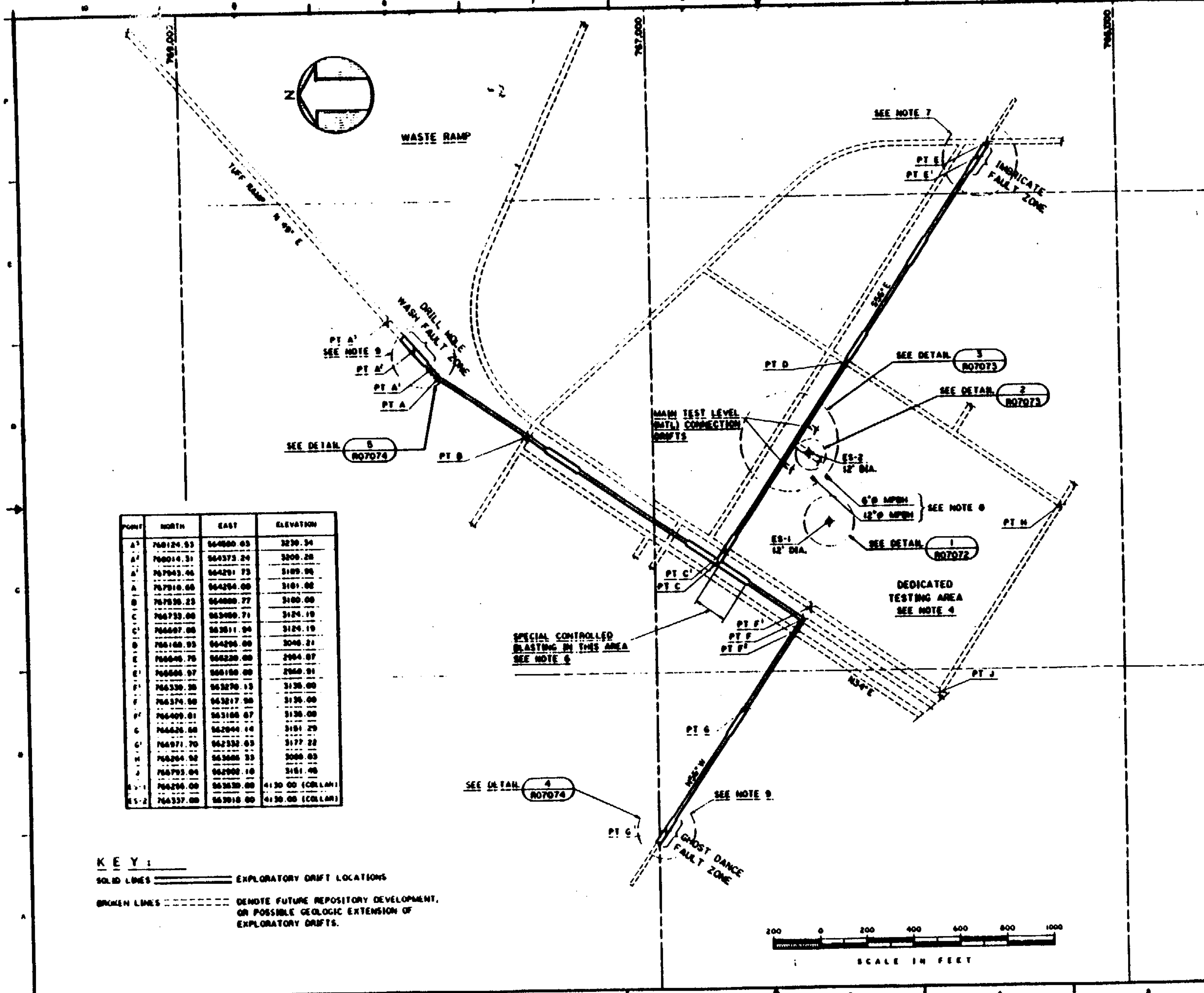

POINT	NORTH	EAST	ELEVATION
A³	768124.53	964580.03	3230.34
A²	768014.31	964373.24	3200.28
A¹	767943.46	964291.73	3189.96
A	767910.60	964254.00	3181.08
B	767838.23	964000.77	3180.00
C	766733.00	963490.71	3124.10
C'	766607.00	963611.94	3124.19
D	766160.93	964296.00	3040.21
E	766646.70	966220.00	2984.87
E'	766606.97	966150.00	2960.91
F¹	766330.30	963270.13	3135.00
F	766374.50	963217.90	3135.00
F²	766409.01	963166.67	3135.00
G	764626.60	962044.14	3181.29
G'	764971.70	962332.63	3177.22
H	768204.92	965086.33	3080.03
J	766793.04	962908.10	3151.40
ES-1	766296.00	963630.00	4130.00 (COLLAR)
ES-2	766337.00	963818.00	4130.00 (COLLAR)

KEY:

SOLID LINES ══════ EXPLORATORY DRIFT LOCATIONS

BROKEN LINES ======= DENOTE FUTURE REPOSITORY DEVELOPMENT, OR POSSIBLE GEOLOGIC EXTENSION OF EXPLORATORY DRIFTS.

NOTES:

1. THESE SEALING DESIGNS ARE CONCEPTS ONLY TO PROVIDE INFORMATION FOR ESF DESIGNERS. FINAL DESIGNS MAY DIFFER.
2. DISTANCES SHOWN ON THESE DRAWINGS OR DERIVED FROM PLANE COORDINATES SHOWN ON THESE DRAWINGS ARE GRID DISTANCES ON THE NEVADA COORDINATE SYSTEM CENTRAL ZONE. CORRECTIONS FOR SCALE FACTOR AND ELEVATION ABOVE MEAN SEA LEVEL ARE TO BE APPLIED TO DERIVE ACTUAL DISTANCES AT SURFACE OR UNDERGROUND LOCATIONS.
3. DIMENSIONS AND ELEVATIONS ARE ROUNDED TO THE NEAREST HUNDREDTH OF A FOOT.
4. DEDICATED ESF AREAS ARE SHOWN BOUNDED BY COORDINATE POINTS D, H, J, AND C'.
5. ANY BACKFILL OR CONSTRUCTION MATERIALS USED ON THE DRIFT FLOORS WITHIN THE ESF MUST BE REMOVABLE TO FACILITATE RESTORATION OF NATURAL PERMEABILITY OF THE FORMATION AT REPOSITORY CLOSURE.
6. ADDITIONAL DEGREE OF CONTROL IS TO BE USED FOR BLASTING IN THIS AREA.
7. NO ADDITIONAL CONSTRUCTION RESTRICTIONS OR FEATURES REQUIRED AT IMBRICATE FAULT ZONE.
8. 6 IN. AND 12 IN. DIA. MULTIPURPOSE BOREHOLE (MPBH) DEVELOPED FROM FENIX AND SCISSON'S PROPOSED MPBH LOCATIONS, FIGURE 10-1, 12-20-88.
9. NO GROUTING IS TO BE PERFORMED DURING OR AFTER CONSTRUCTION IN THE ENLARGED AREA OF DRIFTING THROUGH THE GHOST DANCE AND THE DRILL HOLE WASH FAULTS.

PROPERTY OF
SANDIA NATIONAL LABORATORIES
DEVELOPED BY
Parsons Brinckerhoff Quade & Douglas, Inc.

YUCCA MOUNTAIN PROJECT
SUBSURFACE FACILITY CONCEPTUAL DESIGN

ESF - REPOSITORY INTERFACE SEALING PLAN

SCALE 1"=200' | DWG. NO. R07071 | SIZE D

ES-1 SHAFT CLOSURE

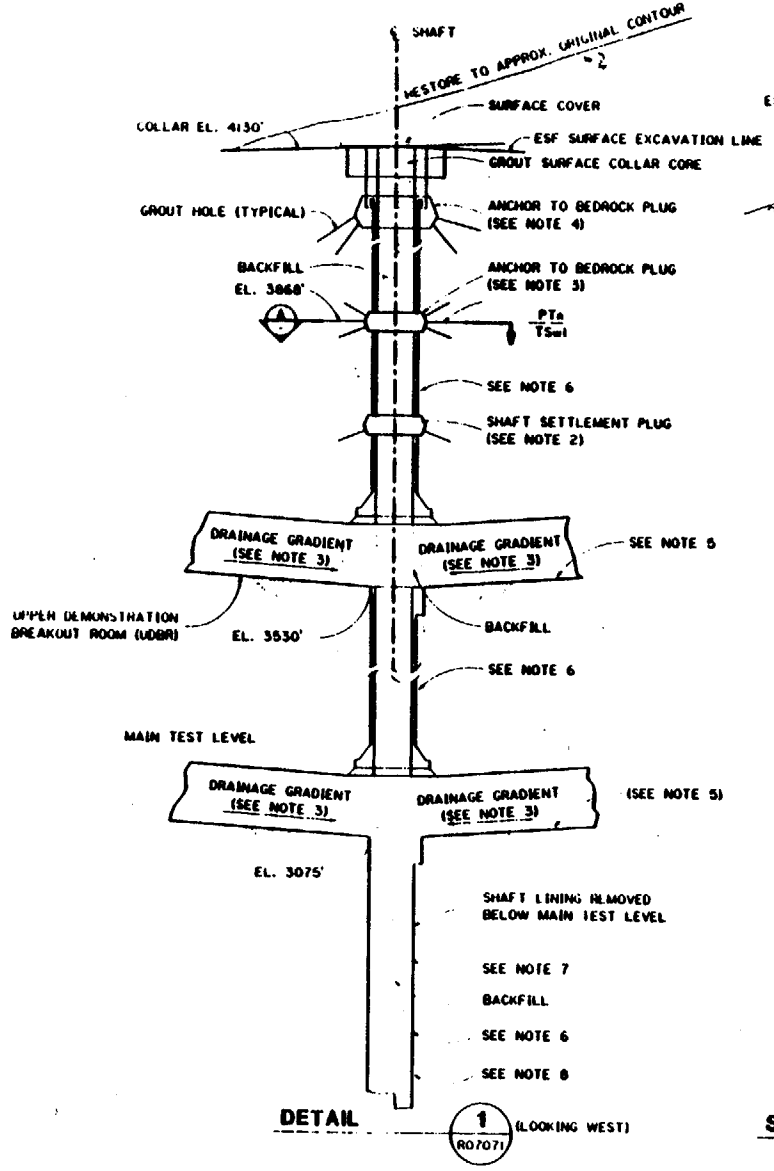

DETAIL 1 R07071 (LOOKING WEST)

TYPICAL BOREHOLE CLOSURE

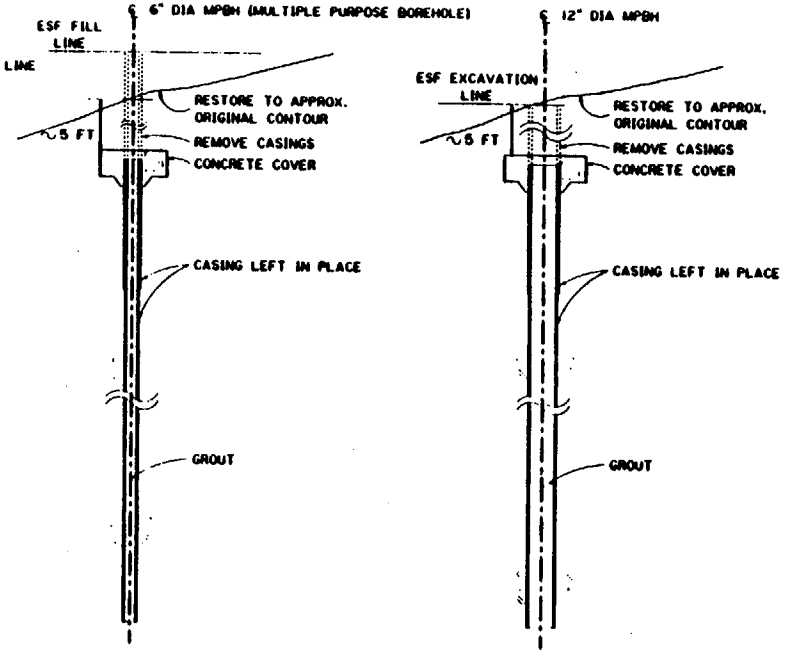

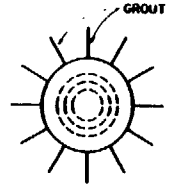

SECTION A

NOTES:

1. SEALING DESIGNS SHOWN ARE CONCEPTS ONLY TO PROVIDE INFORMATION FOR ESF DESIGNERS. FINAL DESIGNS MAY DIFFER.
2. SHAFT SETTLEMENT PLUG MAY NOT BE NECESSARY.
3. WATER WILL FLOW TO THE SHAFT AND DISSIPATE INTO ROCK AT THE BOTTOM OF THE SHAFT.
4. DO NOT PRESSURE GROUT WITHIN 50 FT OF CENTER LINE OF ANCHOR TO BEDROCK PLUGS DURING SHAFT CONSTRUCTION. LINER WILL BE REMOVED IN THESE AREAS DURING PLUG INSTALLATION.
5. ANY BACKFILL OR CONSTRUCTION MATERIALS USED ON THE DRIFT FLOORS WITHIN THE ESF MUST BE REMOVABLE TO FACILITATE RESTORATION OF THE NATURAL PERMEABILITY OF THE FORMATION AT REPOSITORY CLOSURE.
6. TO LIMIT THE EXTENT OF THE MODIFIED PERMEABILITY ZONE (MPZ), CONTROLLED BLASTING WILL BE STANDARD PRACTICE IN ALL AREAS.
7. DO NOT PRESSURE GROUT IN THE SHAFT BELOW THE MAIN ESF TEST LEVEL.
8. WATER CAPACITY OF SUMP BELOW MAIN TEST LEVEL IS TO BE EQUAL TO OR GREATER THAN 150 CUBIC METERS.

PROPERTY OF
SANDIA NATIONAL LABORATORIES
Parsons Brinckerhoff
DEVELOPED BY
Parsons Brinckerhoff Quade & Douglas, Inc.
UNDER CONTRACT NO. 87-0670 CHANGE ORDER
PRIOR APPROVAL OF THE PROCURING AGENCY

YUCCA MOUNTAIN PROJECT
SUBSURFACE FACILITY CONCEPTUAL DESIGN

ESF - REPOSITORY INTERFACE
ES-1 SHAFT AND BOREHOLE SEALING DETAILS

SCALE	PB Dwg. no. - Rev.	REV	SNL Dwg. No.	CAT.
N.T.S.	SS/MM675-0	0	R07072	

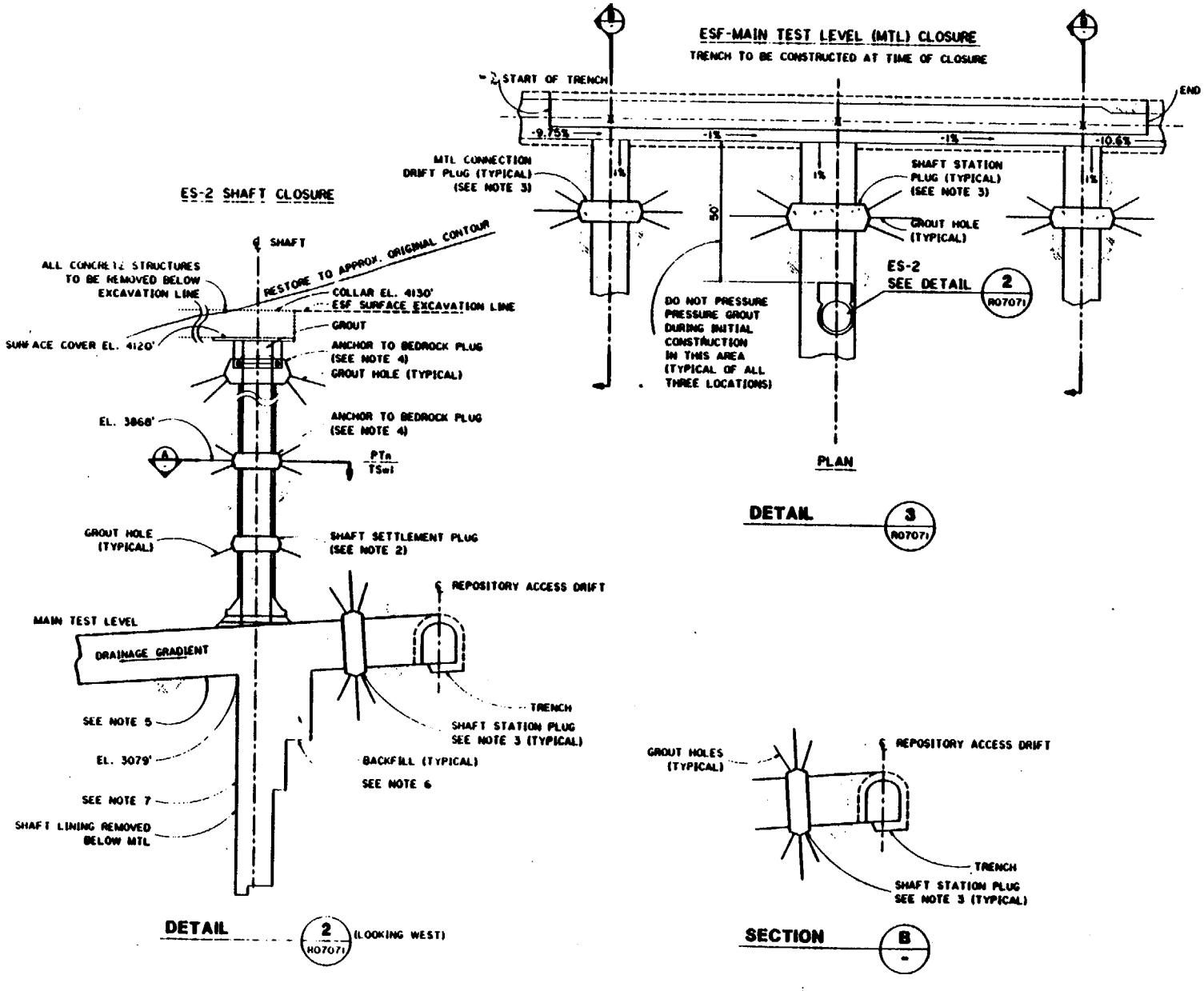

NOTES:

1. SEALING DESIGNS SHOWN ARE CONCEPTS ONLY TO PROVIDE INFORMATION FOR ESF DESIGNERS. FINAL DESIGNS MAY DIFFER.
2. SHAFT SETTLEMENT PLUG MAY NOT BE NECESSARY.
3. SHAFT STATION AND MTL CONNECTION PLUGS ARE OPTIONAL.
4. DO NOT PRESSURE GROUT WITHIN 50 FT OF CENTER LINE OF ANCHOR TO BEDROCK PLUGS DURING SHAFT CONSTRUCTION. LINER WILL BE REMOVED IN THESE AREAS DURING PLUG INSTALLATION.
5. ANY BACKFILL OR CONSTRUCTION MATERIALS USED ON THE DRIFT FLOORS WITHIN THE ESF MUST BE REMOVABLE TO FACILITATE RESTORATION OF THE NATURAL PERMEABILITY OF THE FORMATION AT REPOSITORY CLOSURE.
6. TO LIMIT THE EXTENT OF THE MODIFIED PERMEABILITY ZONE (MPZ), CONTROLLED BLASTING WILL BE STANDARD PRACTICE IN ALL AREAS.
7. DO NOT PRESSURE GROUT IN THE SHAFT BELOW THE MAIN ESF TEST LEVEL.

PROPERTY OF
SANDIA NATIONAL LABORATORIES
Parsons Brinckerhoff DEVELOPED BY
Parsons Brinckerhoff Quade & Douglas, Inc.
UNDER CONTRACT NO. 07-6076, CHANGES REQUIRE PRIOR APPROVAL OF THE PROCURING AGENCY

YUCCA MOUNTAIN PROJECT
SUBSURFACE FACILITY CONCEPTUAL DESIGN

ESF - REPOSITORY INTERFACE
ES-2 SHAFT AND STATION SEALING DETAILS

SCALE	DRAWING NO. - REV.	REV.	SEQ. DRAWING NO.	CAT.
N.T.S.	SS/MM676-D	0	R07073	

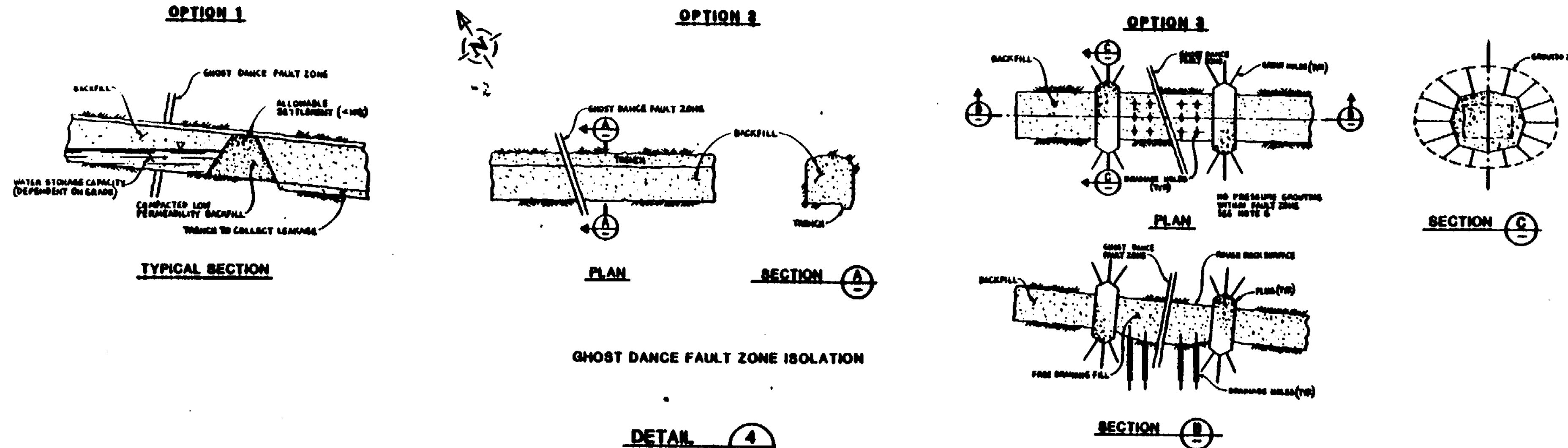

GHOST DANCE FAULT ZONE ISOLATION

DETAIL 4 (RO7071)

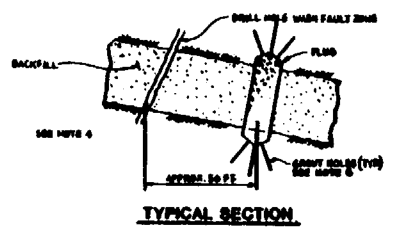

DRILL HOLE WASH FAULT ZONE ISOLATION

DETAIL 5 (RO7071)

DETAIL 5 NOTES:

1. THESE SEALING DESIGNS ARE CONCEPTS ONLY TO PROVIDE INFORMATION FOR ESF DESIGNERS. FINAL DESIGNS MAY DIFFER.
2. BEFORE THE REPOSITORY IS DEVELOPED, THE FAULT ZONE WILL BE GROUTED AND ISOLATED IF NECESSARY.
3. THIS SEALING PLUG WILL BE BUILT BELOW THE FAULT ZONE. SHOTCRETE AND OTHER CONSTRUCTION MATERIALS UP RAMP FROM PLUG FOR 100 FT WILL BE REMOVED TO ALLOW WATER TO DISSIPATE INTO THE GROUND.
4. ANY BACKFILL OR CONSTRUCTION MATERIALS USED ON THE DRIFT FLOORS WITHIN THE ESF MUST BE REMOVABLE TO FACILITATE RESTORATION OF THE NATURAL PERMEABILITY OF THE FORMATION AT REPOSITORY CLOSURE.
5. TO LIMIT THE EXTENT OF THE MODIFIED PERMEABILITY ZONE (MPZ), CONTROLLED BLASTING WILL BE STANDARD PRACTICE IN ALL AREAS.
6. DO NOT PRESSURE GROUT WITHIN 100 FT OF EXTREMITIES OF THE FAULT.

DETAIL 4 NOTES:

1. THESE SEALING DESIGNS ARE CONCEPTS ONLY TO PROVIDE INFORMATION FOR ESF DESIGNERS. FINAL DESIGNS MAY DIFFER.
2. BEFORE THE REPOSITORY IS DEVELOPED, THE FAULT ZONE WILL BE GROUTED AND ISOLATED IF NECESSARY.
3. OPTIONS SHOWN ARE TYPICAL EXAMPLES OF SEALING FEATURES THAT MAY BE USED FOR THE GHOST DANCE FAULT DURING SEALING. FINAL DESIGN MAY DIFFER FROM OPTIONS SHOWN.
4. ANY BACKFILL OR CONSTRUCTION MATERIALS USED ON THE DRIFT FLOORS WITHIN THE ESF MUST BE REMOVABLE TO FACILITATE RESTORATION OF THE NATURAL PERMEABILITY OF THE FORMATION AT REPOSITORY CLOSURE.
5. LIMIT THE EXTENT OF THE MODIFIED PERMEABILITY ZONE (MPZ). CONTROLLED BLASTING WILL BE STANDARD PRACTICE IN ALL AREAS.
6. DO NOT PRESSURE GROUT WITHIN 50 FT. OF THE EXTREMITIES OF THE FAULT.

PROPERTY OF SANDIA NATIONAL LABORATORIES

DEVELOPED BY Parsons Brinckerhoff Quade & Douglas, Inc.

SNL CONTRACT NO. 57-0070 (CHANGES REQUIRE PRIOR APPROVAL OF THE PROCURING AGENCY)

YUCCA MOUNTAIN PROJECT
SUBSURFACE FACILITY CONCEPTUAL DESIGN
ESF-REPOSITORY INTERFACE
FAULT ZONES SEALING DETAILS

SCALE	PB DWG. NO.-REV.	REV.	SNL DWG. NO.	DWG. CLASS	SNL SPEC	SIZE
N.T.S.	88/MN077	0	RO7074	UNC	14213	D

SDRD APPENDIX A.3

THERMAL DESIGN BASIS LOADS FOR THE ESF

CLRT 89-PB02

January 1989

YUCCA MOUNTAIN PROJECT

THERMAL LOADS FOR THE EXPLORATORY SHAFT FACILITY (REVISION 0)

Prepared by

PARSONS BRINCKERHOFF QUADE & DOUGLAS, INC.
San Francisco, California

Prepared for

SANDIA NATIONAL LABORATORIES, INC.
Albuquerque, New Mexico

SANDIA CONTRACT MONITOR
R.E. STINEBAUGH
GEOTECHNICAL DESIGN DIVISION

MEMORANDUM

To: R. E. Steinbaugh

From: R. F. Harig

RE: THERMAL LOADS FOR YUCCA MOUNTAIN PROJECT EXPLORATORY SHAFT DESIGN

1. GENERAL

Analytical methods for design of exploratory shaft liners and underground drifts require a knowledge of the thermal "loads" acting on these underground structures. In this memorandum, loads are defined as free-field stresses and/or strains at the shaft or drift locations. "Free-field" refers to effects that would occur in the ground at the opening location if the openings were non-existent. By defining loads in this manner, they can be specified independent of opening shape, liner thickness and properties, and slip condition at the interface of the liner and the rock.

Because the shaft and drifts are to be designed for use during the operational phase of the repository, the load induced as a result of thermal expansion of the rock as it is heated by emplaced waste is an important component of the total load. The stresses change over time as a result of heat transfer from the waste to the surrounding rock.

A computer model (STRES3D) was used to calculate temperatures and thermal loads in the vicinity of the ESF over 10,000 years. A 100 yr timeframe has been used for this memorandum to be consistent with

other ESF analyses. A complete description of the calculation is contained in Reference 2.

2. SHAFTS

Thermal loads for the shafts are fairly well-defined and can be tabulated for each shaft as a function of elevation. The six components of strain required for shaft and drift loads are shown in Table 1. Note that these are strains at 100 yrs. This time was selected because the critical stresses around a circular unlined opening have been calculated to peak using the 100 year thermal strain components, even though some of the components themselves peak before 100 years.

3. DRIFTS

Thermal loads for the drifts cannot be easily tabulated because of the complex geometry of the drifts. The designer is referred to Reference 2 for a preliminary indication of the thermal stresses in the drifts. Detailed thermal loads and thermal stresses in the various ESF drifts are best determined by computer modeling, using the current ESF layout.

Table 1. Thermal Loads for ES-1 at 100 Years

Unit	Bottom Elevation	ε_{xx}	ε_{yy}	ε_{zz}	γ_{xy}	γ_{yz}	γ_{xz}
COLLAR	4130	-5.12E-07	2.09E-05	-5.82E-06	-3.78E-05	1.26E-07	-1.06E-06
TCw	3990	-5.00E-06	1.23E-05	-6.29E-06	-2.73E-05	-1.24E-06	-1.35E-06
PTn	3868	-5.23E-06	1.23E-05	-1.45E-05	-2.52E-05	-2.97E-06	-2.74E-06
TSw1	3456	1.21E-05	4.61E-05	-7.98E-05	-4.89E-05	1.42E-05	-8.35E-06
TSw2	2783	2.06E-05	4.92E-05	-9.52E-05	-4.21E-05	2.81E-05	3.05E-07
TSw3	2745	1.88E-05	4.45E-05	-8.89E-05	-3.93E-05	2.55E-05	3.59E-06
CHn1	2735	1.83E-05	4.33E-05	-8.72E-05	-3.86E-05	2.49E-05	4.46E-06

Table 2. Thermal Loads for ES-2 at 100 Years

Unit	Bottom Elevation	ϵ_{xx}	ϵ_{yy}	ϵ_{zz}	γ_{xy}	γ_{yz}	γ_{xz}
COLLAR	4130	-4.19E-06	1.64E-05	-3.58E-06	-1.97E-05	2.48E-06	-1.79E-06
TCw	3982	-7.56E-06	1.02E-05	-3.53E-06	-1.13E-05	1.90E-05	-9.88E-06
PTn	3856	-8.00E-06	9.75E-06	-8.57E-06	-9.81E-06	3.01E-05	-1.62E-05
TSw1	3429	7.01E-06	3.93E-05	-5.89E-05	-2.14E-05	9.00E-05	-1.78E-05
TSw2	2759	2.06E-05	5.23E-05	-8.26E-05	-2.19E-05	-5.01E-05	1.94E-06
TSw3	2732	1.79E-05	4.70E-05	-7.66E-05	-2.27E-05	-5.08E-05	5.61E-06
CHn1	2714	1.62E-05	4.36E-05	-7.28E-05	-2.31E-05	-5.08E-05	8.03E-06

REFERENCES

Sandia National Laboratories, "Yucca Mountain Project Preliminary Shaft Liner Design Criteria and Methodology Guide," Approval Draft Revision D. SAND 88-7060. Prepared by Parsons Brinckerhoff Quade & Douglas, Inc., for Sandia National Laboratories, Albuquerque, NM., January 1989 Draft.

Sandia National Laboratories, "Preliminary Evaluation: Three-Dimensional Far-Field Analysis for the Exploratory Shaft Facility." SLTR PDM 75-13, Rev. 1. Report prepared by J.F.T Agapito & Associates, Inc. for Sandia National Laboratories under Contract No. 23-9590, September 16, 1988.

SDRD APPENDIX A.4

SEISMIC DESIGN BASIS LOADS FOR THE ESF

CLRT 89-PB03

January 1989

YUCCA MOUNTAIN PROJECT

SEISMIC LOADS FOR THE EXPLORATORY SHAFT FACILITY (REVISION 0)

Prepared by

PARSONS BRINCKERHOFF QUADE & DOUGLAS, INC.
San Francisco, California

Prepared for

SANDIA NATIONAL LABORATORIES, INC.
Albuquerque, New Mexico

SANDIA CONTRACT MONITOR
R.E. STINEBAUGH
GEOTECHNICAL DESIGN DIVISION

MEMORANDUM

To: R. E. Steinbaugh

From: R. F. Harig

RE: SEISMIC LOADS FOR YUCCA MOUNTAIN PROJECT EXPLORATORY SHAFT DESIGN

1. GENERAL

Analytical methods for design of exploratory shaft liners and underground drifts require a knowledge of the seismic "loads" acting on these underground structures. In this memorandum, loads are defined as a free-field strain tensor at the design location. "Free-field" refers to effects that would occur in the ground at the opening location if the openings were non-existent. By defining loads in this manner, they can be specified independent of opening shape, liner thickness and properties, and slip condition at the interface of the liner and the rock.

Seismic loads have been calculated using the inputs and methods presented in Reference 2.

2. SHAFTS

Seismic loads for exploratory shafts are shown in Table 1. Note that these loads are the same for ES-1 and ES-2. Loads were determined at each of the stratigraphic locations for which data is provided in Reference 2. All input data, equations, and methods are provided in Reference 2.

Table 1. Free-Field Seismic Loads for Shaft Design

Unit	ε_{xx}	ε_{yy}	ε_{zz}	γ_{xy}	γ_{yz}	γ_{xz}	k
TC	148	0	175	54	93	202	2.06
PT	158	0	185	58	100	214	2.36
TSw1(b)	88	0	104	32	56	120	0.734
TSw1(a)	89	0	104	33	57	120	0.752
TSw2	80	0	94	29	51	108	0.612
TSw3	54	0	63	20	34	72	0.272
CHn1v	67	0	79	24	42	91	0.421
CHn1v	86	0	102	31	54	117	0.703

100% SV COMBINATION, THETA=30 DEG, MAXIMIZES HOOP STRESS

The following constraints on use of the seismic loads in Table 1 for shaft design are important.

- The table is for earthquake loads only, based on the assertion in Reference 2 that design earthquake loads for the Yucca Mountain Project have a larger effect on the shaft design than those for underground explosions. If this is not the case, then the loads of Table 1 will not control the design.

- The angle of incidence of the seismic waves on the shaft axis is between 0 and 30° to the shaft axis (vertical).

- The separate effects of the P, S_V, and S_H waves were combined using the 100-40-40 rule described in References 1 and 2.

- All strains in Table 1 were developed using the combination involving 100% of the S_V and 40% of the P and S_H effects at an angle of incidence of 30° to the shaft axis. This

combination was found by calculation to maximize both the hoop stress and axial stress in the unlined shaft wall, using the data, methods, and assumptions of Reference 2. It was assumed that hoop and axial stresses in the concrete liner, which is bonded to the rock, are also maximized by this combination. The designer should check this assumption.

- Reference 1 requires the designer to calculate principal stresses on the inner face of the shaft liner. The designer should demonstrate that the above combination maximizes principal stresses in the liner as part of the design.

- If any changes are made to the data base or ground motions presented in Reference 2, or to the calculation methods and performance criteria presented in Reference 1, the designer must demonstrate that the above combination controls.

- If a different combination maximizes the structural effect of interest, the strains in Table 1 are not valid and must be recalculated for the new combination.

- When calculating out-of-plane shear stresses in the shaft liner using the equations presented in Reference 1, the designer may use 100% of the larger and 40% of the smaller free-field strains shown in Table 1 because they come from difference waves.

3. DRIFTS

The following points regarding seismic loads for drifts are important.

- The criteria, data, and assumptions in Reference 2 pertain primarily to shafts, but are assumed to also hold true for underground drift design.

- The combination involving 100% of the S_V and 40% of the P and S_H effects was found by calculation to maximize the tangential stresses in a horizontal, unlined, circular drift. The strains in Table 1 can be used as loads in designing such drifts.

- The designer must verify whether this combination also maximizes tangential stresses in drifts of other shapes, or of inclinations significantly inclined from horizontal.

- If other effects are of concern (e.g. principal stresses), the designer must verify the controlling combination.

- If any changes are made in the data base or ground motions in Reference 2, the strains in Table 1 are no longer valid for drift design.

REFERENCES

Sandia National Laboratories, "Yucca Mountain Project Preliminary Shaft Liner Design Criteria and Methodology Guide," Approval Draft Revision D. SAND 88-7060. Prepared by Parsons Brinckerhoff Quade & Douglas, Inc. for Sandia National Laboratories, Albuquerque, NM., January 1989 Draft.

Sandia National Laboratories, "Yucca Mountain Project Working Group Report Exploratory Shaft Seismic Design Basis," SAND 88-1203, compiled by C.V. Subramanian, Sandia National Laboratories, Albuquerque, NM., April 1988 Draft.

SDRD APPENDIX A.5

ESF SHAFT DESIGN METHODOLOGY

SAND 88-7060

January 1989

YUCCA MOUNTAIN PROJECT

PRELIMINARY SHAFT LINER DESIGN CRITERIA AND METHODOLOGY GUIDE (APPROVAL DRAFT: REVISION 0)

Prepared by

PARSONS BRINCKERHOFF QUADE & DOUGLAS, INC.
San Francisco, California

Prepared for

SANDIA NATIONAL LABORATORIES, INC.
Albuquerque, New Mexico

SANDIA CONTRACT MONITOR
R.E. STINEBAUGH
GEOTECHNICAL DESIGN DIVISION

ABSTRACT

The Shaft Liner Design Criteria and Methodology Guide outlines a methodology for designing concrete shaft liners for the YMP repository in tuff, the use of which will ensure that all shafts meet the requirements for repository service. These requirements are identified in the guide, then unlined shaft behavior is examined to establish rock behavior modes and to investigate the development of convergence during construction. Ground pressure, induced thermal, and seismic loads imposed on the shaft liner are evaluated. The modes of deformation resulting from loading, which include bending, shear, hoop deformation, and axial strain, are analyzed following a working stress approach that uses closed-form interaction models. Predicted liner stresses are then evaluated using allowable stress criteria. The methodology is illustrated with examples appropriate to the repository site at Yucca Mountain.

YUCCA MOUNTAIN PROJECT

PRELIMINARY SHAFT LINER DESIGN CRITERIA AND METHODOLOGY GUIDE

The following consultants have participated in preparing various sections of this report, and concur with the proposed approach.

Archie M. Richardson
Parsons Brinckerhoff Quade & Douglas, Inc.
12/22/88
Date

Birger Schmidt
Parsons Brinckerhoff Quade & Douglas, Inc.
12/27/88
Date

Michael P. Hardy
J.F.T. Agapito & Associates, Inc.
Date

Christopher St. John
J.F.T. Agapito & Associates, Inc.
Date

Robert P. Kennedy
RPK Structural Mechanics Consulting
12/23/88
Date

Tor L. Brekke
Tor L. Brekke, Inc.
12/24/88
Date

ACKNOWLEDGEMENTS

This report was prepared by Archie M. Richardson of Parsons Brinckerhoff Quade & Douglas, Inc. (PBQ&D), under contract to Sandia National Laboratories (SNL). Considerable input to this effort was provided by a number of individuals from the various organizations comprising the Yucca Mountain Project. Christopher St. John of J.F.T. Agapito & Associates, Inc. was instrumental in development of the equations and methodology for calculating stresses in the liner, and he provided much written input to various sections of the report, especially Chapter 5. He also prepared the material on thermal analysis and the finite element modeling, which appear in the appendices. Michael Hardy, also with Agapito & Assoc., contributed significantly to the development of the performance criteria in Chapter 6. The seismic design methodology was strongly influenced by previous work done for the Salt Repository Program (Fluor/PB-K88, 1987), and the members of the Exploratory Shaft Seismic Design Basis Working Group (SNL, SAND 88-1203, in preparation). Robert Kennedy of RPK Structural Mechanics Consulting provided crucial input during development of the seismic methodology.

A formal technical review was provided by:

Brian Ehgartner	Sandia National Laboratories
Barbara Luke	Sandia National Laboratories

A number of individuals reviewed various drafts of the report and provided informal comments and editorial assistance, including

Bob Stinebaugh	Sandia National Laboratories
Arthur Mansure	Sandia National Laboratories
Tor Brekke	Tor L. Brekke, Inc.
Michael Hardy	J.F.T. Agapito & Associates, Inc.

ACKNOWLEDGEMENTS (concluded)

Christopher St. John	J.F.T. Agapito & Associates, Inc.
Robert Kennedy	Structural Mechanics Consulting
Richard Harig	PBQ&D
Birger Schmidt	PBQ&D
James Monsees	PBQ&D
Matthew Fowler	PBQ&D
Brenda Bohlke	PBQ&D
Jim Owens	Department of Energy, Nevada Operations
Richard Mudd	Fenix and Scisson
Dan Koss	Reynolds Electric Company
Kenneth MacDonald	Science Applications, Inc.
Hobart MacPherson	Harza
Joe Pedalino	Holmes & Narver, Inc.

Other individuals who provided valuable suggestions and other input include:

C. V. Subramanian	Sandia National Laboratories
Thomas Blejwas	Sandia National Laboratories
John Abel	Golden, Colorado
Margaret Asgian	Agapito Associates
K. Arulmoli	Agapito Associates
John Selters	PBQ&D
Ivo Lange	PBQ&D
Mahmoud Mirza	PB/KBB
Prabir Das	PBQ&D
Norman Owen	URS/John A. Blume & Associates
Jay Merrit	The BDM Corporation
Edward Cording	Savoy, Illinois

EXECUTIVE SUMMARY

The Yucca Mountain Project is responsible for the investigation of Yucca Mountain, Nevada, as a prospective site for an underground nuclear waste repository in volcanic tuff rocks. In the current conceptual design, several concrete lined shafts provide access to the proposed underground repository. These shafts will be excavated through a sequence of welded and unwelded Tertiary ash-flow tuffs of variable quality. The primary purposes of the shaft liners are to provide structural support to these strata and to completely secure the shafts against rock fall hazards to personnel. Important secondary purposes of the liners include (1) providing a regular, finished cross section and stable anchorage for ease of installation and alignment of shaft equipment, (2) providing a low friction surface to increase efficiency of ventilation, and (3) protecting the wall rock against weathering.

This Shaft Liner Design Criteria and Methodology Guide (the shaft design guide) outlines a design method for YMP concrete shaft liners to ensure that they meet the requirements for repository service. These requirements are stated in 10 CFR Part 60, the Generic Requirements Document for Mined Geologic Disposal System, and elsewhere. The shaft design guide establishes a framework for design of shaft liners for the YMP and presents a "working stress" approach, which emphasizes closed-form models based on linear elasticity and uses allowable stress criteria. The methodology and criteria presented are conservative for this type of inherently stable structure. This approach does not preclude the application of other methods such as nonlinear numerical analysis with strain criteria. The guide is not intended to restrict a qualified designer's ability to exercise his engineering judgment. Also, more complex analyses may be appropriate for confirming the performance of the final design for repository licensing, as more complete data become available and our understanding of rock behavior improves.

The methodology proposed involves the following steps.

- Define regulatory, functional, design, and performance criteria.

- Analyze unlined shaft behavior to determine rock behavior modes and to investigate the development of convergence during construction.

- Define ground pressure and induced thermal and seismic loads acting on the shaft liner. The designer will either calculate these loads using methods discussed in the design guide and approved design input, or will use loads provided in an approved project data base. Loads are specified as free-field (those that would exist in the ground at the shaft location if the shaft opening did not exist).

- Determine important liner deformation modes, including hoop deformation, axial strain, axial bending, and direct shear.

- Perform a mechanical analysis of the shaft liner. A working stress approach based on elastic closed-form models is suggested because (1) it permits a simplified analysis of ground/liner interaction under generalized plane strain conditions with nonuniform applied loads, (2) the linear models for liner behavior will result in a safe and conservative design when used with the allowable stress criteria proposed in the guide, and (3) the example problems suggest that standard allowable stress criteria can be met readily without unusual design features.

- Establish potential liner failure modes and develop performance criteria. Criteria in this guide protect against compressive crushing and spalling, and tensile cracking.

- Evaluate liner performance and develop alternate designs if unsatisfactory performance is predicted.

Example problems are used to illustrate the salient features of the methodology. Although the framework of this methodology is general, specific analyses proposed in the shaft design guide have been developed that consider the expected underground environment in which the liners will function, and the methodology is, therefore, site specific. Design input appropriate to the exploratory shafts at Yucca Mountain is used in the examples. The methodology is appropriate for design in noncreeping rocks located in a reasonably dry environment with little or no initial rock overstress.

It is not the intent of this guide to provide final recommendations for exploratory shaft design. The example problems suggest that a 1-ft-thick plain (unreinforced) concrete liner (5,000-psi 28-day strength) installed in the exploratory shafts has sufficient compressive strength to sustain all load combinations studied for the preclosure life of the repository, even with the conservative methods and allowables used. Some minor tensile cracking may occur with thermal and seismic loading, which is not considered structurally significant but which requires consideration in the design, and measures such as embedded wire mesh or fiber reinforcing may be required. However, because the example problems are based on preliminary data and do not exhaustively consider all possible load combinations, a complete analysis based on Project-approved data is necessary before any recommendations can be made.

CONTENTS

CONTENTS (concluded)

FIGURES

FIGURES
(continued)

FIGURES
(concluded)

TABLES

TABLES
(concluded)

NOTATION

STRESSES AND STRAINS

σ_a	Axial stress due to uniform axial strain
σ_b	Axial stress induced by axial bending
$\sigma_x, \sigma_y, \sigma_z$	Normal stresses in Cartesian coordinates (see Figure 5-2)
τ_x, τ_y, τ_z	Shear stresses in Cartesian coordinates (see Figure 5-2)
σ_v	Vertical in situ stress
σ_H	Maximum value, horizontal in situ stress
σ_h	Minimum value, horizontal in situ stress and uniform value, horizontal in situ stress
σ_t	Tangential or circumferential stress
σ_1	Maximum principal stress (or maximum in-plane stress in plane strain analysis)
σ_2	Intermediate principal stress
σ_3	Minimum principal stress (or minimum in-plane stress in plane strain analysis)
$\epsilon_x, \epsilon_y, \epsilon_z$	Normal strains in Cartesian coordinates
$\gamma_{xy}, \gamma_{xz}, \gamma_{yz}$	Shear strains in Cartesian coordinates
ϵ_b	Bending strain
p	Internal pressure
p_{lim}	Internal pressure required to prevent formation of inelastic zone
P	Mean stress = $(\sigma_1 + \sigma_3)/2$
S	Stress deviator = $(\sigma_1 - \sigma_3)/2$
S^{ℓ}	Limiting value of stress deviator = $P \sin(\phi) + c \cdot \cos(\phi)$
m	Obliquity = S/S^{ℓ}
K_H	Maximum horizontal stress coefficient = σ_H/σ_v
K_h	Minimum horizontal stress coefficient = σ_h/σ_v

NOTATION
(continued)

K_o	Uniform horizontal stress coefficient = σ_h/σ_v
k	Curvature

PROPERTIES AND PARAMETERS

E	Modulus of elasticity of rock
E'	Modulus of elasticity of concrete
G	Shear modulus of rock = $E/2(1+\upsilon)$
G'	Shear modulus of concrete
υ	Poisson's ratio of rock
υ'	Poisson's ratio of concrete
K_p	Passive pressure coefficient = $(1+\sin\phi)/(1-\sin\phi)$
K_p^*	Dilation coefficient = $(1+\sin\phi^*)/(1-\sin\phi^*)$
q	Unconfined compressive strength of rock
f'_c	Unconfined compressive strength of concrete
P(t)	Instantaneous thermal power as a function of time in years since emplacement
ϕ	Angle of internal friction
ϕ^*	Dilation angle
c	Cohesion = $q\ (1-\sin\phi)/(2\cos\phi)$
α	Coefficient of thermal expansion, or the angle between σ_1 and σ_x directions (depending on context)
K_s	Support stiffness

DIMENSIONS, COORDINATES, DISPLACEMENTS

a	Internal radius of liner
b	Maximum extent of inelastic zone
R	Unlined radius of hole

NOTATION
(continued)

R_p	Radius of inelastic zone
m	a/r
M	r/a (or 1/m)
T	R/a
s	Distance from neutral axis (plane) of beam
x,y	Cartesian coordinates, in-plane of shaft cross section
z	Axial coordinate, out-of-plane of shaft cross section
r,θ	Polar coordinates in plane of cross section when reference direction is x axis
r,t	Polar coordinates in plane of cross section when reference direction is major principal stress direction
u,v	Horizontal displacements in (x,y) directions
u,v	Cylindrical components of displacement
w	Axial component of displacement
U_o	Normalized radial displacement of the shaft wall
θ	Counterclockwise angle from maximum horizontal stress direction

SUPERSCRIPTS AND SUBSCRIPTS

/	Expression applies to liner
^	Expression applies to free field (rock)
~	Effective elastic properties used for plane strain
r	Rock
c	Concrete
lim	Limiting
t	Tangential
p	Plastic (or inelastic)
x	Rectangular coordinate direction

NOTATION
(concluded)

y	Rectangular coordinate direction
z	Rectangular coordinate direction
r	Polar coordinate direction
a	Allowable

Note: Double subscripts on a stress or strain term refer to the plane on which the quantity acts, and the direction in which it acts. For example, τ_{xz} means the shear stress on a plane normal to the x-axis in the z-direction.

SEISMIC NOTATION

P	Compressional
S	Shear
S_V	Vertical component of shear
S_H	Horizontal component of shear
θ	Angle of incidence
C	Seismic velocity
F	Frequency
λ	Wavelength

ACRONYMS

ACI	American Concrete Institute
CH	Calico Hills
ES-1	Exploratory Shaft no. 1
ES-2	Exploratory Shaft no. 2
ESF	Exploratory Shaft Facility
GR	Generic Requirements document
NRC	Nuclear Regulatory Commission
PT	Upper Paintbrush Tuff, nonwelded
RIB	Reference Information Base
SCP-CDR	Site Characterization Plan Conceptual Design Report
TC	Tiva Canyon Member
TS	Topopah Spring (repository horizon)
UNE	Underground Nuclear Event
YMP	Yucca Mountain Project

1.0 INTRODUCTION

1.1 PURPOSE AND SCOPE

This shaft design guide outlines a recommended methodology for designing shaft liners at the proposed repository at Yucca Mountain, Nevada. The methodology is limited to the design of shaft liners. The term "liner" applies to the structure below the collar only. The shaft collar is part of the headframe foundation and will be designed separately according to surface design codes and the needs of the shaft sinking contractor. The collar is not discussed in this document, nor is the design of hoisting systems, conveyances, or other shaft equipment.

Two exploratory shafts (ES-1 and ES-2), a men-and-materials shaft, and an emplacement area exhaust shaft are part of the current conceptual design of the facility (SNL, 1987). According to this design, all four shafts eventually will be used for ventilation of the repository. In addition, the two exploratory shafts initially will be used for exploration activities during the site characterization phase, and the men-and-materials shaft will provide access for personnel, equipment, and supplies to the underground repository during development and subsequent phases. Figure 1-1, a plan view of the northern part of the repository in the vicinity of the exploratory shaft facility (ESF), shows the location of the four shafts.

This document outlines a method for designing repository shaft liners to ensure that they meet the requirements for repository service during the preclosure period. Because a credible accident scenario has not yet been identified that would result in a release of radionuclides to the biosphere, either directly or indirectly, through failure of any shaft liner, the primary concern in this methodology is for worker safety. Design input and safety factors have been selected on this basis. All shaft liners will be designed to the same standards as set forth in this guide.

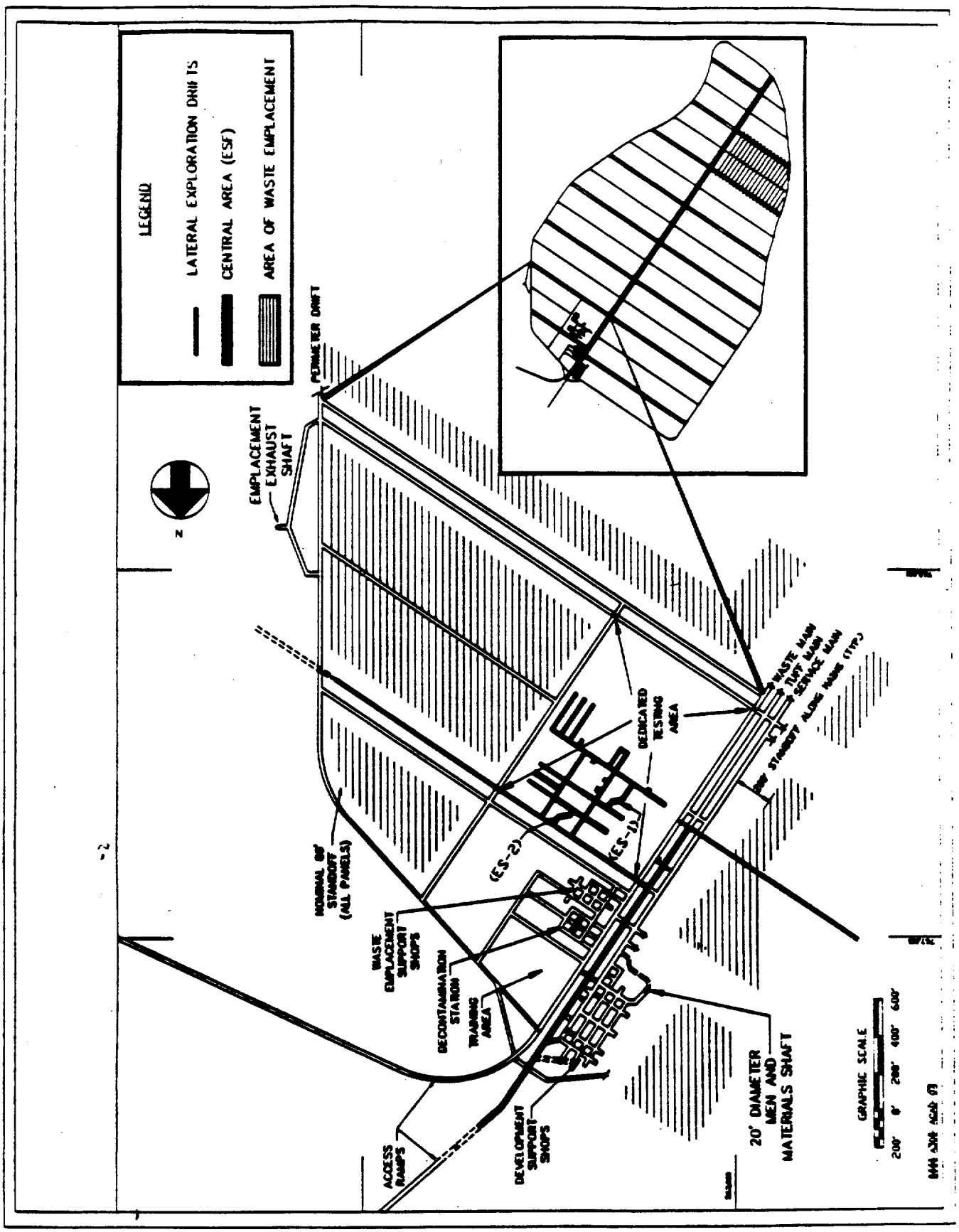

Figure 1-1. Plan View of the Northern Part of the Repository

Current project design concepts specify cast-in-place concrete liners for each of these shafts. A simple concrete liner has a good mix of attractive features, including

- effective structural support of the ground,
- complete security against minor rockfall hazards (especially important during sinking),
- protection of the wall rock against weathering,
- ready installation as part of industry-standard shaft-sinking cycles,
- a regular finished cross section and stable anchorage for optimal installation and alignment of shaft equipment, and
- a low-friction surface for efficient ventilation throughout the life of the repository.

Other options for ground support exist, from a bare shaft (unsupported) or rockbolts and mesh (light support) to steel and reinforced concrete liners (heavy support). However, unsupported or bolts-only support options would present potential safety hazards from rockfall (SNL, 1987). Because the shafts will be excavated from the surface through stratigraphic units of variable quality (based on core logs), this consideration is important in shafts, where any falling object has the potential to achieve high velocity and even small falling rocks pose a considerable hazard to personnel. Bolts, shotcrete, and mesh are frequently used as tunnel and drift supports; however, anchoring, installing, and aligning shaft equipment is difficult without a concrete liner. Watertight liner options can be discarded because the potential for significant water inflow is considered minor at the Yucca Mountain site. Moderate amounts of water can be handled by water rings

and pumping. These considerations, along with the fact that cast-in-place concrete is the industry standard for lining circular shafts in North America and is very familiar to contractors, support the Project position favoring concrete liners.

Despite the wide acceptance of concrete shaft liners, there is no universally accepted method for liner design. This guide establishes a framework for analyzing shaft liners for the Yucca Mountain Project (YMP). The guide includes a collection of relatively simple mechanical models for calculating loads on the liner, determining critical stresses in the liner resulting from these loads, and comparing the strength of the concrete against these stresses. Closed-form solutions are preferred in this methodology because they are more readily followed by reviewers, can be more easily verified, and make sensitivity analysis easier. More elaborate methods may give a more accurate answer if they can be validated and if their input requirements can be met. This methodology is still valid if more elaborate methods are substituted for the simple models proposed in this guide.

The design methodology proposed in this guide is site-specific and was developed considering the expected underground environment in which the liners will function. Thus, the methodology is applicable only to design in noncreeping rocks located in a reasonably dry environment with little or no initial rock overstress.

The models proposed in this preliminary design methodology for calculating liner stresses are analytical stress-strength models in which both the rock mass and the liner are first idealized as elastic engineering media. Inelastic zones are assumed to be stabilized with suitable initial support prior to lining. Equivalent properties are assigned to the rock mass to compensate for the softening effect of the discontinuities, which are not treated explicitly. Elastic-plastic idealizations have only been used to demonstrate that the elastic idealization is reasonable. Stresses generated in the rock mass from

ground pressure and seismic and thermal loading are calculated separately and applied in combination to a simple model of the liner as a thick walled cylinder embedded in an elastic matrix. Critical stresses in the liner resulting from this loading can be calculated and compared with allowable stresses for concrete.

The analytical approach using equivalent continuum models was selected over several excellent alternate methodologies such as empirical methods (the use of rock mass classifications by Bieniawski, 1973) and block methods (e.g., Goodman and Shi, 1985) for the following reasons:

- This approach can readily account for thermal and seismic loading in addition to ground pressure, whereas block and empirical methods currently are used only for evaluating the ground pressure component and must be combined with analytical methods to consider the total load environment.

- This approach is traditional for shaft liners and well established in the literature. Empirical methods are fairly well established for reinforcement of tunnels and drifts, but have not been developed for concrete lined shafts.

- This approach is appropriate for analysis at an early stage when little specific information on joint orientations, spacing, and behavior is available (at this time there is no borehole at the exploratory shaft location). These parameters are required to implement design methods where joints are explicitly considered.

- The equivalent continuum approach can also be applied in blocky ground when initial support (e.g., bolts) is specified to stabilize blocks created by unfavorably oriented fractures detected during mapping. Hence the rock mass in the immediate vicinity of the excavation is assumed to be stabilized using initial support, and blocks will not load the liner.

Accordingly, the analytical approach was selected without further consideration of other possible methods, although these other methods may be used by the designer if appropriate.

1.2 GEOLOGIC SETTING

The following general description of the geologic and stratigraphic setting was derived from the following sources: (1) the NNWSI Reference Information Base (RIB) (SNL, 1987, Appendix Q), (2) the Site Characterization Plan Conceptual Design Report (SCP-CDR) (SNL, 1987), and (3) a report by Spengler and Chornack (1984) that describes an investigation of the USW G-4 borehole, which is the borehole closest to the exploratory shaft location.

The site of the prospective repository is located at Yucca Mountain, Nevada, approximately 85 mi northwest of Las Vegas. The Yucca Mountain site lies within the Basin and Range physiographic province, which is characterized by north-trending fault-block ridges separated by broad valleys. Tectonically the region is dominated by high angle normal faulting.

The upper 2000 m of the total stratigraphic section at Yucca Mountain is dominated by a sequence of Tertiary volcanic rocks, primarily rhyolitic ash-flow tuffs. The planned repository horizon is at a depth of approximately 300 m in the Topopah Spring Member of the Paintbrush Tuff (TS-2). This guide is concerned with the upper 500 m, in which the shafts will be located. Figure 1-2 shows the general stratigraphy for this section of the site, along with a typical shaft.

The exploratory shafts at Yucca Mountain will be collared in the Tiva Canyon Member of the Paintbrush Tuff (TC). The TC Unit is a densely welded to partially welded ash-flow tuff. This unit has a relatively high intact rock strength, but is also relatively highly fractured

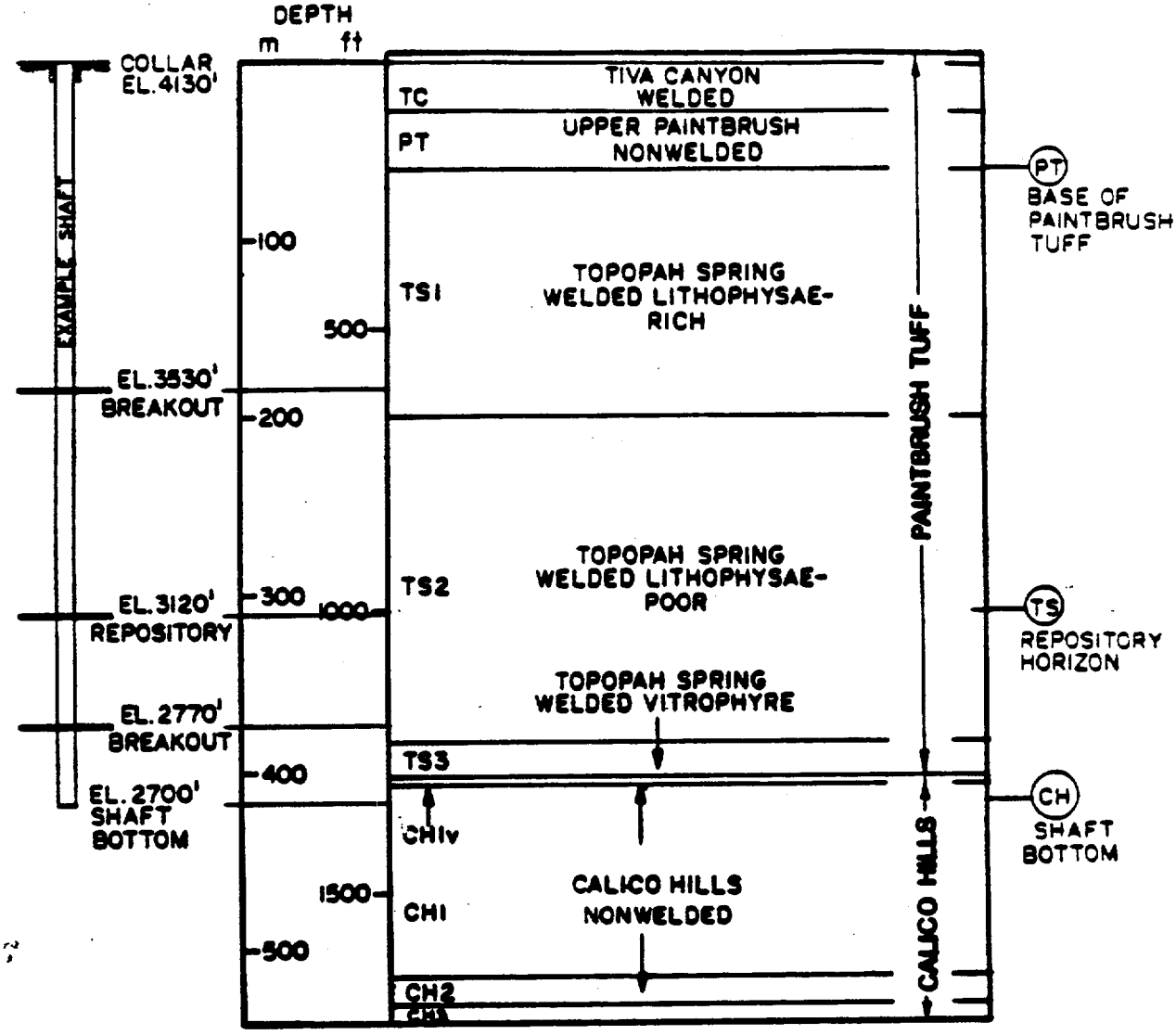

Figure 1-2. Section of Typical Shaft Showing Stratigraphy and Elevations Used in Example Problems

(Spengler and Chornack, 1984). Below the TC are the Yucca Mountain and Pah Canyon Members of the Paintbrush Tuff. These units are nonwelded, vitric ash-flow tuffs collectively referred to as the "PT" Unit. A relatively low fracture frequency in the G-4 core is offset by the low intact rock strength of this unit. Below the PT Unit lies the Topopah Spring Member (TS), which is subdivided into three welded units. From the top, TS-1 is a densely welded ash-flow tuff with a high proportion of lithophysae (voids). TS-2 has a lower void ratio and is the currently designated repository horizon. TS-3 is a thin, densely welded vitrophyre. The TS Member has a moderate fracture density and a generally high strength. Most of the fractures are near vertical and occur in two, obliquely intersecting sets. The rock character changes again in the Calico Hills Formation (CHlv, CHl), which is a generally massive, nonwelded to partially welded ash-flow tuff of relatively low intact strength.

Spengler and Chornack (1984) note a correspondence between the degree of fracturing and the degree of welding, with the most densely welded units being the most fractured. This is reflected in the core index values for borehole G-4, which measure joint frequency, core loss, and broken core.

The water table is thought to be 140-360 m below the repository horizon (SNL, 1987). Although local or perched water may be encountered, conditions in the shafts are generally expected to be dry.

1.3 REPORT ORGANIZATION

The body of this guide is divided into five chapters. Chapter 2 discusses the requirements for repository shaft liners. Chapter 3 analyzes rock behavior during construction and the influence that the timing of support installation will have on the design. Chapter 4 describes each of the major loading mechanisms (static, thermal, and seismic), including summaries of the individual load components and how

individual loads are combined. Chapter 5 describes methods for evaluating liner mechanical behavior, and Chapter 6, liner performance.

Appendix A contains an annotated summary of data used in example problems. Details of thermal analysis calculations are found in Appendix B. Appendix C describes an elastic-plastic finite-element analysis that is intended to check the methodology used in Chapter 3 for calculating unlined shaft behavior and in Chapter 4 for calculating ground pressures. Appendix D demonstrates that the liner design described in Chapter 6 is conservative by showing that a cracked liner has considerable support capacity.

Figure 1-3 is a flow chart of the liner design methodology. This is a roadmap to the design procedure described in this guide. The numbering on the flow chart corresponds to the section numbers in the guide.

1.4 EXAMPLE PROBLEMS

Example problems illustrating the salient features of this methodology are presented throughout this guide. Although the framework of this methodology is general, the details of the methodology are site-specific, as discussed in Section 1.1. To ensure that this methodology is appropriate for conditions expected at the site, design input currently appropriate to the exploratory shafts have been used in these examples.

The exploratory shafts are two 12-ft-diameter, fully furnished exploration shafts (ES-1 and ES-2). The shafts are approximately 1,400 and 1,000 ft deep, respectively, and will be sunk through the tuff formations at Yucca Mountain.

This report does not intend to provide final recommendations for exploratory shaft design. Also, the examples are not necessarily representative of the most severe conditions considered possible in the repository. Not all of the data used in the example problems are

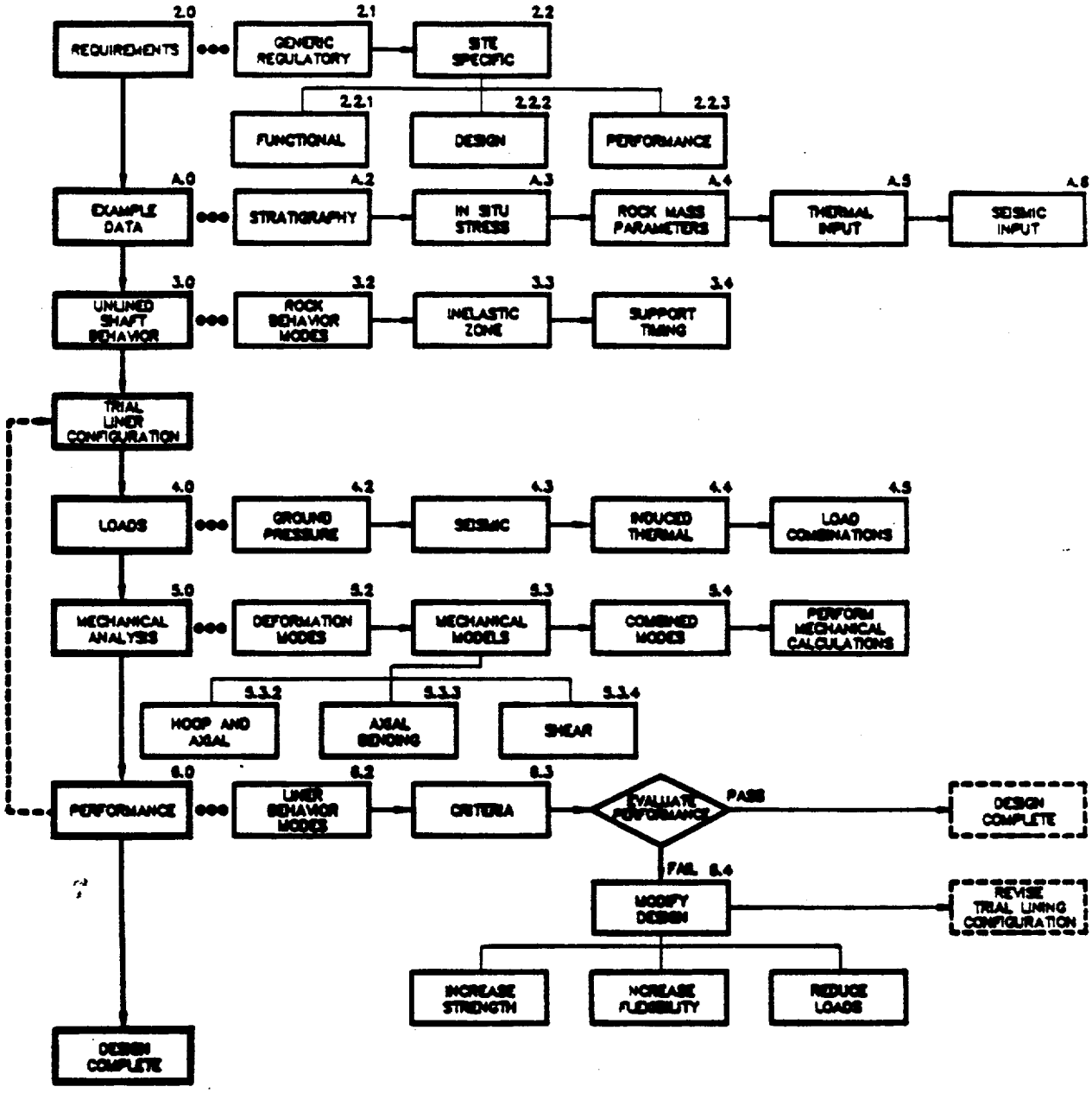

Figure 1-3. Flow Chart of Liner Design Methodology
(numbered boxes refer to report sections)

baselined, and the designer is directed toward the authorized project data base and other approved baseline documents when selecting design input.

Although the examples use single values of input, the designer should be aware that there is a possibility of encountering off-normal conditions in the repository. The results of analyses in the example problems may be sensitive to changes in the recommended values. All designs should be based on recommended values presented in the latest version of the approved data base. The safety factors used to evaluate liner performance in Chapter 6 are based on the use of recommended values. However, the design must consider the possibility of off-normal conditions, which could cause a single parameter to vary or a combination of parameters to vary simultaneously. Credible combinations of off-normal conditions should be developed and analyzed as part of the design.

Example Problem

Thermomechanical stratigraphy for the example problem as illustrated in Figure 1-2 is based on borehole USW G-4 because this is the borehole nearest the exploratory shafts. For convenience in presenting the example problem, three locations along the shafts have been assumed to be critical -- the upper Paintbrush Tuff Unit, the repository horizon, and the shaft bottom.

1. The Paintbrush Tuff Unit near the surface was checked because of its low seismic velocity and low strength. The critical location is referred to as "PT" in this report and is defined at a depth of 74 m (243 ft).

2. The repository horizon in the Topopah Spring formation is the critical location for induced thermal stresses. In this report,

the critical location is referred to as "TS" and is defined at a depth of 305 m (1,000 ft).

3. The shaft bottom at 415 m (1,360 ft) is the region with the greatest potential for stress-related instabilities during construction. This critical location is referred to as "CH" because it is located in the Calico Hills formation.

2.0 REQUIREMENTS

2.1 GENERIC REGULATORY REQUIREMENTS

"Repository shafts" refers to shafts that are used for the repository, including the exploratory shafts after they are converted for repository use. Repository shafts are subject to the provisions of applicable federal regulations and the hierarchy of requirements documents developed for the Nuclear Waste Terminal Storage program. The general requirements for the underground facility are stipulated in 10 CFR 60.133 (NRC, 1986); it is the highest level document that contains requirements applicable to repository shafts. Specific requirements in 10 CFR 60.133 that directly or indirectly apply to shafts include the following:

> "(e) Underground openings. (1) Openings in the underground facility shall be designed so that operations can be carried out safely and the retrievability option maintained. (2) Openings in the underground facility shall be designed to reduce the potential for deleterious rock movement or fracturing of overlying or surrounding rock."
>
> "(f) Rock excavation. The design of the underground facility shall incorporate excavation methods that will limit the potential for creating a preferential pathway for groundwater to contact the waste packages or radionuclide migration to the accessible environment."
>
> "(i) Thermal loads. The underground facility shall be designed so that the performance objectives will be met taking into account the predicted thermal and thermomechanical response of the host rock, and surrounding strata, groundwater system."

The Generic Requirements Document for a Mined Geologic Disposal System (GR) (DOE, 1986) expands on these requirements. An addition to 10 CFR 60 Subpart (f) proposed in the GR would limit, to openings constructed in the saturated zone, the requirement for special excavation methods that minimize preferential pathways for ground water. Nuclear Regulatory Commission (NRC) approval of the addition is pending. The GR also requires the following.

> "Subsurface openings shall be designed and constructed such that they remain stable during operating periods and, if required, retrieval periods to meet personnel, equipment, and ventilation access requirements (GR 1.2.1, PC#1.b)."

> "Adequate subsurface facilities shall be provided to control expected underground water inflow and nonroutine water intrusion events having a reasonably high probability of occurrence during the preclosure period, and to ensure personnel safety and minimum disruption to waste disposal operations (GR 1.2.1, PC#2.b)."

Appendix E of the GR is specific to the exploratory shafts and contains numerous requirements. Four items in the ESF--underground openings, operational seals, shaft liners, and ground support--are considered "permanent" items that must be incorporated into the repository and have additional quality requirements. The GR imposes the following requirements on the shaft liner:

> "SHAFT LINER(S) - all components placed between the inside limits of the shaft and the accessible extent of the underground opening;

Functions:

- to provide structural integrity to shaft opening
- to provide a means for anchoring shaft fittings
- to provide water control
- to complement any operational seals."

Section 6 of Appendix E (of the GR) further stipulates the following requirements for the exploratory shafts and provides justification for the shaft design guide.

> "ESF permanent structures, systems, and components (repository quality) that will be incorporated into the repository shall be designed and constructed with the same criteria, standards, and quality assurance levels as required for the repository to the extent known at the time of ESF design (emphasis added)(PC#2)."

> "Shafts and other underground excavations shall be designed and constructed with reasonably available technology similar to or corresponding with the techniques planned for the candidate repository (PC#6.a)."

> "The predicted thermal and thermomechanical response of the host rock and surrounding strata and the ground water system shall be considered in the ESF design (C#N)."

Appendix E of the GR also outlines the performance requirements for the first exploratory shaft. The criteria relevant to designing the liner for ES-1 include the following:

> "Permanent shaft structures, systems, and components shall be designed and constructed for a maintainable 100-year design life (6.4, PC#1.b)."

"Techniques used for shaft excavation shall control overbreak of rock and minimize disturbance to the integrity of the adjoining rock mass (6.4, PC#1.c)."

"The shaft shall be designed to provide stability and to minimize the potential for deleterious rock movement or fracturing that may create a pathway for radionuclide migration (6.4, PC#1.d)."

"Rock support and other structural anchoring materials shall be compatible with waste isolation and shall neither interfere with radionuclide containment nor enhance radionuclide migration (6.4, PC#1.e)."

Similar requirements are stated for ES-2 under Section 6.5, Appendix E of the GR.

2.2 SITE SPECIFIC REQUIREMENTS

2.2.1 Functional Requirements

All of the generic requirements discussed in the previous section currently apply at the program level to all repositories. Requirements documents that are site-specific at the project and designer levels must be used in conjunction with this guide. Such documents include the Repository Design Requirements for the Yucca Mountain Mined Geologic Disposal System (RDR) (SNL, 1988), and the Nevada Nuclear Waste Storage Investigations Project Exploratory Shaft Facility (ESF) Subsystem Design Requirements Document (NNWSI-SDRD). Some of the generic requirements have been interpreted in this guide to tailor them to the conditions at Yucca Mountain.

The remainder of this chapter consists of site-specific requirements that were discussed by the ESF/Repository Interface Working Group during a series of monthly meetings held in Las Vegas, NV, in 1987.

These requirements will be baselined for ESF design; changes have been made to them for consistency with the content and format of this report. The designer is referred to the baselined document for the original wording (NNWSI-ICWG, 1988).

Several features distinguish the proposed repository at Yucca Mountain from those previously considered at Hanford, Washington (basalt) and Deaf Smith County, Texas (salt): (1) according to the current conceptual design outlined in the SCP-CDR, none of the shafts will be used to transport waste at any time; (2) the proposed repository at Yucca Mountain is situated entirely in the unsaturated zone; therefore, the shaft liners need not be watertight because they do not function as seals or barriers to prevent water from entering the repository; and (3) there are no credible accident scenarios involving the shaft liners that can cause radionuclide release. Thus, the primary functional requirement of the shaft liners is solely to maintain worker safety and operational efficiency; they are not important to public safety.

The functional requirements for the repository shaft liners are to

- enhance the structural integrity of the shaft walls,
- eliminate rockfall hazards to personnel,
- provide a safe and convenient structure for support of shaft equipment,
- provide a smooth surface for efficient ventilation, and
- protect the shaft wall from weathering and other types of deterioration.

The liners for the repository shafts are <u>not</u> intended to

- resist hydrostatic loads from water pressure,
- prevent local yielding of the shaft wall rock,
- rigidly prevent ground movements, or
- function as items important to safety as defined by 10 CFR 60.

2.2.2 Design Requirements

- The liners will be concrete, cast directly against the rock, with a minimum thickness of 0.3 m (12 in.) which is the industry standard.

- The repository shaft liners will be designed for a 100-yr maintainable life.

- The liners will be analyzed for appropriate combinations of the following loads:

  - ground pressure,
  - seismic loads from design-basis underground nuclear events (UNE) and earthquakes, and
  - induced thermal loads.

- The amount of reinforcing (if any) used in the shaft liners will be limited to calculated design requirements.

- Water pressure should be drained, and (weep) holes provided where necessary to prevent water pressure buildup behind the liner.

- The liner design will consider construction activities that might affect liner performance. In competent ground, the design will specify a minimum gap between the curb (bottom) pour of the liner and the shaft bottom to prevent excessive loading due to elastic convergence of the shaft wall and to reduce possible blast damage to fresh concrete. In incompetent ground, the designer may assume that the ground will be stabilized with initial support such as bolts and mesh before the liner is installed. Blast rounds will be carefully designed to minimize overbreak and damage to the formation and the liner. Joints

will be provided between each pour to help localize possible horizontal cracks caused by axial extension and concrete shrinkage. ("Cold" construction joints will satisfy this requirement.)

2.2.3 Performance Requirements

The primary purpose of this guide is to ensure that the liner design meets all performance requirements. The shaft liners shall be designed to meet the design requirements of Section 2.2.2 and to ensure that they will perform all functions described in Section 2.2.1. Specifically, the liners shall be designed to sustain the predicted static and dynamic loads for the design life without collapse or loss of function. Minor damage may be acceptable provided that it does not contribute to failure mechanisms or affect the maintainable performance. Specific criteria for evaluating liner performance and the rationale for their selection are presented in Chapter 6. These criteria pertain to mechanical performance of the liner, and do not address material compatibility concerns.

2.3 SPECIAL CONSIDERATIONS FOR THE EXPLORATORY SHAFTS

The service life of the exploratory shafts is divided into two phases, Phase I and Phase II. In Phase I, before waste emplacement, the shafts will function as openings for site characterization testing operations. In addition to their function of supporting exploration during this phase, the shafts will provide support for the underground ESF. This includes providing access for personnel, materials, utilities, ventilation, and muck handling. After all work associated with the ESF is completed, the exploratory shafts may be used to support repository construction. During Phase I, the shaft liners will be subjected to ground pressure associated with interaction between the liner and the rock, as well as dynamic loading from UNEs and possible natural seismic events.

The conceptual design of the repository currently stipulates that the exploratory shafts will be converted into downcast ventilation shafts before the first waste is emplaced--a step that marks the beginning of Phase II. The shafts will function as downcast ventilation shafts in the waste emplacement area air circuit during the operation, retrieval, and decommissioning periods. During Phase II, the shaft liners will be subjected to induced thermal loads in addition to the loads in Phase I. Appendix E of the GR stipulates that the exploratory shaft liners be designed with the same criteria, standards, and quality assurance levels that are required for the repository to the extent known at the time the shafts are designed (DOE, 1986).

Later designs of the repository shafts will benefit from a more extensive data base obtained from testing in the exploratory shaft facility, but the exploratory shafts must be designed with only preliminary site data obtained by drilling from the surface. When more detailed site data have been collected through testing and monitoring at the underground test facility, it is possible but not likely that these shafts will need to be retrofitted to meet repository performance requirements, especially regarding thermal loading. This possibility can be minimized with a suitably conservative initial design. Retrofitting a shaft with this type of liner, if required, could be performed by several methods that will not present major construction difficulties. Because of uncertainty in estimated thermal loads, the designer should evaluate several retrofit options.

3.0 UNLINED SHAFT BEHAVIOR

3.1 INTRODUCTION

Although shafts can be sunk and lined by several methods, standard mining industry practice is to cast a concrete liner concurrent with sinking. Typically, one or several rounds of the shaft are excavated by drill and blast techniques ahead of the last placed liner segment. The liner is then advanced by lowering the concrete forms and placing the concrete. The liner is advanced concurrent with sinking so that it remains approximately 3-12 m (10-40 ft) from the face. Between the liner and the face, the shaft walls may be unsupported. Rockbolts, wire mesh, shotcrete, and other initial support are installed if necessary to protect workers until the liner can be advanced and has time to cure. The type and quantities of initial support installed will be determined during construction by the parties responsible for worker safety.

The purposes of this chapter are (1) to determine the mode of rock behavior in the unlined shaft section near the face, which is not only important to determining initial support requirements but influences the selection of analytical methods and material models for calculating liner loads, and (2) to establish guidelines for when the liner should be installed. The distance between the face and where the liner is installed during construction is important to the ground pressure that will develop on the shaft liner, as discussed in the following section.

3.2 MODES OF ROCK BEHAVIOR

There are several potential modes of rock behavior around an unlined shaft opening, including both elastic and various inelastic modes such as spalling, crushing, joint slip, wedge fallout, rockburst, etc. This section discusses only the elastic-plastic idealization, which is

considered suitable for initial design of the ESF given the preliminary nature of the available data, as discussed in Section 1.1. Because idealized elastic-plastic behavior is being discussed, the term "yield" is used to describe the onset of any type of inelastic behavior.

In the two-dimensional case, an inelastic zone will form around an opening if the unconfined compressive strength of the rock is less than the peak tangential stress adjacent to the opening. Because a range of values for in situ horizontal stress is possible at the site (Table A-2, Appendix A), two scenarios are evaluated: Case 1, a uniform pressure situation using the upper limit of the minimum horizontal stress, and Case 2, a worst case scenario using the smallest value for the minimum horizontal stress and the largest value for the maximum horizontal stress. The worst case scenario is used to separate the rock into two behavioral regimes (elastic versus inelastic). If the rock remains elastic, no stress-related construction problems are anticipated. If the rock does not remain elastic, the extent of the inelastic zone must be considered.

The strength of each thermomechanical unit is compared with the peak tangential stress (σ_t) induced in the shaft wall at the bottom of the unit, by means of the Kirsch formula (Brady and Brown, 1985, p. 163).

$$\sigma_t \leq q \qquad (1a)$$

where

$\sigma_t = \sigma_H + \sigma_h - 2\,(\sigma_H - \sigma_h)\cos(2\theta)$
q = unconfined compressive strength of the rock mass
σ_H = maximum principal stress in the horizontal plane
σ_h = minimum principal stress in the horizontal plane
θ = counterclockwise angle from maximum horizontal stress direction

At $\theta = 0^{o}$, $\sigma_t = 3\sigma_h - \sigma_H$ and At $\theta = 90^{o}$, $\sigma_t = 3\sigma_H - \sigma_h$.

Alternately,

$$P + 2S \leq q/2 \qquad (1b)$$

where

$P = (\sigma_H + \sigma_h)/2$, mean stress, and
$S = (\sigma_H - \sigma_h)/2$, stress deviator.
(see Figure 3-1)

If Equation 1a or 1b is true, then according to theory the ground will not need to be supported to prevent overstress. No inelastic zone will form. The ratio of the unconfined strength of the rock mass to the peak tangential stress at the edge of the opening conveniently indicates the margin of safety and is termed the "strength/stress ratio."

$$\text{Strength/stress ratio} = q/\sigma_t. \qquad (2)$$

If Equation 1a or 1b is not satisfied, then an inelastic zone will form that may require support for stabilization.

In some situations, block instability due to adversely oriented joints rather than overstress of the rock may dictate initial stabilization requirements. Current indications are that most joints occur in the TC and TS units and that they are subvertical and are not conducive to block-related instability. Additionally, the joints are quite rough, which will contribute to stability. Other formations (PT, CH) are generally massive and overstress is the primary concern. Potentially unstable blocks will be identified and stabilized using rockbolts before the liner is installed, and are not expected to load the liner.

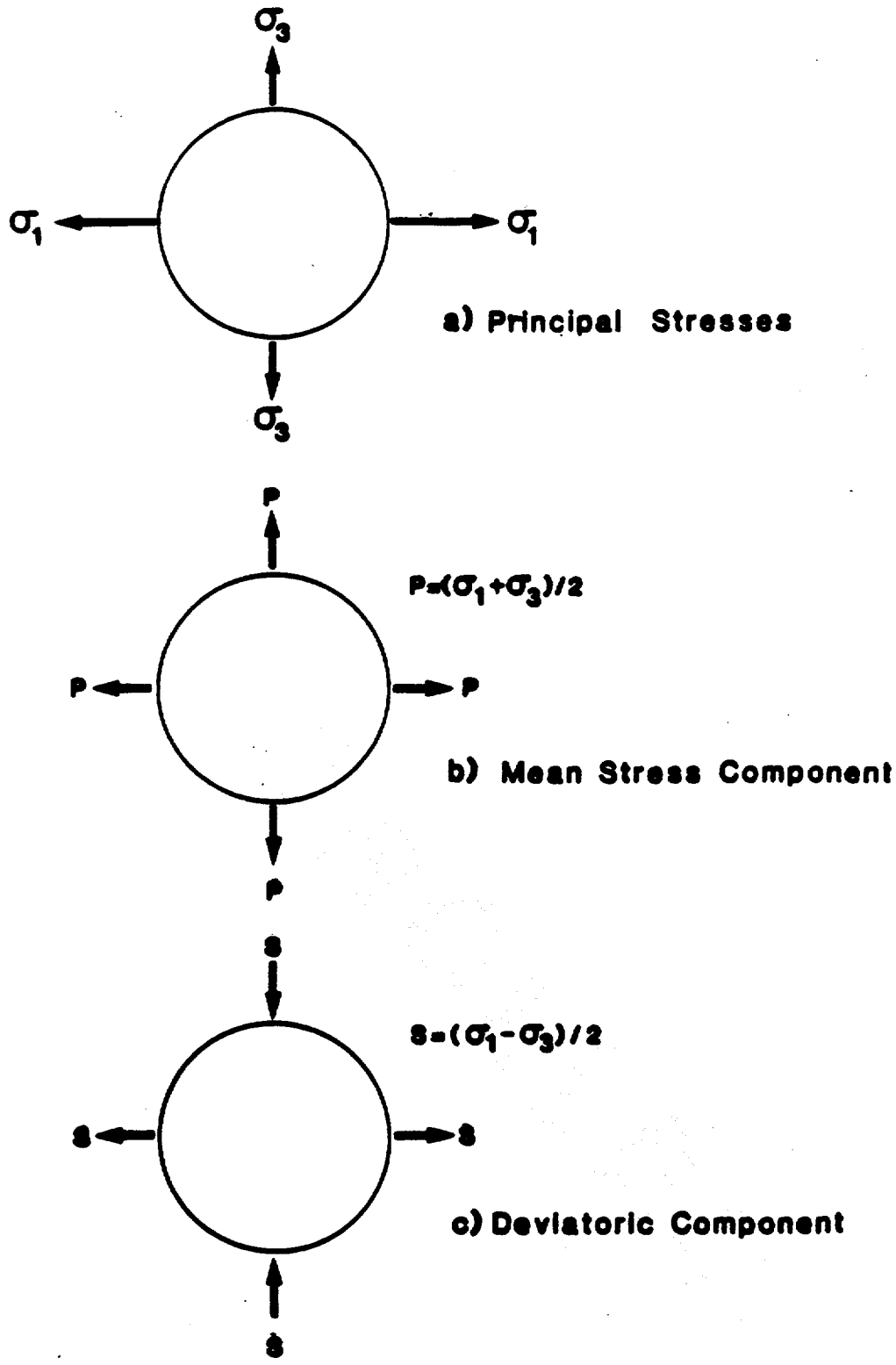

Figure 3-1. Decomposition of the Principal Stresses

3.3 INELASTIC ZONE

The extent and shape of the inelastic zone can be estimated by extending the analysis used to determine the mode of rock behavior developed by Emmanuel Detournay (St. John et al., 1984; Detournay, 1986; Detournay and Fairhurst, 1987). Such an estimate is useful because it gives an indication of the size and shape of regions that may require initial support before the liner is installed. A brief discussion of the method is presented here; details of the analysis can be found in the documents cited above. In its current form, the analysis is based on an elastic-perfectly plastic material and incorporates a Mohr-Coulomb yield criterion.

Figure 3-2 shows how the inelastic zone forms in mean stress-deviatoric stress space. Also shown on the figure is the range of interest for the example problem discussed later. The general position of a particular stress condition on this chart is defined by the levels of mean and deviatoric stress. The "obliquity" is a measure of the anisotropy of the applied stress field as well as a measure of the stress state relative to the yield value defined by the Mohr-Coulomb yield surface, or;

$$\text{Obliquity} = m = S/S^{\ell} \tag{3}$$

where

$$S^{\ell} = P \sin \phi + c \cos \phi$$

$$c = \text{cohesion} = q(1 - \sin \phi)/(2 \cos \phi)$$

$$\phi = \text{friction angle.}$$

It should be emphasized that $m = 0$ is a uniform stress field, $0<m<1$ is a nonuniform stress field, and $m = 1$ is a nonuniform stress field at failure. The obliquity determines the behavior and shape of the relaxed zone, and the mean horizontal stress (P) determines its average radius. Figure 3-2 shows a "critical" obliquity line. The critical obliquity defines the slope of this

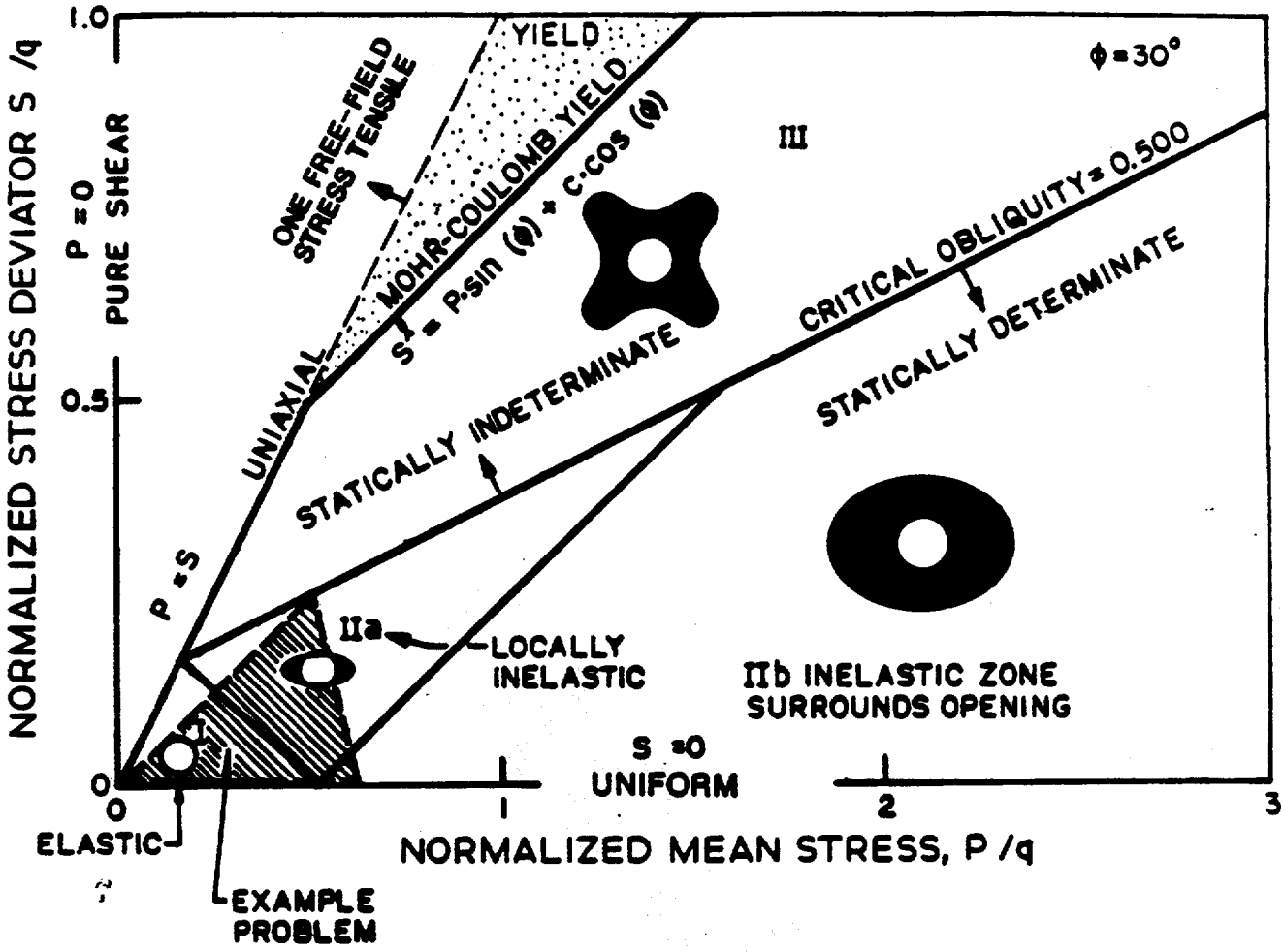

Figure 3-2. Relationship Between the Initial Horizontal Stress State and Failure Modes for an Unlined Shaft in a Mohr-Coulomb Elastic-Plastic Medium, for $\phi = 30°$ (after St. John et al., 1984). (Shaded area represents the approximate zone of interest for example problem: note very limited inelastic behavior.)

line and is a function of friction angle only, ranging from 0.414 for $\phi = 0$ to 0.542 for $\phi = 40°$. Behavior below the critical obliquity line can be determined statically using closed-form solutions; above this line, a numerical method such as finite element is required for solution because the problem becomes statically indeterminate. Note that above the P=S line, one of the field stresses is tensile. This is locally possible, but highly unlikely at any proposed shaft site. Also, Figure 3-2 is strictly valid only for a friction angle of 30° and is used merely for illustrative purposes.

If the in situ stress field is uniform (m = 0), then the inelastic zone is cylindrical, and its radius can be calculated according to the equation (Deere, et al., 1969, p. III - 15)

$$R_p = R\left[(1-\sin\phi)\,\frac{(P + c\cdot\cot\phi)}{(p + c\cdot\cot\phi)}\right]^{\frac{1-\sin\phi}{2\sin\phi}} \qquad (4)$$

where

R = unlined shaft radius
p = internal pressure (= 0 without liner)
R_p = radius of inelastic zone
P = mean horizontal stress.

If the in situ stress field is not uniform, then Equation 4 still provides the average radius of the inelastic zone. The inelastic zone is an oval if the obliquity of the in situ stress state is less than the limiting obliquity. To calculate the shape of this oval and its maximum extent, the following procedure can be used.

1. Calculate the limiting value of the deviator stress (S^2).

2. Calculate the obliquity of the in situ stress condition using Equation 3.

3. Calculate the maximum extent of the inelastic region where b (larger radius of oval) is given by

$$b = [2X/(1 + X)]R_p \qquad (5)$$

and where the intermediate result is the major to minor axis ratio of the inelastic zone (Detournay and Fairhurst, 1987)

$$X = \left[\frac{1+m}{1-m}\right]^{(1-\sin\Phi)} .$$

If the vertical stress is greater than the peak tangential stress (σ_t) given by the left side of inequality (1), then yield in the vertical plane is a possibility. If horizontal stresses are uniform ($\sigma_H = \sigma_h$), yield will first occur in the vertical plane if the horizontal-to-vertical stress ratio (K_o) is less than 0.5. A simple check of the vertical stress (σ_v) against the rock strength (q) is sufficient for this analysis.

The deterministic methodology described above, using Equations 1-5, is based on idealized elastic-plastic behavior. Equation 1 can be used to determine whether or not the rock will yield, but cannot be used to determine the rate at which yield will occur, which is best established by empirical types of evidence. The nature of yield in possible inelastic zones at Yucca Mountain is likely to be minor slabbing and/or spalling of the rock on the shaft walls perpendicular to the principal stress direction. This type of behavior is not uncommon in massive rock with high tangential compressive stresses (Fairhurst and Cook, 1966); slabbing or spalling can be readily stabilized by initial support (rockbolts and possibly mesh). Anchorage for the initial support should extend well into the elastic region.

Other types of inelastic behavior (e.g., rockburst, creep) that sometimes are encountered in mines when the rock strength is exceeded by

stresses are considered unlikely at Yucca Mountain. Blake (1984) indicates that important factors contributing to rockburst conditions are a high stress state, massive and strong brittle rock, a high extraction ratio, and wide spans. The in situ stress levels in this example are not high by mining standards and the indicated overstress is due largely to the low strength of the rock mass reported in the RIB. No core discing has been observed in Yucca Mountain boreholes at shaft depths. Moderate in situ stress levels and low rock strengths do not support the storage of large amounts of elastic strain energy, and the possibility of rockburst must be considered extremely remote. Currently, there are no indications that significant creep will occur in the tuff.

Experience at nearby Rainier Mesa, under similar stress conditions and in rock representative of that at Yucca Mountain, has shown generally favorable ground conditions (Tillerson and Nimick, 1984; Langkopf and Gnirk, 1986). The tuffs at Rainier Mesa have both welded and nonwelded portions. The welded portions, in particular the welded tuff of the Grouse Canyon Member of the Belted Range Tuff at G-Tunnel, have very similar geoengineering properties to the Topopah Spring Member of the Paintbrush Tuff, which is currently the candidate horizon for the repository (Zimmerman et al., 1984). Nonwelded tuffs at Rainier Mesa, particularly Tunnel Bed 5, have geoengineering characteristics similar to the Calico Hills Member, which is below the repository and may be encountered by one of the exploratory shafts. Studies reported by Bauer et al. (1985) and Zimmerman et al. (1984) show that the in situ stress environment at Rainier Mesa is similar to that expected at repository depths.

In G-Tunnel, light support (rockbolts and mesh) has been used to successfully stabilize spans of up to 7.3 m in horizontally-oriented underground drifts. In comparison, the exploratory shaft excavation will be only about 4.3 m in diameter and, because of the vertical orientation, gravity loads from the weight of loosened rock will be relatively small.

Example Problem

Tables 3-1 and 3-2 show the results of example calculations for uniform and nonuniform stress cases using data appropriate for ES-1 (taken from Appendix A; the tables in Appendix A also show the range of the data). A limited inelastic zone develops in the Calico Hills, which is due to moderate overstress. Figure 3-2 illustrates the general region of interest. Inelastic behavior should be quite limited in extent.

Figure 3-3 illustrates the estimated extent of the relaxed zone for two cases of in situ stress. It should be emphasized that these cases represent the worst condition anticipated -- at the bottom of a shaft penetrating the low-strength Calico Hills Formation. With a uniform in situ stress of 8.23 MPa, a relaxed shell approximately 22 cm thick will form near the shaft bottom on the inner wall of the excavation. If a highly anisotropic stress field exists, with the maximum stress being 8.23 MPa and the minimum stress being 3.09 MPa, an oval relaxed zone will form with a maximum extent of 54 cm. In both cases, the relaxed zone is less than one meter thick, within the expected zone of normal blast damage.

In this example, yield will occur in the horizontal plane as a result of tangential stresses. Yield in the vertical plane is precluded because the maximum stress difference in the vertical plane ($\sigma_v - \sigma_h$) is 7.2 MPa at the shaft bottom, less than the strength of 13.5 MPa.

Alternatively, a suitable numerical method such as elastic-plastic finite element analysis may be used to determine the mode of rock behavior and the extent of the inelastic zone. This is required if the obliquity (m) is greater than the limiting obliquity for a given problem, making the solution statically indeterminate (Detournay and Fairhurst, 1987). The example problem is in the statically determinate region and inelastic behavior is extremely limited; thus, the simplified methodology is appropriate under these conditions. Finite-element

TABLE 3-1

RESULTS OF EXAMPLE ROCK BEHAVIOR CALCULATIONS FOR CASE 1
(UNIFORM PRESSURE, K_o = 0.8)[a]

Unit	σ_t Max Tang. Stress (MPa)	q Ave Uniax. Strength (MPa)[b]	Behavior Mode	Strength/Stress Ratio	R_p/R Normalized Plastic Radius	R_p Plastic Radius (m)
TC	1.32	120.00	Elastic	90.64	-	-
PT	2.73	9.50	Elastic	3.48	-	-
TS-1	7.52	16.00	Elastic	2.13	-	-
TS-2/3	15.07	83.00	Elastic	5.51	-	-
CH1V	15.26	13.50	Inelastic	0.88	1.052	2.245
CH1	16.46	13.50	Inelastic	0.82	1.098	2.344

a. Example input data from Appendix A
b. Average uniaxial "rock mass" strength

TABLE 3-2

RESULTS OF EXAMPLE ROCK BEHAVIOR CALCULATIONS FOR CASE 2
(NONUNIFORM PRESSURE, k_h = 0.3, k_H = 0.8) [a]

Unit	σ_t Max Tang. Stress (MPa)	q Ave Uniax. Strength (MPa)[b]	Behavior Mode	Strength/Stress Ratio	R_p/R Normalized Plastic Radius	R_p Plastic Radius (m)	m Obliquity	b Maximum Plastic Radius (m)
TC	1.74	120.00	Elastic	90.06	-	-	0.011	-
PT	3.58	9.50	Elastic	2.65	-	-	0.102	-
TS-1	9.87	16.00	Elastic	1.62	-	-	0.172	-
TS-2/3	19.78	83.00	Elastic	4.20	-	-	0.087	-
CH1V	20.03	13.50	Inelastic	0.67	0.914	1.950	0.370	2.53
CH1	21.60	13.50	Inelastic	0.62	0.931	1.988	0.389	2.67

a. Example input data from Appendix A
b. Average uniaxial "rock mass" strength.

Note: K_o = uniform horizontal stress coefficient = σ_h/σ_v
K_H = maximum horizontal stress coefficient = σ_H/σ_v
K_h = minimum horizontal stress coefficient = σ_h/σ_v

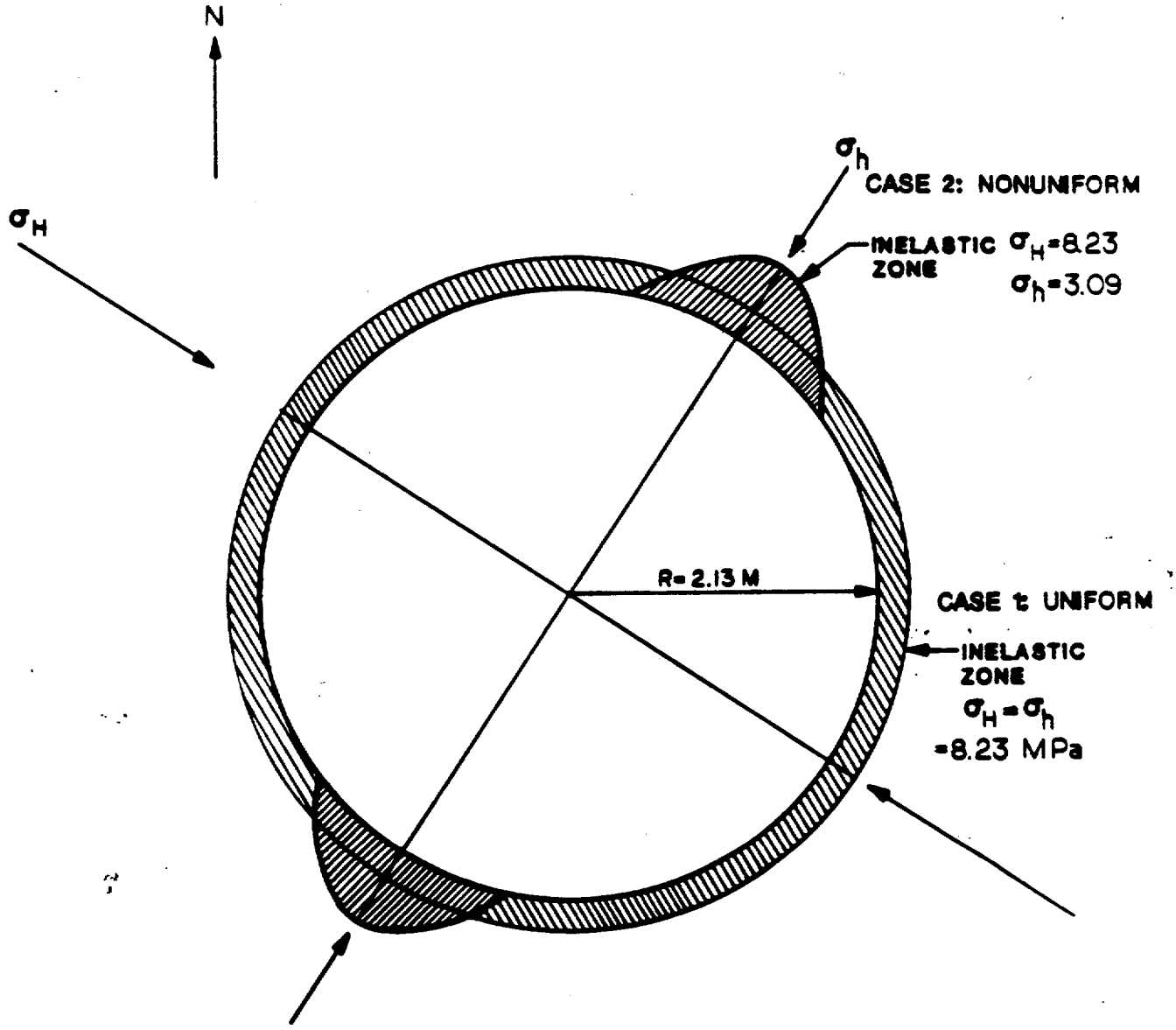

Figure 3-3. Example Problem Showing Two Cases of Yield Zone Formation in the Calico Hills Formation at the Example Shaft Bottom

results described in Figure C-1 (Appendix C) are visually consistent with the closed-form solution illustrated in Figure 3-3.

3.4 SUPPORT TIMING

Convergence associated with shaft sinking can be estimated using an elastic model if the elastic limit of the rock is not exceeded by the ground stresses around the opening. In this case the proportion of ground pressure that is transferred to the shaft liner is a function of when support is installed, which is a construction consideration. In this section, the term "support" refers to the concrete liner.

In the unlined region near the bottom of the excavation, convergence does not fully develop immediately. The shaft bottom exerts a stiffening effect on the shaft opening similar to the manner in which a welded endplate stiffens a steel tube against radial distortion. This effect diminishes with distance from the plate. In the case of the shaft, elastic convergence starts ahead of (below) the face, and develops as the shaft is advanced, with maximum convergence ocurring some distance back from the face. Several studies of this phenomenon have been reported (e.g., Ranken and Ghaboussi, 1975; Pariseau, 1977).

If the ground stresses exceed the elastic limit of the ground, inelastic relaxation will occur as discussed in Section 3.3. Because inelastic zones due to ground pressure are expected to be very small at Yucca Mountain, elastic analysis is used in the example problem to determine the appropriate support installation lag time. (The decision to use elastic analysis is supported by the results of Appendix C.)

Example Problem

Figure 3-4 illustrates the results of an example finite-element analysis of convergence in a situation where the rock walls remain elastic. The example analysis was performed using the elastic material

model option in the finite-element program, VISCOT (ONWI-437, 1983), which uses 8-node isoparametric elements. The deformed mesh is shown in Figure 3-4a. It is evident in the figure that most of the convergence occurs close to the face. In Figure 3-4b, convergence is plotted as a function of distance from the face. If the lining is placed no closer than about 1.2 radii from the face, the liner will experience only about 15% of the total convergence or less. Because elastic convergence is proportional to in situ stress, this is equivalent to saying that the liner will experience no more than 15% of the total in situ stress.

It is evident from this example that the timing of support installation has an important influence on the static pressure that may develop on the liner.

Similar studies (Ranken and Ghaboussi, 1975; Pariseau, 1977) have reported essentially the same results even though the modeling techniques and parameters varied. Ranken and Ghaboussi (1975) indicate that 30% of the radial displacement has already occurred at the shaft bottom and 94% has occurred at one and one-half shaft radii from the shaft bottom. A site-specific finite-element simulation of the exploratory shafts, performed by RE/SPEC (Costin and Bauer, in preparation), showed very low stresses in a shaft liner installed two radii from the bottom and loaded by elastic convergence.

In practice, it is difficult to place the liner closer than 1.2 radii (~ 8 ft) from the face without subjecting the liner to the possibility of damage from blasting. In the case of an exploratory shaft, a longer standoff distance from the bottom of the shaft to the shaft liner will be maintained in an unlined condition for mapping purposes. It is assumed for this methodology that the liner will be installed at least 1.5 radii behind the face. Based on the results shown in Figure 3-4 the liner will not experience more than 15% of the elastic convergence.

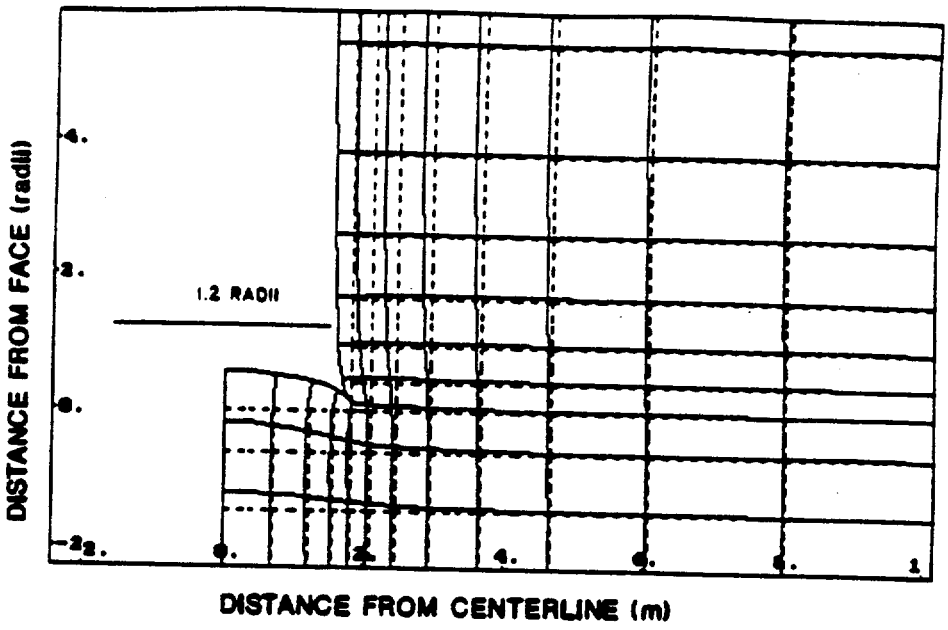

a. Undeformed (dashed) and Deformed (solid) Mesh.

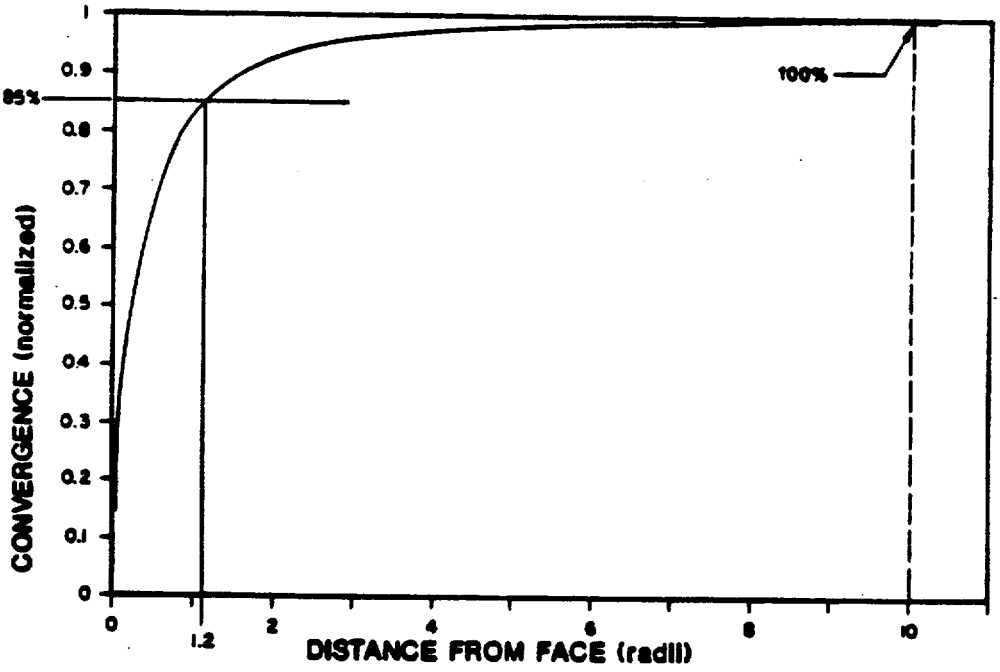

b. Convergence Near Shaft Bottom (as percentage of convergence at 10 radii).

Figure 3-4. Results of Elastic Finite-Element Analysis Showing Development of Convergence Near Shaft Bottom in Example Problem

4.0 LOADS

4.1 GENERAL

To evaluate the liner stresses for the repository shafts, three sources of loading need to be considered: ground pressure, seismic, and induced thermal. (Loads on the liner from rock relaxation are termed ground pressure.) Ground pressure may result from either elastic behavior such as the elastic convergence phenomenon discussed in Section 3.4 or inelastic behavior resulting from the formation and dilation of a relaxed zone as described in Section 3.3. Seismic loads may result from the action of earthquakes or UNEs. Induced thermal loads are generated by thermal expansion of the rock as it is heated after waste emplacement.

Radial and shear tractions develop on the outer surface of a liner as it offers passive resistance to distortions of the surrounding rock mass. Tractions resulting from this interaction between the liner and the rock mass are often used as loads in liner calculations. However, they differ from classic engineering loads in that their magnitude depends on the liner-to-rock stiffness ratio. In this methodology, the free-field stresses, strains, and displacements at the shaft location are collectively termed "loads." "Free-field" refers to effects in the ground that would occur if the shaft opening was not present. By defining loads in this manner, they can be calculated independently without specifying opening shape, liner thickness and properties, and slip condition at the interface of the liner and rock. Analytical techniques later used for liner stress analysis require free-field inputs rather than tractions applied directly to the liner.

Although numerous technical articles have been written about how to determine ground pressures on shaft and tunnel liners, there is no universally accepted method for calculating this component of liner

load. There is evidence that many of the methods in use yield overly conservative designs (Hustrulid, 1984, p. 43).

In rock that is largely self-supporting, like that of the examples in the previous chapter, several authors, including Pariseau (1977), suggest that little ground pressure will actually develop on the liner. Significant pressure may develop (1) if a waterproof liner is used to resist water pressure; (2) if tangential rock stresses are substantially greater than the strength of the rock, which can occur in strong rock in deep shafts or in weak rock at any depth; and (3) in creeping or swelling ground. Because none of these conditions is expected at the Yucca Mountain site, the methodology for calculating ground pressure proposed in this guide does not include design of waterproof liners to resist hydrostatic pressure, nor does it consider loads resulting from creeping or swelling ground conditions.

Although considerable information about how to calculate ground pressure is available, less information has been published for theoretical evaluation of the seismic and thermal effects to which a nuclear waste repository shaft may be subjected. An evolving field, seismic design of underground structures has not received much attention primarily because to date little damage to deep underground structures due to earthquakes has been reported (Owen and Scholl, 1981). Analysis of induced thermal loads on shaft liners is virtually unique to nuclear waste disposal projects and has little precedence in the mining or civil design literature.

When determining liner loads and calculating stresses, the designer must establish an appropriate and consistent coordinate system for the analysis. The Cartesian coordinate system used in this guide is an xyz system with z vertical. For two-dimensional and plane analyses (plane stress or plane strain), stresses and strains may occur in or out of the plane of interest. "In-plane" refers to the xz plane if a vertical section through the shaft is analyzed and the xy plane if a cross section

is considered. "Out-of-plane" refers to both input and results resolved in planes perpendicular to in-plane.

4.2 GROUND PRESSURE

4.2.1 Ground-Support Interaction Analysis

Ground-support interaction analysis (Brady and Brown, 1985, Section 11.2) can be used as a tool to determine design ground pressures for the shaft liner. This is appropriate if the in situ horizontal stresses are assumed to be uniform. If this type of analysis is used, an initial ground displacement is assumed to occur before the support is installed. In the examples accompanying this section, ground-support interaction analysis is used only to illustrate how the timing of support placement, the stiffness of the liner, and the stiffness of the ground are related and how these influence the development of support pressures.

Figure 4-1, a typical ground reaction curve, illustrates the general principles of ground-support interaction analysis. The shape of the ground curve and its slope are determined by the properties of the ground. Convergence, or closure, occurs as the ground relaxes. This convergence can be elastic or inelastic depending on the in situ stress, the properties of the ground, and the internal support pressure provided by the liner. In the case of a concrete liner, the support pressure is passive because it develops solely as a reaction to the converging ground. On the figure, lines or characteristics define the relationship between deformation (closure) and the equilibrium pressures for the rock mass and the liner. Where the support curve intersects the ground curve, equilibrium is established and no further ground movement occurs. The stress developed in the liner at the equilibrium point is the stress in the liner that stabilizes the ground.

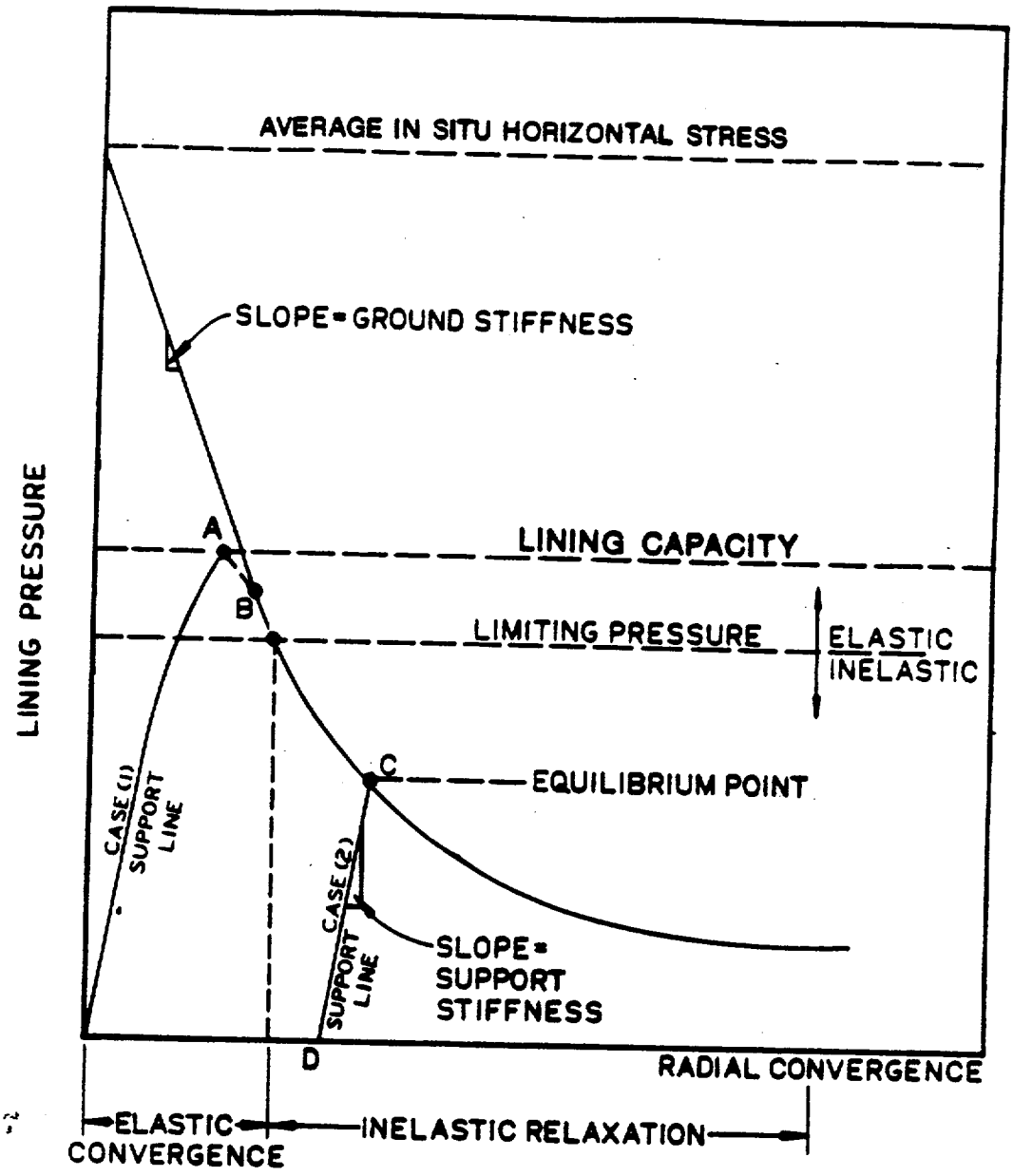

Case 1: LINING IS INSTALLED IMMEDIATELY AND REACHES YIELD AT POINT A (EQUILIBRIUM ESTABLISHED AT POINT B)

Case 2: LINING IS INSTALLED AFTER ELASTIC AND INELASTIC CONVERGENCE (D) OCCURS (EQUILIBRIUM ESTABLISHED AT POINT C)

Figure 4-1. Typical Ground Reaction Curve

In the ground reaction curve of Figure 4-1, two cases illustrate the importance of liner installation timing. In Case 1, a liner with high stiffness is installed immediately. As the face is advanced, the liner is passively loaded by the elastically relaxing ground and yields at Point A before equilibrium is established. After the liner yields, it is expected to retain considerable post-peak strength due to its cylindrical geometry. In this case, equilibrium is established at Point B. The reaction of the liner provides sufficient confining stress in the rock that the rock mass behavior remains linearly elastic.

In practice, it is unrealistic to assume that the shaft liner can be installed instantaneously before any ground movement occurs, as discussed in Chapter 3. A more realistic case is one in which installation of the liner is delayed so that some convergence has had a chance to develop before the liner develops any reaction. Case 2 (Figure 4-1) illustrates this approach. The liner is installed at Point D, after all elastic and some inelastic relaxation has occurred. A relaxed zone has developed, the extent of which is controlled by the passive liner pressure. Equilibrium is established at Point D, and the liner has considerable reserve capacity.

Dilation, or volume expansion, is a phenomenon that should be considered when rock is modeled using elastic-plastic idealizations. In plasticity theory, dilation is related to plastic strain as dictated by the flow rule. The amount of dilation is commonly specified in terms of the dilation angle (ϕ^*), which may assume values between zero and the friction angle (ϕ). The latter value occurs in the case of associated plastic flow. Dilation angles can be experimentally determined in the laboratory by triaxial testing (Ogawa and Lo, 1987, p. 103).

The behavior of tuff is only approximated by idealized elastic-plastic behavior. Although dilation is expected to occur in overstressed tuff, it may result from formation of new fracture

surfaces, sliding on rough fracture surface, and block rotations rather than ideal plastic flow.

When ground-support interaction analysis is used to determine ground pressure acting on the liner, use of a dilational model will increase the calculated ground pressure in the inelastic region because the liner must resist expansion of the rock into the opening. Hence, it is conservative to assume associated plastic flow, with the dilation angle maximized (equal to the friction angle). Given the difficulty of assessing the dilation angle in situ at rock mass scale, such conservatism is warranted. In practice, dilation in the confined rock mass behind the liner tends to increase the normal force on rough fracture surfaces, which will actually contribute to the overall opening stability and may reduce loads on the liner.

In general the ground reaction curve is affected by initial ground support or reinforcement (rock bolts, shotcrete, etc.). The effect is to strengthen the rock mass and reduce displacements, lowering the ground reaction curve and the equilibrium pressure on the liner. In this methodology, the beneficial contribution of the initial support is not considered in calculations of liner loads, an added conservatism.

Example Problem

The bottom of the example shaft was investigated to illustrate the application of ground-support interaction analysis. This location was selected because the strength of the Calico Hills Unit is relatively low and the ground stresses are high. A Mohr-Coulomb model was used to represent the strength of the rock mass. Detournay and St. John (1988) give the equations required to calculate inelastic displacements for a cylindrical hole in a dilational Mohr-Coulomb material. The calculation sequence necessary to develop the ground reaction curve is generally that presented by Brady and Brown (1985), but has been modified for a dilational Mohr-Coulomb material. Figure 4-2 outlines this calculation sequence, which incorporates the following steps.

Step — **Calculation Sequence for Ground Reaction Curve**

1. $$T = R_p/R = \left[(1-\sin\phi)\,\frac{(P + c.\cot\phi)}{(p + c.\cot\phi)}\right]^{\frac{1-\sin\phi}{2\sin\phi}}$$ (see Eq. 4)

2. If $R_p \leq R$; $U_o = 1$ and

$$U = R\,(p-P)/2G.$$

If $R_p > R$; $U_o = 1 + [(\lambda+2K_p+2K_p^*)/(K_p^*+1)(K_p^*+K_p)][T^{(1+K_p^*)} - 1]$

$$+ [(\lambda)/(K_p-1)(K_p^*+K_p)][T^{(1-K_p)} - 1]$$

$$U = (Rq/2G)U_o$$

where

$K_p = (1+\sin\phi)/(1-\sin\phi)$

$K_p^* = (1+\sin\phi^*)/(1-\sin\phi^*)$

$\lambda = (K_p - 1)(K_p^*-1) + (1-2\upsilon)(K_p + 1)(K_p^* + 1).$

(Detournay and St. John, 1988, p. 129)

3. $K_s = E' [R_p^2-R^2]/[(1+\upsilon') [(1-2\upsilon')R^2+R_p^2]]$

where

K_s = liner stiffness.

(Brady and Brown, 1985, p. 496)

Figure 4-2. Calculation Sequence for Preparing Ground Reaction Curves Using a Dilational Mohr-Coulomb Model

1. Calculate normalized radius of inelastic zone (R_p/R) from mean stress (P), internal pressure (p), cohesion (c), and angle of internal friction (ϕ). This calculation is performed for various internal pressures.

2. Determine whether behavior is elastic or inelastic. For each calculation, if the normalized average radius of the inelastic zone is less than 1 ($R_p < R$), no inelastic zone will form. In this case, the elastic solution prevails and can be used to calculate the displacement. This will occur at internal pressures sufficient to prevent inelastic behavior and will generate the linear part of the ground curve.

   If $R_p > R$, a plastic zone will form with radius R_p. The plastic zone will dilate according to the previously selected dilation angle ϕ^*.

   Normalized displacement (U_o) can be converted to absolute displacement (U).

3. Calculate support stiffness (K_s).

A Mohr-Coulomb model was selected for the example problem for two reasons: (1) this type of model is well established in the literature and is well understood and (2) Mohr-Coulomb parameters were available in the RIB at the time of this writing. The same calculation sequence may be used regardless of the yield criteria. Brady and Brown (1985) describe in detail the development of ground reaction curves using non-linear parameters. The designer should use whichever yield criteria are recommended in the approved data base.

A conservative, uniform in situ stress value of 8.23 MPa was used in the example, which is the highest horizontal stress value given in Table A-3, (Appendix A). Rock properties are those for the Calico Hills

Formation selected from Table A-4 (CH1); a modulus of elasticity (E) of 3.6 GPa and a compressive strength (q) of 13.5 MPa were used. Typical values for concrete properties were used (E' = 28 GPa, f'_c = 34.5 MPa). A trial lining thickness of 0.3 m (12 in.) was used for the calculations. (Note that because of overbreak, the actual liner will vary in thickness.)

Figure 4-3 shows the results of the analysis for two different assumptions about the dilation of the rock mass in the inelastic zone: (1) no dilation and (2) dilation = friction angle (ϕ) = 7.6°. The variation in dilation has no visible effect on the results of the analysis because (1) the friction angle (ϕ) (and therefore the maximum possible dilation angle (ϕ^*) of the Calico Hills Unit) is low and (2) only a very limited region of overstress develops, limiting the volume of material able to dilate.

The results of this example ground-support interaction analysis indicate the following.

1. With the data selected for the example problem, elastic behavior predominates, even in the Calico Hills Formation at the shaft bottom. This example analysis would not be greatly affected if inelastic behavior was ignored, a conclusion which is further substantiated by the results of Appendix C.

2. Theoretically, a uniform internal pressure (referred to as limiting pressure in Figure 4-3) of 1.28 MPa or greater would provide sufficient confinement to prevent inelastic rock behavior, provided it was applied early.

3. If the trial 0.3 m-thick liner with a modulus of 28 GPa is installed after 85% of the elastic displacement has occurred, nonlinear rock behavior essentially will be prevented.

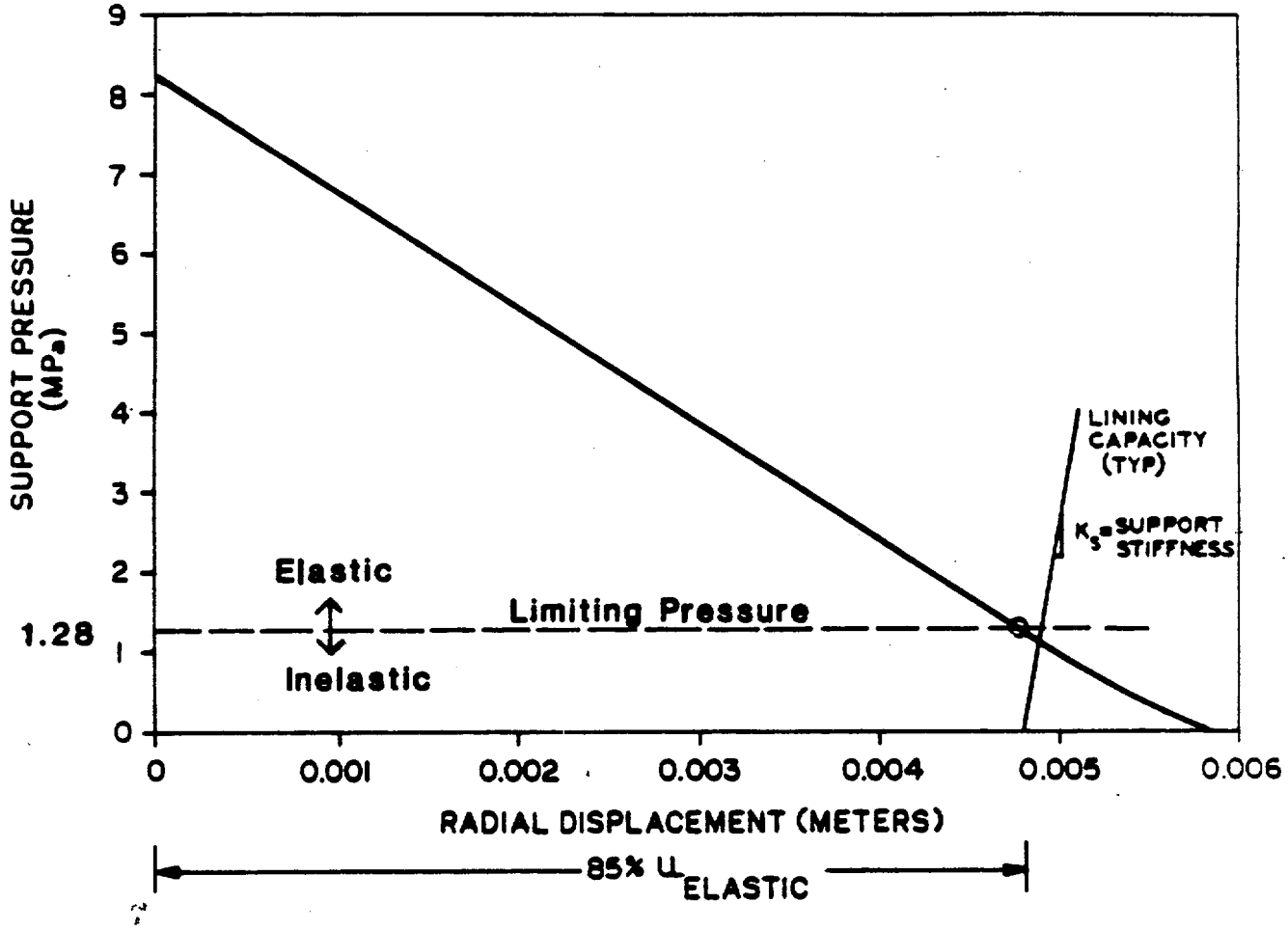

Figure 4-3. Example Ground Reaction Curve at the Bottom of the Example Shaft in the Calico Hills Formation (Location CH from Figure 1-2).

4. Dilation in the relaxed zone has a negligible effect on the pressure on the liner in this case.

Ground-support interaction analysis becomes complex when stresses are anisotropic, and such problems are more readily handled using elastic-plastic finite-element methods. Appendix C describes such a calculation. Engineering judgement must be applied in selecting the type of analysis suited to a given set of conditions.

4.2.2 Ground Pressure Assumptions

If the behavior mode analysis shows that the rock remains in the elastic regime, then no support from the liner is required. Ground pressures generated on the liner will depend entirely on when it is installed, as discussed in Section 3.4. The liner will still be required for its other functions mentioned in Section 2.2.1. If the behavior mode analysis shows that inelastic behavior is a possibility, then support will be required. The classic elastic-plastic method assumes that the maximum pressure the liner is likely to experience is the uniform internal pressure required to confine the rock sufficiently to prevent inelastic behavior (e.g., Hustrulid, 1984; Abel et al., 1979). This calculation is readily performed both in the uniform pressure case and in the anisotropic case. In practice, it is not likely that the liner will generate a uniform internal pressure, nor is it likely to be installed sufficiently early to prevent any possible inelastic behavior. As shown in Section 3.3, anisotropic field stresses will result in an oval inelastic zone that will cause nonuniform loads on the liner. Currently, there is no rigorous closed-form solution for calculating liner stresses when there are localized dilatant inelastic zones caused by overstress of the rock at the shaft periphery under nonuniform stress conditions. In this case, appropriate numerical methods such as nonlinear finite-element analysis may be used. There are also several approximations for addressing this problem using closed-form equations, three of which are discussed below.

The first approximation is to neglect the elliptical shape of the inelastic zone and to work with its mean radius. This approach is acceptable if stress nonuniformity is believed to be small and if conservative in situ stress values are selected; i.e., the greater of the two horizontal stress components should be used to calculate the radius of the inelastic zone.

A second approximation is to assume that no additional ground pressure is produced by dilation of the inelastic zone itself, which is a reasonable simplifying assumption if the inelastic zone is small and stabilized by rock bolts before the liner is installed. In this case the load on the liner becomes a percentage of the original in situ stress, the percentage being a function of the timing of support installation. It is not necessary to assume uniform pressure because suitable closed-form equations exist for nonuniform pressures. In order to implement this strategy, it is necessary to establish percentages of convergence as a function of distance from the face, as in Section 3.4.

The third approximation is to calculate displacements of the shaft walls parallel to the principal stress axes using published design charts based on dilational Mohr-Coulomb theory (Detournay and St. John, 1988). These would be applied as boundary conditions for analysis of the liner as an independent structure. Although displacements along principal axes are readily computed in this manner even in an anisotropic stress field, liner stresses are not. When the rock around the shaft circumference is partially inelastic, the liner must conform to a rock distortion with a complex shape, making stress analysis difficult.

For complex problems with substantial inelastic behavior, the closed-form approach loses its simplicity. It is more appropriate to use a nonlinear numerical method, such as finite-element analysis, to more closely approximate the interaction between the liner and the surrounding rock. This has been done in Appendix C.

The results of Appendix C coupled with the conclusions of Section 4.2.1 indicate that the second approach described above is reasonable for the conditions assumed in the example analysis. Designers should use the method that suits a particular analysis.

Example Problem

In our example problem in Section 4.2.1, it has been shown that possible inelastic zones are quite limited in extent and that inelastic behavior does not dominate the design. In this case, static pressure is determined using the elastic approximation discussed as the second approach above. To ensure a conservative design, two in situ stress cases are analyzed when they are combined with thermal and seismic loading. The in situ stress cases, which were taken from Table A-3, are the following.

- Case 1 (uniform stress)
- Case 2 (nonuniform case, maximum horizontal stress difference)

In both cases, 15% of the appropriate in situ stress value was taken. Rationale for selecting this percentage was presented in Section 3.4. If a limited inelastic zone is predicted, it will be assumed to be stabilized by initial support installed by the shaft sinking contractor. Appendix C supports the adequacy of the elastic simplification for this example.

Table 4-1 shows the values from the two cases used in the example. The principal ground pressure direction is assumed to be the same as the principal in situ stress direction (N30°E).

TABLE 4-1

GROUND PRESSURE CASES[a]

Location[b]	Case 1 (MPa) $\sigma_1 = \sigma_3$	Case 2 (MPa) σ_1	Case 2 (MPa) σ_3
PT	0.20	0.20	0.08
TS	1.13	1.13	0.42
CH	1.23	1.23	0.46

[a]From Table A-3; based on 15% of in situ stress.
[b]See Figure 1-2 for locations.

4.3 SEISMIC*

A seismic event, whether associated with an earthquake or a UNE, generates elastic waves that propagate outward from the source. Body waves may be classified as P (dilational or compressional) waves that consist of alternating compression and tension in the transmission medium, or S (shear or distortional) waves that consist of oscillating shears. Distortional ground motions are typically resolved into S_H waves with horizontal particle motions and S_V waves with motions in a vertical plane. Both shear motions are orthogonal to the incident wave direction as illustrated in Figure 4-4. By definition, particle motions due to S_V waves are in a vertical plane, but not necessarily in a vertical direction. P waves have an inherently higher velocity of propagation than S waves and will always arrive first at the shaft location.

* The seismic design methodology in this guide was largely adapted for the NNWSI Project from that prepared for the Salt Repository Project Office (Fluor/PB-KBB, 1987) and is consistent with the seismic data base prepared by the E.S. Seismic Design Basis Working Group (SNL, in preparation a).

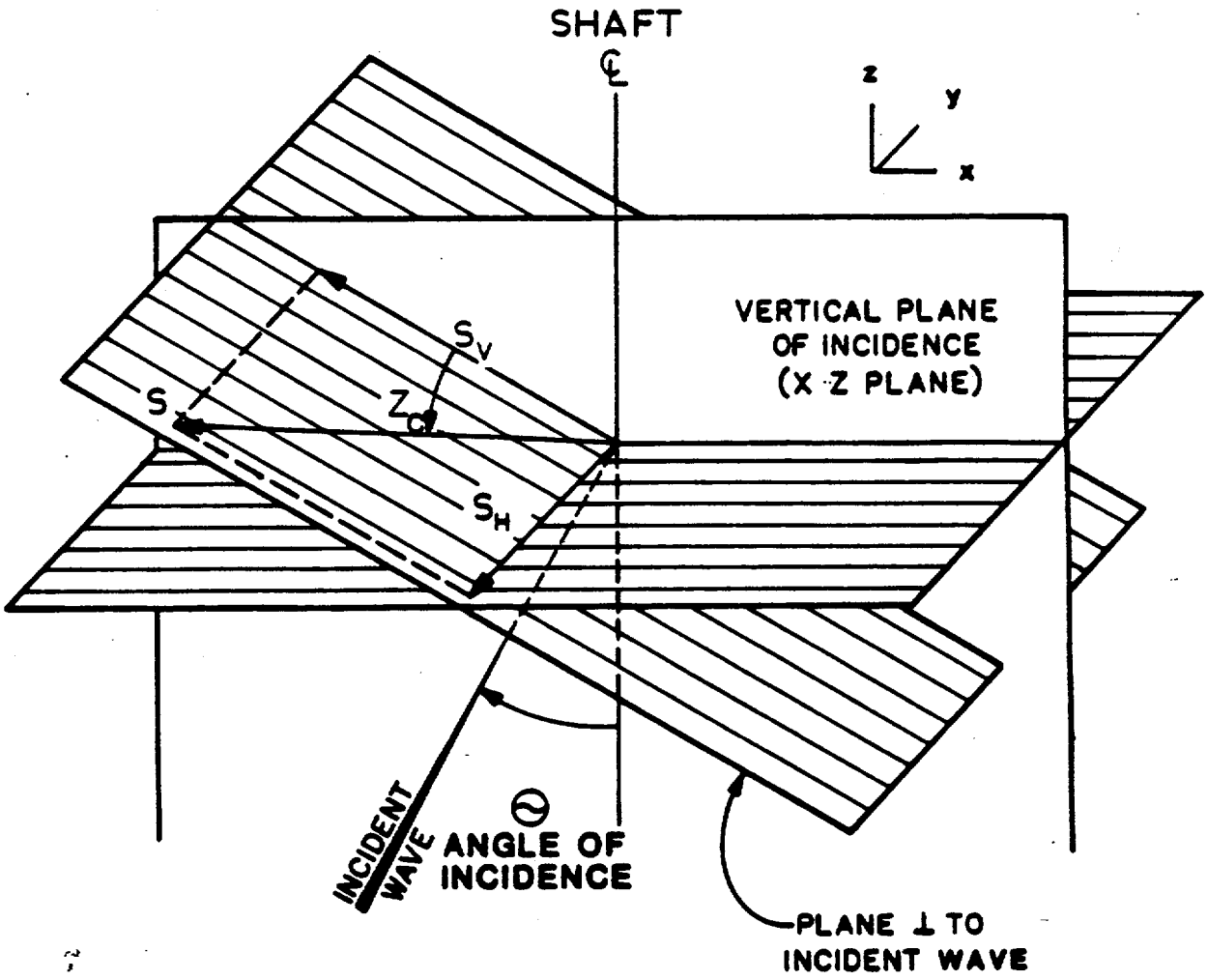

Figure 4-4. Resolution of Shear Wave Motion into S_V and S_H Components

The elastic waves from a seismic event induce transient stresses and strains in a rock mass and, hence, in any embedded structure such as a shaft. The effects on the structure will depend upon a number of parameters, including the physical properties of the rock and the structure and the amplitude, frequency, and duration of the ground motion. Seismic events also may impose direct shear displacements on the shaft liner if they cause movement along faults that transect the shaft axis. Some possible deformation modes resulting from seismic wave action are shown in Figure 4-5, along with the associated strains required for analysis of these deformations.

Unlike surface structures such as buildings, which tend to move and deform independently when excited by earthquake-induced ground motions, shaft liners move and distort compatibly with the ground in which they are embedded. This implies that ground-structure interaction analysis is required. Providing that the wavelength of the seismic pulse is relatively large with respect to the opening diameter (i.e., if the rise time of the seismic impulse is long relative to the transit time of the wavefront across the opening), such analysis can be based on static methods because dynamic amplification will be small. Hendron and Fernandez (1983) propose that there will be little dynamic amplification if the wavelength is at least 8 opening diameters. Because the wavelength associated with the ground motion peak from an earthquake is generally at least 10 times the diameter of a typical shaft, "pseudo-static" analysis will yield sufficient accuracy for most initial liner analyses (see example problem). The designer should consult the Project seismic data base for wavelengths associated with peak ground motions to ensure that the pseudostatic assumption is justified for the opening sizes considered.

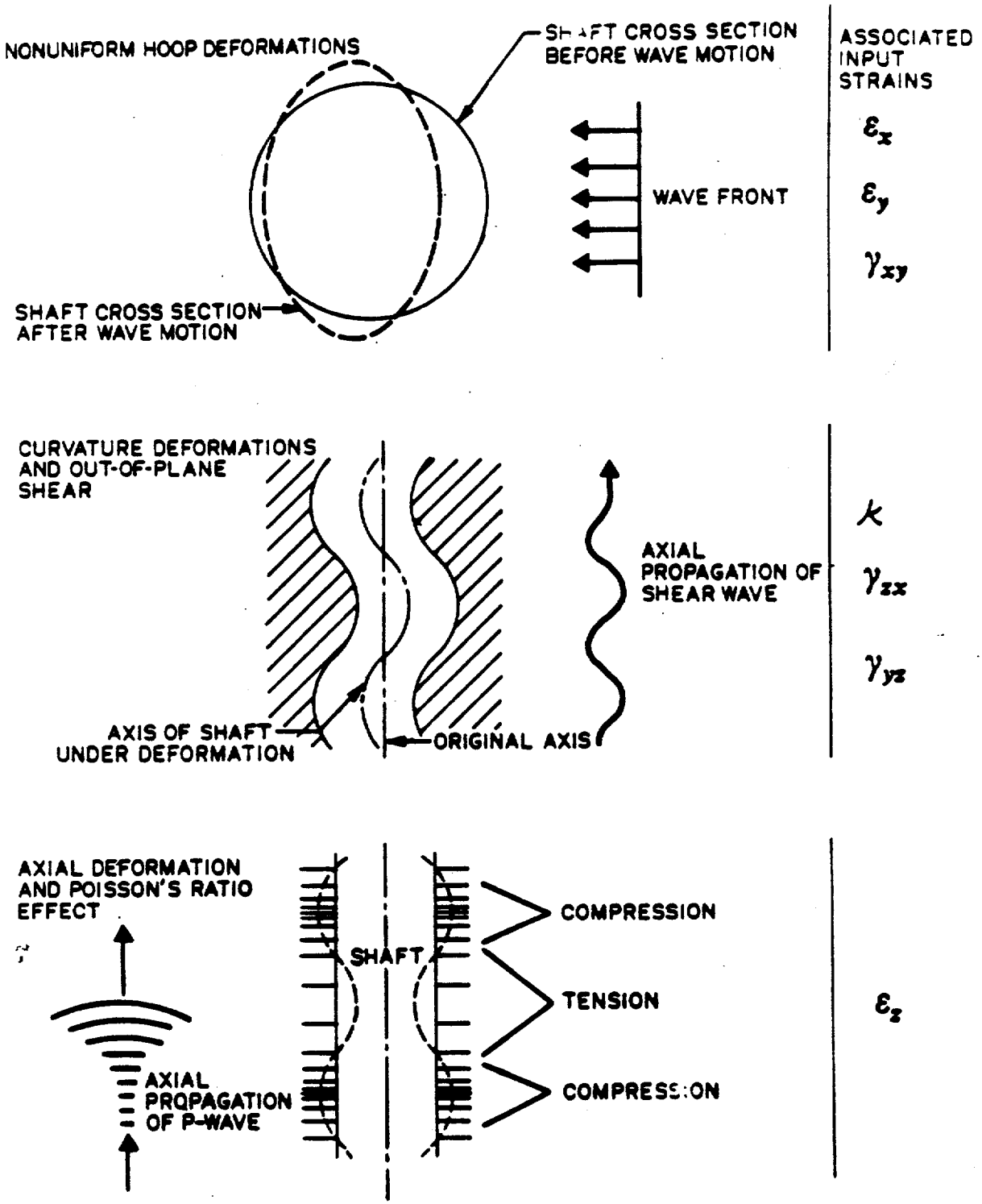

Figure 4-5. Schematic Diagram of Possible Deformation Modes Resulting from Seismic Wave Action (After Owen and Scholl, 1981)

The general procedure for pseudostatic analysis involves the following.

1. Defining ground motions for a control point (usually the intersection of the shaft axis with either the bedrock or ground surface). A deterministic approach can be followed in which the epicentral location and maximum credible magnitude of earthquakes on known faults are estimated, and control motions are calculated using a suitable distance-attenuation function. Alternately, a probabilistic approach may be used in which the spatial and temporal occurrence of earthquakes within each potential earthquake source zone is represented by probabilistic models. Using suitable attenuation functions for each travel path, the annual probability of exceeding a given level of ground motions at the control point can be developed. Defining control ground motions is one of the most difficult parts of the design, and a level of conservatism appropriate to the level of uncertainty and consistent with liner functions should be incorporated in these values. For pseudostatic analysis, the required control motion parameters are particle velocity and acceleration, and three orthogonal components (two horizontal and one vertical) are required for each parameter.

2. Developing a suitable depth-attenuation relationship at the site so that the magnitude of ground motions at various design points along the shaft can be determined from the control motion. This is especially important for soil sites, where dynamic modeling may be appropriate.

3. Determining the ground motion components expected to arrive at the design points, which may include P waves, horizontal S_H and vertical S_V components of S waves, and surface waves. The contribution of each waveform to the control motion must be assessed, and appropriate angles of incidence of the waveforms must be determined.

4. Calculating a tensor of free-field strains at each design point for each waveform using equations for strain components in terms of peak particle velocities, propagation velocities, and angles of incidence. In addition to the strain tensor, curvatures are calculated from accelerations.

5. Assessing the combined effects of different waveforms on the liner. Simplified design approaches commonly assume that all the seismic energy may be assigned to a single, critically oriented waveform or alternately that the effects of each waveform may be analyzed separately (ASCE, 1983). Because of their different propagation velocities, the effects of P and S waves may be assumed to occur separately if the epicentral distance from the shaft is large. Although S_H and S_V waves may occur simultaneously because they have the same propagation velocity, the effects from these waves are likely to be out of phase. For example, the effects due to acceleration (curvatures) will not peak at the same time as the effects due to particle velocities (strains).

   Such assumptions may not always be conservative. Complete P- and S-wave separation cannot be assumed at Yucca Mountain. Some overlap may occur because of the multiplicity of potential seismic sources in close proximity to the shaft. It is possible that several waveforms may act on the shaft simultaneously, and there will be some superposition of effects.

   Newmark and Hall (1977) have suggested that the three orthogonal components of earthquake input motion can be considered to be randomly phased; i.e., the three control motions have statistical independence. Thus, it is an oversimplification to treat them separately. However, because there is only a small probability of the maximum responses occurring simultaneously, they should be combined probabilistically in some fashion rather

than by direct vectorial combination, which would be overly conservative. Rather than a full probabilistic treatment, Newmark and Hall (1977) recommend a conservative simplified approach commonly called the 100-40-40 Combination Rule. Extending this rule to structural effects from earthquakes, 100% of the largest peak effect (e.g. strain in a given direction) from any of the three seismic wave components plus 40 percent of the peak effects from each of the other two components are combined as follows:

$$Z_c = 100\% Z_1 + 40\% Z_2 + 40\% Z_3 \quad (6)$$

where Z_c is the combined value, Z_1 is one component, and Z_2 and Z_3 are the other two components.

The above is suitable for free-field strains. The designer is cautioned that in some cases a vector sum is involved to combine effects acting in different directions. In all cases, the objective is to determine the combination that maximizes a particular structural effect (e.g., strain, hoop stress, maximum principal stress, etc.). The procedure involves trying all possible combinations to determine the one yielding the maximum effect. For example the following is one of the combinations appropriate for bending strains where Z_1 is the S_H component, and Z_2 and Z_3 are from the P and S_V waves.

$$Z_c = \sqrt{(Z_1)^2 + (0.4)^2 [(Z_2)^2 + (Z_3)^2]} \quad (6a)$$

Once all possible combinations are determined, the procedure involves determining the one yielding the maximum effect. Items 1 through 4 are outside the scope of this document and will be provided in the Project seismic data base. The designer should select strain tensors and curvatures at design points from tabulated information provided in the authorized seismic data base (SNL, in preparation a).

A fully dynamic analysis follows the same general approach but requires input from a complete time history of the ground motion.

Loads for pseudostatic analysis consist of a complete free-field stress or strain tensor at design locations along the shaft and curvatures to account for relative displacements of these points. Seismic loads differ from the other loads in that they are transient and oscillate between positive and negative values.

Complete seismic loads for input to the shaft liner analysis will comprise the following.

- In-plane normal strain, ϵ_x
- In-plane normal strain, ϵ_y
- Axial strain, ϵ_z
- In-plane shear strain, γ_{xy}
- Out-of-plane shear strain, γ_{xz}
- Out-of-plane shear strain, γ_{yz}
- Curvature, k (or alternately, bending strain, ϵ_b)

(Note: In this case, the plane is the horizontal (x-y) plane, representing a cross section of the shaft.)

These strains and curvatures can be calculated from ground motion parameters and will be specified as combined strains resulting from critical seismic load combinations, using the 100-40-40 rule.

4.4 INDUCED THERMAL

Because the shafts are to be designed for use during the operational phase of the repository, the load induced as a result of thermal expansion of the rock as it is heated by emplaced waste is an important component of the total load on the shaft liner. Because of the complexities of the waste emplacement geometry relative to the shaft

location, it is not practical to assess the induced thermal loads without computer modeling. Various modeling methods have been applied to this problem. However, the general procedure for solution of the problem comprises the following four steps.

1. Select computer models. Thermal/mechanical analysis for the purpose of shaft design typically involves two uncoupled steps. First, the spatial and temporal rock temperature distribution induced by the waste must be predicted. Second, the predicted temperatures are used to calculate thermally induced stresses and/or strains at the shaft location. Some computer models allow coupled "thermomechanical" analysis to be performed.

2. Prepare input data. The spatial layout, thermal loading, and emplacement sequence of the waste emplacement areas relative to the shaft must be determined. This information should be derived from the approved data base. Figure 4-6 illustrates a conceptual layout of the repository at Yucca Mountain and shows the planned sequence for initial waste emplacement.

   One important decision that must be made in this step is the type of material behavior to be represented in the model. The thermal and mechanical behavior of the rock will be nonlinear, but may initially be approximated by linear models. As more information becomes available the project will achieve a better understanding of rock behavior, and may turn to nonlinear models to more closely approximate this behavior.

   The thermal/mechanical analysis presented in Appendix B uses both a linear thermal model, and a linear equivalent-continuum mechanical model in which the rock mass is represented as an idealized elastic medium. Equivalent (rock mass) properties have been assigned to this medium to compensate for the "softening" effect of discontinuities, which are not treated

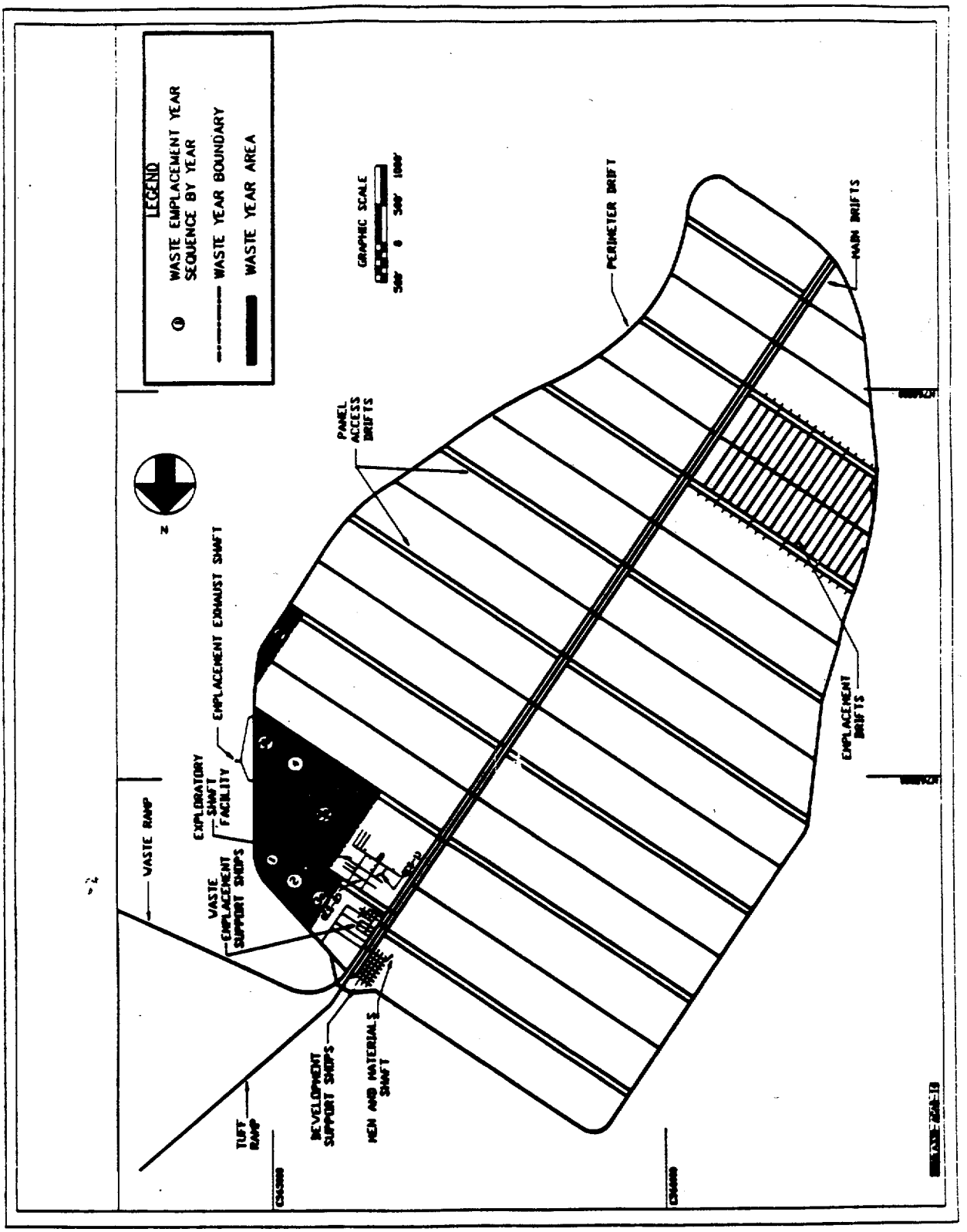

Figure 4-6. Plan View of Repository Showing Planned Sequence for Waste Emplacement for the First 5 Years (SNL, 1987).

explicitly. Nonlinear equivalent continuum models or, alternately, discontinuum models that explicitly model the joints may optionally be used. Also, nonlinear thermal models may be desired.

3. Establish initial conditions and develop model. The initial conditions may be assumed to be zero initial temperature and stress, if the behavior of the rock mass is considered to be linear over the range of temperature and stresses of concern, because the analysis is concerned with changes rather than absolute values. Specific details of the model will depend on the design requirements and the experience of the individual modeler. In general, one-dimensional thermal models that calculate temperature and stress as a function of depth are unsatisfactory because they cannot account for the distribution of waste relative to the shaft. Depending on the specific geometry of waste emplacement relative to the shaft, plane strain, axisymmetric, or complete three-dimensional analysis will be required.

4. Compute temperature distribution and thermally induced stresses (strains) at the shaft location. Appendix B presents a sample thermal/mechanical analysis. In the case investigated, the plane strain assumption was considered appropriate.

Complete thermal loads for input to the shaft liner analysis will comprise the following.

- In-plane normal stress, σ_x
- In-plane normal stress, σ_y
- Axial strain, ϵ_z
- In-plane shear stress, τ_{xy}
- Out-of-plane shear stress, τ_{xz}

- Out-of-plane shear stress, τ_{yz}
- Curvature, k (or bending strain)

Note that this represents a complete stress tensor, except axial strain is presented instead of axial stress for reasons explained later. Curvature is defined as the second derivative of the horizontal displacement, with respect to depth (d^2u/dz^2), and may be calculated as discussed in Section 7.3 of Appendix B. Alternately, strains can be used as suggested in Appendix B.

Most computer models will directly calculate the induced axial stresses. It may be necessary, however, to compute the strain along the shaft axis. This may be computed directly from the distribution of vertical displacements along the axis of the shaft, which may be available directly from modeling results, or calculated from the induced stresses using the following equation:

$$\varepsilon_z = (\sigma_z - \nu(\sigma_x + \sigma_y))/E - \alpha\Delta T, \qquad (7)$$

in which α is the coefficient of linear thermal expansion of the rock and ΔT the temperature change of the shaft location.

Note that Equation 7 defines the axial strain in the rock mass. The axial strain in the shaft will be different if the coefficients of thermal expansion and the temperature of the rock mass and the liner differ significantly. Current conceptual designs show significant standoff (~100 m) between any shaft and the waste emplacement areas. During the preclosure period, temperature at the shaft location will rise only several degrees Celcius (Appendix B), and the thermal strain portion of the equation is likely to be minor. Final design of the repository should include an analysis of the shaft pillar dimensions required to limit thermal loads on the shaft liner to reasonable values.

4.5 LOAD COMBINATIONS

This section discusses a suggested method for evaluating the combined loads that influence the shaft. Chapter 5 presents the methodology for calculating critical stresses that develop in the liner from the combined loads. Some mention of stress analysis is required at this point to explain the development of load combinations.

In general there are two methods for evaluating simultaneous effects: (1) direct combination, in which the effects may be transformed and combined and then a single liner stress calculation performed and (2) superposition of liner stresses, in which a separate stress calculation can be performed for each load condition and the resulting stresses linearly superimposed. If linear elastic stress analysis is performed, the results of the two methods will be identical according to the principle of superposition (Timoshenko and Goodier, 1970).

In this simplified methodology, a mix of these two methods is used to emphasize important differences between the different loads. "Static" loads, including ground pressures and thermal loads, are combined following the first method. Liner stresses due to combined static and dynamic loads are evaluated using the second method. The rationale for this distinction between static and dynamic loads consists of the following points.

- Static loads represent a relatively steady preload that must be sustained for long periods of time and upon which the oscillatory dynamic transient is applied. Hence, static loads remain after dynamic loads have passed.

- Static loads act in specified directions. (Although uncertainty currently exists about determining these directions, it will be reduced in the future with thermal analysis and in situ stress measurements.) There are numerous potential seismic

sources at Yucca Mountain, and dynamic effects must be assumed to arrive from the direction resulting in the highest combined stresses, because this uncertainty is likely to remain.

- Static rock properties are used in models of rock structures under the influence of static loads, but dynamic rock properties are used for dynamic modeling situations.

In general, the principal stress directions for in situ and thermal stresses are different, and principal stresses must be transformed to the xyz coordinate system selected for liner stress analysis. For shaft design situations, the vertical (z) axis is approximately a principal stress direction for both in situ and thermal stress. Thus, stress transformation involves rotation about the (z) axis. For loads that affect a horizontal section of the shaft, the biaxial transformation equations apply (e.g., Brady and Brown, 1985, p. 28). In transforming from principal to xy stress components, there is no initial shear stress and the equations become

$$\sigma_x = 1/2\ (\sigma_1 + \sigma_3) + 1/2\ (\sigma_1 - \sigma_3) \cos 2\alpha \quad (8)$$

$$\sigma_y = 1/2\ (\sigma_1 + \sigma_3) - 1/2\ (\sigma_1 - \sigma_3) \cos 2\alpha \quad (9)$$

$$\tau_{xy} = - 1/2\ (\sigma_1 - \sigma_3) \sin 2\alpha, \quad (10)$$

where α is the angle between σ_1 and σ_x directions. Note that the minimum principal stress has been designated "σ_3" rather than "σ_2". This notation is used here for plane strain and biaxial problems even though there may be only two stress axes.

The designer must consider all possible combinations of seismic, thermal, and ground pressure loads to ensure that the liner will survive the worst-case combination.

Example Problem

Table 4-2 shows the principal directions of static loads for the example problem. The ground pressure direction coincides with the mean in situ stress direction (see Table A-2, Appendix A). The thermal load direction is the direction of maximum emplacement density relative to the shaft. If the in situ stress direction is arbitrarily taken as the x-direction, then $\alpha = 0$ for ground pressure and Equations 8 through 10 reduce to

$$\sigma_x = \sigma_1$$
$$\sigma_y = \sigma_3$$
$$\tau_{xy} = 0.$$

The maximum thermal loads are oriented almost orthogonally to the maximum ground pressure. Hence, for thermal loads, Equations 8 through 10 reduce to

$$\sigma_y = \sigma_1$$
$$\sigma_x = \sigma_3$$
$$\tau_{xy} = 0.$$

TABLE 4-2

ORIENTATIONS OF STATIC
LOADS FOR EXAMPLE PROBLEM

Loads	Maximum	Minimum
Ground Pressure	N30E(x)	N60W(y)
Thermal	N60W(y)	N30E(x)

Because of the multiplicity of potential sources for seismic events, no single azimuth of incidence can be defined for seismic loading, and it was assumed that a seismic impulse arrives from the direction that results in the maximum combined static and seismic stresses. This is accomplished by keeping static and seismic loads separate so that the peak liner stresses resulting from each can be calculated separately and combined properly, as explained in the next section.

Table 4-3 shows the load cases examined in the example analysis. Two ground pressure cases are examined: STATIC-1, a uniform ground pressure and STATIC-2, a nonuniform pressure. In two other cases (STATIC-3 and STATIC-4) thermal loads are combined with uniform and nonuniform ground pressure. Table 4-4 shows values of ground pressure and thermal loads.

Seismic loads may only be specified as equivalent free-field static strains if pseudostatic analysis is appropriate. The example shaft is 12 ft (3.66 m) in diameter. As discussed in section 4.3, the minimum wave length for pseudostatic analysis is 8 times the opening diameter, or approximately 30m. The minimum seismic velocity in the geologic units traversed by the shaft occurs in the PT Unit, which has a shear wave velocity of 1040 m/s (SNL, in preparation a). Since:

$$c = f\lambda \qquad (11)$$

(Ref: Sears and Zemansky, 1970)

where

c = seismic velocity
f = frequency
λ = wavelength

(in consistent units)

then $f = c/\lambda = (1040 \text{ m/s})/30\text{m} = 35$ Hz.

TABLE 4-3

LOAD CASES FOR EXAMPLE PROBLEM

Load Case	Loads	Time Period
STATIC-1	Uniform ground	Pre-emplacement
STATIC-2	Anisotropic ground	Pre-emplacement
STATIC-3	Uniform ground and thermal	100 yrs*
STATIC-4	Anisotropic ground and thermal	100 yrs*
SEISMIC-1	Orthogonal Seismic	Preclosure
SEISMIC-2	Inclined Seismic	Preclosure

*Until approximately 100 years after first emplacement

Hence, if the peak ground motion occurs at frequencies below about 35 Hz, then pseudostatic analysis is justified. Seismic design spectra in project literature (SNL, 1984) clearly show peak ground motions occur at frequencies below 1 Hz, with a substantial decrease in magnitude above 6 Hz. The pseudostatic assumption is clearly justified for the example problem.

Two seismic cases are considered. SEISMIC-1 is an orthogonal seismic case based on a simplified assumption that all dilational energy is concentrated in a single P wave propagating axially, and all distortional energy is concentrated in a single S_H wave form propagating horizontally. P and S waves are assumed to be in phase and are simultaneously considered. This simplified example is representative of assumptions that have been used for many years by civil engineers to analyze the response of buried pipes and other structural components to ground motions (ASCE, 1983). This approach is included here for illustrative purposes although it is not recommended in this methodology because a detailed data base is available (SNL, in preparation a), permitting use of a more precise approach.

TABLE 4-4

FREE-FIELD STATIC LOADS FOR EXAMPLE PROBLEM

Load Case	Ground[a] σ_x (MPa)	Ground[a] σ_y (MPa)	Thermal[b] x	Thermal[b] y	Thermal[b] zy	Thermal[b] z
			PT			
	Stresses (MPa)			Strains ($\times 10^{-6}$)		
STATIC -1	0.20	0.20	--	--	--	--
STATIC -2	0.20	0.08	--	--	--	--
STATIC -3	0.20	0.20	0	40	32	-20
STATIC -4	0.20	0.08	0	40	32	-20
			TS-2			
	Stresses (MPa)					Strain ($\times 10^{-6}$)
STATIC -1	1.13	1.13	--	--	--	--
STATIC -2	1.13	0.42	--	--	--	--
STATIC -3	1.13	1.13	-0.05	1.60	0.50	-150
STATIC -4	1.13	0.42	-0.05	1.60	0.50	-150
			CH			
	Stresses (MPa)			Strains ($\times 10^{-6}$)		
STATIC -1	1.23	1.23	--	--	--	--
STATIC -2	1.23	0.46	--	--	--	--
STATIC -3	1.23	1.23	0	91	32	-120
STATIC -4	1.23	0.46	0	91	32	-120

a. Ground pressure from Table 4-1
b. Thermal loads from Appendix B; in PT and CH units these are strains as discussed in Appendix B.
c. The x-direction is taken as N30E for this example
d. Compression positive

Case SEISMIC-2 (inclined seismic) is based on inclined P, S_V, and S_H waves. It is assumed that these waves follow the same path, with an incidence cycle of 30° from vertical. The waves are assumed to be randomly phased, so their effects may be combined using the 100-40-40 rule discussed in Section 4.3. It should be recognized that different angles of incidence are likely for earthquakes and UNEs and that strains are a function of the assumed angle of incidence. Also, the 100-40-40 combination assumed for the example is not necessarily the most conservative case. Several cases may require analysis to ensure that the most critical combination is selected. Table 4-5 shows the seismic loads for the example problem, taken from Appendix A, Tables A-6 through A-8, which were estimated for this example. Seismic data should be drawn directly from the approved seismic data base.

TABLE 4-5

FREE-FIELD SEISMIC LOADS ASSUMED FOR EXAMPLE PROBLEM[a]

Location[c]	Load Case	Strain (x 10^{-6}) ε_x	ε_y	ε_z	γ_{xy}	γ_{xz}	γ_{yz}[d]	k (1/m)
PT	SEISMIC-1	0	0	67	164	0	0	0
PT	SEISMIC-2[b]	158	0	185	58	214	40	2.36
TS	SEISMIC-1	0	0	44	109	0	0	0
TS	SEISMIC-2[b]	80	0	94	29	108	20	0.61
CH	SEISMIC-1	0	0	67	153	0	0	0
CH	SEISMIC-2[b]	86	0	102	31	117	22	0.70

Notes: [a]Seismic loads taken from Appendix A, Table A-6, A-7 and A-8 (rounded off).
[b]This is a vector sum using the 100-40-40 rule (SNL, in preparation a).
[c]See Figure 1-2 for locations.
[d]40% of the values shown in Appendix A per 100-40-40 rule.

5.0 MECHANICAL ANALYSIS

5.1 INTRODUCTION

In the previous chapter, loads were defined as free-field stresses and strains at the shaft location resulting from combined ground pressure and thermal and seismic effects. Loads have been defined in this fashion for two reasons: (1) to facilitate transforming and combining them and (2) to make them independent of the liner.

Once the loads have been established, a trial liner configuration is selected and its mechanical behavior under the prescribed loads is analyzed. This chapter discusses the four general steps for analyzing the mechanical behavior of a shaft liner.

1. Identify important deformation modes. These modes must reflect the nature and direction of action of the loads and are selected on the basis of experience and engineering judgment.

2. Select or develop mathematical models that represent the deformation modes. These models may be quite simple or extremely complex, depending on the degree of refinement considered necessary in the analysis. The degree of complexity of the models also should be consistent with the quality of input data as determined by the designer.

3. Demonstrate that the assumptions inherent in a particular model will lead to an appropriately safe and conservative design.

4. Analyze the behavior of the liner in each of the different deformation modes, being sure to exercise each model with appropriate load combinations to ensure that the conditions critical to design have been considered.

Typically, the above process is applied iteratively. A trial liner of the minimum practical thickness with little or no reinforcement is selected. Simple models based on conservative assumptions are initially applied. If the results of the analysis meet the criteria, the design is conservative and further analysis may not be required. If, on the other hand, the results fail to meet the criteria, the analysis may be refined to eliminate some of the inherent conservatism. If the refined analysis still fails to meet the criteria, then the design must be revised. The objective of the next two chapters is to define the characteristics of a methodology that formalizes this iterative process. It is recognized that the design process requires a considerable degree of engineering judgment in selecting models, and it is not the intent of this guide to restrict that judgment.

Accordingly, this chapter presents the general framework of a methodology together with a set of closed-form models for liner stress analysis. Linear elastic stress analysis models were selected for several reasons: (1) they permit a simplified analysis of ground/liner interaction behavior under generalized plane strain conditions with nonuniform applied loads (which is useful for situations involving complex load combinations); (2) linear models are considered to be appropriate for initial design of the exploratory shaft liners at the NNWSI site and, when coupled with the other methods and criteria proposed in the guide, will result in a design that is both safe and conservative; and (3) the example problems suggest that accepted allowable stress criteria (Chapter 6) can be met readily at the site with a practical shaft liner design. The designer may select alternate models if they can be shown to be more suitable. If the simplified analyses suggest that unusual design provisions such as heavy reinforcing are required, a more detailed nonlinear analysis should be performed that considers the nonlinear behavior of the concrete. More complex analyses also may be appropriate for detailed performance verification before submittal of the final design for repository licensing. Discussion of such analyses is

beyond the scope of this work, since present indications imply that such steps are unnecessary, as illustrated by the examples in this guide.

In the notation of this section, a distinction is drawn between the rock and the liner and between free-field conditions and those influenced by the proximity of the shaft. The superscript "'" means the quantity applies to the liner. Similarly, "^" means it applies to the free field, which refers to conditions in the rock mass away from the influence of the shaft opening. Additionally, the superscript ~ has been used to denote where effective elastic properties are used. For conditions in which axial strain is constrained (plane strain), the following definition applies:

$$\tilde{E} = \frac{E}{1-\upsilon^2} \; ; \; \tilde{\upsilon} = \frac{\upsilon}{1-\upsilon} \; .$$

In this section the stresses and strains are generally defined relative to a cylindrical coordinate reference, illustrated in Figure 5-1. The reference axis is any horizontal axis in that system (referred to as the x axis in the following discussions). Cartesian and cylindrical components of the stress tensor are shown in Figure 5-2.

5.2 IMPORTANT DEFORMATION MODES

Figure 5-3 schematically illustrates three independent deformation modes: (a) hoop deformation and axial strain, (b) bending, and (c) shear. Hoop and axial deformation are combined because they are always coupled by Poisson's effect.

Hoop deformation is caused by inward radial rock pressure acting on the exterior of the liner and axial compression or extension. The resulting stresses in the liner are referred to as radial and hoop (tangential), stresses. In structural engineering terminology, the hoop stresses arise from thrust and moment. It is not necessary to distinguish between these two sources in this methodology. Design of nonrepository shaft liners has typically been limited to considering only

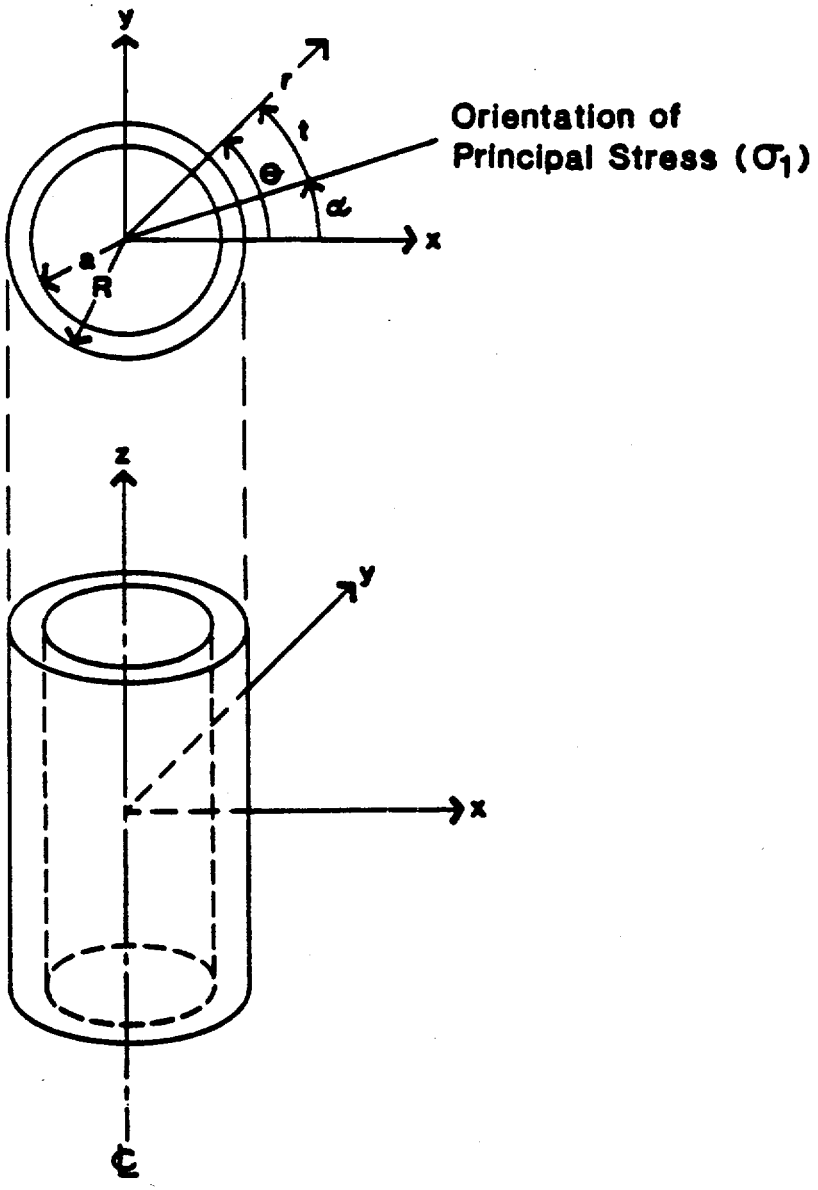

Figure 5-1. Coordinate System for Shaft Liner Analysis

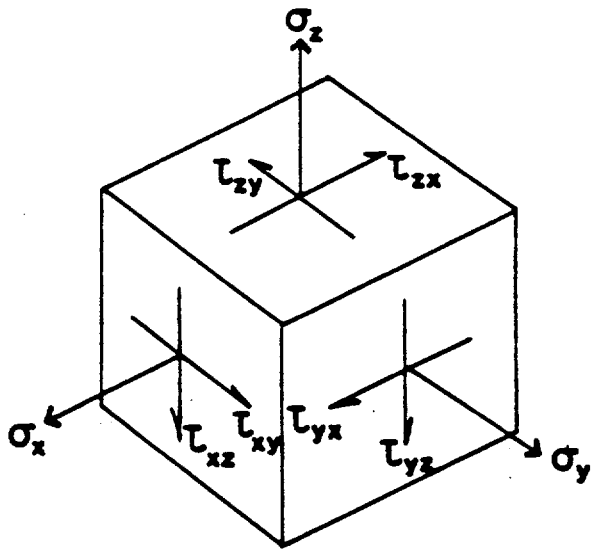

a) Cartesian Components

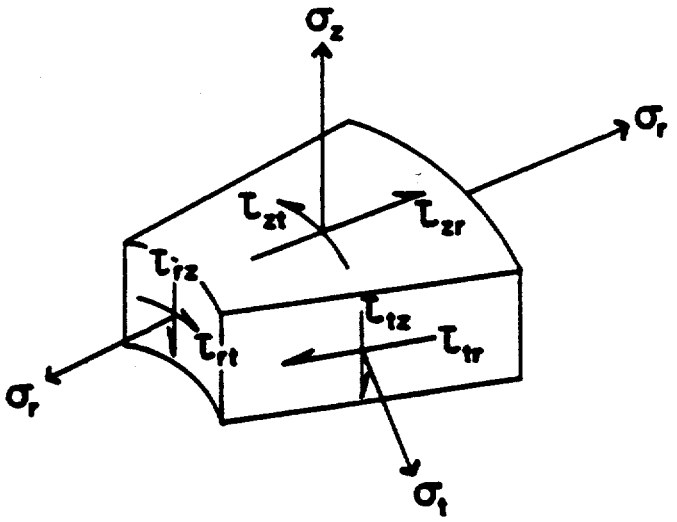

b) Cylindrical Components

Figure 5-2. Cartesian and Cylindrical Components of the Stress Tensor

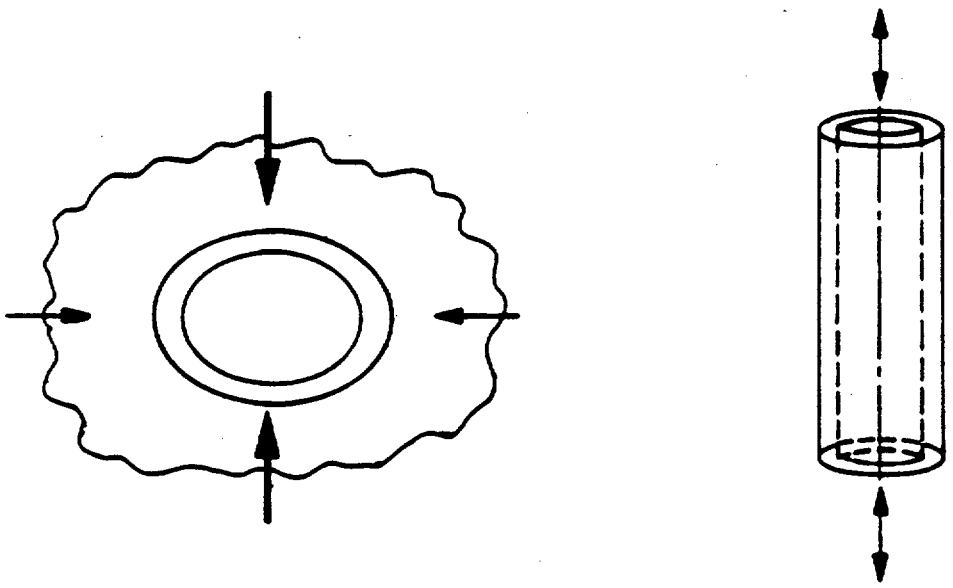

(a) HOOP DEFORMATION AND AXIAL STRAIN

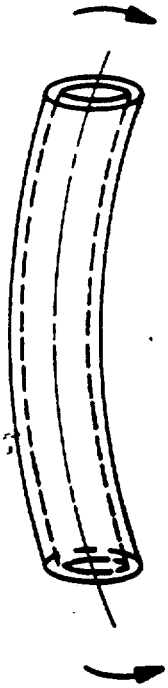

(b) BENDING

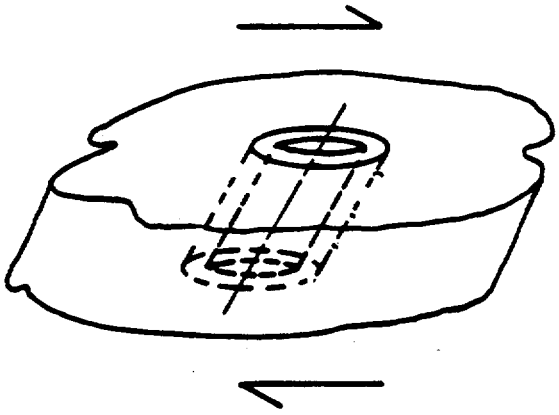

(c) SHEAR

Figure 5-3. Schematic Diagram of Modes of Deformation

hoop deformation, with the implicit assumption that there will be no change in the average axial dimension of the liner. This implies that there will be no vertical stress in the liner, providing it is cast directly against the rock, because the vertical weight of the liner will be supported by the surrounding rock mass. Design of nonrepository shaft liners also has typically ignored curvature and shear unless differential subsidence caused by mining or consolidation is expected.

For repository shaft liners, hoop deformation is also considered the most important mode because it directly relates to the liners structural function, which is to radially confine the wall rock. Other modes are only considered for possible impacts to shaft liner functions.

Even though hoop deformation is likely to dominate, the other modes should be considered because the loads experienced by a repository shaft liner will be complex. In particular, the repository shaft liner may bend or flex as a result of the variation with stratigraphy and depth of stresses and strains associated with thermal loading of the repository and from seismic loading as shown in Figure 4-5. These effects can be enhanced at the edges of the repository and at the interface between different stratigraphic members, so particular attention should be devoted to these locations. Also, shear deformation of the shaft liner may occur as a result of shear strains induced in the rock mass that are associated with thermal and seismic loading.

Stresses induced in a shaft liner experiencing the deformations illustrated in Figure 5-3 may be complex. Figure 5-4 illustrates the typical stresses due to the action of an inclined S_V wave on the lining. The wave form is incident in the x-z plane, and particle motions are confined to this plane, so it contains $\hat{\varepsilon}_x$, $\hat{\varepsilon}_z$, and $\hat{\gamma}_{xz}$ strain components, as well as curvature in the x-z plane. Hoop stresses result in the liner from the $\hat{\varepsilon}_x$ and $\hat{\varepsilon}_z$ free-field strain components. Non-uniform axial stresses are also caused by the axial

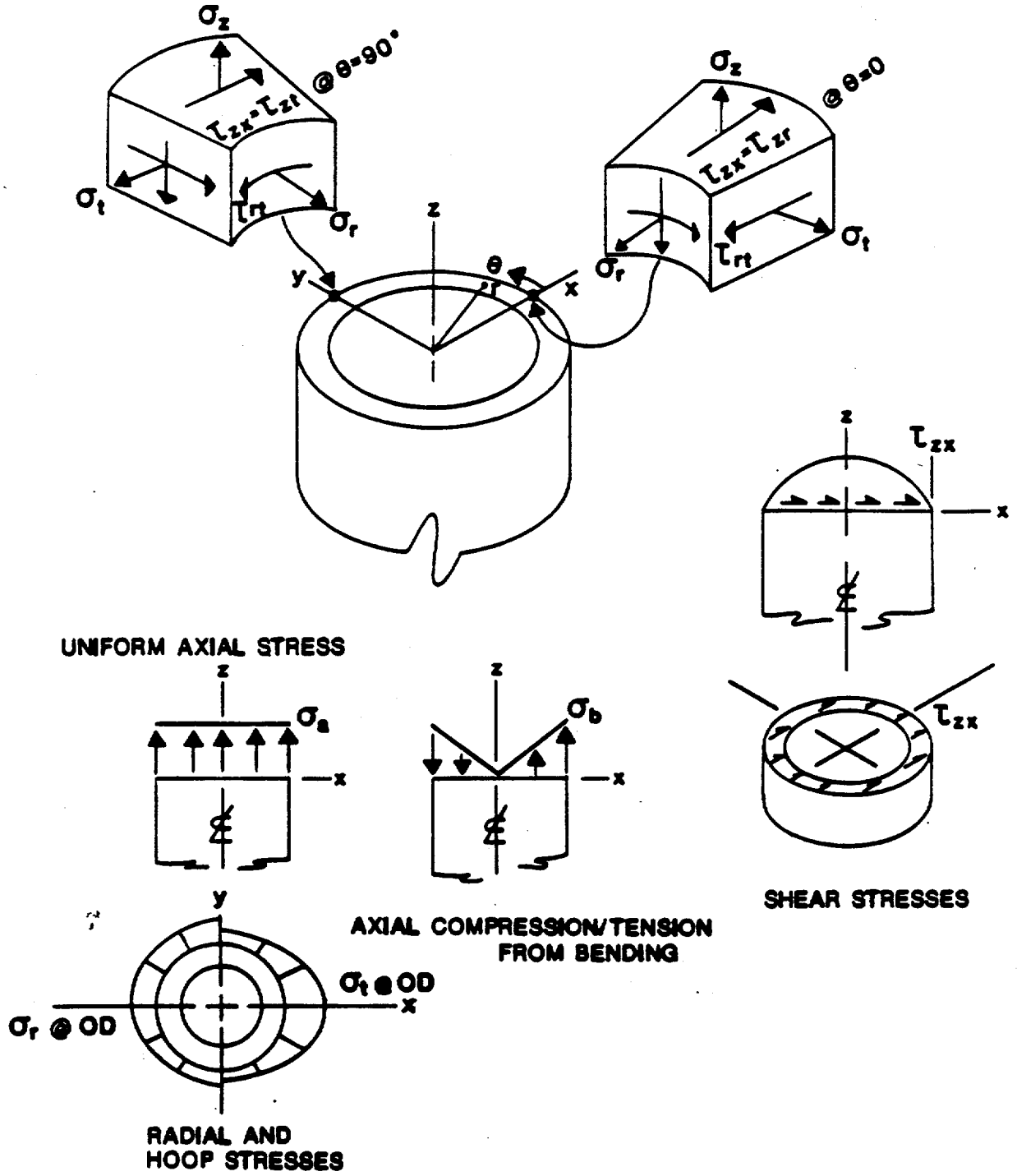

Figure 5-4. Typical Stresses due to Inclined S_V Wave
(After Fluor/PB-KBB, 1987)

curvature. Shear stresses are caused by $\hat{\gamma}_{xz}$ in the plane of particle motion.

Figure 5-5 shows stresses resulting from inclined S_H loading. Again, the direction of incidence is in the xz-plane, but particle motions are in the y-direction, and the wave contains $\hat{\gamma}_{xy}$ and $\hat{\gamma}_{yz}$ free-field strain components as well as y-z plane curvature. Peak hoop stresses occur at a 45° angle to the x-direction because of the pure shear condition. Nonuniform axial stresses are caused by the curvature, and shear stresses are caused by $\hat{\gamma}_{yz}$.

Although Figures 5-4 and 5-5 specifically show stresses from inclined seismic wave action, they also generally serve to illustrate the stress components that result from static loading because they involve all liner stress components of importance in this methodology.

5.3 MECHANICAL MODELS

5.3.1 General

Models for liner stress analysis can be divided into three progressively more complex categories: (1) those that assume the strains in the liner are exactly the same as the free-field strains in the rock; (2) those that analyze the liner as a free-standing structure subjected to loads imposed on it by the rock mass, and (3) those that analyze the liner and rock together as a system and consider the interaction between them. The first type of model involves the least computation, but is extremely conservative if the liner is significantly stiffer than the surrounding rock mass. The second type of model assumes that it is possible to calculate a set of loads exerted on the exterior of the liner by the rock mass. These loads can then be used to calculate the moments and thrusts in the liner, usually by assuming that the liner behaves like a beam. The obvious difficulty with this second method is the need to calculate the loads imposed on the liner. As discussed in Chapter 4, those loads depend on the interaction between the rock and the liner

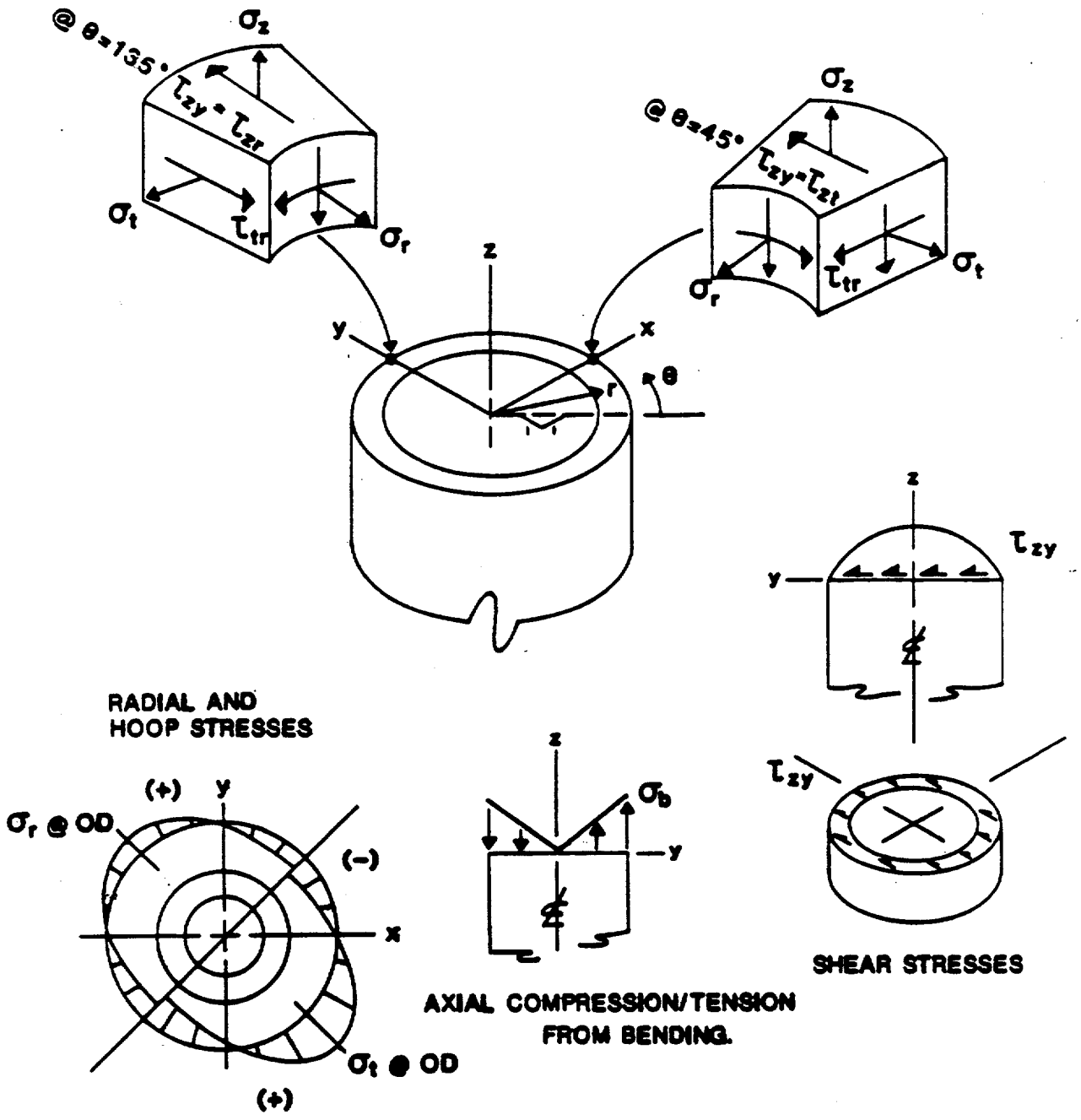

Figure 5-5. Typical Stresses due to Inclined S_H Wave
(After Fluor/PB-KBB, 1987)

and are influenced by their relative stiffnesses. Hence, it is difficult to avoid performing an interaction analysis, which is the basis of the third type of model. In general, it is more convenient and more accurate to directly consider the interaction between the liner and the ground. Simple ground-support interaction analysis such as described in Section 4.2 can be used if uniform loading assumptions apply. Otherwise, more involved interaction analyses must be performed. These may rely upon closed-form models, such as the hoop deformation models described in this chapter. Alternately, numerical models such as those based on the finite-element method can be used to analyze interaction under a variety of conditions.

5.3.2 Hoop Deformation and Axial Strain

Hoop deformation is considered to be the most significant mode of deformation in vertical shafts because it is directly related to the structural function of the shaft liner. It is recommended that interaction between the liner and the rock mass be considered in all hoop stress analyses.

This section presents a method of interaction analysis in which free-field loads (stresses and strains) are applied to a model composed of a thick walled cylinder (liner) embedded in a matrix (rock). The applied loads may be nonuniform, and the liner and the rock may have different properties. The case of plane strain, in which an arbitrary axial strain can be defined, was considered appropriate for the shaft liner problem (Jaeger and Cook, 1986, p. 116). The equations in this section have been incorporated in a computer program SHAFT (SNL, in preparation b).

Input for the hoop deformation calculations comprises the strains ($\hat{\varepsilon}_x$, $\hat{\varepsilon}_y$, $\hat{\gamma}_{xy}$) or stresses ($\hat{\sigma}_x$, $\hat{\sigma}_y$, $\hat{\tau}_{xy}$) in the rock mass in a horizontal plane (cross section of the shaft), and the vertical or axial

strain ($\hat{\varepsilon}_z$). The latter is assumed to be the same in the liner as in the rock because the two are bonded to each other.

Because the analysis presented in this section is based on the theory of linear elasticity, it does not matter whether loads are specified as stresses or as equivalent strains. However, it is more convenient to present the interaction equations in terms of stresses. Hence, if in-plane strains are initially specified as input, then they should be converted to stresses, using Lame's relationships (e.g., Goodman, 1980, p. 172).

$$\hat{\sigma}_z = (2G + \lambda)\hat{\varepsilon}_z + \lambda\hat{\varepsilon}_y + \lambda\hat{\varepsilon}_x, \tag{11}$$

$$\hat{\sigma}_y = \lambda\hat{\varepsilon}_z + (2G + \lambda)\hat{\varepsilon}_y + \lambda\hat{\varepsilon}_x, \text{ and} \tag{12}$$

$$\hat{\tau}_{xy} = G\hat{\gamma}_{xy}. \tag{13}$$

The material constant λ [Lame's constant, (Brady and Brown, 1985, p. 37)] in the above equations is related to the elastic constants E and ν by

$$\lambda \text{ - Lame's constant} = \nu E/(1+\nu)(1-2\nu) \tag{14}$$

As a matter of convenience, the solution for the liner stresses is given in terms of the free-field values of the mean and deviator stresses P and S (see Figure 3-1), which are defined from the changes in the free-field principal stresses, $\hat{\sigma}_1$ and $\hat{\sigma}_3$. The transformation equations necessary to obtain those principal stresses from any set of free-field normal and shear stresses can be taken from any of several rock mechanics books (e.g., Goodman, 1980, p. 340)

$$\hat{\sigma}_1 = \frac{1}{2}(\hat{\sigma}_z + \hat{\sigma}_y) + [\hat{\tau}_{zy}^2 + (\hat{\sigma}_z - \hat{\sigma}_y)^2/4]^{1/2} \tag{15}$$

and

$$\hat{\sigma}_3 = \frac{1}{2}(\hat{\sigma}_z + \hat{\sigma}_y) - [\hat{\tau}_{zy}^2 + (\hat{\sigma}_z - \hat{\sigma}_y)^2/4]^{1/2} \tag{16}$$

Note that $\hat{\sigma}_3$ has been used to designate the minimum in-plane principal stress. Because out-of-plane stresses are not being considered, no confusion should result from the "3" subscript, even though there are only two principal stresses possible in any given plane.

The principal stress directions are orthogonal, and the direction of σ_1 is given by

$$\alpha = \frac{1}{2}\tan^{-1}\left(\frac{2\hat{\tau}_{xy}}{\hat{\sigma}_x - \hat{\sigma}_y}\right) \tag{17}$$

As indicated in Figure 5-2, α is measured counterclockwise from the positive x direction. Defining the changes in the mean and deviator stresses as in Equation 1b, the liner stresses are (SNL, in preparation b)

$$\sigma'_r = \frac{A'}{r^2}(1 - M^2) - \left[\frac{C'}{r^4}(M^4 - 1) + \frac{2D'}{r^2}(M^2 - 1)\right]\cos 2(\theta - \alpha), \tag{18}$$

$$\sigma'_t = -\frac{A'}{r^2}(1 + M^2) + \left[\frac{C'}{r^4}(1 - M^4 + 4M^6) + \frac{2D'}{r^2}(3M^4 - M^2)\right]\cos 2(\theta - \alpha), \text{ and} \tag{19}$$

$$\tau'_{rt} = \left[\frac{C'}{r^4}(2M^6 - M^4 - 1) + \frac{D'}{r^2}(3M^4 - 2M^2 - 1)\right]\sin 2(\theta - \alpha), \tag{20}$$

$$\sigma'_z = \nu'(\sigma'_r + \sigma'_t) + E'\hat{\varepsilon}_z \tag{21}$$

in which θ is measured counterclockwise from the x-axis, and A', C', and D' are constants that depend upon the properties of the liner, the rock mass, and the applied loads, and M=r/a, where r is the radial distance of the calculation point from the axis of the shaft, and a is the inside radius of the liner. The coefficients A' and B' are related to the mean applied stress (P), and are defined by (SNL, in preparation b)

$$A' = \frac{-2PR^2 - B'R^2\varepsilon_z}{\frac{E}{E'}[(1+\tilde{\nu}')+T^2(1-\tilde{\nu}')] - (1+\tilde{\nu})(1-T^2)}$$

where $T = R/a$

$$B' = \hat{E}(\nu' - \nu) \text{ .}$$

The values of C' and D' are related to the deviatoric component of the applied stress field (S) and also depend on the condition of the liner and rock at their interface. If the liner is cast against a rough rock wall and it can be assumed that there will be no slip between the two, then the coefficients are

$$C' = \frac{12S \cdot R^4}{\Delta}[(1+\tilde{\nu})T^4 - (2F_3 + F_4 + 1 + \tilde{\nu})]$$

$$D' = \frac{4S \cdot R^2}{\Delta}[-2(1+\tilde{\nu})T^6 + (F_1 + F_2 + 2(1+\tilde{\nu}))]$$

in which S = deviatoric component of stress field.

$$\Delta = (\tilde{\nu}+1)(\tilde{\nu}-3)T^8 + 4[(5-\tilde{\nu})F_3 + (2-\tilde{\nu})F_4 - (\tilde{\nu}+1)(\tilde{\nu}-3)]T^6$$
$$+[(\tilde{\nu}-5)F_1 + 2(\tilde{\nu}-2)F_2 + 6(\tilde{\nu}-3)F_3 + 3(\tilde{\nu}-3)F_4 + 6(\tilde{\nu}+1)(\tilde{\nu}-3)]T^4$$
$$-2[(\tilde{\nu}-3)(F_1+F_2) + 2(\tilde{\nu}+1)(\tilde{\nu}-3)]T^2$$
$$+[F_1(F_4 - 1 + \tilde{\nu}) - 2F_3(F_2 + 1 + \tilde{\nu}) + F_4(1+\tilde{\nu}) - 2F_2 + (\tilde{\nu}+1)(\tilde{\nu}-3)],$$

and

$$F_1 = \frac{\hat{E}}{E'}[4\tilde{\nu}'T^6 - (1+\tilde{\nu}')(1+3T^4)],$$

$$F_2 = \frac{\hat{E}}{E'}[-2(3+\tilde{\nu}')T^6 + (1+\tilde{\nu}')(3T^4 - 1)],$$

$$F_3 = \frac{\hat{E}}{E'}[\tilde{\nu}'T^4 - (1+\tilde{\nu}')T^2 - 1], \text{ and}$$

$$F_4 = \frac{\hat{E}}{E'}[-(\tilde{\nu}'+3)T^4 + 2(1+\tilde{\nu}')T^2 + (1-\tilde{\nu}')].$$

Inspection of Equation (19) reveals that hoop stresses in the liner reach extreme values along radial lines parallel to the directions of the applied principal stresses. Critical locations for hoop stress relative to the free-field principal stresses are shown in Figure 5-6.

5.3.3 Axial Bending

Analysis of bending is based on the assumption that the liner conforms exactly to the free-field displacement of the rock mass. The liner is treated as a beam subjected to the free-field curvature. Two stress components are of concern. The first is the axial stress, which is given by (Timoshenko & Young, 1968)

$$\sigma_b = \pm E'rk \tag{22}$$

where

- E' = Young's modulus of the lining material
- r = distance from the shaft centerline to the fiber under consideration
- k = free-field ground curvature.

From Equation 22, it is clear that the extreme value of axial stress associated with bending occurs at the outside of the liner.

The second stress induced by curvature is the shear stress on horizontal sections perpendicular to the neutral plane of the liner. Again, considering the liner as a beam, the average value of this shear stress is given by (Timoshenko and Young, 1968)

$$\tau_{ave} = \frac{E'I'}{A} \frac{d^3u}{dz^3} \tag{23}$$

in which I' is the second moment of area (moment of inertia) of the liner, A the cross-sectional area, and d^3u/dz^3 the third

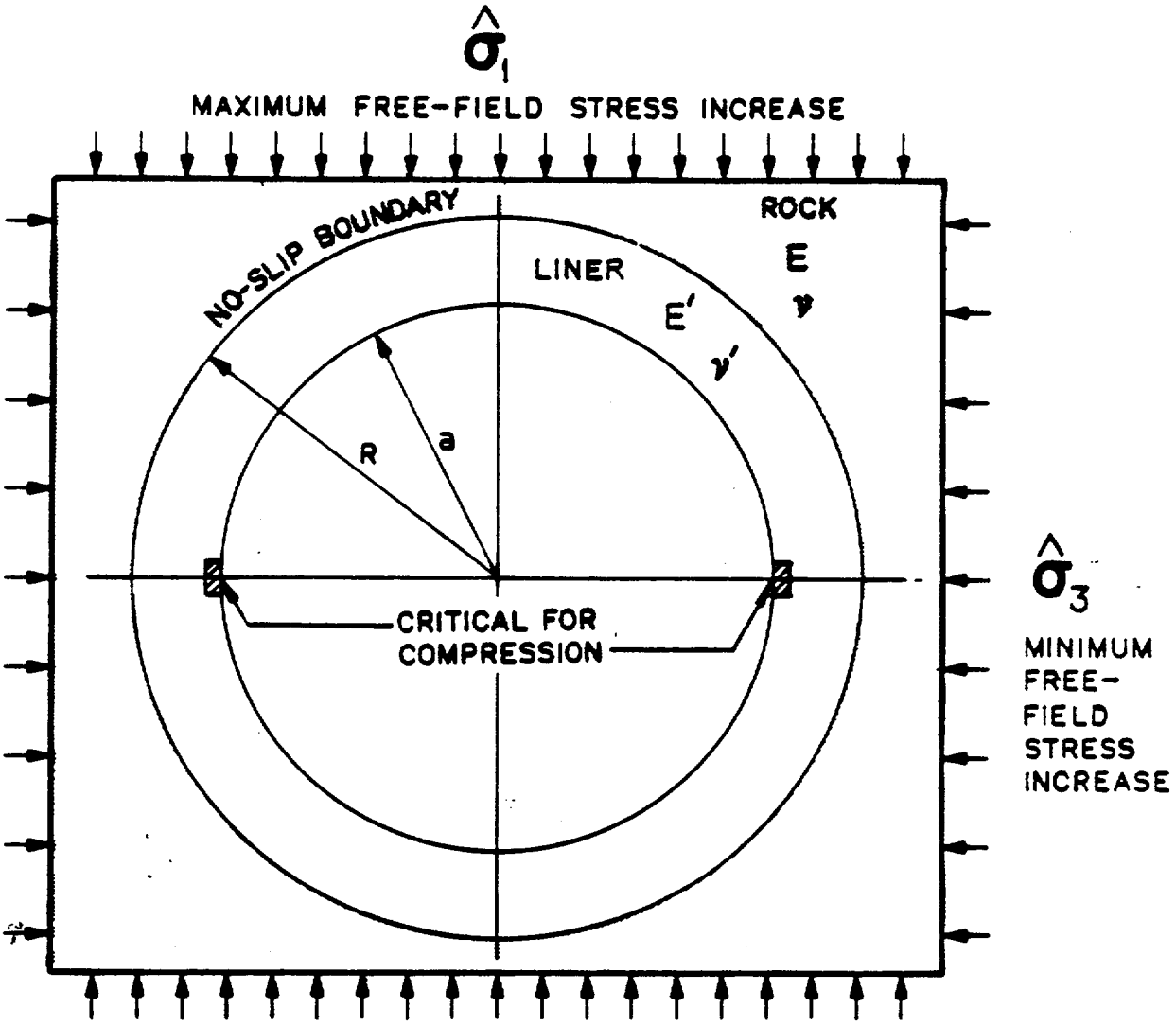

Figure 5-6. Cross Section of Interaction Model Used for Hoop Stress Analysis Showing Critical Tangential Stress Locations

derivative with depth of the horizontal displacement of the axis of the shaft liner (i.e., the first derivative of the curvature). The maximum value of the shear stress is given by

$$\tau_{max} = \alpha \tau_{ave} \tag{24}$$

where α is a factor that depends upon the shape of the cross section and for a thin cylinder is approximately 2.0 (Popov, 1968). This value is conservative for a thick cylinder. The maximum value of this shear stress occurs at the neutral plane.

Input for the bending deformation analysis is the curvature (k) of the axis of the shaft. This information should be obtained directly from the seismic input if bending is associated with shear wave action. In the case of induced thermal bending, the curvature is computed from the horizontal displacements of points along the shaft axis as discussed in Section 4.4.

5.3.4 Shear Deformation

This section deals with the effect of changes in the shear stress on planes perpendicular to the shaft axis. (Note: when considering the hoop stress, it was assumed that there was no shear stress on those planes.) In the free field, these out-of-plane stresses are the $\hat{\tau}_{xz}$ and $\hat{\tau}_{yz}$ stresses. The corresponding shear stresses induced in the liner are computed using a model given by Equations 25 and 26 that accounts for interaction between the liner and the rock mass (SNL, in preparation b).

$$\tau_{rz}' = \frac{2(1-m^2)}{G/G'(1+a^2/R^2)+(1-a^2/R^2)}(\hat{\tau}_{xz}\cos\theta + \hat{\tau}_{yz}\sin\theta) \tag{25}$$

and

$$\tau'_{rr} = \frac{2(1+m^2)}{G/G'(1+a^2/R^2)+(1-a^2/R^2)}(-\hat{\tau}_{xx}\sin\theta + \hat{\tau}_{yz}\cos\theta). \quad (26)$$

where

a is the internal radius of the liner
R is the external radius of the liner
Θ is measured relative to the x axis, as Figure 5-1 indicates
G' is the linear shear modulus,
G is the shear modulus, and
m = a/r.

Input for the shear deformation analysis comprises the shear strains ($\hat{\gamma}_{xz}$ and $\hat{\gamma}_{yz}$) or shear stresses ($\hat{\tau}_{xz}$ and $\hat{\tau}_{yz}$) experienced by the rock mass in the absence of the shaft. If the shear strains are supplied, then they need to be converted to stresses using the following relationships:

$$\hat{\gamma}_{xz} = \hat{\tau}_{xz}/G \; : \; \hat{\gamma}_{yz} = \hat{\tau}_{yz}/G. \quad (27)$$

5.3.5 Assumptions

The assumptions needed to apply the models of Section 5.3 relate to the material behavior of the liner and surrounding rock mass, the degree of bonding between the liner and the rock mass, the nature of any interaction between the liner and the rock, and the nature of the applied loads.

Material Behavior

In all cases the liner and rock mass are assumed to behave as linearly elastic materials. This assumption is important to the derivation of the interaction equations used to define the state of

stress in the liner, and it allows the results of independent analyses to be superimposed to obtain the total effect of various load combinations. For a typical concrete, the linear elastic assumption is valid provided that the compressive stresses remain below 50-60% f'_c, where f'_c is the strength of the concrete in uniaxial compression (Winter and Nilson, 1972). As discussed by O'Rourke (1984, Appendix B), the assumption of linear concrete behavior results in a conservative design if its linear range is exceeded. Also, tensile cracking in the liner will reduce its stiffness, and actual stresses in a cracked liner will be much lower than calculated using linear assumptions The use of linear models for the rock mass was discussed earlier in the introduction to this chapter.

Bonding

For the interaction calculations it is assumed that the liner and the rock mass are bonded to each other. This implies that there is no shear displacement, or slip, at the liner/rock interface and that the liner remains in contact with the rock, even if there is a tendency for the two to separate because the stress normal to the interface becomes tensile. The assumption of no slip at the interface is appropriate when the liner is cast directly against the wall of a shaft excavated in rock using drill and blast methods. In this case, relative shear displacement would involve shearing through intact rock and concrete because the interface is typically irregular. The validity of the assumption also can be checked by calculating the shear stress at the interface and comparing it with the strength of the rock and the liner. Similarly, the normal, or radial, stress at the interface can be checked to determine whether it is compressive all around the liner.

Interaction

In the hoop and shear deformation models, liner/rock interaction is considered directly and does not require simplifying assumptions. When

considering axial bending deformation, it is assumed that the liner will deform conformably with the rock mass. Thus, no account is taken of any interaction that would cause the liner to deform less than the surrounding rock. Because the conformable deformation assumption results in an over estimate of the bending deformation of the liner, the estimate of the stresses associated with this deformation mode is conservative. This conservatism is considered necessary and acceptable because simple models of axial bending of an embedded liner are not available, and the associated stresses are relatively low. Such conservatism is not necessary when considering the shear and hoop deformation modes because complete solutions for the case of interaction between the liner and the rock mass are available.

5.4 COMBINED DEFORMATION MODES

Hoop deformation and axial strain are directly coupled modes and should be considered together (Section 5.3.2). Also, axial stresses resulting from axial strains should be combined with those from axial bending.

The relationship between shear stress and principal tensile stress criteria was considered by the developers of the ACI concrete codes. Section 6.3.7 of the commentary to the ACI code for structural plain concrete (ACI, 1983b) states, "In special cases, investigation for principal tensile stresses in a homogenous material may be appropriate."

The designer may wish to analyze secondary principal stresses at a number of critical locations in the shaft liner, resulting from axial, hoop, and out-of-plane shear stresses. The principal stresses in the tz plane may be calculated using equation 16. Although these equations are presented in terms of free-field stresses, they are equally valid for calculating principal stresses in the liner.

Example Problem: Load Cases STATIC-3 and STATIC-4

The design methodology is illustrated by an example performed at the repository horizon (TS). Input loads are taken from load case STATIC-3 in Table 4-4, considering uniform ground pressures combined with thermal loads, and load case STATIC -4, considering anisotropic ground pressures combined with thermal loads.

The inner radius of the liner is 1.83 m, and the outer radius is 2.13 m. The deformability parameters used to represent the concrete shaft liner are taken from Appendix A as follows.

- $E' = 28{,}000$ MPa
- $\upsilon' = 0.15$

Static deformability parameters are used for the rock mass.

1. Hoop stresses

   Hoop stresses due to static loading were calculated using Equation 19 incorporated in the SHAFT code (SNL, in preparation b). Sample output from the shaft code is shown in Appendix E. The peak hoop stress is 11.14 MPa for load case STATIC-3, and 7.91 for load case STATIC-4. This is compressive and occurs at the inner face of the liner. The upper part of Figure 5-7 illustrates the results of the static load interaction analysis for load case STATIC-4.

2. Out-of-plane shear stresses

   Free-field out-of-plane shear stresses are associated with thermal loading. A peak value of approximately 0.5 MPa occurs after approximately 100 years at a location approximately 100 m

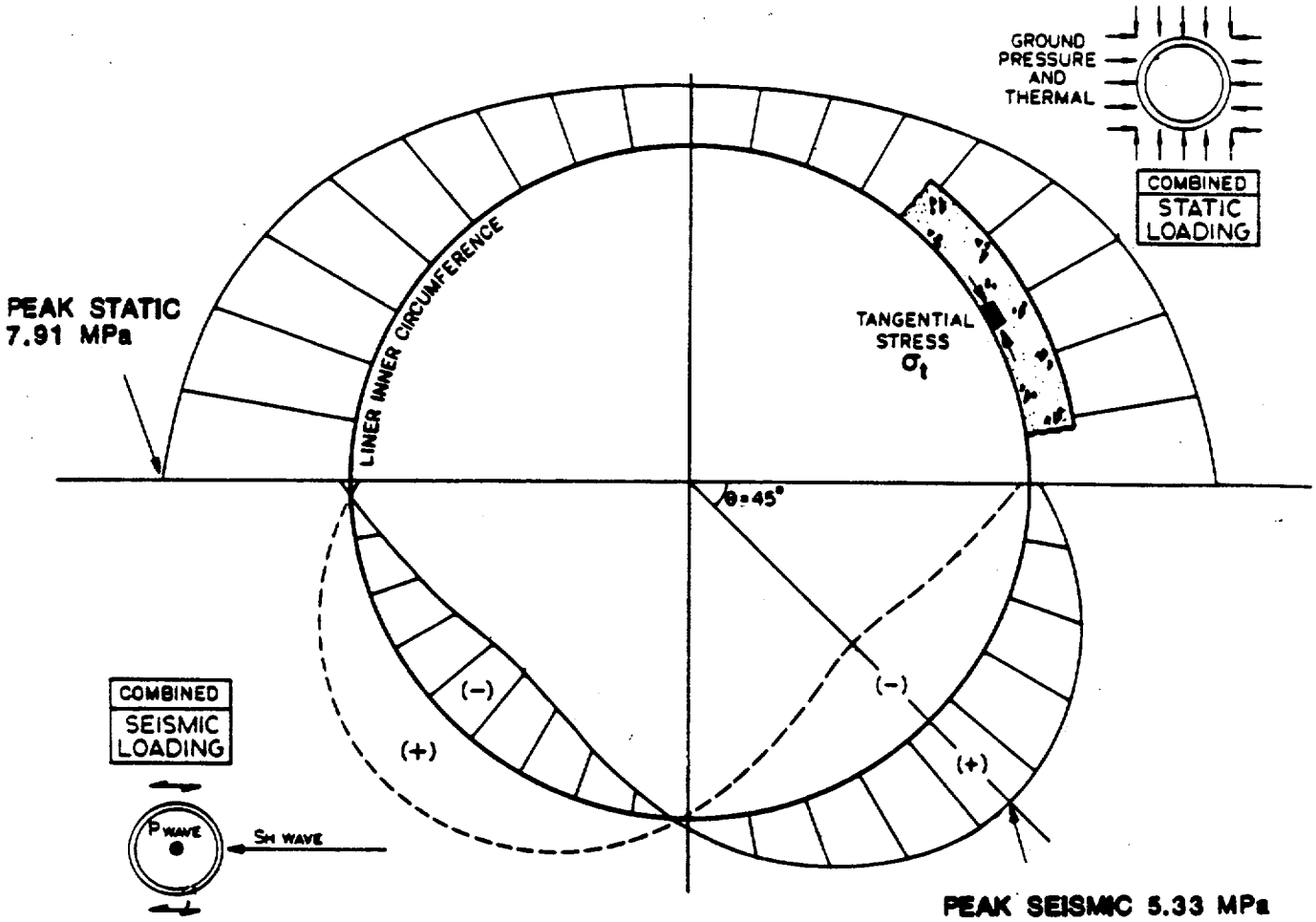

Figure 5-7. Tangential Stresses on the Interior Face of the Example Problem Shaft Liner (Upper portion shows stresses from load case STATIC-4; lower portion shows stresses from seismic load case SEISMIC-1.)

above the repository horizon (Appendix B). Using Equation 26, this results in an out-of-plane shear stress of 1.74 MPa.

3. Axial strains

A free-field tensile axial strain of 150×10^{-6} was taken from Table 4-4. This is associated with thermal loading and is assumed to be transmitted directly to the liner.

Example Problem: Load Case SEISMIC-1

This seismic load case comprises a vertically propagating P wave and a horizontally propagating S_H wave. The nonzero strains associated with those waves are given in Table 4-5 as

- $\hat{\varepsilon}_z = 44 \times 10^{-6}$, and
- $\hat{\gamma}_{xy} = 109 \times 10^{-6}$.

1. Hoop Stresses

The lower portion of Figure 5-7 illustrates the results of the interaction analyses using load case SEISMIC-1. The maximum magnitude of the hoop stresses is approximately 5.33 MPa at the interior face based on analysis using the SHAFT code (SNL, in preparation b). These stresses oscillate between compression and tension.

2. Out-of-plane shear stresses

Because there is no curvature of the shaft axis associated with the seismic loading conditions, there are no out-of-plane shear stresses due to seismic loading.

3. Axial strains

An axial strain of 44×10^{-6} (0.0044%) occurs in the liner as a result of the action of the P wave. This alternates between compression and tension. No calculation is necessary; the free-field axial strain is assumed to be transmitted directly to the liner and can be directly taken from Table 4-5.

Example Problem: Load Case SEISMIC-2

This seismic load combination is composed of P, S_V, and S_H waves at a 30° angle of incidence to the shaft axis. The free-field strain tensor was estimated from the strain components associated with the individual waveforms. It is taken from Table 4-5.

$$\hat{\varepsilon}_x = 80 \times 10^{-6}$$
$$\hat{\varepsilon}_y = 0 \times 10^{-6}$$
$$\hat{\varepsilon}_z = 94 \times 10^{-6}$$
$$\hat{\gamma}_{xy} = 29 \times 10^{-6}$$
$$\hat{\gamma}_{xz} = 108 \times 10^{-6}$$
$$\hat{\gamma}_{yz} = 20 \times 10^{-6}$$

Liner stresses are calculated as follows.

1. Hoop stress/axial strain

Substituting the values for $\hat{\gamma}_{xy}$, $\hat{\varepsilon}_x$, and $\hat{\varepsilon}_z$ into the plane-strain analysis of Equation 19 as incorporated in the SHAFT code, we obtain a peak tangential stress of

$$\sigma_{t(max)} = 8.12 \text{ MPa.}$$

Note that the dynamic rock mass modulus (Appendix A) was used in the liner stress calculations (see Appendix E).

2. Out-of-plane shear stresses

Using Equation (27) to convert the out-of-plane shear strains γ_{xz} and γ_{yz} to free-field stresses, then substituting into Equations (25) and (26) as shown in Appendix E, we have

$$\tau_{tz'} = 2.54 \text{ MPa.}$$

3. Axial stresses

Using Equation 21, incorporated in the SHAFT code, we obtain the direct axial stress:

$$\sigma'_a = 3.85 \text{ MPa (uniform axial stress).}$$

The axial stress due to bending (σ_b), with a curvature of 0.73×10^{-6}/m from Table 4-5, and bending calculated from Equation 22, is

$$\sigma'_b = E'rk = (28{,}000 \text{ MPa})\ (2.13 \text{ m})(0.61\times10^{-6})$$
$$= 0.04 \text{ MPa.}$$

Axial stresses due to the axial strain are combined with those due to bending:

$$\sigma'_z = \sigma'_a + \sigma'_b$$
$$= 3.85 \text{ MPa} + 0.04 \text{ MPa}$$
$$= \pm 3.89 \text{ MPa.}$$

The axial strain due to bending is a negligible contribution to the overall axial strain. The axial strain alternates between compression and tension.

Tables 5-1, 5-2, and 5-3 show the results of similar calculations for other units, using example inputs taken from Appendix A. To simplify the tables only seismic load case SEISMIC-2 is shown because this case follows the project seismic data base.

TABLE 5-1

PEAK TANGENTIAL (HOOP) STRESSES*

Load Case STATIC	Load Case SEISMIC	Peak σ_t (Static) (MPa)	Peak** σ_t (Seismic) (MPa)	Static + Seismic (MPa)
		PT		
1	2	1.82	7.86	9.68
2	2	2.36	7.86	10.22
3	2	2.78	7.86	10.64
4	2	2.17	7.86	10.03
		TS		
1	2	3.53	8.12	11.65
2	2	4.54	8.12	12.66
3	2	11.14	8.12	19.26
4	2	7.91	8.12	16.03
		CH		
1	2	9.28	7.46	16.75
2	2	11.41	7.46	18.87
3	2	12.05	7.46	19.52
4	2	10.49	7.46	17.95

*See Table 4-3 for definition of load cases.
**Stresses due to seismic waves may be (+) or (-)

TABLE 5-2

PEAK AXIAL COMPRESSION/TENSION STRESSES

Location[a]	Static Load Case	Seismic Load Case	Peak σ_a (MPa)	Peak σ_b (MPa)	Combined σ_z (MPa)
PT	STATIC-1,2	SEISMIC-2	6.36	0.14	6.50
TS	STATIC-1,2	SEISMIC-2	3.85	0.04	3.89
CH	STATIC-1,2	SEISMIC-2	3.98	0.04	4.02

[a]See Figure 1-2 for locations.

TABLE 5-3

OUT-OF-PLANE SHEAR STRESSES

Location[a]	Static Load Case	Seismic Load Case	Stresses		
			Thermal	Seismic	Combined[b]
			τ_{tz}	τ_{tz}	τ_{tz}
PT	STATIC-1,2	SEISMIC-2	0	2.90	2.90
PT	STATIC-3,4	SEISMIC-2	2.27	2.90	3.18
TS	STATIC-1,2	SEISMIC-2	0	2.54	2.54
TS	STATIC-3,4	SEISMIC-2	1.74	2.54	4.28
CH	STATIC-1,2	SEISMIC-2	0	2.60	2.60
CH	STATIC-3-4	SEISMIC-2	0.41	2.60	3.01

[a]See Figure 1-2 for locations.
[b]The combination is formed by direct superposition.

Example Problem: Principal Stresses

1. Critical Combination for Tension (SEISMIC-2 (-), NO STATIC)

The seismic wave alternates between (+) and (-) values. During the (-) cycle, tensile stresses are predicted in the liner. If sufficient compressive prestress can be guaranteed in the liner from ground pressure and thermal loads, the predicted tensile stresses from seismic loads would be mitigated.

However, the ground pressure is a function of the liner installation sequence, and it is quite possible that little or no ground pressure will act on the liner. The magnitude of compressive thermal load depends upon a number of programmatic and design variables, and in any case thermal loads will not develop until late in the operations period. Hence, it is unreasonable to assume that these loads will result in a compressive prestress in the liner.

The critical combination considered here involves the (-) excursion of the seismic wave in the TS Unit. A worst-case condition is assumed in which negative axial and hoop stresses are combined with out-of-plane shear stresses, yielding a general tensile condition on the inner face of the liner. The following components were taken from Tables 5-1 through 5-3:

hoop stresses = σ_t = -8.12 MPa
axial stress = σ_z = -3.89 MPa
shear stress = γ_{tz} = 2.54 MPa

Using equation 16 to calculate the maximum tensile principal stress, we have:

σ_3 = maximum tensile principal stress = -9.31 MPa

2. Critical Combination for Compression (STATIC-3 + SEISMIC-2 (+))

The critical case for compression is when all three loads (ground pressure, thermal, and seismic) are acting on the liner, and the seismic wave is in its positive (+) cycle. From Tables 5-1 through 5-3, we have:

hoop stresses = σ_t = 19.26 MPa
axial stress = σ_z = 3.89 MPa
shear stress = τ_{tz} = 4.28 MPa

σ_1 = maximum compressive principal stress = 20.37 MPa

Other values for critical compressive and tensile principal stresses for the two combinations considered above are tabulated in Table 5-4.

Table 5-4

Critical Principal Stresses for Two Combinations

Location[a]	Static Load Case	Seismic Load Case	Critical Tension (MPa)	Critical Compression (MPa)
PT	NONE	SEISMIC-2(-)	-10.16	-
PT	STATIC-3	SEISMIC-2(+)	-	12.36
TS	NONE	SEISMIC-2(-)	-9.31	-
TS	STATIC-3	SEISMIC-2(+)	-	20.37
CH	NONE	SEISMIC-2(-)	-8.86	-
CH	STATIC-3	SEISMIC-2(+)	-	20.08

6.0 PERFORMANCE

6.1 GENERAL

In the preceding chapters of this guide, methods for calculating potentially critical stresses in the concrete shaft liner have been developed. This chapter presents a methodology for evaluating liner performance.

6.1.1 The Liner as a Structural Member

In the United States, most design of concrete structures is performed using the methods and criteria developed by the American Concrete Institute (ACI) and described in its concrete codes (ACI, 1983a; 1983b). The design and analysis provisions of the ACI codes are intended primarily for surface buildings and are not specific to the design of shaft liners. These codes are supported by vast testing and construction experience, and their use will result in a safe and efficient design. Concrete shaft liners are inherently stable structural elements that differ in several significant respects from the beams, columns, and similar elements used in buildings. The following general points highlight these differences.

1. The only structural function of concrete liners for the NNWSI project is to counter the tendency of the rock mass to ravel and collapse into the opening by providing a passive outward radial pressure in response to possible inward radial displacements. The liner is <u>not</u> required to

   - provide resistance against thermal uplift of the ground surface,

- rigidly prevent normal and shear strains occurring in the earth from seismic and/or thermal loading,
- support its own weight, or the weight of the rock mass,
- provide lateral resistance to strata movements causing axial bending,
- act as a vertical beam, chimney, column, or other structural member encountered in building construction.

2. A concrete shaft liner cast against the rock is not a free-standing structure affected by independent external loads. Although loads develop in and are transmitted by the rock mass surrounding the liner, the rock mass is also part of the structure and in most cases is largely or entirely self supporting. The liner serves primarily to reinforce the rock mass through interaction.

3. A concrete liner will deform in a ductile manner when subjected to external loading, despite the brittle nature of the concrete material. The liner derives this inherent ductility from its shape and loading geometry.

4. Except for water pressure (which is not expected at Yucca Mountain), loads on shaft liners are displacement-dependent. They are not "following" loads as are typically assumed for surface structures. Loading a liner will cause it to yield slightly, after which some of the excess load will be redistributed into the surrounding rock mass, and the stress in the liner will be reduced. Often detrimental to other concrete structures, limited creep and shrinkage may be beneficial to liner performance because they result in the reduction and redistribution of liner stresses.

Overloading a beam or column may ultimately result in sudden, catastrophic collapse and complete loss of its load-bearing function. This behavior was considered by the ACI when the building codes were developed, and an appropriate amount of conservatism was built into these codes. Unlike a beam or column, the liner/rock system inherently achieves a stable equilibrium through load redistribution. Hence, less conservatism should be necessary when designing shaft liners than beams or columns. However, in the absence of appropriate design codes for liners, the methodology presented herein draws on ACI design codes for performance criteria. The designer should recognize that these procedures and criteria are very conservative for shaft liner applications. Shear strength criteria in the concrete codes are not appropriate for concrete liners, as discussed later.

6.1.2 Strength and Working Stress Methods

ACI codes allow two design methods: (1) the "ultimate strength" or "strength" design method, which is the primary method, and (2) the "working stress" method, which is an alternate. In the strength design method, the required strength of the structure must be less than or equal to its design strength. The required strength is calculated using standard methods specified for each type of structural member used in building construction, after multiplying the service loads by load factors (1-1.7) to allow for the effects of excess load and simplifying assumptions in structural analysis. The design strength is obtained by multiplying the yield or ultimate strength by a strength reduction factor (<1) to account for uncertainties due to material imperfections, dimensional tolerance, and stability concerns. In the working stress (alternate) method, linear analysis is used to calculate working stresses in the concrete, which are compared to allowable stresses. For this reason, the working stress method is sometimes called the "elastic" method.

The strength method is favored in modern building design for the following reasons:.

1. It is generally easier and more accurate to analyze the ultimate load capacity of a reinforced concrete structural element than to compute the critical stresses in the element under working loads.

2. The strength method accounts for redistribution of stresses between the concrete and reinforcing steel in the element caused by the nonlinear behavior of the concrete, enabling calculation of a true safety factor and resulting in efficient use of materials.

The working stress method generally results in a more conservative design in reinforced concrete. In plain concrete, the two methods give virtually identical results.

The linear elastic interaction analysis of the preceding chapter has been selected for reasons of convenience and versatility as discussed earlier. Because this method enables calculations of working stresses in a liner and does not directly provide liner strength, a working stress approach is recommended in this guide.

6.2 LINER BEHAVIOR MODES UNDER CONDITIONS OF OVERSTRESS

6.2.1 Types of Overstressed Concrete Behavior

As discussed in Chapter 2, the shaft liners must protect and support the rock and provide for worker safety throughout the design life. Hoisting-shaft liners must also provide stable anchorage for the hoisting equipment, and utilities also may be anchored to the liner.

There are several modes of inelastic behavior (cracking, crushing) that could develop if the liner is overstressed. Not all of these are equally likely, nor will all of them affect the maintainable performance of the liner. Table 6-1 summarizes the modes of overstressed behavior that could occur, along with the deformation modes responsible for each type.

6.2.2 Damage Categories

Three possible overall levels of liner damage have been defined for the purpose of this guide. Level 1 involves minor tensile cracking. Level 2 involves compressive crushing and spalling, possibly combined with more severe tensile cracking. Complete collapse and failure of the liner occur in level 3. The potential effect of each of these levels of damage on the shaft liner functional requirements will largely determine appropriate acceptance criteria for analysis.

Level 1: Minor tensile cracking

Axial (horizontal) tension cracks may arise from induced axial tension caused by thermal loading or from alternating compression and tension caused by vertical components of P and S_V waves. These tension cracks are likely to be quite small, evenly distributed along the length of the shaft, and similar to cracks resulting from shrinkage of the concrete. Hairline cracking is almost unavoidable in concrete and can be observed in perfectly stable structures. More continuous axial tension cracks, should they occur, will be similar to axial construction joints that naturally occur between successive liner pours during construction. A liner consisting of rings separated by joints has the same lateral restraining capacity as a continuous liner. Neither distributed hairline cracks nor the more continuous axial tensile cracking are expected to affect any of the liner functions.

TABLE 6-1

POSSIBLE MODES OF OVERSTRESSED CONCRETE BEHAVIOR

Mode of Behavior	Liner Deformation Mode	Loading Mechanism
Compressive (crushing or spalling)	Hoop compression (uniform or nonuniform)	Ground pressure, induced thermal, inclined* P and S waves
	Axial compression	Inclined P and S_V waves
	Axial bending	Inclined P and S waves, induced thermal
Shear (tension cracks)	Direct shear	Inclined P and S waves
	Axial bending	Inclined P and S waves, induced thermal
Extensile (tension cracks)	Axial extension	Inclined P and S_V waves, induced thermal
	Axial bending	Axial P and S waves, induced thermal
	Nonuniform hoop compression	Nonuniform ground pressure, induced thermal, inclined P and S waves.

*Note that axial incidence is a special case of inclined incidence

Radial (vertical) tensile cracks may occur from nonuniform hoop distortions. If the liner is subjected to a nonuniform load, moments (nonuniform hoop stresses created by bending or flexure) will develop in

the liner. Moments may result in tension or compression in the liner. If there is insufficient thrust (uniform hoop stress) to counter the negative moments, a radial tension crack will form. The crack will generally start at the inner face of the liner and propagate radially outward. If the liner is not bonded to the rock and carries some compressive thrust in addition to the moments, it is unlikely that such tension cracks will fully penetrate the liner because the thrust will become concentrated in the liner ahead of the tension crack and will eventually arrest its development. Where full bonding exists between the liner and the rock, the crack may fully penetrate the liner under cyclic loading conditions (seismic), or if thrust is transferred into the surrounding rock. However, a fully bonded but partially cracked liner still retains most of its thrust capacity and consequently its support function. (An analysis of this situation is presented in Appendix D.) Once formed, radial tension cracks add to the flexibility of the liner, thus tending to relieve excess moments and to result in a more even distribution of stress in the liner.

It could be postulated that further loading of a radially cracked liner could push blocks formed by radial cracking into the shaft and cause the liner to fail (level-3 damage). However, this type of failure is highly unlikely because (1) normal stresses are generated across the failure surfaces as an individual block is pushed in; this is caused by wedging of the inward tapering blocks; (2) the loads typically are not "following" loads; their intensity decreases as the liner is displaced in response to the loads; (3) any distortion of the liner will increase the loads on the liner in the areas where the liner moves outward (toward the surrounding rock), tending to eliminate instability and collapse; and (4) there may be some interlocking between the liner and the rough rock surface.

A case history of a sewer tunnel in Mexico City clay (Schmitter and Moreno, 1983) illustrates the limits to which these principles may be carried. A 6-m-diameter sewer tunnel was constructed under compressed

air and was lined with four unbolted segments plus a key. As the air pressure was eliminated in one section of the tunnel, the horizontal diameter of the liner increased by up to 340 mm, or about 5.5%. Tension cracks were noted at a distortion of 2.3% and compressive spalling at 5.5% distortion. In spite of these unusually large distortions, the liner did not collapse even with five unbolted radial joints (which correspond to cracks that penetrate the liner completely). Taken to its unlikely extreme condition, a combination of radial and circumferential tension cracks could cause a condition similar to a liner made of bricks or blocks. In fact, brick and block liners have a long history of successful application in mining and tunneling. Any tendency toward inward distortion increases the thrust in the liner and consequently the frictional forces between blocks holding them in place. Although tension cracks will certainly occur before level-3 damage, major distortion and crushing of the liner must accompany the tensile cracking before the liner can collapse. Thus, tensile cracking may be a symptom of liner problems, but does not in itself constitute a failure mechanism. This is especially the case for seismically induced cracks, which close after the disturbance passes.

Level 2: Compressive Crushing and Spalling, Major Tensile Cracking

The primary concern in concrete shaft liner design is crushing or spalling of the concrete, which results from excess compressive stress at the interior face of the liner. Severe combinations of all three types of loading (ground pressure, thermal, and seismic) could cause this type of inelastic behavior. The principal causative deformation mode is hoop compression or distortion caused by radial compressive and shear loads and horizontal shears acting on the liner. Although tangential and hoop stresses are usually the controlling factor, axial compression and axial bending in combination also can cause vertical compressive stresses in the liner. The onset of spalling does not represent loss of the ground support or ventilation functions of the liner. However, flakes of concrete could become detached from the liner, possibly resulting in

hazards associated with falling objects. In hoisting shafts, level-2 damage raises questions about the integrity of the conveyance anchorages. For these reasons, it is appropriate to limit the allowable compressive stresses or strains in the concrete to prevent level-2 damage.

Severe tensile cracking can also be considered level-2 damage.

Level 3: Complete Collapse

Complete collapse of a thick concrete liner would not occur unless the liner experienced severe distortions, as discussed above. Such distortions are highly unlikely at Yucca Mountain. Complete collapse of the liner would result in loss of all liner functions and could affect repository ventilation. A structure designed against level-2 damage will have a large factor of safety against level-3 damage.

6.3 CRITERIA

6.3.1 General

To establish appropriate criteria for evaluating liner performance, an acceptable level of damage must be selected. Level-1 damage involves tensile cracking which is probably unavoidable in shaft liners subjected to seismic loading and should not interfere with any shaft functions. For the Yucca Mountain Project, criteria have been established to ensure that level -1 damage will not progress to level -3 damage.

It is appropriate to develop criteria to guard against the onset of level-2 damage in shafts used for hoisting and shafts where personnel will be present and might be exposed to falling objects. Currently, it is appropriate to apply these criteria equally to all repository shafts, including ES-1 and ES-2.

Criteria against level -1 and level -2 damage will preclude the possiblity of level -3 damage.

Damage criteria will be in terms of principal compressive and tensile stresses and strains. The prinicipal stresses are caused by combinations of axial, hoop, and shear stresses, acting simultaneously. Separate criteria will not be established for axial, hoop, and shear stresses since it is the principal stresses that initiate damage.

6.3.2 Compression

As discussed in Section 6.1.1, the only structural function of concrete liners for the NNWSI project is to apply a passive internal pressure to the shaft walls. In generating such a pressure, compressive stresses are developed in a ring-shaped compression member such as the shaft liner. It is necessary to establish criteria to maintain the support function, by limiting these compressive stresses and strains to prevent level -2 damage. A two-stage criterion is proposed. The first stage involves an allowable stress criterion. If this is exceeded, the designer should refine the analysis to include nonlinear concrete behavior and apply a strain criterion.

Because shafts must withstand the ground pressure as a working load, a standard safety margin of 0.45 f'_c (concrete cylinder strength) is proposed for this load. At least some shafts must remain functional throughout the retrievability period and will be exposed to prolonged thermal effects. Concrete will creep in response to gradually imposed induced thermal strains; therefore, theoretically deduced stresses that ignore concrete creep will be higher than actual stresses. In the example problem, no distinction is made between ground pressure and thermal loads. Under these conditions the standard safety margin is considered to be quite conservative; the designer may consider concrete creep for long-term loading if required.

Compressive stresses resulting from a seismic event are transient. The controlling seismic event is an earthquake, which has a low probability of occurrence during the lifetime of the structure. Considerable conservatism exists in the methods used for determining seismic loads in the Project data base, and load factors greater than 1 will introduce excessive conservatism in the design. However, an overall safety factor of 0.65 f'_c, based on the standard strength reduction factor, is recommended for combinations involving seismic loads. Table 6-2 shows recommended allowable compressive stress criteria.

The designers should note that use of principal compressive stress, which involves a shear stress component, rather than hoop stress may be conservative in cases involving seismic loading. Since seismic loads alternate between compression and tension, but concrete is weaker in tension, tensile cracking is likely to precede any compressive damage. This will reduce the shear modulus of the concrete, and limit its ability to transmit shear stresses from the free-field. Designers have traditionally ignored out-of-plane stresses in buried pipe design for this reason (ASCE, 1983).

TABLE 6-2

ALLOWABLE COMPRESSIVE STRESS CRITERIA

Loading	Reinforced Concrete (f_c/f'_c)	Plain Concrete (f_c/f'_c)
Static	0.45[a]	0.45[a]
Static + Dynamic	0.65[b]	0.65[b]

a. Calculated from ACI 318.1-83 (ACI, 1983b), part 6.2.2 (strength reduction factor of .65) and part 6.1.2 (load factor of 1.4).
b. Calculated from ACI 318.1-83, part 6.2.2 (strength reduction factor of 0.65) using load factor of 1.

Allowable compressive stresses for reinforced concrete and plain concrete are the same because the primary purpose for the compressive safety factors is to guard against spalling of the shaft wall. Reinforcing cannot be installed close enough to the face of the shaft to completely eliminate the possibility of spalling while maintaining the required minimum coverage.

If the allowable compressive stress is exceeded, the linear analysis recommended in this guide is no longer applicable. For cases involving static and dynamic loads, the designer should perform a nonlinear analysis and calculate principal compressive strains in the liner. A peak compressive strain of 0.003 (0.3%) is permitted by the concrete codes (ACI-318, 1983, part 10.2.3).

6.3.3 Tension

Maintenance of the tensile capacity of the concrete liner is not required for the liner to function in resisting radial compression but tensile cracking should be limited to maintain adequate appearance and to limit fall out of slabs or blocks of the liner. The allowable tensile strength of concrete is provided by the ACI code as:

$$\text{Allowable Tensile Stress} = 3.25\sqrt{f'_c}$$

where

f'_c is the compressive strength of concrete (in psi)
(Source: ACI, 1983b)

If principal tensile stresses exceed this allowable strength, the designer should consider minimum reinforcing, light wire or fibre reinforcing. This light reinforcement should be designed to ensure distribution of cracks and to increase ductility of the concrete. If tensile strains in excess of 0.001 (0.1%) are expected, alternate designs, as listed in section 6.4, should be considered. The designer

should check that the orientation and location of tensile cracks do not inhibit the ability of the liner to withstand compressive hoop stresses.

Example Problem

In our example problem, we specify a concrete with 28-day strength f'_c = 5,000 lb/in² (34.5 MPa). The allowable compressive stress for the two cases are

$$0.45 \times \sqrt{f'_c} = 0.45 \times 34.5 \text{ MPa} = 15.5 \text{ MPa} \quad \text{(combined static), and}$$

$$0.65 \times \sqrt{f'_c} = 0.65 \times 34.5 \text{ MPa} = 22.4 \text{ MPa} \quad \text{(static and seismic).}$$

The allowable tensile stress is:

$$3.5 \times \sqrt{f'_c} = 3.5\ (70.7)/145 = 1.71 \text{ MPa}$$

Several critical combinations are considered below.

The stress checking procedure is illustrated by considering the principal stresses in Table 5-4.

Tension

At all locations, the load combination involving the negative excursion of the seismic wave (without static loads) exceeds the allowable tensile stress of 1.71 MPa. The designer should calculate the range of possible orientations of these cracks. If they deviate signficantly from horizontal and vertical, the designer should consider embedded wire mesh or some similar measure to increase the ductility of the concrete, as discussed in Section 6.4.

Compression

The load combination involving the positive excursion of load case SEISMIC-2 combined with load case STATIC-3 in all cases results in maximum compressive principal stresses below the allowable of 22.4 MPa. Hence, nonlinear analysis is not required, and the designer need not consider the special measures for compression discussed in Section 6.4.

6.4 DESIGN ALTERNATES

If the principal tensile stress criterion is exceeded, the designer must add minimal reinforcement, welded wire mesh, or fiber reinforcement. The purpose of these measures is not to prevent level-1 damage, but to preclude the possibility of level-1 damage progressing to level-3 damage or otherwise impairing the liner's function.

This means that the reinforcement need not be designed to carry the tensile stresses. The purpose of this reinforcement is to maintain the ductility of the liner when undergoing tensile strains greater than those at which cracking is predicted using linear elastic methods.

If the allowable compressive stress criteria are exceeded in a linear analysis, then the designer should perform a nonlinear analysis using an allowable strain of 0.003. If that criterion is exceeded, or if the principal tensile strains in the rock wall exceed 0.001, the designer may consider one of the following alternates:

1. Increase concrete strength. Although some advantage may be gained using high strength concrete, this option has limited value because the stiffness (and thus the liner stresses) increases with strength. Also, 28-day strengths in excess of 5,000 psi are not standard practice in shaft construction.

2. Increase liner thickness. This option also has limited value because if the liner modulus is greater than that of the rock, a thicker liner will attract more stress.

3. Add embedded steel, either structural ring members or reinforcing. If reinforcing is used, the lining may be designed according to ACI 318, Appendix B.

4. Use frangible backpacking to absorb rock displacement without loading the liner.

5. Investigate alternate means for increasing liner flexibility.

6. Require a larger shaft pillar with more standoff from the waste storage areas to reduce thermal stresses.

7. Install an inner steel liner to confine the concrete. If this option is selected, the 0.3% strain limit will be too conservative.

7.0 REFERENCES

Abel, J.F., Jr., J.E. Dowis, and D.P. Richards, "Concrete Shaft Lining Design," Proc. 20th U.S. Symposium on Rock Mechanics, Austin, TX, pp. 627 - 633, 1979.

ACI-318, "Building Code Requirements for Reinforced Concrete," American Concrete Institute, Detroit, MI, 1983a.

ACI-318.1-83, Building Code Requirements for Structural Plain Concrete," American Concrete Institute, Detroit, MI, 1983b.

ASCE (American Society of Civil Engineers) "Seismic Response of Buried Pipes and Structural Components, Committee on Seismic Analysis," New York, NY, pp. 15-16, 1983.

Bauer, S.J., J. F. Holland, and D.K. Parrish, "Implications About In Situ Stress at Yucca Mountain," Resource and Engineering Applications in Rock Masses, Proceedings of the 26th U.S. Symposium on Rock Mechanics, Rapid City, SD, June 26-28, 1985, Eileen Ashworth, ed., A.A. Balkema, Boston, MA, 1985, Vol. II, pp. 1113-1120.

Bieniawski, Z.T., "Engineering Classification of Jointed Rock Mass," Transactions, South African Institution of Civil Engineers, Vol. 15, No. 12, pp. 335-344, 1973.

Blake, W., "Assessment of Rock Burst Potential in Basalt at the Hanford Site," SD-BWI-ER-010, Rockwell Hanford Operation, Richland, WA, 1984.

Brady, B.H.G. and E.T. Brown, Rock Mechanics for Underground Mining, George Allen & Unwin, Ltd., London, England, 1985.

Costin, L.S., and S.J. Bauer, "Preliminary Analyses for the Excavation Investigation Experiments Proposed for the Exploratory Shaft at Yucca Mountain, Nevada Test Site," SAND87-1575, Sandia National Laboratories, Albuquerque, NM, in preparation.

Deere, D.U., R.B. Peck, J.E. Monsees, and B. Schmidt, "Design of Tunnel Liners and Support Systems," prepared by the University of Illinois for the U.S. Department of Transportation, NTIS: PB183 799, Washington, DC, February 1969.

Detournay, E., "Elastoplastic Model of a Deep Tunnel for a Rock with Variable Dilatancy," Rock Mechanics and Rock Engineering, Vol. 19, Springer-Verlag, New York, NY, pp. 99-108, 1986.

Detournay, E., and C. Fairhurst, "Two-dimensional Elastoplastic Analysis of a Long, Cylindrical Cavity Under Non-hydrostatic Loading," Int. Jour. Rock Mech. Min. Sci. & Geomech., Abstr, Vol. 24, No. 4, Pergamon Press, Oxford, Eng., pp. 197-211, 1987.

Detournay, E., and C.M. St. John, "Design Charts for a Deep Circular Tunnel Under Non-uniform Loading," Rock Mechanics and Rock Engineering, Vol. 21, pp. 119-137, 1988.

DOE (U.S. Department of Energy), "Generic Requirements Document for a Mined Geologic Disposal System, OGR/B-2, DOE/RW-0090, Office of Civilian Radioactive Waste Management, Washington, DC, June 1986.

Fairhurst, C., and N.G.W. Cook, "The Phenomenon of Rock Splitting Parallel to a Free Surface Under Compressive Stress," Proc. 1st. Cong. Int'l. Soc. Rock Mech., Lisbon, Vol. 1: 687-692-1966.

Fluor Technology, Inc., and Parsons Brinckerhoff/PB-KBB, in conjunction with Morrison-Knudsen Engineers, Inc., Science Applications International Corporation, Woodward-Clyde Consultants, and Rockwell International, Inc., "Salt

Repository Project Shaft Design Guide," (DOE/CH/46656-16-Rev 0.) prepared for the U.S. Department of Energy, Salt Repository Project Office, Hereford, TX, December 1987.

Goodman, R.E., and G. Shi, Block Theory and Its Application to Rock Engineering," Prentice-Hall, Inc., Englewood Cliffs, NJ, 1985.

Goodman, R.E., Introduction to Rock Mechanics, John Wiley & Sons, New York, NY, 1980.

Hendron, A.J., Jr., and G. Fernandez, "Dynamic and Static Design Considerations for Underground Chambers," Seismic Design of Embankments and Caverns, Proceedings of a symposium sponsored by the ASCE Geotechnical Engineering Division in conjunction with the ASCE National Convention, Philadelphia, PA, May 16-20, 1983, T.R. Howard, ed., pp. 157-197.

Hustrulid, W., "Lining Considerations for a Circular Vertical Shaft in Generic Tuff," SAND 83-7068, prepared for Sandia National Laboratories, Albuquerque, NM, December, 1984.

Jaeger, J.C. and N.G.W. Cook, Fundamentals of Rock Mechanics, Second Edition, Chapman and Hall, Ltd., London, England, 1976.

Langkopf, B.S., and P.R. Gnirk, 1986. Rock-Mass Classification of Candidate Repository Units at Yucca Mountain, Nye County, Nevada, SAND 82-2034, Sandia National Laboratories, Albuquerque, N. Mex.

Link, H., H. Lutendorf, and K. Stross, translated by B. Schmidt and S.A.G. Poppen, "Guidelines for Calculating Shaft Linings in Incompetent Strata," 2nd. Edition, Coal Mining Association, Glukauf, Essen, FRG, 1985.

NNWSI-SDRD (Nevada Nuclear Waste Storage Investigation-Exploratory Shaft Facility-Subsystem Design Requirements Document), prepared by U.S. Department of Energy, Nevada Operations Office, Rev. 1.

NNWSI-ICWG (Nevada Nuclear Waste Storage Investigation - Interface Control Working Group), "Repository Design Requirements, Shaft Collars and Linings, Preclosure Period," Engineering Change Request #005, January 8, 1988.

Newmark, N.M., and W.J. Hall, "Development of Criteria for Seismic Review of Selected Nuclear Power Plants" NUREG/CR-0098, prepared for the U.S. Nuclear Regulatory Commission, Washington, DC, September 1977.

NRC (U.S. Nuclear Regulatory Commission), "Disposal of High Level Radioactive Wastes in Geologic Repositories," Code of Federal Regulations, Energy, Title 10, Part 60, Washington, DC, January 1986.

Ogawa, T., and K.Y. Lo, "Effects of Dilatancy and Yield Criteria on Displacements around Tunnels," Canadian Geotechnical Journal, Vol. 24, 1987, pp. 100-113.

ONWI (Office of Nuclear Waste Isolation) "VISCOT: A Two-dimensional and Axisymmetric Nonlinear Transient Thermovisoelastic and Thermoviscoplastic Finite-Element Code for Modeling Time Dependent Viscous Mechanical Behavior of a Rock Mass," ONWI-437, Battelle Project Management Division, Columbus, OH, April 1983.

O'Rourke, T.D., ed. Guidelines for Tunnel Lining Design, American Society of Civil Engineers, New York, NY, 1984.

Owen, G.N., and R.E. Scholl, "Earthquake Engineering of Large Underground Structures," prepared for the Federal Highway Administration, FHWA/RD-80/ 195, Washington DC, January 1981.

Pariseau, W.G., "Estimation of Support Load Requirements for Underground Mine Openings by Computer Simulation of the Mining Sequence," Transactions, Society of Mining Engineers, AIME, Vol. 262, June 1977.

Popov, E.P., Introduction to Mechanics of Solids, Prentice-Hall, Inc., Englewood Cliffs, NJ, 1968.

Ranken, P.E., and J. Ghaboussi, "Tunnel Design Considerations. Analysis of Stresses and Deformations Around Advancing Tunnels," FRA OR&D 75-84, prepared for the University of Illinois for the Federal Railroad Administration, Washington, D.C., August 1975.

SNL (Sandia National Laboratories), "Site Characterization Plan Conceptual Design Report," SAND84-2641, compiled by H.R. MacDougall, L.W. Scully, and J.R. Tillerson, Sandia National Laboratories, Albuquerque, NM, September 1987.

SNL (Sandia National Laboratories) "NNWSI Project - Working Group Report Exploratory Shaft Seismic Design Basis," SAND88-1203, compiled by C.V. Subramanian, Sandia National Laboratories, Albuquerque, NM, in preparation[a].

SNL (Sandia National Laboratories), "Documentation and Verification of the SHAFT Code," SAND88-7065, prepared by J.F.T. Aqapito Assoc. for Sandia National Laboratories, Alburquerque, NM, in preparation[b].

SNL (Sandia National Laboratories), "Ground Motion Evaluations at Yucca Mountain, Nevada, with Applications to Repository Conceptual Design and Siting," SAND 85-7104, prepared by URS/John A. Blume & Associates for Sandia National Laboratories, Albuquerque, NM, May 1985.

SNL (Sandia National Laboratories), "Repository Design Requirements for the Yucca Mountain Mined Geologic Disposal System," SAND 85-0260, compiled by R.R. Hill, Nuclear Waste Engineering Projects Divison, Sandia National Laboratories, Albuquerque, NM, June 1988.

Schmitter, J.M., and A.F. Moreno, "Tunel con Deformaciones Excesivas," Proceedings of the Seventh Panamerican Conference on Soil Mechanics and Foundation Engineering, Canada, published by the Canadian Geotechnical Society, Montreal, Quebec, June 1983.

Sears, F.W., and M.W. Zemansky, University Physics, Fourth Edition Addison-Wesley Publishing Company, Inc., Reading, MA. 1970.

Spengler, R.W., and M.P. Chornack, "Stratigraphic and Structural Characteristics of Volcanic Rocks in Core Hole USW G-4, Yucca Mountain, Nye County, Nevada," USGS-OFR-84-789, Denver, CO, 1984.

St. John, C.M., E. Detournay, and C. Fairhurst, "Design Charts for a Deep Circular Tunnel Under Non-Hydrostatic Loading," Rock Mechanics in Productivity and Protection, Proc. 25th Symp. Rock Mechanics, Northwestern University, Evanston, IL, pp. 849-857, June 1984.

Tillerson, J.R., and F.B. Nimick "Geoengineering Properties of Potential Repository Units at Yucca Mountain, Southern Nevada," SAND 84-0221, Sandia National Laboratories, Albuquerque, NM, December 1984.

Timoshenko, S.P., and J.N. Goodier, Theory of Elasticity, Third Ed., McGraw-Hill Book Company, Inc., New York, NY, 1970.

Timoshenko, S.P., and D.H. Young, Elements of Strength of Materials, Fifth Edition, Van Nostrand Reinhold Company, New York, NY, 1968.

Winter, G., and A.H. Nilson, Design of Concrete Structures, Eighth Edition, McGraw-Hill Book Company, New York, NY, 1972.

Zimmerman, R.M., F.B. Nimick, and M.P. Board, "Geoengineering Characteristics of Welded Tuffs from Laboratory and Field Investigations," Proceedings of the Material Resources Society Annual Meeting, Boston, pp. 547-554, 1984.

APPENDIX A

EXAMPLE DATA

APPENDIX A. EXAMPLE DATA

A.1 GENERAL

This appendix presents an annotated listing of data used in the example problems. Although these data were derived from a number of project sources and are generally representative of expected site conditions, in all cases the designer is referred to the approved Project data base(s) for design input.

A.2 STRATIGRAPHY

Stratigraphic data used in the example problems and listed in Table A-1 have been derived from the SCP-CDR (SNL, 1987, Appendix Q). Elevations for borehole USW-G4 were used because this is the borehole closest to the exploratory shaft location. Precise elevations of stratigraphic boundaries are currently somewhat subjective because of limited data. The designer should use elevations of stratigraphic boundaries given in the approved project data base.

A.3 IN SITU STRESS

Table A-2 shows average expected in situ stress values at the repository horizon, along with ranges of values both for the vertical stress and the two horizontal stress components.

In reviewing the results of a large number of in situ stress measurements, Hoek and Brown (1980) have shown that measured vertical stresses typically are in fair agreement with calculations of the weight of overlying rock. However, horizontal stresses may differ widely from calculations based on elasticity considerations. The reasons for this

TABLE A-1

ELEVATIONS OF STRATIGRAPHIC BOUNDARIES USED IN EXAMPLE PROBLEMS[a]

Unit[b]	USW G-4 Corrected Elevations (ft)	(m)	Corrected Depth to Top (ft)	(m)
Ground Level				
Ground Surface	4167	1270	0	0
TC	4137	1261	30	9
PT	4049	1234	118	36
TS1	3924	1196	243	74
TS2	3497	1066	670	204
TS3	2876	877	1288	393
CH1v	2824	861	1343	409
CH1z	2807	856	1360	415

a. SCP-CDR (SNL 1987, Appendix Q)
b. Unit names are as described in the main text (Section 1.2)

variation include

- residual stresses,
- tectonic stresses,
- anisotropy, and
- creep.

The regional tectonic setting at Yucca Mountain is predominantly one of extensional normal faulting (Carr, 1984), making it unlikely that horizontal stresses are greater than, or even approach, vertical stress levels. Jamison and Cook (1980) suggest that values of the horizontal stress ratio (K_o) of 0.5 are typical for regions of normal faulting.

There is considerable uncertainty about the in situ stress magnitudes and orientations due to uncertainties in the methods that must be used to measure stresses when access from the surface is through long, small-diameter boreholes. This is evidenced by the wide ranges in suggested values. Because

TABLE A-2

MEAN VALUES AND RANGES OF PRINCIPAL STRESS MAGNITUDES AND DIRECTIONS AT THE CANDIDATE HORIZON[a]

Parameter	Average Value[b]	Range
Vertical Stress, σ_v	7.0 MPa	4.0 to 10.0 MPa
Ratio of Minimum Horizontal Stress to Vertical Stress (σ_h/σ_v)	0.5	0.3 to 0.8
Ratio of Maximum Horizontal Stress to Vertical Stress (σ_H/σ_v)	0.6	0.3 to 1.0
Bearing of Minimum Horizontal Stress	N57°W	N50°W to N65°W
Bearing of Maximum Horizontal Stress	N33°E	N25°E to N40°E

a. RIB Version 3.001
b. Average value for a depth of approximately 1,000 ft.

of this uncertainty and the fact that the liner stresses are directly proportional to the magnitude of the stresses, conservative cases for uniform and nonuniform horizontal stress are investigated in the example problem. The in situ conservative uniform value is 0.8 times the vertical stress. The conservative nonuniform horizontal stresses (σ_H and σ_h) are 0.8 and 0.3 times the vertical stress. It is possible but unlikely that in situ stress values will be as unfavorable as the cases selected for analysis.

Stress values in the Project literature (SNL, 1987, Appendix Q) are given for a depth of approximately 1,000 ft, which is the current elevation of the candidate repository horizon. In the example, vertical stresses (σ_v) at other elevations were calculated by

$$\sigma_v = 0.023 \text{ MPa/m} \times \text{depth from surface (m)}. \quad \text{(A-1)}$$

Case 1 (uniform pressure) horizontal stress was calculated from

$$\sigma_h = K_o \times \sigma_v, \quad \text{(A-2)}$$

where

σ_h = uniform horizontal stress
K_o = horizontal to vertical stress ratio
= 0.8.

Case 2 (anisotropic) horizontal stress was calculated from

$$\sigma_H = K_H \times \sigma_v, \text{ and} \quad \text{(A-3)}$$

$$\sigma_h = K_h \times \sigma_v, \quad \text{(A-4)}$$

where

$\sigma_{H(h)}$ = extreme maximum (minimum) horizontal stress
$K_{H(h)}$ = max (min) horizontal to vertical stress ratio
= 0.8 (0.3).

Design stresses for each unit are those calculated at the base of the unit. This represents the worst case situation.

Table A-3 tabulates the vertical and horizontal stresses at key elevations.

A.4 ROCK MASS PARAMETERS

In fractured materials such as rock, data from tests on small specimens of "intact" rock generally are not representative of the behavior of large rock volumes. Discussions of this phenomenon are available in most standard rock mechanics texts (e.g., Goodman, 1980). The precise relationship between intact and rock mass strength and deformability properties in jointed rock is highly rock and site

TABLE A-3

STRESS VALUES USED FOR EACH THERMOMECHANICAL UNIT IN EXAMPLE PROBLEM

	In Situ Stresses			Case 1	Case 2	
	Formation Bottom Depth		Vertical Stress	Uniform Horiz. Stress	Min. Value Min. Horiz. Stress	Max. Value Max. Horiz. Stress
Unit	(ft)	(m)	(MPa)	(MPa)	(MPa)	(MPa)
TC	118	36.0	0.83	0.66	0.25	0.66
PT	243	74.1	1.70	1.36	0.51	1.36
TS-1	670	204.3	4.70	3.76	1.41	3.76
TS-2/3	1343	409.5	9.42	7.53	2.83	7.53
CH1v	1360	414.6	9.54	7.63	2.86	7.63
CH1z	1467*	447.3*	10.29	8.23	3.09	8.23

*Example shaft bottom

specific, difficult to measure, and in general poorly understood. Rock mass properties rather than intact properties are appropriate for the scale of the analyses described in this guide because the joint spacing is small relative to the shaft diameter. The rock mass strength and deformability properties (uniaxial strength, cohesion, modulus) have been reduced to account for scale effects as described in the SCP-CDR (SNL, 1987, Appendix O). These have been used as a basis for the example problem.

In addition to uniaxial strength and stiffness parameters, a yield criterion for the rock mass is needed for shaft analysis to define the increase in rock strength with confining pressure. A number of different criteria exist; some of these are complex and permit a close fit to experimental data, if suitable data exist. The linear Mohr-Coulomb (or Coulomb) criterion was selected for the example problems in this report for two reasons: (1) it has a long history of application and is well-understood and (2) the RIB specifies Mohr-Coulomb parameters. This methodology does not

preclude the use of alternate yield criteria, if such are recommended in the approved data base.

The Mohr-Coulomb criterion (Goodman, 1980) is of the following form:

$$\sigma_1 = q + K_p \sigma_3 \qquad \text{(A-5)}$$

where

σ_1 = major principal stress
σ_3 = minor principal stress
q = unconfined compressive strength
K_p = passive pressure coefficient
= $(1+\sin\phi)/(1-\sin\phi)$
ϕ = friction angle.

Table A-4 lists the parameters that were selected for the example calculations.

TABLE A-4

ROCK PROPERTY VALUES SELECTED FOR EXAMPLE PROBLEM

Thermal/ Mechanical Unit	Static Modulus of Elasticity E (MPa)	Static and Dynamic Poisson's Ratio	Unconfined Compressive Strength (MPa)	Angle of Friction (°)	Dynamic* Modulus of Elasticity E (MPa)
TC	20000	0.10	120.0	44.7	---
PT	1900	0.19	9.5	8.5	4100
TS1	7600	0.16	16.0	12.5	14900
TS2/3	15200	0.22	83.0	23.5	23500
CH1v	3600	0.15	13.5	12.0	25500
CH1	3600	0.16	13.5	7.6	16300

* Source: RIB Version 3.001

A.5 THERMAL INPUT

Analysis of thermally induced stresses is an important part of repository design, and a fully detailed methodology for thermal analysis for the NNWSI Project may be developed for repository licensing. Of the three loading mechanisms discussed in Chapter 4, thermal loading of the shaft liner is the only one that is heavily dependent on details of the future repository design. Thermal analyses are also sensitive to any modifications to the thermal properties of the emplaced waste and the host rock, neither of which are currently completely defined. For the example problems used in the simplified methodology presented here (and supplemented in Appendix B), the following properties are important.

WASTE

- Type and age
- Emplacement sequence
- Emplacement density
- Decay characteristics

HOST ROCK

- Thermal conductivity
- Coefficient of thermal expansion
- Thermal capacity.

Waste type used for example analysis is 8.55-yr-old spent fuel, using an assumed 60:40 (pressurized-water reactor fuel: boiling-water reactor fuel) mix (SNL, 1987, Appendix G-3). The waste emplacement sequence from the SCP-CDR was used, as discussed in Appendix B. The normalized waste decay curve and the allowable thermal loading completely specify the heat input term.

Average thermal load density (emplacement density) and decay characteristics of the waste are required for the example problem. An emplacement density of 57 kW/acre (14.1 W/m^2) was used in the example. The waste-normalized decay characteristics are given by the following equation (see Appendix B, this report).

$$P(t) = 0.15602 \exp(-0.0013539t) + 0.59786 \exp(-0.019142t) + 0.15227 \exp(-0.051888t) + 0.09384 \exp(-0.43768t), \quad \text{(A-6)}$$

in which the instantaneous power P is expressed as a function of time t, in years since emplacement.

Table A-5 lists the values of host rock thermal parameters selected for use in the example analysis, including thermal conductivity, coefficient of thermal expansion, and thermal capacity.

A.6 SEISMIC INPUT

Table A-6 through A-8 shows seismic data used in the example problem. Two cases are considered, as discussed in Section 4.5.

A.7 CONCRETE PROPERTIES

The concrete strength value of 34.5 MPa (5000 psi) used in the example problems is a specified 28-day design strength value and is compatible with concrete mixes and placement procedures appropriate to shaft sinking.

The modulus of the concrete (E_c) with a given unit weight (w_c) and unconfined compressive strength (f'_c) can be calculated according to ACI standard practice (ACI, 1983, Section 8.5.1), as follows:

TABLE A-5

VALUES FOR ROCK THERMAL/MECHANICAL PARAMETERS USED IN THE EXAMPLE PROBLEM[a]

Unit	Elevation of Top (m)	Density (gm/cc)	Coeff. Linear Expansion ($10^{-6}K^{-1}$)	Thermal Capacity (J/cm^3K)	Thermal Conductivity (kW/mK)	Young's Modulus (GPa)	Poisson's Ratio
TC	1326	2.32	10.7	2.24	2.00	15.4	0.10
TS 1	1240	2.27	10.7	1.88	1.16	7.6	0.16
TS 2/3	1022	2.34	10.7	2.25	2.07	15.1	0.20
CH	901	1.89	6.7	2.46	1.35	3.5	0.17
PP[b]	756	2.15	8.3	2.42	1.86	6.1	0.20

a. These values were taken from Appendix B. The stratigraphy and properties differ slightly from those used in other example problems. The minor differnces are of no importance to the utility of the examples.

b. The Prow Pass Unit is below the shaft bottom and has no major importance to any of the analyses. However, in the stratified thermal analysis of Appendix B, the Prow Pass was included as part of the finite element model.

$$E_c = w_c^{1.5}\, 33\sqrt{f'_c}, \qquad \text{(A-7)}$$

with E_c and f'_c in psi, w_c in lb/cu ft.

For normal weight concrete, $w_c \approx 145$ lb/cu ft.

$$E_c = 57{,}000\sqrt{f'_c}. \qquad \text{(A-8)}$$

Data on concrete properties are not site specific and are not included in the RIB. Specific concrete properties are dependent on the mix design and are not the subject of this report. However, the values for concrete strength and deformability parameters that were used in the example problem include the following.

Compressive strength:	34.5 MPa
Tensile strength:	2.9 MPA
Elastic modulus:	28 GPA
Poisson's ratio:	0.15

These values can readily be achieved during shaft sinking. The designer must specify required strength and design modulus values.

A.8 DESIGN DATA

Design data used in the example problem include the following:

Shaft diameter (lined):	3.28 m
Shaft depth:	425 m

Design data specific to the example thermal analysis is listed in Appendix B.

TABLE A-6

ASSUMED PT UNIT FREE-FIELD SEISMIC LOADS FOR EXAMPLE PROBLEM

Load Case	Wave Component	Strain ($\times 10^{-6}$) ε_x	ε_y	ε_z	γ_{xy}	γ_{xz}	γ_{yz}	k (1/m)
SEISMIC-1	P	0.0	0.0	67.0	0.0	0.0	0.0	0.0
SEISMIC-1	S_V	0.0	0.0	0.0	0.0	0.0	0.0	0.0
SEISMIC-1	S_H	0.0	0.0	0.0	164	0.0	0.0	0.0
SEISMIC-2	P	34.4	0.0	103	0.0	119	0.0	0.45
SEISMIC-2	S_V	144	0.0	144	0.0	167	0.0	2.04
SEISMIC-2	S_H	0.0	0.0	0.0	144	0.0	250	2.04
SEISMIC-2	$S_V+0.4(P+S_H)$	158	0.0	185	57.7	214	99.9	--
SEISMIC-2*	$\sqrt{(SV+0.4P)^2+0.4SH^2}$	--	--	--	--	--	--	2.36

*This is a vector sum using the square root of the sum of the squares. The P and S_V waves cause bending at 90° to the S_H wave (SNL, in preparation).

NOTES:

- The xyz coordinate system for seismic is referenced to the direction of incidence of the seismic wave (the x-direction). It is not related to the global xyz coordinate system, since it is assumed that the earthquake can come from any direction.
- The values of γ_{xz} and γ_{yz} can be further combined using the 100-40-40 rule, since they come from different waves but act together vectorially to produce a net out-of-plane shear strain.

TABLE A-7

ASSUMED TS UNIT FREE-FIELD SEISMIC LOADS FOR EXAMPLE PROBLEM

Load Case	Wave Component	Strain ($\times 10^{-6}$) ε_x	ε_y	ε_z	γ_{xy}	γ_{xz}	γ_{yz}	k (1/m)
SEISMIC-1	P	0.0	0.0	44.0	0.0	0.0	0.0	0.0
SEISMIC-1	S_V	0.0	0.0	0.0	0.0	0.0	0.0	0.0
SEISMIC-1	S_H	0.0	0.0	0.0	109	0.0	0.0	0.0
SEISMIC-2	P	17.0	0.0	50.9	0.0	58.8	0.0	0.11
SEISMIC-2	S_V	73.5	0.0	73.5	0.0	84.9	0.0	0.53
SEISMIC-2	S_H	0.0	0.0	0.0	73.5	0.0	127	0.53
SEISMIC-2	SV+0.4(P+SH)	80.3	0.0	93.9	29.4	108	50.9	--
SEISMIC-2*	$\sqrt{(SV+0.4P)^2+0.4^2SH^2}$	--	--	--	--	--	--	0.61

*These are vector sums using the square root of the sum of the squares. (SNL, in preparation).

NOTES:

- The xyz coordinate system for seismic is referenced to the direction of incidence of the seismic wave (the x-direction). It is not related to the global xyz coordinate system, since it is assumed that the earthquake can come from any direction.
- The values of γ_{xz} and γ_{yz} can be further combined using the 100-40-40 rule, since they come from different waves but act together vectorially to produce a net out-of-plane shear strain.

TABLE A-8

ASSUMED CH UNIT FREE-FIELD SEISMIC LOADS FOR EXAMPLE PROBLEM

Load Case	Wave Component	Strain ($\times 10^{-6}$) ϵ_x	ϵ_y	ϵ_z	γ_{xy}	γ_{xz}	γ_{yz}	k (1/m)
SEISMIC-1	P	0.0	0.0	67.0	0.0	0.0	0.0	0.0
SEISMIC-1	S_V	0.0	0.0	0.0	0.0	0.0	0.0	0.0
SEISMIC-1	S_H	0.0	0.0	0.0	153	0.0	0.0	0.0
SEISMIC-2	P	19.2	0.0	57.5	0.0	66.4	0.0	0.14
SEISMIC-2	S_V	78.5	0.0	78.5	0.0	90.7	0.0	0.60
SEISMIC-2	S_H	0.0	0.0	0.0	78.5	0.0	136	0.60
SEISMIC-2	$S_V+0.4(P+S_H)$	86.2	0.0	102	31.4	117	54.4	--
SEISMIC-2*	$\sqrt{(SV+0.4P)^2+0.4^2SH^2}$	--	-	---	---	--	--	0.70

*These are vector sums using the square root of the sum of the squares. (SNL, in preparation).

NOTES:

- The xyz coordinate system for seismic is referenced to the direction of incidence of the seismic wave (the x-direction). It is not related to the global xyz coordinate system, since it is assumed that the earthquake can come from any direction.
- The values of γ_{xz} and γ_{yz} can be further combined using the 100-40-40 rule, since they come from different waves but act together vectorially to produce a net out-of-plane shear strain.

REFERENCES

ACI-318, "Building Code Requirements for Reinforced Concrete," American Concrete Institute, Detroit, MI, 1983.

Carr, W.J., "Regional Structural Setting of Yucca Mountain, SW Nevada, and Late Cenozoic Rates of Tectonic Activity in Part of the Southwestern Great Basin, Nev. and Calif.," USGS OFR 84-854, 109 pp., 1984.

Goodman, R.E., Introduction to Rock Mechanics, John Wiley & Sons, Inc., New York, NY, 1980.

Hoek, E. and E.T. Brown, Underground Excavations in Rock, The Institution of Mining and Metallurgy, London, 527 pp., 1980.

Jamison, D.B. and N.B. Cook, "Note on Measured Values for the State of Stress in the Earth's Crust," J. Geophys. Research, v. 85., pp 1833-1838, April 10, 1980.

SNL (Sandia National Laboratories), "Site Characterization Plan Conceptual Design Report," SAND84-2641, compiled by H. R. MacDougall, L. W. Scully, and J. R. Tillerson, Sandia National Laboratories, Albuquerque, NM, September, 1987.

SNL (Sandia National Laboratories), "NNWSI Project - Working Group Report Exploratory Shaft Seismic Design Basis," SAND88-1203, compiled by C.V. Subramanian, Sandia National Laboratories, Albuquerque, NM, in preparation.

APPENDIX B

THERMAL ANALYSIS MEMO

J. F. T. AGAPITO & ASSOCIATES, INC.

MEMORANDUM

To: Archie M. Richardson
Parsons Brinckerhoff Quade & Douglas, Inc.

From: Christopher M. St. John

Date: January 3, 1989

Memorandum: 87-88-0024/Rev 5

Subject: Analysis of Thermally-Induced Stresses and Strains at the Location of a Shaft of Repository at Yucca Mountain

1.0 INTRODUCTION

The purpose of this memorandum is to document the findings of a brief study of the loads to which the shafts of the proposed repository at Yucca Mountain will be subjected during the operational period of that facility. The primary purpose in preparing this memorandum was to illustrate a methodology that may be used to compute stresses and strains at the shaft locations. Results are presented for a specific set of assumptions with respect to the repository layout, waste emplacement schedule, thermal loading, and waste form. These results are intended to be used only to support example problems for the NNWSI shaft design methodology and guide.

2.0 CONCLUSIONS AND RECOMMENDATIONS

- Before undertaking design of the shafts of a repository, it is important that analyses accounting for the location of the shaft relative to the waste emplacement panels, be performed. Those analyses should be made using the best available data on the repository layout, the waste to be emplaced, and the rock mass properties. Output from the analyses should comprise predictions of the stresses, strains, and displacements that are predicted at the location of the shaft as a result of the thermal loading of the repository.

- Thermal loading of the repository imposes stresses and strains on the shaft liner. If the shaft is set off from the emplacement area, the axial strains will be tensile, and the horizontal stresses applied to the liner will not be uniform. These stresses and strains are greatest close to the emplacement areas, and decay rapidly with standoff distance.

- To compute the thermally-induced stresses in the liner, it is necessary to perform analyses of the interactions between the rock mass and the liner. Input to those calculations comprises the changes in the stress or strain in the rock mass.

- The thermally induced horizontal stresses are strongly anisotropic unless waste is emplaced symmetrically around the shaft. In the case investigated, at the repository horizon the principal horizontal stresses induced by thermal loading are approximately 1.6 MPa compression and 0.01 MPa tension, 100 years after waste emplacement. The axial strain is extensile, and has a magnitude of approximately 150 microstrains. The curvature that would be induced in the shaft, if it conforms to the displacement of the rock mass, is insignificant.

- The induced stresses in the rock and the liner will be directly dependent on the assumed expansion coefficient of the rock mass. However, the induced stresses and the axial strain in the liner are insensitive to variations in the rock mass modulus.

3.0 ANALYSIS METHODS

Two computer models of the repository illustrated schematically in Figure 1 were used in order to develop results presented in this memorandum. First, a boundary element code, HEFF, was used to develop two models of a repository in a homogeneous elastic medium with the thermal and thermal-mechanical properties of the candidate horizon. Those models were used to investigate thermally-induced stress at the locations of the ES1 and ES2 shafts and also at an exhaust shaft located at the repository boundary. Second, the finite element codes, DOT and VISCOT, were used to develop simple models of a repository comprising two waste emplacement panels and a comparison was made between the thermally-induced stress when the rock mass is homogeneous and when a representative stratigraphy is assumed. Description of the HEFF, DOT, and VISCOT codes and a discussion of how they have been applied in repository analyses can be found in SAND86-7005 (St. John, 1987).

3.1 Shaft Liner Analysis

Analysis of the effect of the repository thermal loading on the shafts and the shaft liners involved consideration of four different deformation modes. These are: hoop deformation, that is associated with stresses in the horizontal plane normal to the shaft axis; axial deformation, that is associated with thermally-induced extension of the rock against which a liner would be cast; shear deformation, that is associated with thermally-induced shear stresses in a vertical plane passing through the shaft; and bending, that is associated with thermally-induced displacements of the rock mass through which the shaft passes. Each of these deformation modes is discussed briefly below. The purpose of this discussion is to identify the information that is required from the repository analysis.

Hoop Deformation and Axial Strain: Hoop deformation and axial strain should be considered together because the two are intimately coupled to each other in the shaft line analysis. Specifically, the analysis should consider the case of an initially stress-free liner that is installed within a cylindrical hole in the rock mass. That condition corresponds to the case of a liner installed after the rock mass has reached a state of equilibrium following excavation of the shaft. The effect of thermal loading of the repository is to change the stresses and strains in the rock mass, by an amount calculated using numerical models such as those developed using the HEFF, DOT and VISCOT codes. For the sake of convenience, we designate the thermally-induced stresses at the shaft location as:

- σ_{xx} - the horizontal direct stress in the plane of a two-dimensional model of the repository.
- σ_{yy} - the horizontal direct stress normal to the plane of a two-dimensional model of the repository.
- σ_{zz} - the vertical direct stress.

Note that these are stresses that would exist in the rock if the shaft were not present. They are illustrated schematically in Figure 2.

The interaction calculations for the shaft liner require definition of the induced horizontal stresses, σ_{xx} and σ_{yy}, and also prescription of the axial strain, ε_{zz}. For a long cylindrical structure,

such as a shaft or tunnel liner, it is common to assume plane strain conditions. Namely, it is assumed that axial deformation is impossible. This assumption is not appropriate in the present instance because thermal expansion of the rock mass surrounding the repository causes strains parallel to the axis of the shaft. Those strains are transmitted directly to the shaft liner, which is assumed to be insufficiently stiff to constrain the large-scale deformation of the rock mass to any significant degree. The strains can be computed from the induced stresses from the equation:

$$\varepsilon_{zz} = \frac{[\sigma_{zz} - \nu(\sigma_{xx} + \sigma_{yy})]}{E},$$

in which ν and E are, respectively, the Poisson's ratio and elastic modulus of the rock mass. Note that the equation should properly include a term for the thermal strain. This has been ignored in the present instance because the temperature changes at the proposed shaft locations are very small during the time frames of concern (up to 100 years after emplacement) and because the thermal expansion coefficients of the concrete and the surrounding rock mass are similar. If a shaft were to pass directly through an emplacement area rather than be separated from the emplacement area by a significant standoff distance, then the thermal strain would need to be considered. The thermal strains are not insignificant close to the emplacement areas and are correctly included within the repository models.

Shear Deformation: In cases where waste is not emplaced symmetrically around a shaft location, the shaft liner may experience shear stresses. These can be amplified if there are significant variations in the thermal-mechanical properties of the rock mass through which the shaft passes, but are also present if the rock mass is homogeneous. Adopting the same coordinates defined earlier for the direct stresses, the shear stress is designated σ_{xz}, which indicates a shear stress in the direction of the x-axis on a plane normal to the z-axis. The maximum value of the corresponding shear stress is parallel to the shaft wall on a plane normal to the z-axis (denoted σ'_{xz}). It is defined by (J. F. T. Agapito & Associates, Inc., 1988):

$$\sigma'_{xz} = \frac{2\left(1 + \frac{a^2}{r^2}\right)}{\frac{G}{G'}\left(1 + \frac{a^2}{R^2}\right) + \left(1 - \frac{a^2}{R^2}\right)} \cdot \sigma_{xz},$$

in which a and R are, respectively, the internal and external radii of the shaft liner, r is the radial distance from the center of the shaft, and G and G' are shear moduli of the rock and liner, respectively. For an isotropic elastic material, the shear modulus is related to the parameters E and ν by:

$$G = \frac{E}{2(1+\nu)}.$$

Bending Deformation: It is assumed that the shaft is initially vertical and straight. Unless the waste is emplaced symmetrically with respect to the shaft, there will be horizontal displacement of the shaft axis that causes bending. The bending induces both axial stresses and shear stresses. These are defined by the following equation:

$$\sigma'_{zz} = E' X \frac{d^2u}{dz^2},$$

and

$$\sigma'_x = \frac{E'I}{A}\frac{d^3u}{dz^3},$$

in which X is the distance from the neutral axis to the fiber of concern, E' is the liner modulus, I is moment of inertia, and A the cross-sectional area. u is the displacement normal to the long axis of the shaft and $\frac{d^2u}{dz^2}$ and $\frac{d^3u}{dz^3}$ are, respectively, the second and third derivatives of that displacement with respect to z. The second derivative is also the curvature. The displacement needed to evaluate the bending stresses are obtained directly from the repository models.

4.0 ANALYSIS DATA AND ASSUMPTIONS

The source of data for all repository analyses was the NNWSI Reference Information Base and drawings of the repository layout in the Draft SCP Conceptual Design Report (MacDougall, et al., 1987). The configuration for emplacement of waste in short vertical holes in the floors of the emplacement drifts was considered specifically, but the results of analyses of the horizontal emplacement option would be the same providing the emplacement density and waste form are identical.

Geometrical Data:

Emplacement Drift Spacing	102 ft.	(31.1 m)
Main Drift Width	25 ft.	(7.6 m)
Main Drift Spacing	63 ft.	(19.2 m)
Standoff of Emplacement Drift from Main	200 ft.	(61.0 m)

Waste Characteristics:

Emplacement Density	57 kW/acre (14.1 W/m^2)
Waste Type	8.55 Year-Old Spent Fuel
Waste Normalized Decay Characteristics	$P(t)$ = 0.15602exp(-0.0013539t)
	+ 0.59786exp(-0.019142t)
	+ 0.15227exp(-0.051888t)
	+ 0.9384exp(-0.43768t)

in which the instantaneous power, P, is expressed as a function of time, t, in years, since emplacement.

Thermal and Thermal-Mechanical Properties:

The following data is provided for a representative stratigraphy that is described in the Unit Evaluation Report (Johnstone, et al., 1984). The material parameters are taken from Nimick, et al. (1984) for material that is 80% saturated. The values differ slightly from those listed in Version 02.002 of the RIB, dated August 6, 1987. However, the differences are sufficiently minor that the conclusions presented in this memorandum would not be affected.

Thermal-Mechanical Unit	Elevation of Top* (m)	Density (gm/cc)	Linear Expansion ($10^{-6}K^{-1}$)	Thermal Capacity (J/cm^3K)	Thermal Conductivity (kW/mK)	Young's Modulus (GPa)	Poisson's Ratio (-)
Tiva Canyon	1326	2.32	10.7	2.24	2.00	15.4	0.10
Topopah Springs 1	1240	2.27	10.7	1.88	1.16	7.6	0.16
Topopah Springs 2/3	1022	2.34	10.7	2.25	2.07	15.2	0.20
Calico Hills	901	1.89	6.7	2.46	1.35	3.5	0.17
Prow Pass	756	2.15	8.3	2.42	1.86	6.1	0.20

* *From hole USWG-1 (Nimick and Williams, 1984)*

5.0 REPOSITORY MODELS

As noted in Section 3, repository models were developed using both the HEFF code and the DOT/VISCOT code. These models are described briefly in the following paragraphs and are illustrated schematically in Figure 1.

5.1 Boundary Element Models

The two boundary element models were based on the assumption that the repository is located within a homogeneous medium, with the thermal and thermal-mechanical properties of the candidate horizon (TS2/3), at a depth of 300 m below a horizontal ground surface. From the current repository plans, two simplified models of the repository were developed:

- Section through the exploratory shaft, with a space of 450 m between the nearest emplacement drifts of adjacent panels. As viewed in Figure 1, the panel to the right of the ES1/2 comprised 12 parallel drifts and the panel to the left 35 drifts. Emplacement in those two panels was assumed to occur instantaneously in years 1 and 17, respectively, and the shafts were located 124 m and 186 m from the nearest emplacement drift in the left-hand panel.

- Section through an exhaust shaft on the eastern perimeter of the repository. As viewed in Figure 1, each panel comprised 35 emplacement drifts, separated by the narrow pillar (102.5 m diagonal width) containing the repository main entries. It was assumed that the waste in the panel nearer the shaft was emplaced after 3 years and that in the other panel 13 years later.

In both models, the thermal load of the repository was idealized as a line heat source located beneath the center of each emplacement drift and the waste was assumed to be an average of 8.55 years out of the reactor at the time of emplacement. The standoff distance between the last emplacement drift and the exhaust shaft was 100 m, or approximately 85 m from the edge of a panel, if it is assumed to extend a half the drift spacing from the last drift. The strength of the heat sources was calculated directly from the areal power density (APD) and the drift spacing. (i.e., for a spacing of 31 m, it has a value of 438.4 w/m of drift).

5.2 Finite-Element Models

For the finite-element models, the repository was assumed to comprise two long panels 770 m wide separated by a pillar 320 m wide. Consistent with data used during the unit evaluation, the candidate horizon was assumed to be 348 m below the surface. (This value is greater than that used in the boundary element models because the candidate horizon lies within the TS2 member, which lies between 304 m and 425 m below the surface in the idealized stratigraphy.)

Finite-element analyses were performed for a homogeneous rock mass and a rock mass with the stratigraphy defined in Section 4.0. In both cases, the thermal loading was represented by uniform heat generation in a layer 10 m thick centered about the repository horizon. The strength of the heat source was computed in the same manner as for the boundary element models.

6.0 RESULTS OF A REPOSITORY ANALYSIS

Since the purpose of the repository analyses was merely to define the boundary conditions for the shaft liner investigation, detailed results are not presented.[1] Instead, selected results are presented in a series of figures, for which the following brief commentary is provided. Note that in all cases, the quantities plotted in the figures are those induced by the thermal load alone.

Figures 3 through 5: These figures illustrate the stress and strain profiles at the candidate locations for the shafts for both the boundary element and finite-element models. The following observations may be made.

- There is good agreement between the results of the boundary element analysis of conditions at the exhaust shaft location and those of homogeneous finite-element model.
- The direct stresses peak at the repository horizon.
- The axial strains peak at the repository horizon, except in the case of the stratified model when the strains are higher in the adjacent strata because they have a lower elastic modulus.
- The layering has a pronounced effect on the stresses and strains in the rock mass, with higher induced stresses predicted in the stiffer layers.

Note that for some shaft locations, the out-of-plane stress is observed to decrease (Figure 4). As discussed below in relation to Figures 6 through 8, this is an effect of the thermally-induced axial tensile strain at those locations. Note also that for the finite-element analyses, the stresses are plotted at the gauss (integration) points of the elements. When a coarse finite-element mesh is used, as in this case, this can give rise to significant discontinuities in the stress between adjacent elements.

Figures 6 through 8: These figures illustrate the development of stresses and strains at the shaft locations, as predicted by the boundary element models. The following observations may be made:

- The in-plane horizontal stresses increase steadily and continue to increase at least until 100 years after emplacement.

---

1 Note: There is no discussion of temperature changes since these are small for the first 100 yrs after emplacement: less that 0.5°C for the ES1 and ES2 and less that 5°C for the Exhaust Shaft.

- The out-of-plane horizontal stresses initially decrease, but subsequently increase as the lateral extent of the heated rock mass extends.

- The axial strain to which the liner is subject increases steadily and appears to peak later than 100 years after waste emplacement.

- The conditions experienced at the exploratory shaft locations are more moderate than at the exhaust shafts because of the greater standoff.

When reviewing the time history of the out-of-plane stress (Figure 6), it is important to recall that this quantity is computed from the induced horizontal and vertical stresses in the plane of the section, the temperature change, and the thermal-mechanical properties of the rock mass. Because plane strain conditions are assumed, the temperature increase might be expected to result in an increase in the out-of-plane stress. However, when there is significant induced tension in the vertical direction, the net affect can be a decrease in the out-of-plane stress.

Figures 9 and 10: These figures illustrate the relationship between the induced stress and strain as a function of distance from the edge of the repository. The following observations may be made:

- The effect of the thermal loading is comparatively local, even 100 years after waste emplacement, and is reduced to modest levels within 100 m of the boundary of the adjacent panel.

- The horizontal stresses at the repository horizon are compressive close to the waste emplacement panel, and because they are not equal, will cause the shaft to deform to an oval-shaped cross section.

- The vertical stresses in the rock and the axial straining in the rock and the liner are extensile.

- The affect of the relatively higher modulus of the candidate member is to increase the horizontal stresses, but decrease the axial strain.

Figures 11 and 12: The induced shear stress from the homogeneous model along the axes of ES1 and ES2 is illustrated. The maximum shear stress above the repository occurs approximately 119 years after emplacement, 100 m above the repository. The stratigraphy shown was constructed from the idealized stratigraphy used for the finite-element analysis, but adjusted to the 300 m repository depth used in the boundary element analysis.

7.0 INPUT FOR ANALYSIS OF THE SHAFT LINER

Consistent with the discussion of Section 3.0, discussion of the data for analysis of the shaft liner is divided into three groups. The first deal with hoop and axial deformation, the second shear stress, and the third bending.

7.1 Hoop Deformation and Axial Strain

The computed stresses and strains at the repository horizon are tabulated below.

Location	Induced Stress xx-stress (MPa)	yy-stress (MPa)	zz-stress (MPa)	Induced Axial Strain Microstrains
ES1 (BE)	+1.483	-0.0814	-1.988	-150.
ES2 (BE)	+1.608	-0.0139	-2.040	-156.
Exhaust Shaft (BE)	+2.860	+0.9880	-2.018	-185.
Exhaust Shaft (FE) (Homogeneous Model)	+2.770	+0.7980	-2.010	-180.
Exhaust Shaft (FE) (Stratified Model)	+3.360	+1.1100	-1.195	-137.

The close correspondence between the boundary element and finite-element analyses of the homogeneous model is evident in this table. However, it is also clear that the variation in thermal-mechanical properties of the rock mass is important in determining the stresses sand strains in the individual units. For units other than the Topopah Springs 2/3 units, the thermally-induced strains are recommended as inputs for evaluation of the shaft liner stresses and deformations. Additional repository analyses need to be performed in order to obtain reliable estimates of the stresses and strains along the entire depth of the shafts. Until such analyses are performed, the following values may be used for analysis of the exploratory shafts.

Unit	Δ Maximum (In-plane) Stress (MPa)	Δ Minimum (Out-of-plane) Stress (MPa)	In-Plane Strain (micro strains)	Δ Axial Strain (micro strains)
Tiva Canyon	0.6	0.10	40	-20.
Topopah Springs 1	1.0	0.05	34	-100.
Topopah Springs 2/3	1.6	-0.05	134	-150.
Calico Hills	1.0	-0.09	91	-120.

Note: Out-of-plane strain zero.

7.2 Shear Deformation

The shear stress in the shaft liner is maximum at the outside edge of the liner. Substitution of typical dimensions and material parameters in the equation given in Section 3.1 indicates that the maximum shear stresses for the liner in the TS2/3 unit would be approximately three times the value in the rock mass.

Review of the results of the boundary element repository models shown in Figures 11 and 12 indicates that maximum shear stresses at the shaft locations considered occur some 100 m above the repository horizon. The magnitudes of the stresses depend upon the emplacement sequence adopted. For the first 100 years after emplacement and the particular cases discussed here, the maximum values of the shear stress above the repository are approximately 0.13 MPa and 0.55

MPa for ES1 and ES2, respectively. It is concluded that the thermally induced shear stresses in the exploratory shaft liner are generally small. However, detailed modeling of the stratigraphy and the location of the shaft relative to the waste emplacement panels will be required to obtain a reliable estimate of the shear stresses that will be experienced. For shaft liner design in units other than the Topopah Springs 2/3, the thermally-induced shear strains should be used. The recommended thermally-induced shear stresses and strains are as follows:

Unit	Out-of-Plane Shear Stress (MPa)	Out-of-Plane Shear Strain (micro strains)
Tiva Canyon	0.2	32
Topopah Springs 1	0.5	80
Topopah Springs 2/3	0.5	80
Calico Hills	0.2	32

7.3 Bending Deformation

The axial stress induced by bending of the shaft liner can be computed from the equation given in Section 3.1, providing the curvature $\frac{d^2u}{dz^2}$ is known. This can be calculated from the results of the repository model using the finite difference approximation for irregularly-spaced sample points.

$$\frac{d^2u}{dz^2} = \frac{\left(\frac{u_{i-1}-u_i}{z_{i-1}-z_i} - \frac{u_i-u_{i+1}}{z_i-z_{i+1}}\right)}{\left(\frac{z_{i-1}-z_{i+1}}{2}\right)}$$

where u_i is the x displacement at the i^{th} sample point and z_i is the elevation of that sample point.

If the above procedure is used to compute the curvature along the location of the axis of the exhaust shaft, then maximum values on the order of 1×10^{-6} 1/m are obtained for the stratified and homogeneous cases. The corresponding axial stress at the extreme fiber of the shaft liner are on the order of 0.05 MPa. The affect of bending is, therefore, considered to be insignificant.

REFERENCES

J. F. T. Agapito & Associates, Inc. (1988), "Documentation and Verification of the SHAFT Code," SAND88-7065 (Draft) prepared for Sandia National Laboratories, Albuquerque, NM.

Johnstone, J, Peters, R. R., and Gnirk, P. F. (1984), "Unit Evaluationa at Yucca Mountain, Nevada Test Site: Summary Report and Recommendation," SAND83-0372, Sandia National Laboratories, Albuquerque, NM.

MacDougall, H. R., Scully, L. W., and Tillerson, J. R. (1987), "Draft Site Characterization Plan Conceptual Design Report," SAND84-2641, Sandia National Laboratories, Albuquerque, NM, July.

Neville, A. M. (1975), Properties of Concrete, Pitman Publishing, London.

Nimick, F. B., Bauer, S. J., and Tillerson, J. R. (1984). "Recommended Matrix and Rock Mass Bulk, Mechanical and Thermal Properties for Thermomechanical Stratigraphy of Yucca Mountain," Version 1, Keystone Document No. 6310-85-1, Sandia National Laboratories, Albuquerque, NM, October.

Nimick, F. B. and Williams, R. L. (1984). "A Three-Dimensional Geologic Model of Yucca Mountain, Southern Nevada, SAND83-2593, Sandia National Laboratories, Albuquerque, NM.

St. John, C. M. (1987), "Reference Thermal and Thermal-Mechanical Analysis of Drifts for Vertical and Horizontal Emplacement of Nuclear Waste in a Repository in Tuff," SAND86-7005, Sandia National Laboratories, Albuquerque, NM.

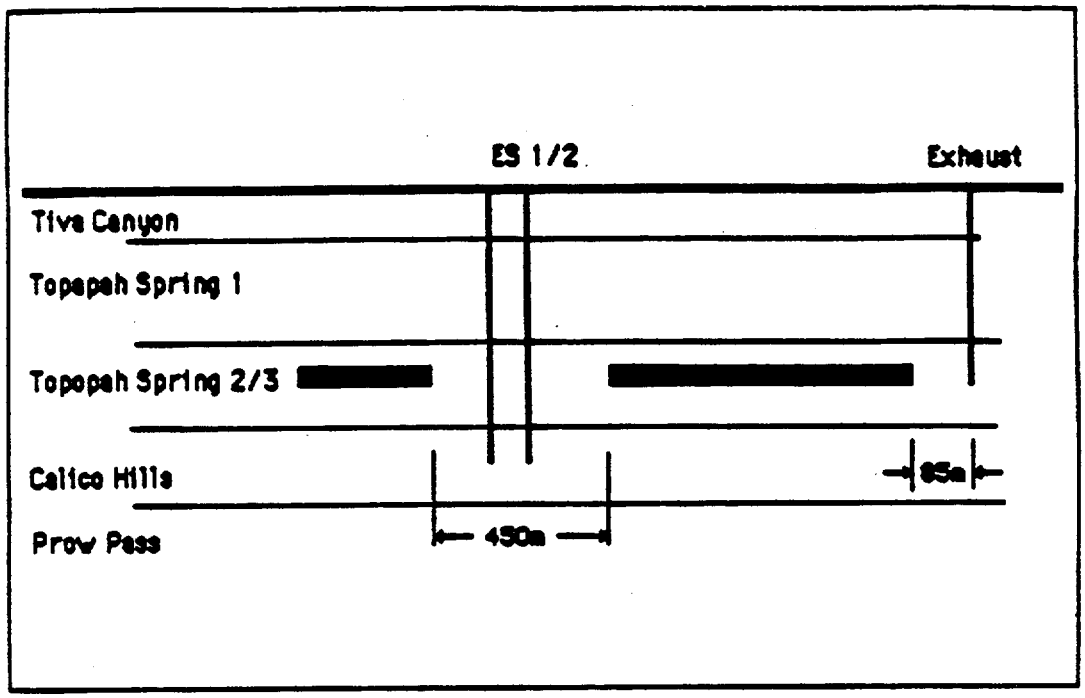

Figure 1. Conceptual Model of the Repository at Yucca Mountain

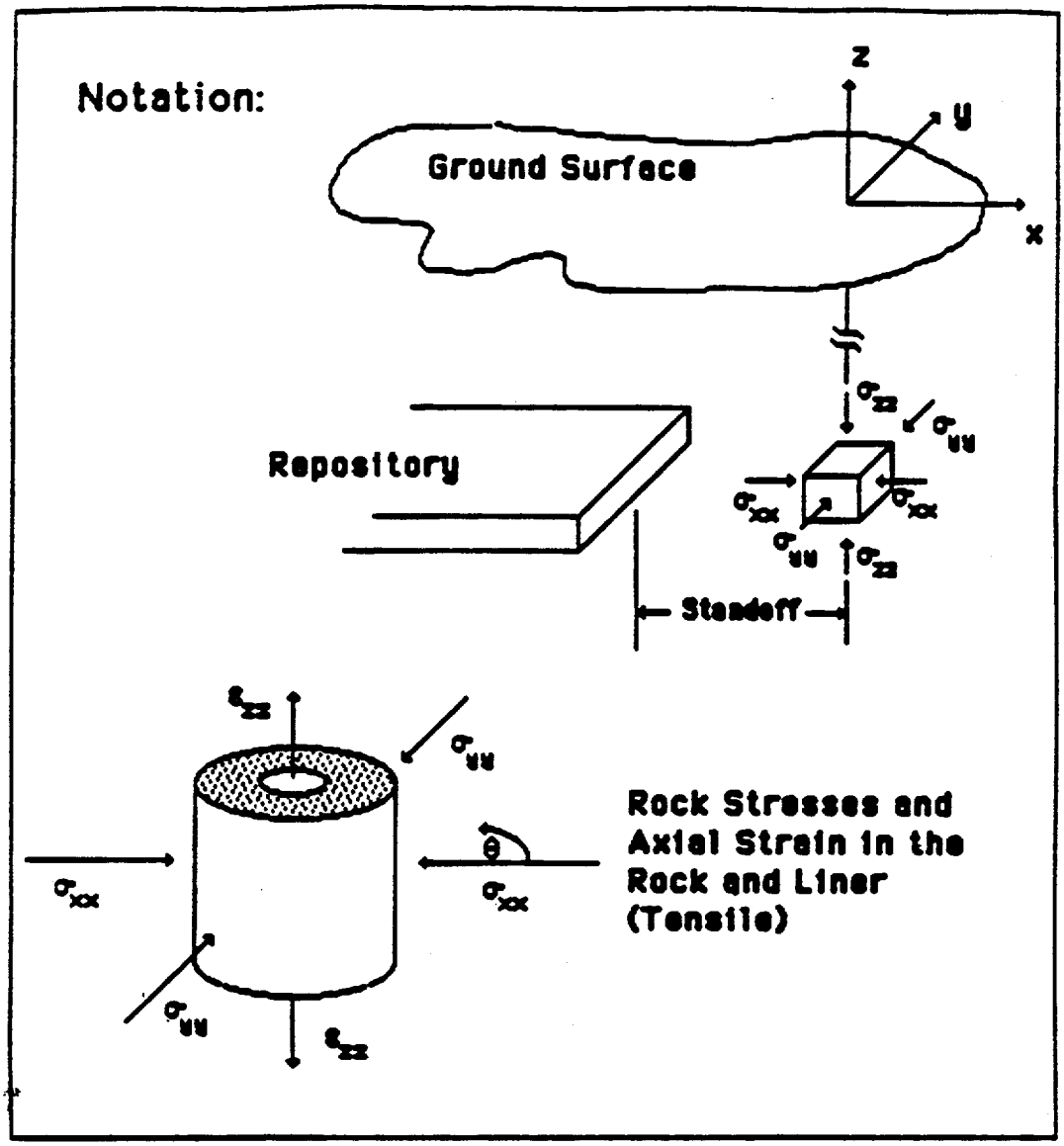

Figure 2. Notation for Repository and Shaft Analysis

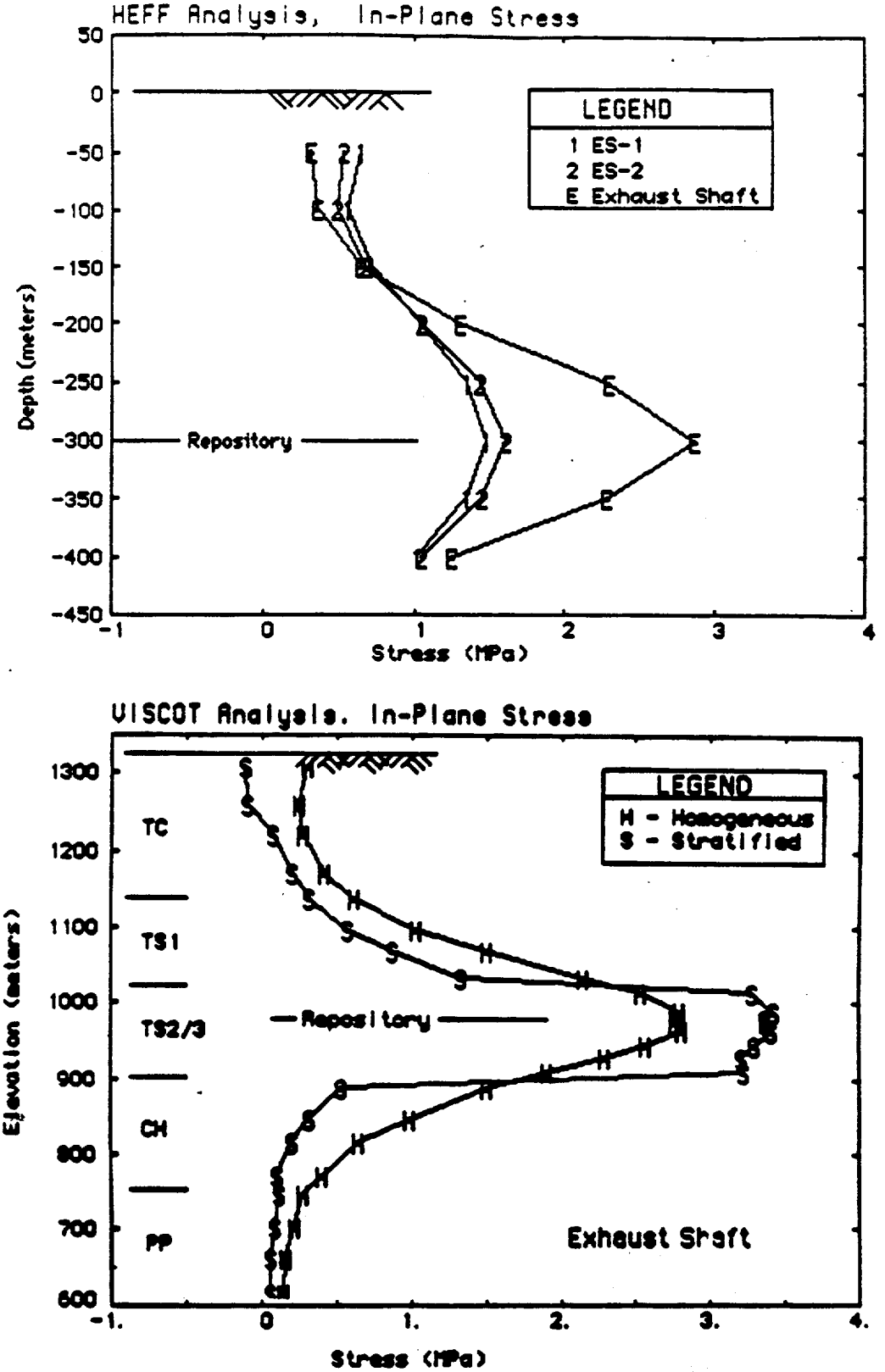

Figure 3. Profile of Induced In-Plane Horizontal Stresses at Selected Shaft Locations, 100 Years After Waste Emplacement

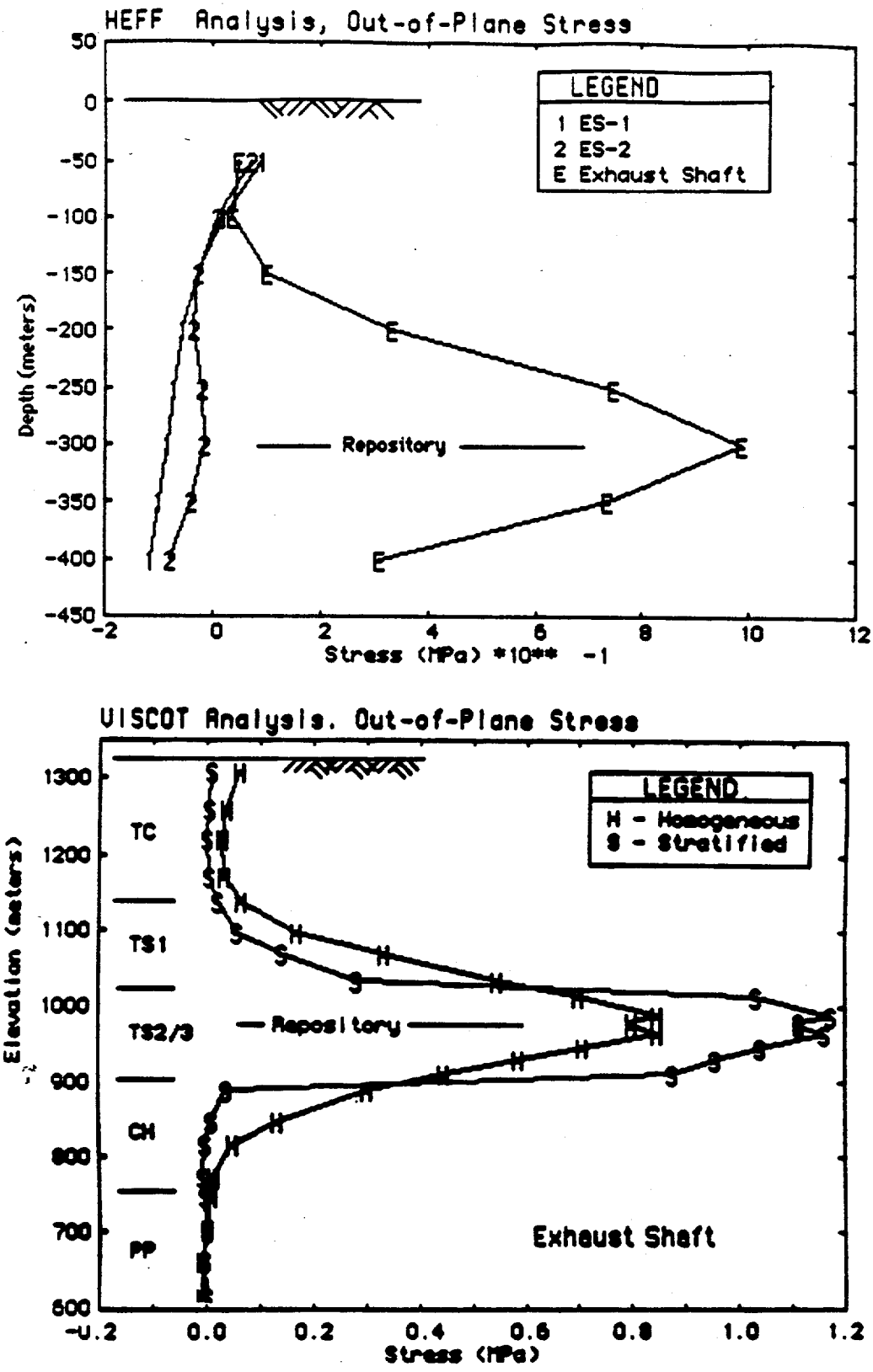

Figure 4. Profile of Induced Out-of-Plane Horizontal Stresses at Selected Shaft Locations, 100 Years After Waste Emplacement

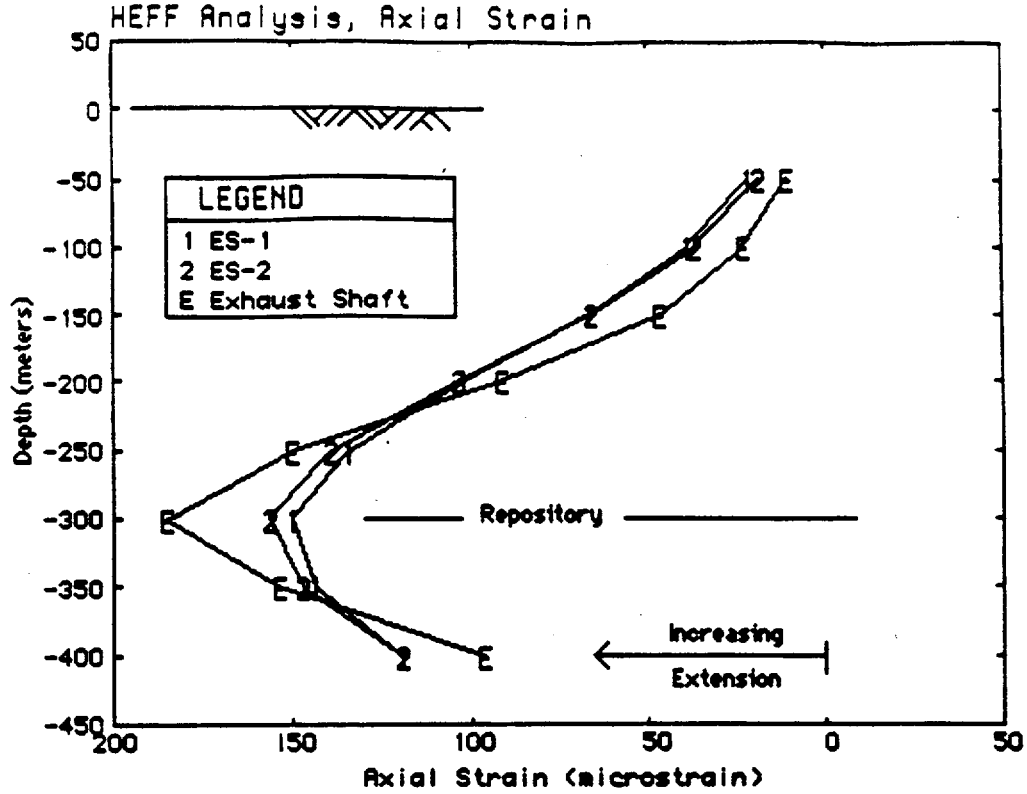

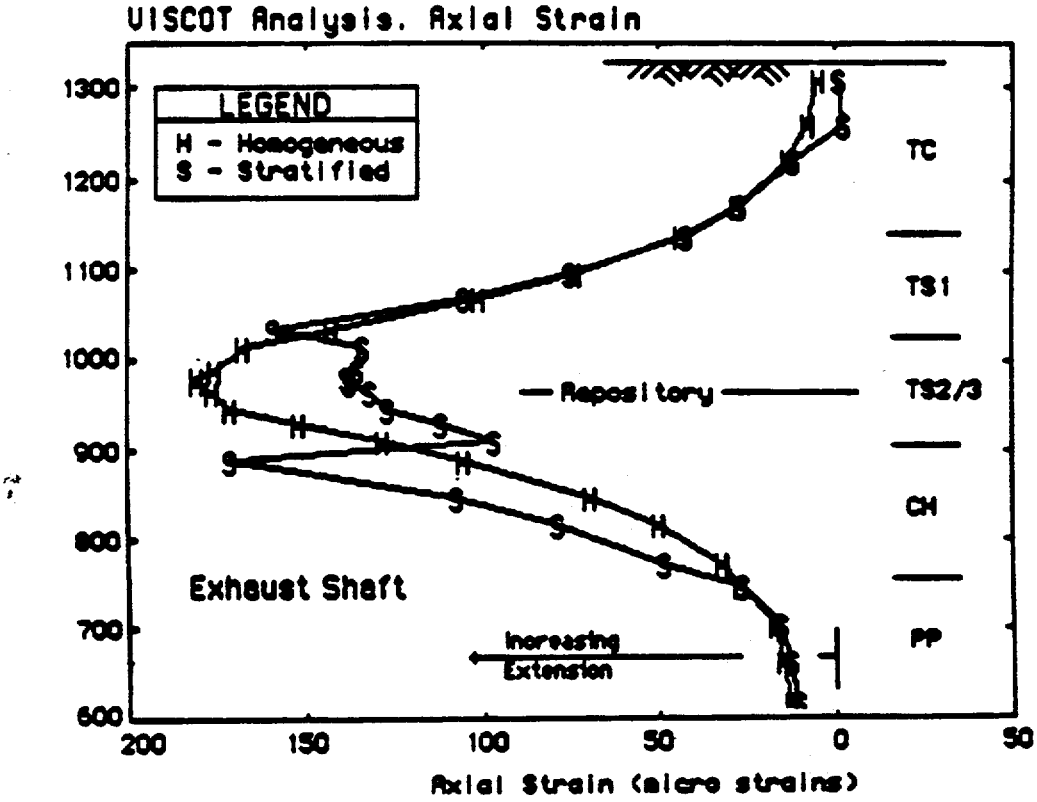

Figure 5. Profile of Induced Axial Strain at Selected Shaft Locations, 100 Years After Waste Emplacement

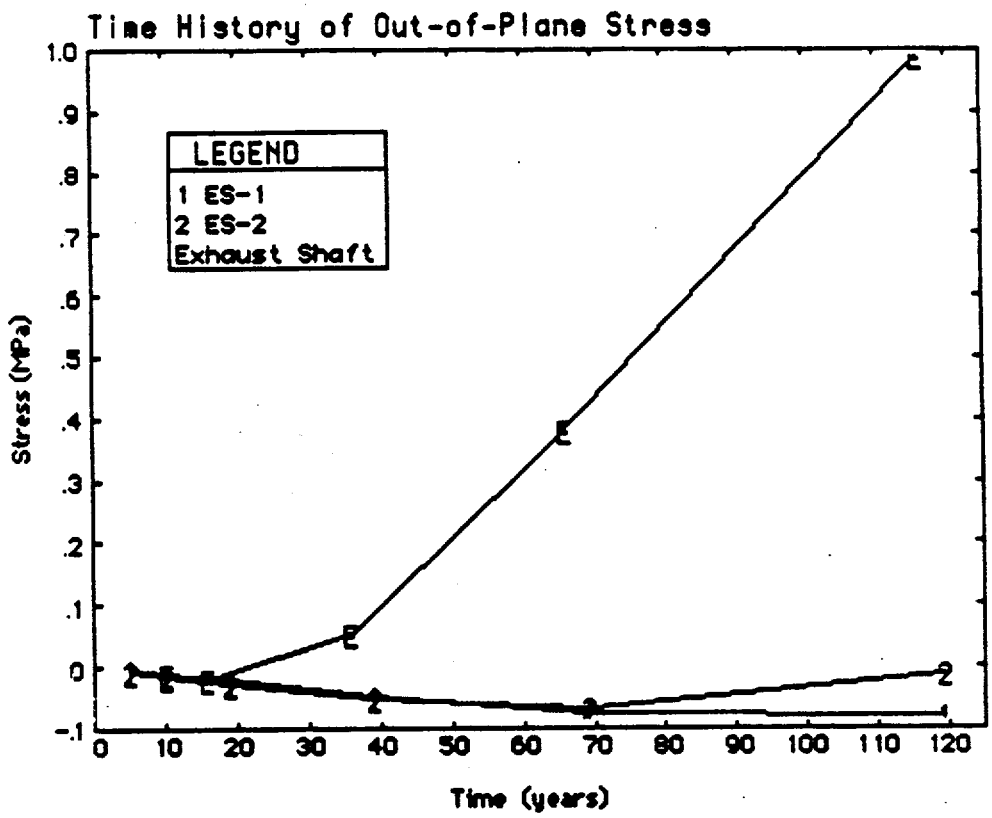

Figure 6. Time History of Induced Out-of-Plane Horizontal Stresses at the Shaft Locations, Computed Using the Boundary Element Models

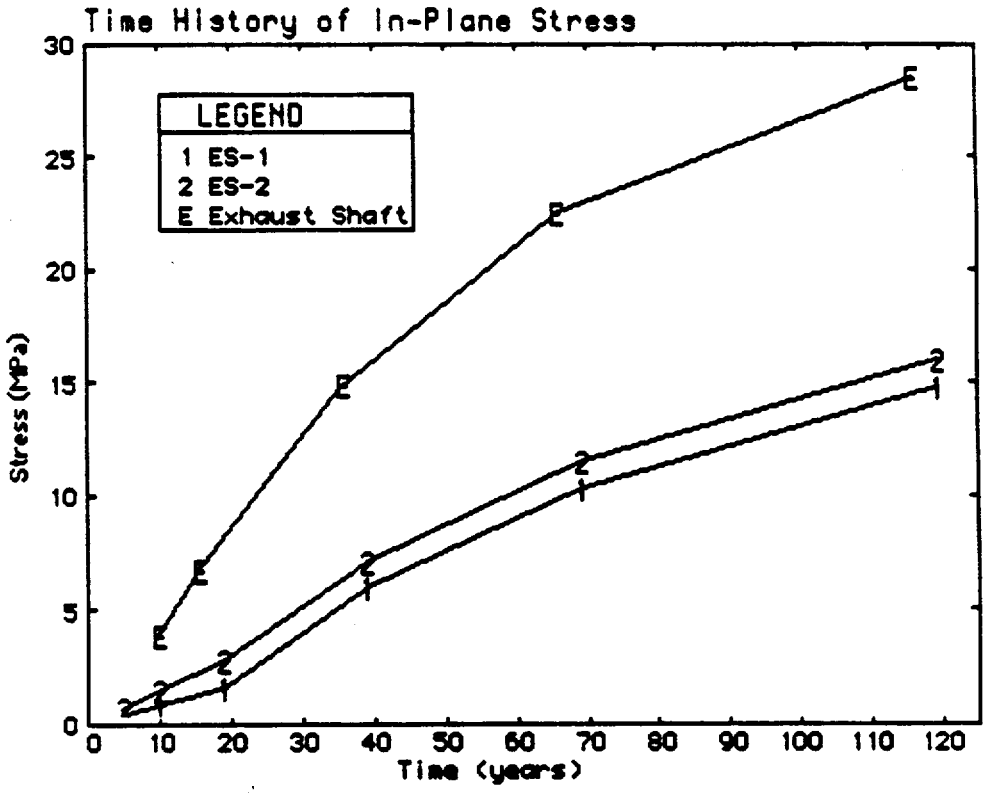

Figure 7. Time History of Induced In-Plane Horizontal Stresses at the Shaft Locations, Computed Using the Boundary Element Models

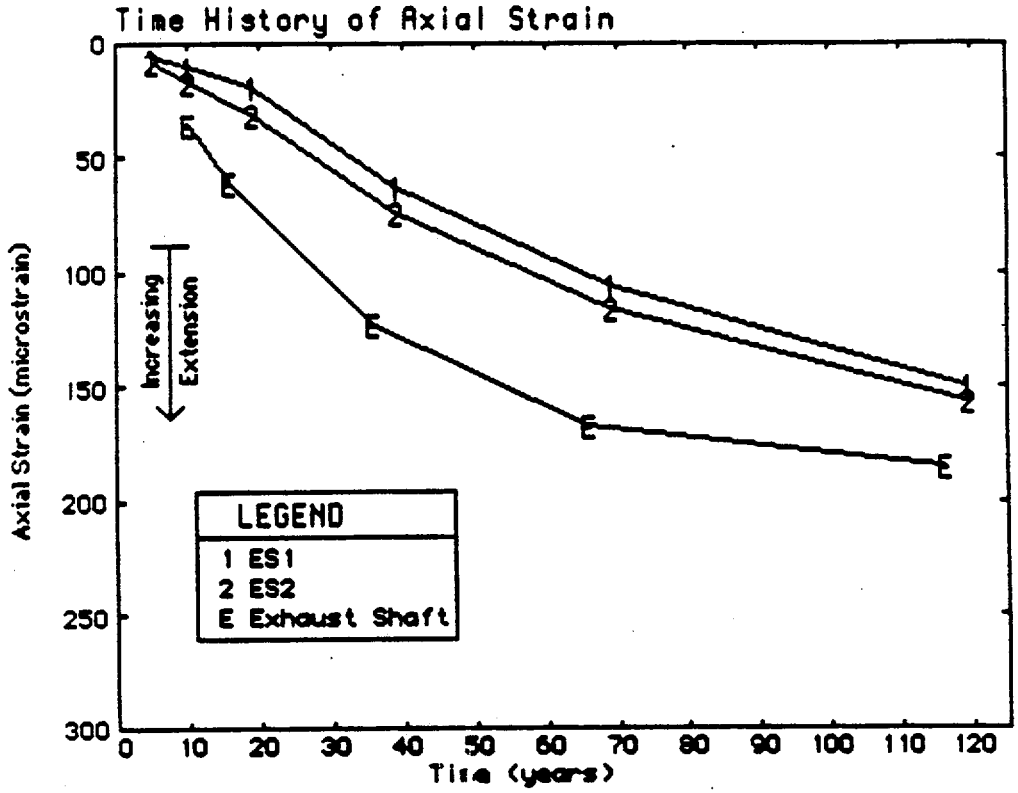

Figure 8. Time History of Induced Axial Strain at the Shaft Locations, Computed Using the Boundary Element Models

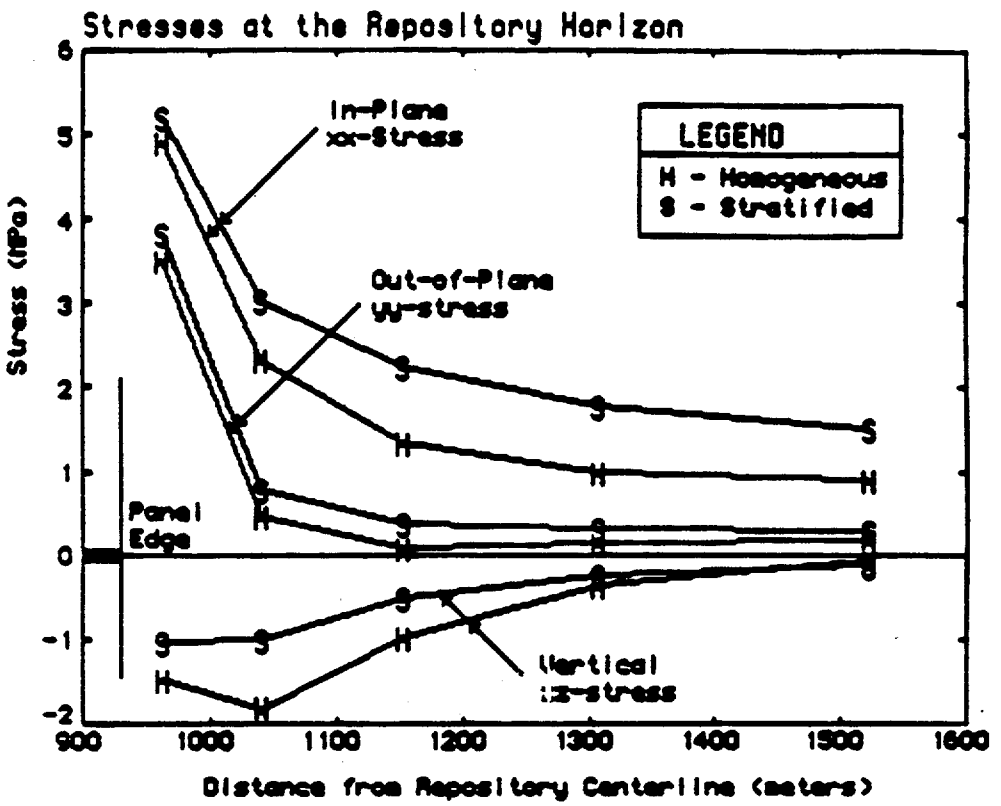

Figure 9. Induced Stress as a Function of Distance, 100 Years After Waste Emplacement, as Computed by the Finite-Element Model

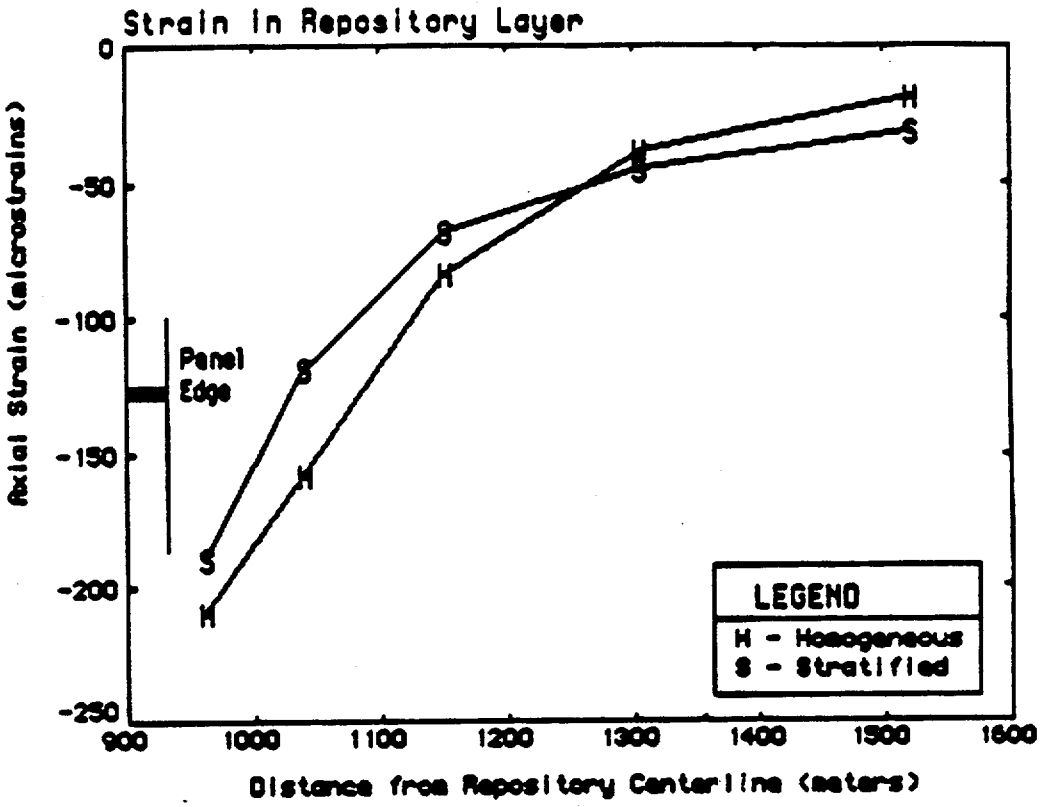

Figure 10. Induced Axial Strain as a Function of Distance, 100 Years After Waste Emplacement, as Computed by the Finite-Element Model

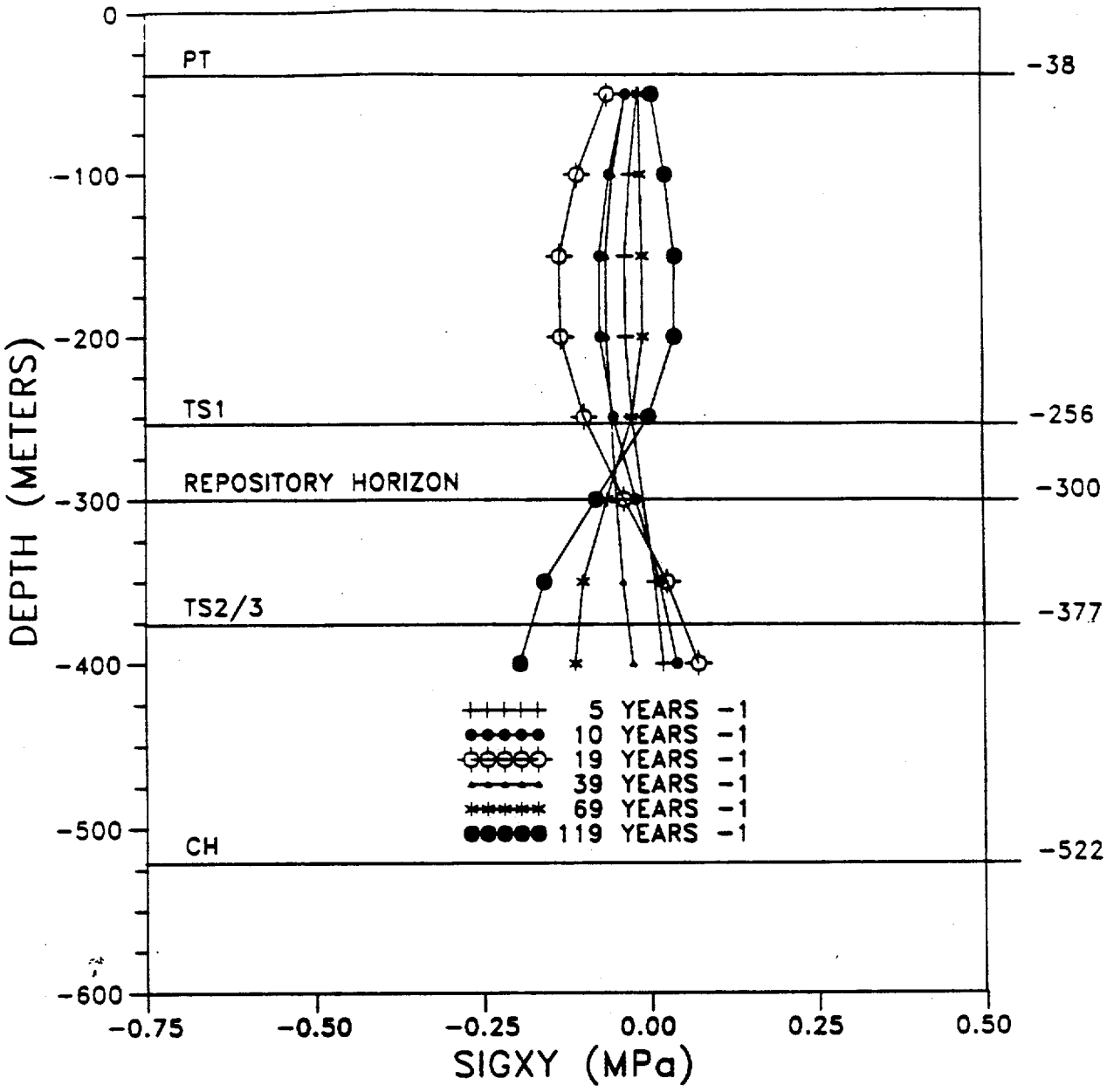

Figure 11. Induced Shear Stress Versus Depth at the ES1 Shaft Location, Computed Using the Boundary Element Model

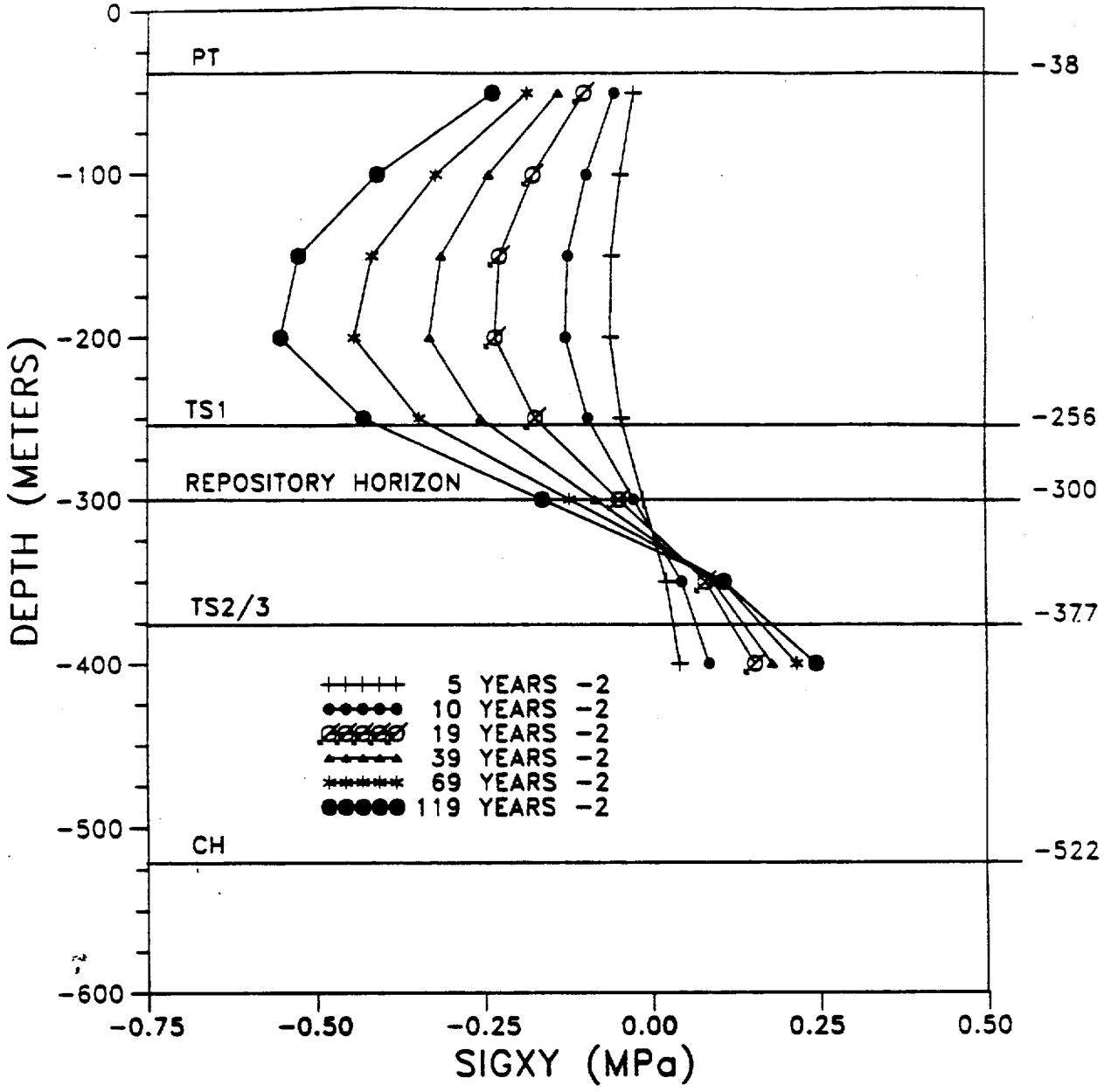

Figure 12. Induced Shear Stress Versus Depth at the ES2 Shaft Location, Computed Using the Boundary Element Model

APPENDIX C

INVESTIGATION OF THE EFFECT OF NONLINEAR BEHAVIOR OF THE ROCK MASS AROUND A LINED SHAFT

APPENDIX C
AN INVESTIGATION OF THE EFFECT OF NONLINEAR BEHAVIOR OF THE ROCK MASS AROUND A LINED SHAFT

C.1 BACKGROUND

The methodology described in the main body of the shaft design guide is based on the application of a closed-form solution for an embedded liner (SNL, in preparation). Both the liner and the rock mass are assumed to behave as linearly elastic materials. The purpose of this appendix is to document the results of a brief study of the effect on the liner of limited nonlinear behavior of the rock mass. The study has been performed to justify the assumptions of linear elastic behavior used to calculate loads on the liner in Chapter 4 of the shaft design guide.

C.2 APPROACH

To investigate the effect of nonlinear behavior of the rock mass, a series of example finite-element analyses has been performed using the VISCOT finite element code (ONWI, 1983). A case in which nonlinear rock mass behavior had been predicted was selected for analysis. The analyses were performed for both a lined and unlined shaft. In the case of the lined shaft, the liner is installed after 85% of the in situ stress had been allowed to relax. Hence, the liner experiences loads equivalent to 15% of the original in situ stresses.

The following liner properties have been assumed.

- Liner outside radius: 2.13 m
- Liner thickness: 0.30 m
- Elastic modulus: 28,000 MPa
- Poisson's ratio: 0.15

The selected material properties and in situ states of stress are representative of the Calico Hills Unit, CH1 (Appendix A).

- Rock mass modulus: 3,600 MPa
- Rock mass Poisson's ratio: 0.15
- Rock mass cohesion: 5.47 MPa
- Rock mass friction angle: 12.0°
- Maximum horizontal stress: 8.23 MPa
- Minimum horizontal stress: 3.09 MPa
- Vertical stress: 10.29 MPa

The rock-mass strength parameters, which define a Mohr-Coulomb strength model, have been used for the nonlinear analyses. Associated plastic behavior has been assumed for that model (Chapter 4), which implies a dilatation angle equal to the friction angle.

C.3 RESULTS

Figure C-1 illustrates and Table C-1 lists the results of analysis of the unlined shaft. The effect of the inelastic deformation on the induced displacements around the shaft can be judged by comparing the results of the linear and nonlinear analyses in Table C-1.

These results indicate that the response is predominantly elastic even though a small yield zone develops. The most obvious difference is that the displacements parallel to the direction of the minimum principal stress for the elastic and inelastic case are in opposite directions at the end of 100% unloading. This occurs because locally the dilatation of the elasto-plastic material is larger than the elastic deformation.

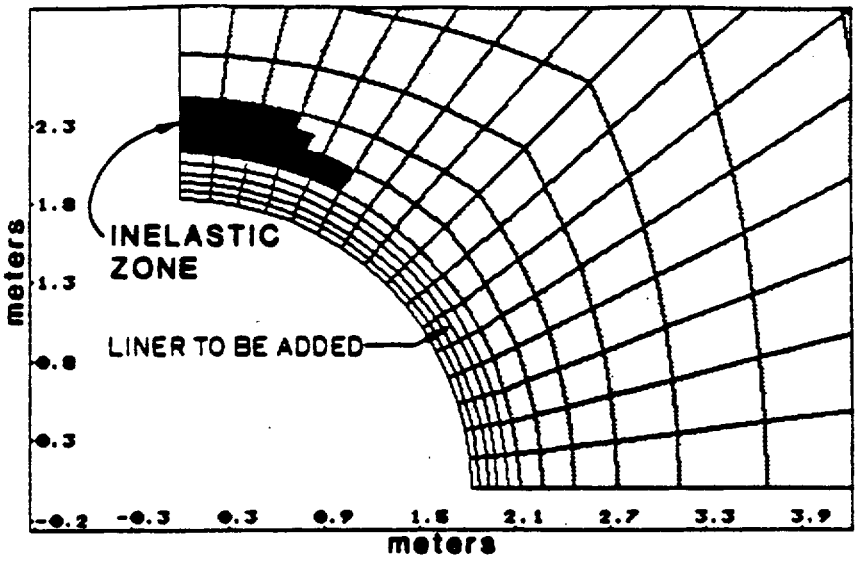

a) Extent of inelastic behavior after relaxation of 85% of in situ stress (σ_H horizontal, σ_h vertical on diagram)

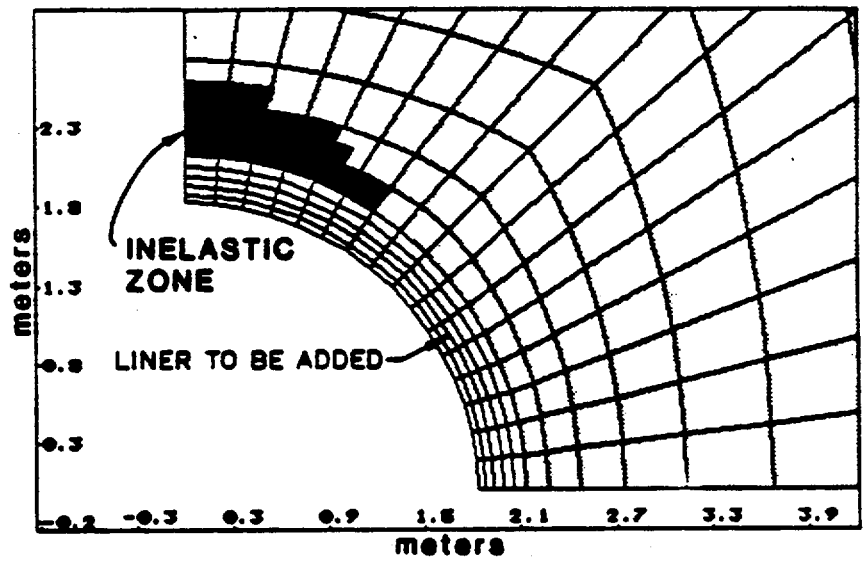

b) Extent of inelastic behavior after complete (100%) relaxation of in situ stress

Figure C-1. Results of Finite-Element Analysis of an Unlined Shaft. Elements in liner location have been given a very small modulus and do not affect the calculation.

TABLE C-1

DISPLACEMENT OF ROCK WALL[a]

Material Behavior	Parallel to Maximum Stress	Parallel to Minimum Stress
Elastic		
85% unload	-7.527	+0.736
100% unload	-8.855	+0.866
Elasto-plastic		
85% unload	-7.744	+0.178
100% unload	-9.232	-0.116

[a]Negative values represent convergence

The primary purpose of the analyses summarized above has been to develop initial conditions for a second set of analyses in which the liner was emplaced after 85% of the initial stresses had been relaxed. Hence, data files containing the state of stress after relaxation of 85% of the initial stresses have been prepared for both the linear and nonlinear cases. When those data files are used as initial conditions for a second set of analyses with the liner in place, then the balance of the stress relaxation takes place. The medium thus experiences the full in situ stress, and the liner experiences only the loads that result from medium/liner interaction during relaxation of the final 15% of the initial stresses. Table C-2 shows displacements of two points on the inner face of the liner. Note that the differences between elastic and inelastic analyses are negligible in this case.

TABLE C-2

DISPLACEMENT OF LINER INTERIOR (MM)

Material Behavior	Parallel to Maximum Stress	Parallel to Minimum Stress
Elastic	-0.6960	+0.2119
Elasto-plastic	-0.6958	+0.2116

C.4 CONCLUSIONS

The results of these analyses indicate that limited inelastic deformation might be anticipated around an unlined shaft sunk to planned ES-1 depths in a rock mass with properties representative of the Calico Hills Unit. Inelastic deformation starts somewhat before 85% of the in situ stress has relaxed. However, it is inhibited as soon as the liner is in place. The beneficial effect of rockbolts in controlling inelastic deformation was not modeled. In the particular case examined, the response after liner installation was entirely elastic, with previously overstressed material having returned to an elastic state as confinement was added. This behavior is a function of the idealization used in the model and is not a completely accurate representation of the actual behavior of the rock. However, this analysis shows that a model based on the assumption that the response of both the liner and the medium is elastic appears entirely reasonable in this case and illustrates the use of numerical methods to solve problems of this type.

REFERENCES

ONWI (Office of Nuclear Waste Isolation), "VISCOT: A Two-Dimensional and Axisymmetric Nonlinear Transient Thermoviscoelastic and Thermoviscoplastic Finite-Element Code for Modeling Time-Dependent Viscous Mechanical Behavior of a Rock Mass," ONWI-437, Battelle Project Management Division, Columbus, OH, April 1983.

SNL (Sandia National Laboratories), "Documentation and Verification of the SHAFT Code," SAND 88-7065, prepared by C.M. St. John for Sandia National Laboratories, Albuquerque, NM, in preparation.

APPENDIX D

AN EVALUATION OF THE EFFECT OF RADIAL CRACKING OF A LINER

APPENDIX D

AN EVALUATION OF THE EFFECT OF RADIAL CRACKING OF A LINER

D.1 BACKGROUND

Unless a liner is subjected to uniform loading, the hoop stresses and the thrust will vary around the circumference of the section. If the loading is sufficiently anisotropic, then tensile stresses develop in some portions of the section, with the maximum tensile stress occurring on the extreme interior fibres of the liner on a radial line parallel to the direction of the more compressive principal stress. This suggests that if a liner is subjected to an anisotropic load there is a possibility of developing radial cracks that will propagate from the interior and may penetrate the full depth of the liner. The purpose of this appendix is to evaluate the effect that such crack propagation may have on the liner.

D.2 APPROACH

Because no simple solution for the case of a cracked liner is available, a numerical modeling approach has been adopted and a particular case has been selected for examination. The liner properties for that case are as follows.

- External radius of liner: 2.13 m
- Thickness of liner: 0.30 m
- Elastic modulus of liner: 28,000 MPa
- Poisson's ratio of liner: 0.15

A rock/liner interaction calculation has been performed for the case of external loading of a liner in the TS-2 Unit. Input to those calculations comprises the following.

- Elastic modulus of rock mass: 15,200 MPa
- Poisson's ratio of rock mass: 0.22
- Direct stress in x-direction: 0.679 MPa
- Direct stress in y-direction: -0.679 MPa

The loads correspond to a pure shear strain of 109 microstrains, which is the value used in the example of a shaft subjected to seismic loading due to an S wave.

The analysis uses two models. First, the SHAFT code is used to compute the stresses in the liner, assuming it behaves as a linear elastic ring capable of sustaining tension (SNL, in preparation). Second, the intact liner analysis is repeated using a finite element model developed using the VISCOT code (ONWI-437). The finite element model is then modified to simulate development of a radial crack through the section.

Because this is intended only as an example calculation, a very simple method of simulating the development of a crack has been adopted. This method is best explained by Figure D-1, in which the finite-element mesh in the vicinity of the liner is illustrated. Application of a compressive load in the horizontal direction and a tensile load in the vertical direction induces tensile stress at the location of the horizontal plane of symmetry. That plane of symmetry is defined by applying constraints to the nodes that lie along it. If those constraints are relaxed by "uncoupling" the nodes from the plane of symmetry, then the liner will no longer sustain tension.

D.3 RESULTS

Table D-1 lists the values of the hoop and radial stresses computed using the closed-form solution and the finite-element analysis for the case of an intact liner. Note that values are given for a series of

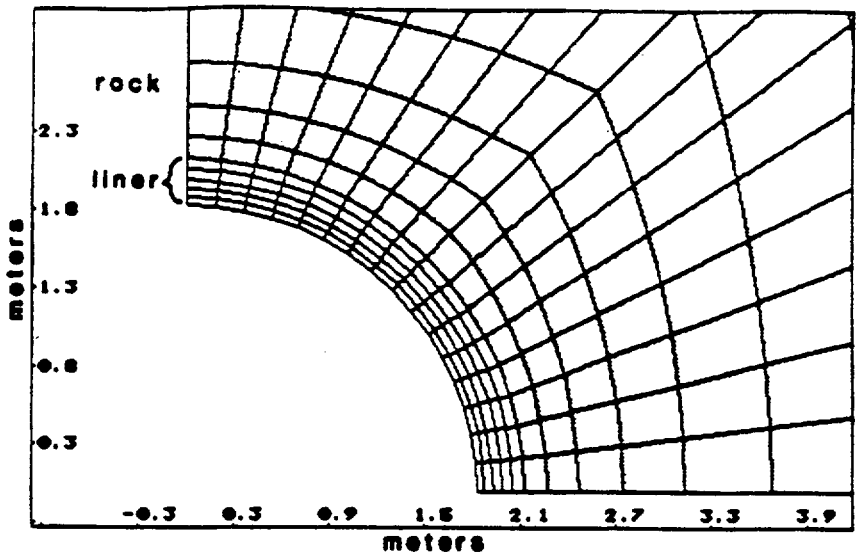

a) Details of the Finite-Element Mesh for the Lined Shaft Model

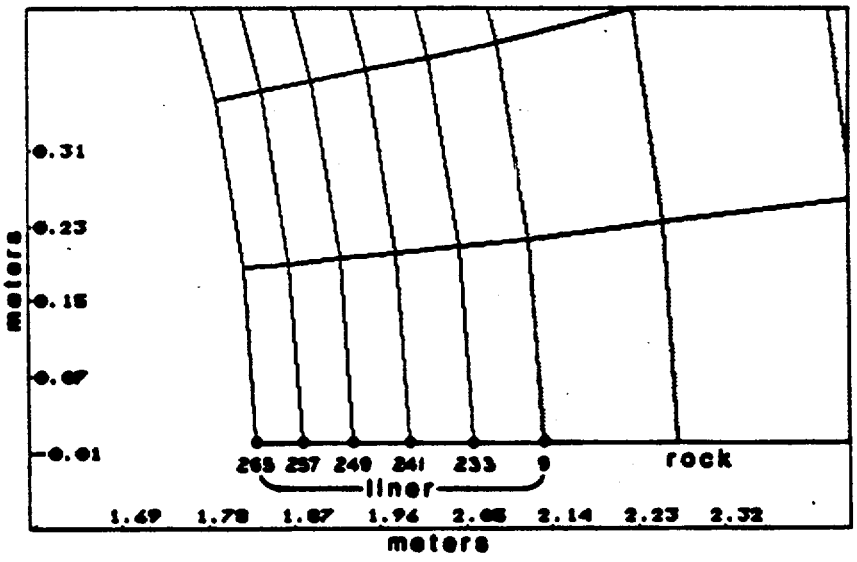

b) Nodal Connections Along the Plane of Symmetry Parallel to the Direction of the Applied Compressive Stress

Figure D-1. Finite-Element Analysis of the Shaft Liner

TABLE D-1

HOOP AND RADIAL STRESSES

Sample Point Radial Distance (m)	Closed Form Analysis		Finite-Element Model	
	Hoop Stress (MPa)	Radial Stress (MPa)	Hoop Stress (MPa)	Radial Stress (MPa)
1.830	4.050	0.0	4.409	0.0684
1.878	3.703	0.0940	3.995	0.0815
1.931	3.362	0.1730	3.616	0.1731
1.991	3.029	0.2353	3.253	0.2389
2.057	2.707	0.2799	2.905	0.2826
2.130	2.397	0.3060	2.027	0.2955

sample points in the liner that lie on the radial line parallel to the direction of the applied compressive stress. The stresses along the radial line parallel to the direction of the applied tensile stress are identical, except that the signs are opposite. Note that the hoop stress results of the closed-form analysis and the finite-element analysis differ by about 10%. This difference is attributed to modeling idealizations with the finite element model, and could be substantially reduced with more detailed modeling. Because the primary purpose of the finite-element analysis has been to evaluate the relative behavior of cracked and uncracked liners, the slight difference between the closed-form analysis and the finite-element analysis is considered unimportant.

The finite-element analysis is then repeated after initially uncoupling the first three nodes along the plane of symmetry (nodes 265, 257, and 249 in Figure D-1), and subsequently the next three nodes (241, 233, and 9). The effect of partial cracking is to increase the tension in the uncracked portion of the liner, which suggests that a crack will propagate entirely through the section once started. However, detailed

discussion of the state of stress around the crack is inappropriate as the method of simulating the presence of the crack is obviously approximate. It is appropriate to examine the effect of the liner at a point remote from the crack and, in particular, along a vertical plane of symmetry where the hoop stresses will be highest.

Table D-2 lists hoop stresses and radial displacements along a radial sample line perpendicular to the crack direction. Data are presented for all three cases considered. However, the values for the fully cracked and uncracked liner are of particular interest.

TABLE D-2

HOOP STRESSES AND RADIAL DISPLACEMENTS ALONG
A RADIAL SAMPLE LINE PERPENDICULAR TO THE CRACK DIRECTION

Sample Point Radial Distance (m)	Hoop Stress (MPa)			Radial Displacement 10^{-4} m		
	No Crack	Partially Cracked	Fully Cracked	No Crack	Partially Cracked	Fully Cracked
1.830	4.409	4.422	4.524	3.180	3.239	3.607
1.878	3.995	4.008	4.112	3.191	3.251	3.619
1.931	3.616	3.630	3.736	3.201	3.261	3.630
1.991	3.253	3.268	3.376	3.209	3.269	3.638
2.057	2.905	2.920	3.029	3.215	3.275	3.644
2.130	2.027	2.039	2.126	3.220	3.279	3.648

In Figure D-2, contours of horizontal stresses in the vicinity of the liner are plotted for the uncracked and fully cracked liner. It can be seen from those figures that the presence of the crack has very little influence on the stresses, except in the immediate vicinity of the crack.

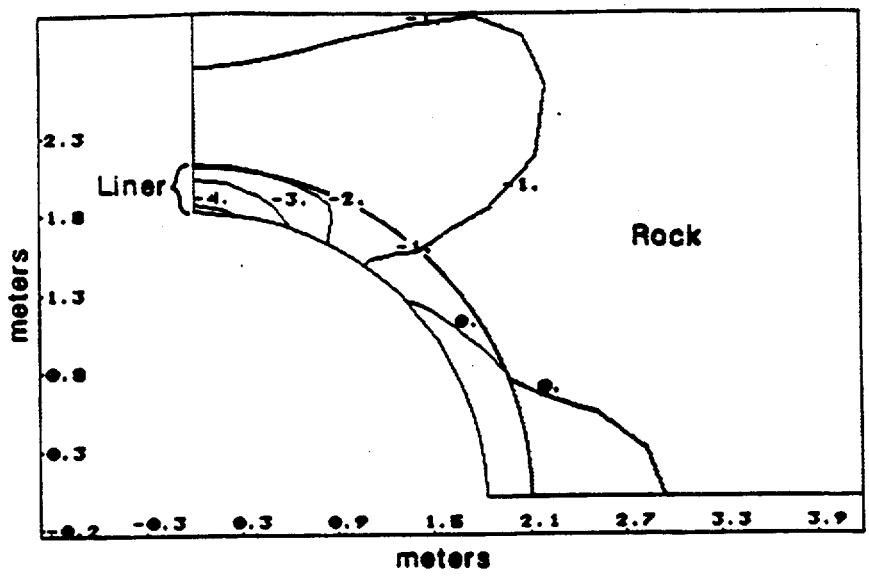

a) Uncracked Liner

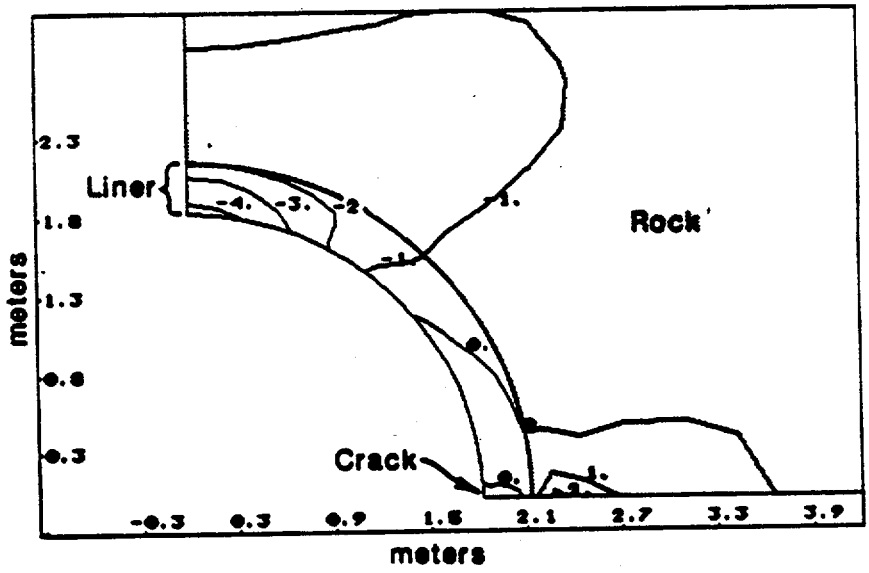

b) Fully Cracked Liner

Figure D-2. Contours of the Horizontal Stress (MPa) in the Shaft Liner for Uncracked and Fully Cracked Cases

D.4 CONCLUSIONS

The results presented in the preceding sections indicate that the analysis of the liner as an uncracked ring provides a good estimate of the maximum compressive stresses in the liner even if it is completely cracked. The computed maximum compressive stresses vary less than 3% between the uncracked and fully cracked cases. Also, reasonable correspondence between the closed-form and finite-element models is demonstrated.

Although it is not possible to draw completely general conclusions from these limited example analyses, the general nature of the behavior seems clear. First, radial cracks in the liner may develop. If there is nothing else to initiate those cracks, they will occur along radial planes parallel to the direction of the major applied compressive stress. Any blocks that might tend to be created by such cracking cannot move inward because they will taper towards the center of the shaft (as described in Chapter 6). Hence, radial cracking alone is not anticipated to influence the utility of the liner. Second, radial cracking within any section does not significantly influence the hoop stresses, and hence the thrust and moment, in the portion of the section carrying the highest compressive loads. This is because the liner and the surrounding rock mass behave as an integral structure, and the load that cannot be sustained by the cracked liner is transferred to the rock. This behavior also illustrates the important difference between a typical structural member, such as a beam, column, or arch, and the embedded shaft liner (as discussed in Chapter 6).

REFERENCES

ONWI (Office of Nuclear Waste Isolation), "VISCOT: A Two-Dimensional and Axisymmetric Nonlinear Transient Thermoviscoelastic and Thermoviscoplastic Finite-Element Code for Modeling Time-Dependent Viscous Mechanical Behavior of a Rock Mass," ONWI-437, Battelle Project Management Division, Columbus, OH, April 1983.

SNL (Sandia National Laboratories), "Documentation and Verification of the SHAFT Code," SAND 88-7065, prepared by J.F.T. Agapito & Associates, Inc. for Sandia National Laboratories, Albuquerque, NM, in preparation.

APPENDIX E

EXAMPLE SHAFT CODE PRINTOUTS

```
**********************************************************************************************
*                                                                                            *
*     SSSSSSSS        HH        HH          AA          FFFFFFFFFFF   TTTTTTTTTTTTTT     *
*    SS      SSS      HH        HH         AAAA         FFFFFFFFFFF   TTTTTTTTTTTTTT     *
*   SS                HH        HH        AA  AA        FF                TT             *
*    SSS              HHHHHHHHHHHH       AA    AA       FF                TT             *
*       SSS           HHHHHHHHHHHH      AAAAAAAAAA      FFFFFF            TT             *
*          SSS        HH        HH     AAAAAAAAAAAA     FFFFFF            TT             *
*            SS       HH        HH    AA          AA    FF                TT             *
*   SSS      SS       HH        HH   AA            AA   FF                TT             *
*    SSSSSSSS         HH        HH   AA            AA   FF                TT             *
*                                                                                            *
**********************************************************************************************
```

Analytical solutions for a lined circular hole

Code: SHAFT. Version 3.00, upgraded for SANDIA/NNWSI May 5, 1988
J.F.T. Agapito and Associates
Grand Junction (303) 242 4220

Comments

TS-STATIC-SHAFT GUIDE EXAMPLE PROBLEM

Static Load Cases For TS-2 Unit (From Table 4-3)

Analysis completed by :A.M.RICHAR

Plane strain analysis

Bonding between shaft wall and liner is assumed

Geometry and Properties of Shaft and Liner

(In Consistent Metric Units)

Radius of unlined hole..... =	2.1300
Lining thickness..... =	.3000
Elastic modulus of medium.... =	.1520E+05
Poissons ratio of medium..... =	.2200E+00
Elastic modulus of liner..... =	.2800E+05
Poissons ratio of liner..... =	.1500E+00

HOOP AND AXIAL DEFORMATION CALCULATION

Comments (cont.)

Input in-plane stresses are :
.1130E+01 .1130E+01 .0000E+00
Axial strain is :
.0000E+00

Load Case Static - 1
Uniform Ground Pressures
(From Table 4-4)

The Interaction Calculation for the liner predicts the stresses listed below. Note that the reference angle is the first principal stress direction

Hoop Stresses in the Liner

Radius	At 0.(Pt 1)	At 90.(Pt 2)	Minimum	Maximum
			.3071E+01	.3533E+01
1.83	.3533E+01	.3533E+01		
1.86	.3471E+01	.3471E+01		
1.90	.3411E+01	.3411E+01		
1.93	.3355E+01	.3355E+01		
1.96	.3302E+01	.3302E+01		
2.00	.3251E+01	.3251E+01		
2.03	.3203E+01	.3203E+01		
2.06	.3156E+01	.3156E+01		
2.10	.3113E+01	.3113E+01		
2.13	.3071E+01	.3071E+01		

Peak Tangential Stress for Table 5-1

Radial Stresses in the Liner

Radius	At 0.(Pt 1)	At 90.(Pt 2)	Minimum	Maximum
			.0000E+00	.4626E+00
1.83	.0000E+00	.0000E+00		
1.86	.6265E-01	.6265E-01		
1.90	.1220E+00	.1220E+00		
1.93	.1783E+00	.1783E+00		
1.96	.2318E+00	.2318E+00		
2.00	.2826E+00	.2826E+00		
2.03	.3310E+00	.3310E+00		
2.06	.3770E+00	.3770E+00		
2.10	.4208E+00	.4208E+00		
2.13	.4626E+00	.4626E+00		

Axial Stresses in the Liner

Radius	At 0.(Pt 1)	At 90.(Pt 2)	Minimum	Maximum
			.5300E+00	.5300E+00
1.83	.5300E+00	.5300E+00		
1.86	.5300E+00	.5300E+00		
1.90	.5300E+00	.5300E+00		
1.93	.5300E+00	.5300E+00		
1.96	.5300E+00	.5300E+00		
2.00	.5300E+00	.5300E+00		
2.03	.5300E+00	.5300E+00		
2.06	.5300E+00	.5300E+00		
2.10	.5300E+00	.5300E+00		
2.13	.5300E+00	.5300E+00		

HOOP AND AXIAL DEFORMATION CALCULATION

Comments (cont.)

Input in-plane stresses are :
.1130E+01 .4200E+00 .0000E+00
Axial strain is :
.0000E+00

Load Case Static - 2
Non-uniform Ground
Pressures
(From Table 4-4)

The Interaction Calculation for the liner
predicts the stresses listed below.
Note that the reference angle is the
first principal stress direction

Hoop Stresses in the Liner

Radius	At 0.(Pt 1)	At 90.(Pt 2)	Minimum	Maximum
			.3062E+00	.4541E+01
1.83	.3062E+00	.4541E+01	1	2
1.86	.3912E+00	.4370E+01	1	2
1.90	.4685E+00	.4211E+01	1	2
1.93	.5388E+00	.4063E+01	1	2
1.96	.6030E+00	.3926E+01	1	2
2.00	.6618E+00	.3797E+01	1	2
2.03	.7156E+00	.3677E+01	1	2
2.06	.7651E+00	.3565E+01	1	2
2.10	.8108E+00	.3459E+01	1	2
2.13	.8530E+00	.3359E+01	1	2

Peak Tangential Stress
For Table 5-1

Radial Stresses in the Liner

Radius	At 0.(Pt 1)	At 90.(Pt 2)	Minimum	Maximum
			.0000E+00	.4773E+00
1.83	.0000E+00	.0000E+00	+	
1.86	.7578E-02	.7035E-01	1	2
1.90	.1873E-01	.1486E+00	1	2
1.93	.3287E-01	.2118E+00	1	2
1.96	.4952E-01	.2685E+00	1	2
2.00	.6924E-01	.3195E+00	1	2
2.03	.8867E-01	.3653E+00	1	2
2.06	.1105E+00	.4066E+00	1	2
2.10	.1334E+00	.4438E+00	1	2
2.13	.1573E+00	.4773E+00	1	2

Axial Stresses in the Liner

Radius	At 0.(Pt 1)	At 90.(Pt 2)	Minimum	Maximum
			.4593E-01	.6811E+00
1.83	.4593E-01	.6811E+00	1	2
1.86	.5982E-01	.6672E+00	1	2
1.90	.7308E-01	.6539E+00	1	2
1.93	.8575E-01	.6413E+00	1	2
1.96	.9788E-01	.6291E+00	1	2
2.00	.1095E+00	.6175E+00	1	2
2.03	.1206E+00	.6064E+00	1	2
2.06	.1313E+00	.5957E+00	1	2
2.10	.1416E+00	.5854E+00	1	2
2.13	.1515E+00	.5755E+00	1	2

HOOP AND AXIAL DEFORMATION CALCULATION

Comments (cont.)

Input in-plane stresses are :
-.5000E-01 .1500E+01 .0000E+00
Axial strain is :
-.1500E-03

Thermal
(From Table 4-4)

The Interaction Calculation for the liner
predicts the stresses listed below.
Note that the reference angle is the
first principal stress direction

Hoop Stresses in the Liner

Radius	At 0.(Pt 1)	At 90.(Pt 2)	Minimum	Maximum
			-.2235E+01	.7606E+01
1.83	.7606E+01	-.2235E+01	!2	1 !
1.86	.7261E+01	-.1985E+01	!2	1 !
1.90	.6942E+01	-.1756E+01	! 2	1 !
1.93	.6646E+01	-.1545E+01	! 2	1 !
1.96	.6370E+01	-.1352E+01	! 2	1 !
2.00	.6114E+01	-.1173E+01	! 2	1 !
2.03	.5875E+01	-.1007E+01	! 2	1 !
2.06	.5652E+01	-.8537E+00	! 2	1 !
2.10	.5443E+01	-.7111E+00	! 2	1 !
2.13	.5246E+01	-.5782E+00	! 2	1 !

Peak Tangential Stress
For Table 5-1

Radial Stresses in the Liner

Radius	At 0.(Pt 1)	At 90.(Pt 2)	Minimum	Maximum
			-.7821E-01	.7234E+00
1.83	.0000E+00	.0000E+00	! +	!
1.86	.1299E+00	-.3462E-01	! 2 1	!
1.90	.2437E+00	-.5822E-01	!2 1	!
1.93	.3434E+00	-.7231E-01	!2 1	!
1.96	.4306E+00	-.7821E-01	!2 1	!
2.00	.5067E+00	-.7708E-01	!2 1	!
2.03	.5730E+00	-.6990E-01	!2 1	!
2.06	.6306E+00	-.5755E-01	!2 1	!
2.10	.6805E+00	-.4078E-01	! 2 1	!
2.13	.7234E+00	-.2020E-01	! 2 1	!

Axial Stresses in the Liner

Radius	At 0.(Pt 1)	At 90.(Pt 2)	Minimum	Maximum
			-.4535E+01	-.3059E+01
1.83	-.3059E+01	-.4535E+01	!2	1 !
1.86	-.3091E+01	-.4503E+01	!2	1 !
1.90	-.3122E+01	-.4472E+01	! 2	1 !
1.93	-.3152E+01	-.4443E+01	! 2	1 !
1.96	-.3180E+01	-.4414E+01	! 2	1 !
2.00	-.3207E+01	-.4387E+01	! 2	1 !
2.03	-.3233E+01	-.4362E+01	! 2	1 !
2.06	-.3258E+01	-.4337E+01	! 2	1 !
2.10	-.3282E+01	-.4313E+01	! 2	1 !
2.13	-.3305E+01	-.4290E+01	! 2	1 !

OUT-OF-PLANE SHEAR CALCULATION

Input shear stresses are :
.0000E+00 .5000E+00

RZ-Shear Stresses across the Liner

Radius	At 0.(Pt 1)	At 90.(Pt 2)	Minimum .0000E+00	Maximum .2274E+00
1.83	.0000E+00	.0000E+00	!+	!
1.86	.0000E+00	.3080E-01	!1 2	!
1.90	.0000E+00	.5999E-01	!1 2	!
1.93	.0000E+00	.8768E-01	!1 2	!
1.96	.0000E+00	.1140E+00	!1 2	!
2.00	.0000E+00	.1390E+00	!1 2	!
2.03	.0000E+00	.1627E+00	!1 2	!
2.06	.0000E+00	.1853E+00	!1 2	!
2.10	.0000E+00	.2069E+00	!1 2	!
2.13	.0000E+00	.2274E+00	!1 2	!

TZ-Shear Stresses across the Liner

Radius	At 0.(Pt 1)	At 90.(Pt 2)	Minimum .1267E-04	Maximum .1737E+01
1.83	.1737E+01	.1458E-04	!2	1 !
1.86	.1706E+01	.1432E-04	!2	1 !
1.90	.1677E+01	.1408E-04	!2	1 !
1.93	.1650E+01	.1385E-04	!2	1 !
1.96	.1623E+01	.1363E-04	!2	1 !
2.00	.1598E+01	.1342E-04	!2	1 !
2.03	.1574E+01	.1322E-04	!2	1 !
2.06	.1552E+01	.1303E-04	!2	1 !
2.10	.1530E+01	.1285E-04	!2	1 !
2.13	.1510E+01	.1267E-04	!2	1 !

Comments (cont.)

Load Cases Static - 3 and Static - 4 (Shear Stresses from Appendix B)

Peak Shear Stress For Table 5-3

```
**********************************************************************************
*                                                                                *
*    SSSSSSSS     HH       HH          AA          FFFFFFFFFFF   TTTTTTTTTTTTTT  *
*   SS      SSS   HH       HH         AAAA         FFFFFFFFFFF   TTTTTTTTTTTTTT  *
*  SS             HH       HH        AA  AA        FF                  TT        *
*   SSS           HHHHHHHHHHH       AA    AA       FF                  TT        *
*      SSS        HHHHHHHHHHH      AAAAAAAAAA      FFFFFF              TT        *
*         SSS     HH       HH     AAAAAAAAAAAA     FFFFFF              TT        *
*           SS    HH       HH    AA          AA    FF                  TT        *
*  SSS      SS    HH       HH   AA            AA   FF                  TT        *
*   SSSSSSSS      HH       HH   AA            AA   FF                  TT        *
*                                                                                *
**********************************************************************************
```

Analytical solutions for a lined circular hole

Code: SHAFT. Version 3.00, upgraded for SANDIA/NNWSI May 5, 1988
J.F.T. Agapito and Associates
Grand Junction (303) 242 4220

Comments

TS-SEISMIC-SHAFT DESIGN GUIDE EXAMPLE PROBLEM ← **Seismic Load Case Seismic-1 For TS-2 Unit (From Table 4-3)**

Analysis completed by :A.M.RICHAR

Plane strain analysis

Bonding between shaft wall and liner is assumed

Geometry and Properties of Shaft and Liner ← **(In Consistent Metric Units)**

Radius of unlined hole.......	=	2.1300
Lining thickness.............	=	.3000
Elastic modulus of medium....	=	.2350E+05
Poissons ratio of medium.....	=	.2200E+00
Elastic modulus of liner.....	=	.2800E+05
Poissons ratio of liner......	=	.1500E+00

HOOP AND AXIAL DEFORMATION CALCULATION

Input in-plane strains are :
.0000E+00 .0000E+00 .1090E-03
Calculated in-plane stresses are :
.3330E+00 .3330E+00 .1050E+01
Axial strain is :
.4400E-04

Comments (cont.)

Seismic Load Case
Seismic -1
(From Table 4-5)

Free Field Stresses Calculated

The principal stresses are :
.1383E+01 -.7168E+00
The major stress is inclined at:
45.0
relative to the X axis

The Interaction Calculation for the liner
predicts the stresses listed below.
Note that the reference angle is the
first principal stress direction

Hoop Stresses in the Liner

Radius	At 0.(Pt 1)	At 90.(Pt 2)	Minimum	Maximum
			-.4015E+01	.5330E+01
1.83	-.4015E+01	.5330E+01	!1	2 !
1.86	-.3771E+01	.5063E+01	!1	2 !
1.90	-.3549E+01	.4818E+01	! 1	2 !
1.93	-.3344E+01	.4593E+01	! 1	2 !
1.96	-.3157E+01	.4385E+01	! 1	2 !
2.00	-.2984E+01	.4194E+01	! 1	2 !
2.03	-.2825E+01	.4017E+01	! 1	2 !
2.06	-.2678E+01	.3853E+01	! 1	2 !
2.10	-.2543E+01	.3701E+01	! 1	2 !
2.13	-.2417E+01	.3560E+01	! 1	2 !

Peak Tangential Stresses
For Table 5-1

Radial Stresses in the Liner

Radius	At 0.(Pt 1)	At 90.(Pt 2)	Minimum	Maximum
			-.2801E+00	.4523E+00
1.83	.0000E+00	.0000E+00	! + !
1.86	-.6668E-01	.8999E-01	! 1 2 !
1.90	-.1216E+00	.1670E+00	! 1 2 !
1.93	-.1661E+00	.2325E+00	! 1 2 !
1.96	-.2017E+00	.2880E+00	! 1 2 !
2.00	-.2295E+00	.3347E+00	! 1 2 !
2.03	-.2504E+00	.3736E+00	! 1 2 !
2.06	-.2653E+00	.4056E+00	!1 2 !
2.10	-.2750E+00	.4316E+00	!1 2 !
2.13	-.2801E+00	.4523E+00	!1 2 !

Axial Stresses in the Liner

Radius	At 0.(Pt 1)	At 90.(Pt 2)	Minimum .6298E+00	Maximum .2031E+01
1.83	.6298E+00	.2031E+01	!1	2 !
1.86	.6563E+00	.2005E+01	!1	2 !
1.90	.6815E+00	.1980E+01	! 1	2 !
1.93	.7054E+00	.1956E+01	! 1	2 !
1.96	.7282E+00	.1933E+01	! 1	2 !
2.00	.7499E+00	.1911E+01	! 1	2 !
2.03	.7707E+00	.1891E+01	! 1	2 !
2.06	.7905E+00	.1871E+01	! 1	2 !
2.10	.8094E+00	.1852E+01	! 1	2 !
2.13	.8275E+00	.1834E+01	! 1	2 !

← Peak Axial Stress For Table 5-2

```
**********************************************************************************
*                                                                                *
*     SSSSSSSS       HH       HH          AA          FFFFFFFFFFF   TTTTTTTTTTTTT  *
*    SS     SSS      HH       HH         AAAA         FFFFFFFFFFF   TTTTTTTTTTTTT  *
*   SS               HH       HH        AA  AA        FF                TT        *
*    SSS             HHHHHHHHHHH       AA    AA       FF                TT        *
*      SSS           HHHHHHHHHHH      AAAAAAAAAA      FFFFFF            TT        *
*         SSS        HH       HH     AAAAAAAAAAAA     FFFFFF            TT        *
*           SS       HH       HH    AA          AA    FF                TT        *
*   SSS     SS       HH       HH   AA            AA   FF                TT        *
*    SSSSSSSS        HH       HH   AA            AA   FF                TT        *
*                                                                                *
**********************************************************************************

Analytical solutions for a lined circular hole

Code: SHAFT.  Version 3.00, upgraded for SANDIA/NNWSI May 5, 1988
              J.F.T. Agapito and Associates
              Grand Junction (303) 242 4220

TS-SEISMIC-SHAFT DESIGN GUIDE EXAMPLE PROBLEM

Analysis completed by :A.M.RICHAR

Plane strain analysis

Bonding between shaft wall and liner is assumed

Geometry and Properties of Shaft and Liner

Radius of unlined hole..... =      2.1300
Lining thickness.......... =       .3000

Elastic modulus of medium.... =  .2350E+05
Poissons ratio of medium..... =  .2200E+00

Elastic modulus of liner..... =  .2800E+05
Poissons ratio of liner...... =  .1500E+00
```

Comments

Seismic Load Case Seismic-For TS-2 Unit (From Table 4-3)

(In Consistent Metric Units)

HOOP AND AXIAL DEFORMATION CALCULATION

Input in-plane strains are :
.8000E-04 .3000E+00 .2900E-04
Calculated in-plane stresses are :
.2858E+01 .1317E+01 .2793E+00
Axial strain is :
.9400E-04

The principal stresses are :
.2907E+01 .1268E+01
The major stress is inclined at:
10.0
relative to the X axis

The Interaction Calculation for the liner predicts the stresses listed below. Note that the reference angle is the first principal stress direction

Hoop Stresses in the Liner

Radius	At 0.(Pt 1)	At 90.(Pt 2)	Minimum .8241E+00	Maximum .8119E+01
1.83	.8241E+00	.8119E+01	!1	2 !
1.86	.9439E+00	.7841E+01	!1	2 !
1.90	.1051E+01	.7583E+01	!1	2 !
1.93	.1148E+01	.7344E+01	! 1	2 !
1.96	.1234E+01	.7122E+01	! 1	2 !
2.00	.1312E+01	.6916E+01	! 1	2 !
2.03	.1382E+01	.6724E+01	! 1	2 !
2.06	.1445E+01	.6544E+01	! 1	2 !
2.10	.1502E+01	.6376E+01	! 1	2 !
2.13	.1553E+01	.6219E+01	! 1	2 !

Radial Stresses in the Liner

Radius	At 0.(Pt 1)	At 90.(Pt 2)	Minimum .0000E+00	Maximum .8713E+00
1.83	.0000E+00	.0000E+00	!+	!
1.86	.1812E-01	.1404E+00	!1 2	!
1.90	.4179E-01	.2870E+00	! 1 2	!
1.93	.7008E-01	.3813E+00	! 1 2	!
1.96	.1022E+00	.4845E+00	! 1 2	!
2.00	.1375E+00	.5779E+00	! 1 2	!
2.03	.1753E+00	.6624E+00	! 1 2	!
2.06	.2152E+00	.7390E+00	! 1 2	!
2.10	.2568E+00	.8084E+00	! 1 2	!
2.13	.2998E+00	.8713E+00	! 1 2	!

Comments (cont.)

Seismic Load Case
Seismic - 2
(From Table 4-5)

Free Field Stresses Calculated

Peak Tangential Stresses For Table 5-1

Comments (cont.)

Axial Stresses in the Liner

Radius	At 0.(Pt 1)	At 90.(Pt 2)	Minimum .2756E+01	Maximum .3850E+01
1.83	.2756E+01	.3850E+01	!1	2 !
1.86	.2776E+01	.3829E+01	!1	2 !
1.90	.2796E+01	.3810E+01	! 1	2 !
1.93	.2815E+01	.3791E+01	! 1	2 !
1.96	.2832E+01	.3773E+01	! 1	2 !
2.00	.2849E+01	.3756E+01	! 1	2 !
2.03	.2866E+01	.3740E+01	! 1	2 !
2.06	.2881E+01	.3724E+01	! 1	2 !
2.10	.2896E+01	.3710E+01	! 1	2 !

← Peak Axial Stress For Table 5-2

OUT-OF-PLANE SHEAR CALCULATION

Input shear strains are :
.1080E-03 .2000E-04
Input shear stresses are :
.1040E+01 .1926E+00

RZ-Shear Stresses across the Liner

Radius	At 0.(Pt 1)	At 90.(Pt 2)	Minimum .0000E+00	Maximum .3328E+00
1.83	.0000E+00	.0000E+00	!+	!
1.86	.4506E-01	.8345E-02	!2 1	!
1.90	.8777E-01	.1625E-01	! 2 1	!
1.93	.1283E+00	.2376E-01	! 2 1	!
1.96	.1668E+00	.3088E-01	! 2 1	!
2.00	.2033E+00	.3765E-01	! 2 1	!
2.03	.2381E+00	.4409E-01	! 2 1	!
2.06	.2712E+00	.5022E-01	! 2 1	!
2.10	.3027E+00	.5606E-01	! 2 1	!
2.13	.3328E+00	.6163E-01	! 2 1	!

TZ-Shear Stresses across the Liner

Radius	At 0.(Pt 1)	At 90.(Pt 2)	Minimum -.2542E+01	Maximum .4707E+00
1.83	.4707E+00	-.2542E+01	!2	1 !
1.86	.4623E+00	-.2497E+01	!2	1 !
1.90	.4544E+00	-.2454E+01	!2	1 !
1.93	.4469E+00	-.2413E+01	! 2	1 !
1.96	.4398E+00	-.2375E+01	! 2	1 !
2.00	.4330E+00	-.2338E+01	2	1 !
2.03	.4266E+00	-.2304E+01	! 2	1 !
2.06	.4205E+00	-.2271E+01	! 2	1 !
2.10	.4146E+00	-.2239E+01	! 2	1 !
2.13	.4091E+00	-.2209E+01	! 2	1 !

Comments (cont.)

Free Field Shear Strain (Inputs from Table 4-5)

Free Field Stresses Calculated

Peak Shear Stress For Table 5-3

SDRD APPENDIX A.6

ESF UNDERGROUND EXCAVATIONS DESIGN METHODOLOGY

CLRT 89-PB01

January 1989

YUCCA MOUNTAIN PROJECT

STRATEGY FOR TITLE II GROUND SUPPORT DESIGN AND CONSTRUCTION FOR THE EXPLORATORY SHAFT FACILITY (REVISION 0)

Prepared by

PARSONS BRINCKERHOFF QUADE & DOUGLAS, INC.
San Francisco, California

Prepared for

SANDIA NATIONAL LABORATORIES, INC.
Albuquerque, New Mexico

SANDIA CONTRACT MONITOR
R.E. STINEBAUGH
GEOTECHNICAL DESIGN DIVISION

STRATEGY FOR TITLE II GROUND SUPPORT DESIGN AND CONSTRUCTION FOR THE EXPLORATORY SHAFT

An important part of the Exploratory Shaft Facility (ESF) design is the design of the ground support for the facility's underground openings. Acceptable documentation of this design requires adherence to an accepted standard or procedure. This memo outlines the procedure for ground support design and implementation. The procedure incorporates theoretical and empirical analyses, as well as fundamental considerations of rock mass behavior. Implementation in the field requires observations and measurements of rock mass quality, and certain types of monitoring. Details of the procedure and supporting analytical methods will be presented in reports by Parsons Brinckerhoff and J.F.T. Agapito & Associates, respectively, later in the year.

Drifts and other openings in the underground repository facility must be designed and constructed so that they remain stable and functional for the required length of time. This also applies to the ESF. A stable design is achieved by appropriate selection of spacings between openings, shapes of openings, method of excavation, and ground support components. The selection of these engineered parameters, followed by the preparation of construction drawings and specifications, constitute the design of the openings.

Design of rock openings is complicated by the variability of the rock mass and the great difficulty of determining rock mass parameters, particularly rock mass strength, at an appropriate scale. Because of this complexity, it is generally recognized that analytical methods cannot be relied upon as the sole design tools. Analytical methods used alone do not have a good track record for underground opening design, and the output of such analyses, typically in the form of stresses, strains, and definition of yielded zones, is difficult to interpret for real opening behavior. Therefore, underground designers primarily rely on

empirical and observational methods to achieve ground control and stability.

For repository openings it is necessary to use a strategy that incorporates elements of analytical, empirical, and observational methods in a pragmatic, yet formal design process. This process, and the interrelations between the analytical and empirical elements of the process, are summarized in the following.

There are several ways to break up the design process into individual steps or procedures. The process described herein is complete and involves nine steps, each of which is broken into several elements (see Figure 1).

The first step is the assembly of the data base used to develop the design, including site-specific geotechnical and geologic parameters and their variability, design data gathered from functional requirements (e.g., required cross section area and minimum dimensions), and temperature and thermal stress data. Analytical heat transfer and thermomechanical models are usually used to derive temperatures and thermal stresses, based on design geometry and heat output from the decaying nuclear waste.

Step 2 is the selection of opening shape; spacing between openings also may be analyzed in this step. Often the rough opening shape is dictated by functional requirements, but the detailed opening shape is selected based on stress analyses so as to minimize stress concentrations and regions of overstress or yield. In these analyses a rock mass strength or yield function is used, derived from laboratory and field data fitted to an empirical triaxial strength formulation.

In these and other analyses, seismic effects are incorporated pseudo-statically, i.e., the static modeling will incorporate seismic stress or strain components superimposed on the static boundary

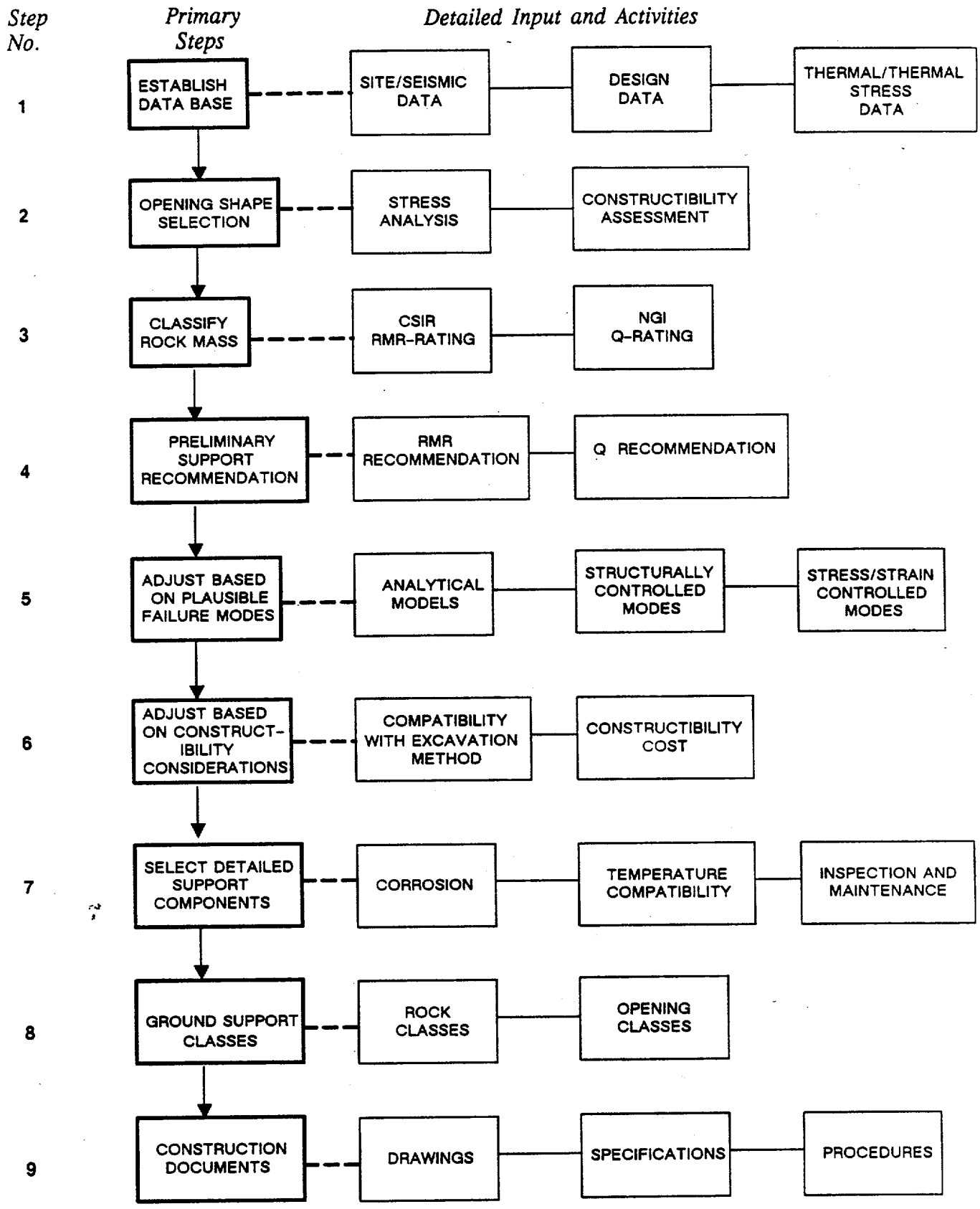

Figure 1. Design Steps for Underground Openings

conditions. These are derived from ground motions specified in the project seismic data base.

The opening shape also must be matched to the proposed excavation method (e.g., an opening excavated by tunnel boring machine should be circular).

Step 3 consists of classifying the rock mass for empirical assessment of ground support requirements, using not one but two or more classification methods. It is important here to assess the variability of the rock mass (ranges and distribution of rock mass classes). Certain input to the empirical classification systems requires determination of the stress state around the opening, initially and later, subject to the thermal load. The stress state will be determined using mechanical and thermomechanical modeling.

A preliminary support recommendation is derived from the empirical classification in Step 4. Typically a range of support schemes is derived commensurate with the range of rock mass classes, but generally using the same types of support components, applied to a different degree.

Step 5 is very important. It has been found that the empirical methods do not always bring out recommendations that match potential failure modes derived from fundamental analyses. It is therefore necessary to examine these potential failure modes to verify if the recommended support, in fact, will counteract them. These potential failure modes are usually classified as structurally controlled (controlled largely by joints, faults, or bedding planes), or stress controlled; other modes, such as those controlled by deterioration of the rock mass, are also considered. Analyses of these failure modes usually involve fundamental geologic input data (such as frequency, direction, and character of joints) and input from analytical modeling. These analyses also provide specific input to the design of individual rock support components (e.g., length and required capacity of rock bolts).

In Step 6 the construction process is examined to ensure that the installation of ground support components is compatible with the method and sequence of excavation. Costs of different support methods are also compared. The ground support scheme is modified as required to produce a practical, constructible, and economical design.

Step 7 is the final selection of ground support components. Here, the long-term performance of the components under the particular local environment is analyzed, considering issues of corrosion and deterioration (dependent on temperature, humidity, and available chemical species), temperature and thermal strain compatibility, and the accessibility of the particular location for inspection and maintenance.

In Step 8 practical definitions of rock classes and opening classes are formulated, and different support schemes (different levels and types of support) are matched to the class and quality of the rock mass and the size, function, and environment of the openings. A system is devised by which the rock is classified during construction so that the local selection or verification of ground support class can be made.

The final step is the production of the end product, which consists of construction drawings and details, specifications, and procedures for rock classification and for testing of ground support components as required. Instructions for monitoring opening performance are also prepared, as well as procedures for inspection. Procedures for long-term monitoring, inspection, and maintenance during the operational phase are also required.

As described previously, the design process is a fairly complex one that involves an interplay between empirical methods of ground support selection, analytical modeling, evaluation of fundamental rock behavior, practical considerations of constructibility and durability, an observational approach to be taken during construction, and consideration of long-term maintainability. It is generally not possible in this

process to separate the analytical activities from the empirical and more fundamental considerations and to perform the analytical modeling or the empirical support selection independently. The needs for analytical modeling in the design process are driven by the strategic progression from the raw data and functional requirements to the end product, the construction documents.

The design as described herein will be presented in detail in a report by Parsons Brinckerhoff later in the year. This report will also contain certain data input for the design, including thermomechanical and sesimic design input, and criteria for acceptable performance to be used in the interpretation of design analyses. Description of and criteria for fundamental geological analyses also will be presented. The report will contain solved example problems, and examples of acceptable ground support systems. The examples will use rock mass characteristics and opening sizes and shapes typical of the ESF.

Several steps of the design procedure use numerical modeling of rock mass behavior, including thermal as well as mechanical modeling. A report containing modeling methods and examples for these purposes also will be presented by J.F.T. Agapito & Associates later in the year.